

**Stabilization of water-in-oil (W/O)
emulsions using food grade materials**

Morfo Zembyla

Submitted in accordance with the requirements for the degree of

Doctor of Philosophy

The University of Leeds

School of Food Science and Nutrition

October 2019

The candidate confirms that the work submitted is her own, except where work which has formed part of jointly-authored publications has been included. The contribution of the candidate and the other authors to this work has been explicitly indicated below. The candidate confirms that appropriate credit has been given within the thesis where reference has been made to the work of others. Details of the jointly-authored publications and the contributions of the candidate and the other authors to the work are outlined on the page –v-.

This copy has been supplied on the understanding that it is copyright material and that no quotation from the thesis may be published without proper acknowledgement.

The right of Morfo Zembyla to be identified as Author of this work has been asserted by her in accordance with the Copyright, Designs and Patents Act 1988.

Further details of the jointly-authored publications and the contributions of the candidate and the other authors to the work are included below:

Patent

Murray, B. S., Zembyla, M. & Sarkar, A. (2019). Emulsions in foods. WO/2019/008059A1.

<https://patentscope2.wipo.int/search/en/detail.jsf?docId=WO2019008059>

Chapter 3

Zembyla, M., Murray, B.S. and Sarkar, A. (2018). Water-In-Oil Pickering Emulsions Stabilized by Water-Insoluble Polyphenol Crystals. *Langmuir*. 34 (34), 10001-10011.

Chapter 4

Zembyla, M., Murray, B.S., Radford, S.J. and Sarkar, A. (2019). Water-in-oil Pickering emulsions stabilized by an interfacial complex of water-insoluble polyphenol crystals and protein. *Journal of colloid and interface science*, 548, 88-99.

Chapter 5

Zembyla, M., Lazidis, A., Murray, B.S., and Sarkar, A. (2019). Water-in-Oil Pickering Emulsions Stabilized by Synergistic Particle-Particle Interactions. *Langmuir*, 35 (40), 13078-13089.

Chapter 6

Zembyla, M., Lazidis, A., Murray, B.S., and Sarkar, A. (2019). Shear and Temperature Stability of Water-in-Oil Emulsions Co-Stabilized by Polyphenol Crystals- Protein Complex. *Submitted to Journal of Food Engineering*.

Details of authorship contributions:

Morfo Zembyla: designed the experiments and conducted the measurements, data analysis and interpretation as well as drafted and edited the manuscripts and replied to the comments from reviewers.

Brent S. Murray and Anwasha Sarkar: provided supervision, feedback and contributed to the proofreading and editing of the manuscript and to the comments from the reviewers.

Stewart Radford and Aris Lazidis: provided industrial supervision and feedback.

List of accepted conference abstracts and awards

Poster presentations

Zembyla, M., Murray, B. S. & Sarkar, A. (2016). Stabilization of Water-in-Oil Emulsions Using Food Grade Materials. *SOFI CDT Showcase*. University of Leeds, UK.

Zembyla, M., Murray, B. S. & Sarkar, A. (2016). Stabilization of Water-in-Oil Emulsions Using Food Grade Materials. *3rd PhD Conference*. University of Leeds, UK.

Zembyla, M., Murray, B. S. & Sarkar, A. (2016). How about a tasty and healthy chocolate?. *University of Leeds PGR Conference*. University of Leeds, UK.

Zembyla, M., Murray, B. S. & Sarkar, A. (2017). Stabilization of Water-in-Oil Emulsions Using Food Grade Materials. *SOFI CDT Showcase*. University of Durham, UK.

Zembyla, M., Murray, B. S. & Sarkar, A. (2017). Stabilization of Water-in-Oil Emulsions Using Food Grade Materials. *UK colloids conference: An international colloids and interface science symposium*. Manchester, UK.

Zembyla, M., Murray, B. S. & Sarkar, A. (2018). Stabilization of Water-in-Oil Emulsions Using Food Grade Materials. *17th Food Colloids Conference*. University of Leeds, UK.

Zembyla, M., Murray, B. S. & Sarkar, A. (2018). Stabilization of Water-in-Oil Emulsions Using Food Grade Materials. *EPSRC Centres for Doctoral Training (CDTs) Poster Event*. University of Leeds, UK.

Zembyla, M., Murray, B. S. & Sarkar, A. (2018). Stabilization of Water-in-Oil Emulsions Using Food Grade Materials. *SOFI CDT Showcase*. University of Edinburgh, UK.

Zembyla, M., Murray, B. S. & Sarkar, A. (2019). Water-in-Oil (W/O) Pickering Emulsions Stabilized by Polyphenol Crystals-Biopolymer Complex. *Industry Day Event*. University of Leeds, UK.

Zembyla, M., Murray, B. S. & Sarkar, A. (2019). Water-in-Oil Emulsions Stabilized by an Interfacial Complex of Polyphenol Crystals and Protein. *9th International Colloids Conference*. Sitges, Barcelona, Spain.

Oral presentations

Zembyla, M., Murray, B. S. & Sarkar, A. (2017). Stabilization of Water-in-Oil Emulsions Using Food Grade Materials. *SOFI CDT Showcase*. University of Durham, UK.

Zembyla, M., Murray, B. S. & Sarkar, A. (2017). Stabilization of Water-in-Oil Emulsions Using Food Grade Materials. *4th PhD Conference*. University of Leeds, UK.

Zembyla, M., Murray, B. S. & Sarkar, A. (2018). Water-in-Oil (W/O) Pickering Emulsions Stabilized by Polyphenol Crystals-Biopolymer Complex. *32nd EFFoST International Conference*. Nantes, France.

Zembyla, M., Murray, B. S. & Sarkar, A. (2018). Water-in-Oil (W/O) Pickering Emulsions Stabilized by Polyphenol Crystals-Biopolymer Complex. *5th PhD Conference*. University of Leeds, UK.

Zembyla, M., Murray, B. S. & Sarkar, A. (2019). Pickering Water-in-Oil Emulsions Stabilized by an Interfacial Complex of Polyphenol Crystals and Protein. *SOFI CDT Showcase*. University of Leeds, UK.

Zembyla, M., Murray, B. S. & Sarkar, A. (2019). Dual delivery of water-soluble compounds and water-insoluble polyphenols using complex interfaces. *8th International Symposium on "Delivery of Functionality in Complex Food Systems"*. Porto, Portugal.

Awards

Inside Cover:

Journal of Colloids and Interface Science (Volume 550, 15 August 2019)
based on the published manuscript:

Zembyla, M., Murray, B.S., Radford, S.J. and Sarkar, A. (2019). Water-in-oil Pickering emulsions stabilized by an interfacial complex of water-insoluble polyphenol crystals and protein. *Journal of colloid and interface science*, 548, 88-99.

Best Poster Prizes:

Zembyla, M., Murray, B. S. & Sarkar, A. (2017). Stabilization of Water-in-Oil Emulsions Using Food Grade Materials. *SOFI CDT Showcase*. University of Durham, UK.

Zembyla, M., Murray, B. S. & Sarkar, A. (2017). Stabilization of Water-in-Oil Emulsions Using Food Grade Materials. *UK colloids conference: An international colloids and interface science symposium*. Manchester, UK.

Zembyla, M., Murray, B. S. & Sarkar, A. (2018). Stabilization of Water-in-Oil Emulsions Using Food Grade Materials. *17th Food Colloids Conference*. University of Leeds, UK.

Zembyla, M., Murray, B. S. & Sarkar, A. (2018). Stabilization of Water-in-Oil Emulsions Using Food Grade Materials. *EPSRC Centres for Doctoral Training (CDTs) Poster Event*. University of Leeds, UK.

Zembyla, M., Murray, B. S. & Sarkar, A. (2019). Water-in-Oil Emulsions Stabilized by an Interfacial Complex of Polyphenol Crystals and Protein. *9th International Colloids Conference*. Sitges, Barcelona, Spain.

Acknowledgements

Undertaking this PhD has been a truly-life changing experience for me and it would not have been possible to do without the support and guidance I received from many people.

First of all I would like to express my sincere gratitude to my supervisors, Professor Brent Murray and Dr Anwasha Sarkar, whose expert guidance and advices in all aspects helped make this possible. Their vision, sincerity and motivation have deeply inspired me and made me feel confident about my abilities. Their support and advices have helped shape my professional career and improved as a scientist. Thank you very much!!

I gratefully acknowledge Soft Matter and Functional Interfaces (SOFI) CDT, EPSRC and Nestlé PTC Confectionery (York, UK) for the financial support during my studies (Grant Ref. No. EP/L015536/1).

Many thanks go to colleagues and staff in School of Food Science and Nutrition, particularly from the Food Colloids group for supporting me throughout my research and making my life in the laboratory enjoyable. I am incredibly proud to be a part of this team. I particularly would like to thank: Panayiotis Klitou, Dr Elena Simone, Dr Papoole Valadbaigi, Dr Alessandro Gulotta, Lorenzo Metilli, Zachary Glover, Sam Stubbley, Andrea Araiza-Calahorra, Dr Nataricha Phisarnchananan, Neil Rigby and Miles Ratcliffe, who were always there to help and offer valuable support during my PhD.

Last but not least, I would like to express my gratitude to my parents and my brother, who have always supported me throughout my career and helped out in their special way. Words cannot express how grateful I am to my incredible family for their unconditional love and unlimited support. Special thanks go to my grandparents, uncles, aunts and cousins who, stayed close to me and supported me throughout these years. This thesis is dedicated to all of you!!

Abstract

Considering the global uprise of obesity and food-linked cardiovascular diseases, the addition of water into fat-based products, in the form of water-in-oil (W/O) emulsions, seems the most promising way to reduce the fat and calorific content of these products. Although this appears to be the most promising approach in theory, lack of stability of these emulsion systems presents one of the key challenges because they are thermodynamically unstable and prone to phase separation over time. Traditionally, chemically-synthesized surfactants (e.g., polyglycerol polyriconeate (PGPR)) and/or chemically modified particles (e.g., silica particles), that contain *E-numbers*, have widely used as stabilizers for W/O emulsions. However, owing to the growing interests for '*clean label*' products by consumers, such products tend to be less appealing. Consequently, there is a huge driving force from food industries to replace these chemically-synthesized materials with natural and biodegradable ingredients that will give a '*clean label*' on the final product.

This thesis addresses this research challenge of providing longer term stability to water droplets dispersed in an oil continuous matrix using biocompatible materials. The design of novel W/O emulsion droplets stabilized by an interfacial complex formation produced by a combination of nature-derived polyphenol crystals (curcumin or quercetin particles), present in the oil phase, and protein (WPI) or protein-based particles (WPM particles), in the aqueous phase, is shown in this work. The stability of these water droplets depends on the concentration of WPI or WPM particles present in the aqueous phase, as well as, the pH of the aqueous phase. An improvement of the stability was observed at an acidic pH (~ 3.0) due to hydrogen bonding and electrostatic attraction between the oppositely charged WPI or WPM particles (positive) and polyphenol crystals (negative). In addition, the effect of different processing conditions such as shear rates and temperatures on the stability of these emulsions, is shown in this thesis. It was concluded that the emulsions stabilized by interfacial complexes provided longer term stability, compared to those stabilized only by curcumin or quercetin crystals, and were stable under shear and temperatures without any coalescence or phase separation.

Table of Contents

Details of authorship contributions:	v
List of accepted conference abstracts and awards	vi
Acknowledgements.....	ix
Abstract.....	x
Table of Contents	xi
List of Tables	xvi
List of Figures	xx
List of Abbreviations.....	xxix
Nomenclature	xxx
Chapter 1 General Introduction.....	1
1.1. Research motivation	1
1.2. General insight about emulsions	2
1.3. Research aim	3
1.3.1. Research hypothesis & proposed stabilization mechanism.....	4
1.4. Rationale behind the selection of polyphenol crystals	5
1.4.1. Classification of polyphenols.....	6
1.4.2. Interactions of polyphenols with proteins	10
1.5. Rationale behind the selection of biopolymers and their derivatives	12
1.5.1. Whey protein isolate.....	13
1.5.2. Whey protein microgel particles	14
1.6. Rationale behind the selection of characterization techniques.....	15
1.6.1. Interfacial tension	15
1.6.2. Contact angle and wettability	16
1.6.3. Static light scattering	17
1.6.4. Dynamic light scattering	18
1.6.5. Zeta-potential (ζ -potential)	19
1.6.6. Microscopy across length scales.....	22
1.6.7. Langmuir trough experiments	25
1.6.8. Rheology	27
1.6.9. Interfacial shear viscosity	29
1.7. Outline of the thesis	31

References.....	35
Chapter 2 Water-in-oil emulsions stabilized by surfactants, proteins and particles: A literature review	41
Abstract.....	41
2.1. Introduction	41
2.2. Emulsions characteristics.....	44
2.2.1. Definition	44
2.2.2. Thermodynamic and kinetic stability of the emulsions	44
2.2.3. Instability of W/O emulsions	46
2.2.4. Stabilizers/ Emulsifiers	49
2.3. Emulsification parameters influencing the stability of W/O emulsions	50
2.4. Stabilization of W/O emulsions by surface active agents (surfactants)	57
2.4.1. Definition & characteristics	57
2.4.2. W/O emulsions stabilized by low molecular weight surfactants.....	57
2.5. W/O emulsions stabilized by biopolymers	59
2.5.1. Definition & characteristics.....	59
2.5.2. Biopolymer & surfactant-stabilized W/O emulsions	60
2.6. Stabilization of W/O emulsions by particles (Pickering stabilization)	63
2.6.1. Definition & characteristics	63
2.6.2. Wettability.....	64
2.6.3. Macroscopic configurations and stabilization mechanisms	65
2.6.4. Particle-stabilized W/O emulsions	67
2.7. Rheological properties of W/O emulsions	75
2.8. Conclusion	78
References.....	79
Chapter 3 Water-in-Oil Pickering Emulsions Stabilized by Water-Insoluble Polyphenol Crystals	89
Abstract.....	89
3.1. Introduction	90
3.2. Material and methods.....	94
3.2.1. Materials.....	94

3.2.2.	Contact angle and wettability	94
3.2.3.	Interfacial tension	95
3.2.4.	Preparation of oil dispersions and W/O emulsions	95
3.2.5.	Particle and emulsion droplet size measurements	96
3.2.6.	ζ -Potential measurements.....	96
3.2.7.	Optical microscopy.....	97
3.2.8.	Scanning electron microscopy (SEM)	97
3.2.9.	Confocal laser scanning microscopy (CLSM)	97
3.2.10.	Interfacial shear viscosity (η_i)	98
3.2.11.	Statistical analysis.....	99
3.3.	Results and discussion	99
3.3.1.	Assessment of polyphenol crystals as Pickering stabilizers	99
3.3.2.	W/O emulsions.....	105
3.4.	Conclusion	115
	References.....	117
Chapter 4 Water-in-Oil Pickering Emulsions Stabilized by an Interfacial Complex of Water-Insoluble Polyphenol Crystals and Protein		
	Abstract.....	120
4.1.	Introduction	121
4.2.	Material and methods.....	124
4.2.1.	Materials	124
4.2.2.	Preparation of W/O emulsions	125
4.2.3.	Particle size measurements	126
4.2.4.	Confocal laser scanning microscopy (CLSM) ...	126
4.2.5.	Interfacial tension	127
4.2.6.	Interfacial shear viscosity (η_i)	127
4.2.7.	Optical microscopy.....	128
4.2.8.	Statistical analysis.....	128
4.3.	Results and discussion	129
4.3.1.	Stability measurements of W/O Pickering emulsions.....	129
4.3.2.	Effect of increase in volume fraction of water droplets	136
4.3.3.	Interfacial shear viscosity	137

4.4. Discussion	145
4.5. Conclusion	147
References	149
Chapter 5 Water-in-Oil Pickering Emulsions Stabilized by Synergistic Particle-Particle Interactions	152
Abstract	152
5.1. Introduction	153
5.2. Material and methods	156
5.2.1. Materials	156
5.2.2. Preparation of aqueous dispersion of whey protein microgel (WPM) particles	156
5.2.3. Particle size measurement of WPM particles	157
5.2.4. Electrophoretic mobility	157
5.2.5. Preparation of W/O emulsions	158
5.2.6. Droplet size measurement of emulsions	159
5.2.7. Confocal laser scanning microscopy (CLSM)....	160
5.2.8. Langmuir trough measurements	160
5.2.9. Interfacial shear viscosity (η_i)	161
5.2.10. Statistical analysis	162
5.3. Results and discussion	162
5.3.1. Characterization of aqueous dispersion of WPM particles	162
5.3.2. Characterization of polyphenol particles in the oil phase	163
5.3.3. W/O Pickering emulsions stabilized by WPM-polyphenol crystal complexes	165
5.3.4. Interfacial shear viscosity (η_i)	179
5.4. Discussion	181
5.5. Conclusion	183
References	185
Chapter 6 Shear and Temperature Stability of Water-in-Oil Emulsions Co-Stabilized by Polyphenol Crystals- Protein Complex	189
Abstract	189
6.1. Introduction	190
6.2. Materials and methods	193
6.2.1. Materials	193

6.2.2.	Preparation of oil dispersion of curcumin or quercetin crystals	193
6.2.3.	Preparation of aqueous dispersion of whey protein isolate (WPI).....	193
6.2.4.	Preparation of aqueous dispersion of whey protein microgel (WPM) particles	194
6.2.5.	Preparation of W/O emulsions	194
6.2.6.	Rheology.....	195
6.2.7.	Particle size measurements	195
6.2.8.	Confocal laser scanning microscopy (CLSM) ...	196
6.2.9.	Statistical analysis.....	196
6.3.	Results and discussion	196
6.3.1.	Control experiments.....	196
6.3.2.	Stability of 10 wt% W/O emulsions stabilized by curcumin or quercetin crystals with or without 2 wt% WPI or WPM particles.....	200
6.3.3.	Stability of 10 wt% W/O emulsions stabilized by curcumin or quercetin crystals + wt% different concentrations of WPM particles.....	209
6.3.4.	Stability of 20 wt% W/O emulsions stabilized by curcumin or quercetin crystals + 2.0 wt% WPM particles.....	211
6.4.	Conclusion	214
	References.....	214
	Chapter 7 General Discussion	218
7.1.	Introduction	218
7.2.	Summary of the main results.....	222
7.2.1.	Assessment of particles as Pickering stabilizers	222
7.2.2.	W/O emulsions.....	226
7.3.	Concluding remarks and recommendations for future studies.....	231
7.3.1.	Concluding remarks	231
7.3.2.	Future studies	232
	References.....	234
	Appendix A Supporting information for Chapter 3	235
	Appendix B Supporting information for Chapter 4	239
	Appendix C Supporting Information of Chapter 5.....	244

List of Tables

Table 2.1. Summary of homogenizers that have been used in literature to prepare W/O emulsions and their physicochemical characteristics (applied energy (Tadros, 2013) and size of droplets (Dickinson, 1992; McClements, 2015))	52
Table 2.2. Summary of surfactants, biopolymers or particles (bio-derived and non-bio-derived) used for stabilizing W/O emulsions.....	55
Table 2.3. Summary of processing experiments for W/O emulsions stabilized by surfactants, biopolymers or particles.	78
Table 3.1. Measured contact angles of water droplets (pH 3.0 and 7.0) on polyphenol crystals in air (θ_w) and oil droplets on polyphenol crystals in air (θ_o). Also shown is the calculated three-phase contact angle (θ) at the W-O interface in the aqueous phase (pH 3.0 and 7.0). Samples with the same letter do not differ significantly ($p > 0.05$) according to Tukey's test.....	104
Table 3.2. ζ -potential (mV) of curcumin and quercetin particles (0.14 wt%) dispersed in the aqueous phase at pH 3.0 and 7.0. Samples with * do not differ significantly ($p > 0.05$) according to Tukey's test.	105
Table 4.1. Interfacial tension (γ_T) data, with or without the presence of curcumin or quercetin particles (0.14 wt%) and WPI (0.5 wt%), between the soybean oil and aqueous phases. Samples with the same letter do not differ significantly ($p > 0.05$) according to Tukey's test.	133
Table 5.1. Size and ζ -potential of 0.5 wt% WPM particles in the aqueous phase at pH 3.0 and 7.0.	163
Table 5.2. Mobility of 0.14 wt% polyphenol crystals in the oil phase (at 150 V).	164
Table 6.1. d_{32} and d_{43} values (μm) before and after shearing of 10 wt% W/O emulsions stabilized by 0.14 wt% curcumin crystals & water, 2.0 wt% WPI or 2.0 wt% WPM particles as an aqueous phase (pH 3.0) at different temperatures; 25, 35 and 50 °C. Samples with the same letter differ significantly ($p < 0.05$) according to Tukey's test for each component in the aqueous phase before and after shearing.	207
Table 6.2. d_{32} and d_{43} values (μm) before and after shearing of 10 wt% W/O emulsions stabilized by 0.14 wt% quercetin crystals & water, 2.0 wt% WPI or 2.0 wt% WPM particles as an aqueous phase (pH 3.0) at different temperatures; 25, 35 and 50 °C. Samples with the same letter differ significantly ($p < 0.05$) according to Tukey's test for each component in the aqueous phase before and after shearing.	208

Table 6.3. d_{32} and d_{43} values (μm) before and after shearing of 10 wt% W/O emulsions stabilized by 0.14 wt% curcumin crystals & WPM particles as an aqueous phase (pH 3.0) at different concentrations; 0.1, 0.5, 1.0 and 2.0 wt%. Samples with the same letter differ significantly ($p < 0.05$) according to Tukey's test for each WPM particle concentration.....	210
Table 6.4. d_{32} and d_{43} values (μm) before and after shearing of 10 wt% W/O emulsions stabilized by 0.14 wt% quercetin crystals & WPM particles as an aqueous phase (pH 3.0) at different concentrations; 0.1, 0.5, 1.0 and 2.0 wt%. Samples with the same letter differ significantly ($p < 0.05$) according to Tukey's test for each WPM particle concentration.....	211
Table 6.5. d_{32} and d_{43} values (μm) before and after shearing of 20 wt% W/O emulsions stabilized by 0.14 wt% curcumin or quercetin crystals & 2.0 wt% WPM particles as an aqueous phase (pH 3.0) at different temperatures; 25, 35 and 50 °C. Samples with the same letter differ significantly ($p < 0.05$) according to Tukey's test for each polyphenol crystal before and after shearing.	213
Table 7.1. Comparison of the characteristics of 0.14 wt% curcumin and quercetin crystals based on their size in oil (d_{32}), contact angle of water droplet (θ_w), oil droplet (θ_o) at pH 3.0 and 7.0, interfacial tension (γ_T) at oil-water (O-W) interface, ζ-potential (in water, pH 3.0 and 7.0) and electrophoretic mobility (in oil). Samples with the same letter do not differ significantly ($p > 0.05$) according to Tukey's test.....	224
Table 7.2. d_{32} values for 0.14 wt% curcumin and quercetin crystals dispersed in oil under different treatments; ultra-Turrax only (9,400 rpm for 5 min), ultra-Turrax (9,400 rpm for 5 min) followed by: ultrasound bath for 2, 5 or 10 min, heat (60 °C for 1 h) or Jet homogenizer (twice at 300 bar). Samples with the same letter do not differ significantly ($p > 0.05$) according to Tukey's test.	226
Table A1. Average size of curcumin and quercetin crystals (0.14 wt%) dispersed in oil under different mixing conditions; Ultra-Turrax at 9,400 rpm/ 5 min or after passing through all stages of emulsification process (Ultra-Turrax at 9,400 rpm/ 5 min, 13,400 rpm/ 2 min and Jet homogenization for two passes, at 300 bar). Samples with the same letter do not differ significantly ($p > 0.05$) according to Tukey's test.....	236
Table A2. Surface tension (γ) between aqueous phase and air (A-W) and non-purified soybean oil phase and air (O-A) in the presence or not of 0.14 wt% curcumin and quercetin crystals. Samples with the same letter do not differ significantly ($p > 0.05$) according to Tukey's test.....	237

Table A3. Interfacial tension (γ_T) between aqueous phase at pH 3.0 and curcumin or quercetin crystals (0.14 wt%) dispersed in purified or non-purified soybean oil phase. Samples with the same letter do not differ significantly ($p > 0.05$) according to Tukey's test.....	237
Table B1. Size of water droplets (d_{32}) over time of 5 wt% W/O emulsions stabilized by 0.14 wt% curcumin particles containing 0, 0.05, 0.5, 1, 2 and 4 wt% WPI in the aqueous phase at pH 3.0. Samples with the same letter differ significantly ($p < 0.05$) according to Tukey's test for each concentration of WPI.	240
Table B2. Size of water droplets (d_{32}) over time of 5 wt% W/O emulsions stabilized by 0.14 wt% quercetin particles containing 0, 0.05, 0.5, 1, 2 and 4 wt% WPI in the aqueous phase at pH 3.0. Samples with the same letter differ significantly ($p < 0.05$) according to Tukey's test for each concentration of WPI.	241
Table B3. Size of water droplets (d_{32}) over time of 5 wt% W/O emulsions stabilized by 0.14 wt% curcumin particles containing 0, 0.05, 0.5, 1, 2 and 4 wt% WPI in the aqueous phase at pH 7.0. Samples with the same letter differ significantly ($p < 0.05$) according to Tukey's test for each concentration of WPI.	242
Table B4. Size of water droplets (d_{32}) over time of 5 wt% W/O emulsions stabilized by 0.14 wt% quercetin particles containing 0, 0.05, 0.5, 1, 2 and 4 wt% WPI in the aqueous phase at pH 7.0. Samples with the same letter differ significantly ($p < 0.05$) according to Tukey's test for each concentration of WPI.	242
Table C1. Size of water droplets (d_{32}) over time of 10 wt% W/O emulsions stabilized by 0.14 wt% curcumin crystals containing 0.05, 0.1, 0.5, 1 and 2 wt% WPM particles in the aqueous phase at pH 3.0. Samples with the same letter differ significantly ($p < 0.05$) according to Tukey's test for each concentration of WPM particles.....	245
Table C2. Size of water droplets (d_{32}) over time of 10 wt% W/O emulsions stabilized by 0.14 wt% quercetin crystals containing 0.05, 0.1, 0.5, 1 and 2 wt% WPM particles in the aqueous phase at pH 3.0. Samples with the same letter differ significantly ($p < 0.05$) according to Tukey's test for each concentration of WPM particles.....	246
Table C3. Size of water droplets (d_{32}) over time of 15, 20 and 30 wt% W/O emulsions stabilized by 0.14 wt% curcumin crystals & 2 wt% WPM particles in the aqueous phase at pH 3.0. Samples with the same letter differ significantly ($p < 0.05$) according to Tukey's test for each concentration of WPM particles.	248

Table C4. Size of water droplets (d_{32}) over time of 15, 20 and 30 wt% W/O emulsions stabilized by 0.14 wt% quercetin crystals & 2 wt% WPM particles in the aqueous phase at pH 3.0. Samples with the same letter differ significantly ($p < 0.05$) according to Tukey's test for each concentration of WPM particles.248

Table C5. Interfacial shear viscosity at W-O interface with 0.14 wt% curcumin and quercetin crystals dispersed in purified oil with different concentrations of WPM particles in the aqueous phase after 24 h of adsorption at pH 3.0. Samples with the same letter differ significantly ($p < 0.05$) according to Tukey's test for each polyphenol crystal.249

List of Figures

Figure 1.1. “Dual” delivery system for delivering both water insoluble polyphenol crystals, present in the oil phase, and water-soluble compounds, present in the aqueous phase, through W/O Pickering emulsions.....	5
Figure 1.2. Classification of polyphenols.....	7
Figure 1.3. Structure of (a) quercetin molecule, (bi) curcumin molecule in α,β -unsaturated- β -diketonic tautomeric form and (bii) two isomers of curcumin molecule in an equilibrating keto-enol tautomeric form.	9
Figure 1.4. Mechanism of interactions between proteins and polyphenols.	12
Figure 1.5. Contact angle (θ) of an aqueous drop on a solid (particle) substrate; (a) θ is smaller than 90° indicating hydrophilic particles and (b) θ is bigger than 90° indicating hydrophobic particles.....	17
Figure 1.6. An illustration of different scattering patterns displayed a small (a) vs big (b) particle as illuminated by a laser beam.....	18
Figure 1.7. Schematic representation of a negatively charged particles and the presence of its ions at the "stern layer", "diffuse layer" and "slipping plane".....	21
Figure 1.8. Schematic representation of surface pressure (π) versus area per molecule (A) plot of a surface-active molecule. The π - A plot is divided to different regimes (gas, liquid, solid and collapse) during compression, depending on the strength of the solute-solute interactions.	27
Figure 1.9. Relationship between the force and velocity of an applied stress on the displacement of a material (Mezger, 2014).	28
Figure 1.10. Comparison of viscosity functions of Newtonian and non-Newtonian fluids.....	29
Figure 1.11. Schematic representation of interfacial shear viscometer.	31
Figure 1.12. Schematic framework of this thesis.	32
Figure 2.1. Activation energy (ΔG^*) required to form kinetically stable emulsions which prevents the phase separation arising from thermodynamically unstable systems for a certain time period.	46
Figure 2.2. Physical emulsions destabilization mechanisms for W/O emulsions; (a) original emulsion, (b) flocculation, (c) sedimentation, (d ₁ -d ₂) Ostwald ripening, (e) coalescence and (f) phase separation.	46

Figure 2.3. Schematic diagram of a W/O emulsion droplet showing different interfacial stabilization by surfactant, biopolymers or particles.	50
Figure 2.4. (a) The three-phase contact angle is related to the balance of surface free energies at the particle-water, particle-oil and water-oil interfaces. (b) Hydrophilic particle ($\gamma_{po} > \gamma_{pw}$) with contact angle smaller than 90° form O/W emulsions (left). Hydrophobic particles ($\gamma_{po} < \gamma_{pw}$) with contact angle bigger than 90° form W/O emulsions (right).	65
Figure 2.5. Possible configurations of particles in solid-stabilized emulsions (Binks <i>et al.</i> , 2006).	66
Figure 2.6. Possible mechanisms responsible for stability of particles in solid-stabilized emulsions (Binks <i>et al.</i> , 2006)....	66
Figure 2.7. Preparation of water-in-toluene emulsions stabilized by silica nanospheres with different contact angles (volume fraction of water: 0.20, silica concentration: 5 kg m^{-3}) (Yan <i>et al.</i> , 2001).	68
Figure 2.8. Cryo-SEM images of W/O emulsions with 20 vol% water. (a) Water droplets in oil with zein particles circled in the inset on one of the droplet surface; one droplet is cut-open during freeze-fracture. (b - c) A network of zein particles observed within the etched core of the water droplets (Rutkevičius <i>et al.</i> , 2018).	75
Figure 3.1. Structure of curcumin (a) and quercetin (b) molecules.	93
Figure 3.2. Particle size distribution of curcumin (black solid line, 0.14 wt%) and quercetin (red dashed line, 0.14 wt%) particles dispersed in soybean oil, respectively.	100
Figure 3.3. Microstructure of curcumin dispersion (0.14 wt%) in soybean oil at various length scales: (a) optical microscopy, (b) CLSM at 488 nm excitation, (c) SEM at lower magnification (250 \times) and (d) SEM at higher magnification (2,000 \times). Scale bar is 20 μm	101
Figure 3.4. Microstructure of quercetin dispersion (0.14 wt%) in soybean oil at various length scales: (a) optical microscopy, (b) CLSM at 405 nm excitation, (c) SEM at lower magnification (250 \times) and (d) SEM at higher magnification (2,000 \times). Scale bar is 20 μm	102

Figure 3.5. Mean water droplet size distributions and corresponding visual images of W/O Pickering emulsions (5:95 wt% w:o ratio) stabilized by curcumin (a) and quercetin (b) crystals at different particle concentrations; 0.06 wt% [■] and [I], 0.14 wt% [●] and [II], 0.25 wt% [▲] and [III], 0.5 wt% [□] and [IV], 1.5 wt% [○] and [V] curcumin or quercetin particles at pH 3.0. Dashed line separates the unabsorbed particles remained into the continuous phase ($\leq 1 \mu\text{m}$) and water droplets.107

Figure 3.6. Mean droplet size of water droplets (d_{32}) stabilized by curcumin [■] or quercetin [●] particles at different concentrations; 0.06, 0.14, 0.25, 0.5 and 1.5 wt%. The pH of the aqueous phase was adjusted to pH 3.0. Error bars represent standard deviation of at least three independent experiments. Samples with * do not differ significantly ($p > 0.05$) according to Tukey's test.108

Figure 3.7. Mean water droplet size distributions and corresponding visual images of W/O Pickering emulsions (5:95 wt% w:o ratio) stabilized by curcumin (a) and quercetin (b) crystals at different particle concentrations; 0.14 wt% [●] and [I], 0.25 wt% [▲] and [II] and 0.5 wt% [□] and [III] curcumin or quercetin particles at pH 7.0. Dashed line separates the unabsorbed particles remained into the continuous phase ($\leq 1 \mu\text{m}$) and water droplets.109

Figure 3.8. Mean droplet size (d_{32}) of the W/O Pickering emulsions versus pH for curcumin (a) and quercetin (b) at different particle concentrations; 0.14 wt% [black], 0.25 wt% [gray] and 0.5 wt% [white]. Error bars represent standard deviation of at least three independent experiments. Bars with the same letter do not differ significantly ($p > 0.05$) according to Tukey's test for each polyphenol crystal at the two different pH values used.110

Figure 3.9. Confocal images of W/O Pickering emulsions (5:95 wt% w:o ratio) stabilized by curcumin (red) particles at different concentrations; 0.06 (a), 0.14 (b), 0.25 (c), 0.5 (d) and 1.5 wt% (e). The pH of the aqueous phase was adjusted to pH 3.0. The scale bar is equal with $20 \mu\text{m}$. The brightness in the images is caused by auto-fluorescence of curcumin particles (488 nm excitation).111

Figure 3.10. Confocal images of W/O Pickering emulsions (5:95 wt% w:o ratio) stabilized by quercetin (green) particles at different concentrations; 0.06 (a), 0.14 (b), 0.25 (c), 0.5 (d) and 1.5 wt% (e). The pH of the aqueous phase was adjusted to pH 3.0. The scale bar is equal with $20 \mu\text{m}$. The brightness in the images is caused by auto-fluorescence of quercetin particles (405 nm excitation).112

- Figure 3.11. Confocal images of W/O Pickering emulsions stabilized by 0.14 wt% curcumin particles. The arrows indicate the sequence of images collected at depths of focus in order to visualize the particles at the W-O interface. The brightness in the image is caused by auto-fluorescence of the curcumin particles (488 nm excitation). 113
- Figure 3.12. Confocal images of W/O Pickering emulsions stabilized by 0.14 wt% quercetin particles. The arrows indicate the sequence of images collected at depths of focus in order to visualize the particles at the W-O interface. The brightness in the image is caused by auto-fluorescence of the quercetin particles (405 nm excitation). 113
- Figure 3.13. Interfacial shear viscosity at interface of Milli-Q water with non-purified oil [■], non-purified oil with 0.14 wt% curcumin particles [●] and non-purified oil with 0.14 wt% quercetin particles [▲]. The pH of the aqueous phase was adjusted to pH 3.0. Error bars represent standard deviation of at least two independent experiments. 115
- Figure 4.1. PSD [(a) and (c)] and mean particle size (d_{32}) of water droplets over time with visual images [(b) and (d)] of 5 wt% W/O emulsions stabilized by 0.14 wt% curcumin [(a) and (b)] and quercetin [(c) and (d)] particles containing 0 wt% [■] [I], 0.05 wt% [●] [II], 0.5 wt% [▲] [III], 1 wt% [□] [IV], 2 wt% [○] [V] and 4 wt% [X] [VI] WPI in the aqueous phase at pH 3.0, respectively. For statistical analysis according to Tukey's test see Appendix B, Table B1 and Table B2 for curcumin and quercetin, respectively. 131
- Figure 4.2. Confocal images of 5 wt% W/O Pickering emulsions stabilized by 0.14 wt% curcumin (a) and quercetin (b) crystals with 0.5 wt% WPI in the aqueous phase, at pH 3.0. The green brightness in the images is caused by auto-fluorescence of curcumin (488 nm excitation) or quercetin (405 nm excitation) crystals. The red brightness is due to WPI stained by Rhodamine B (568 nm excitation). The scale bar represents 20 μm 132
- Figure 4.3. PSD [(a) and (c)] and mean particle (d_{32}) size of water droplets over time with visual images [(b) and (d)] of 5 wt% W/O emulsions stabilized by 0.14 wt% curcumin [(a) and (b)] and quercetin [(c) and (d)] particles containing 0 wt% [■] [I], 0.05 wt% [●] [II], 0.5 wt% [▲] [III], 1 wt% [□] [IV], 2 wt% [○] [V] and 4 wt% [X] [VI] WPI in the aqueous phase at pH 7.0, respectively. For statistical analysis according to Tukey's test see Appendix B, Table B3 and Table B4 for curcumin and quercetin, respectively. 135

Figure 4.4. Confocal images of 5 wt% W/O Pickering emulsions stabilized by 0.14 wt% curcumin (a) and quercetin (b) crystals with 0.5 wt% WPI in the aqueous phase at pH 7.0. The green brightness in the images is caused by auto-fluorescence of curcumin (488 nm excitation) or quercetin (405 nm excitation) crystals. The red brightness is due to WPI stained by Rhodamine B (568 nm excitation). The scale bar represents 20 μm136

Figure 4.5. Mean size of water droplets (d_{32}) over time of W/O emulsions containing 5 wt% (black), 10 wt% (grey) and 20 wt% (white) water stabilized by 0.14 wt% curcumin (a) and quercetin (b) particles at 0.5 wt% WPI in the aqueous phase at pH 3.0, respectively. Samples with the same letter do not differ significantly ($p > 0.05$) according to Tukey's test.....137

Figure 4.6. Interfacial shear viscosity at W-O interface of 0.14 wt% curcumin [■] and quercetin [●] particles dispersed in purified oil with different concentrations of WPI in the aqueous phase after 24 h of adsorption at pH 3.0 (a) and pH 7.0 (b), respectively. Samples with the same letter do not differ significantly ($p > 0.05$) according to Tukey's test for each polyphenol + WPI system at each pH value.....139

Figure 4.7. Interfacial shear viscosity at W-O interface of 0.14 wt% particles of curcumin [black] and quercetin [grey] dispersed in purified oil and 0.5 wt% WPI at different NaCl concentrations in aqueous phase at pH 3.0, after 24 h of adsorption. Samples with the same letter do not differ significantly ($p > 0.05$) according to Tukey's test.142

Figure 4.8. Interfacial shear viscosity at W-O interface against time of 0.14 wt% curcumin (a) and quercetin (b) particles with Milli-Q water [black], 0.5 wt% WPI in aqueous phase [red] at 25 °C [filled symbols] or 45 °C [open symbols] at pH 3.0 for the first 3 h of adsorption. The embedded graph shows the interfacial shear viscosity at 25 or 45°C, for curcumin (a) or quercetin (b) particles with Milli-Q water [black] and 0.5 wt% WPI [red] at pH 3.0, after 24 h of adsorption. Error bars represent standard deviation of at least two independent experiments. Samples with the same letter do not differ significantly ($p > 0.05$) according to Tukey's test.144

Figure 4.9. Optical microscope images of curcumin or quercetin dispersions (0.14 wt%) at 25 °C (a), during heating at 45 °C (b) and after cooling down to 25 °C (c). The scale bar represents 20 μm145

Figure 4.10. Schematic representation (not to scale) of curcumin or quercetin + WPI-stabilized W/O emulsions, illustrating the effects of pH and WPI concentration and the possible mechanisms of interaction between the proteins and polyphenols at the interface.....147

Figure 5.1. Droplet size distribution [(a) and (c)] and mean droplet size (d_{32}) of water droplets over time with visual images [(b) and (d)] of 10 wt% W/O emulsions stabilized by 0.14 wt% curcumin [(a) and (b)] and quercetin [(c) and (d)] crystals in the oil phase and 0.05 wt% [■] [I], 0.1 wt% [●] [II], 0.5 wt% [▲] [III], 1.0 wt% [□] [IV] and 2.0 wt% [○] [V] WPM particles in the aqueous phase at pH 3.0, respectively. For statistical analysis according to Tukey's test, see Appendix C, Table C1 and Table C2 for curcumin and quercetin, respectively..... 167

Figure 5.2. Confocal images of 10 wt% W/O Pickering emulsions stabilized by 0.14 wt% curcumin (a) and quercetin (b) crystals in the oil phase and different concentrations of WPM particles in the aqueous phase; 0.1 (i), 0.5 (ii), 1.0 (iii) and 2.0 wt% (iv) for freshly prepared samples. The green brightness in the images is caused by the auto-fluorescence of curcumin (488 nm excitation) or quercetin (405 nm excitation) crystals. The red brightness is due to the WPM particles stained by Rhodamine B (568 nm excitation). The scale bar represents 50 μm 169

Figure 5.3. Confocal images of 10 wt% W/O Pickering emulsions stabilized by 0.14 wt% curcumin (a) and quercetin (b) crystals in the oil phase and 2.0 wt% WPM particles in the aqueous phase (pH 3.0) for 21 days old samples. The green brightness in the images is caused by the auto-fluorescence of curcumin (488 nm excitation) or quercetin (405 nm excitation) crystals. The red brightness is due to WPM particles stained by Rhodamine B (568 nm excitation). The scale bar represents 50 μm 170

Figure 5.4. Mean size of water droplets (d_{32}) over time and confocal images (i-iii) of W/O emulsions stabilized by 0.14 wt% curcumin (a) and quercetin (b) crystals containing 15 wt% (■, i), 20 wt% (●, ii) and 30 wt% (▲, iii) water with 2.0 wt% WPM particles at pH 3.0. For statistical analysis according to Tukey's test, see Appendix C, Table C3 and Table C4 for curcumin and quercetin, respectively. The green brightness in the images is caused by the auto-fluorescence of curcumin (488 nm excitation) or quercetin (405 nm excitation) crystals. The red brightness is due to WPM particles stained by Rhodamine B (568 nm excitation). The scale bar represents 50 μm 172

Figure 5.5. Surface pressure (π) versus (A_p) isotherms at A-W interface (aqueous phase at pH 3.0) spread solution of 0.34 wt% WPM particles (a), 0.5 wt% curcumin (b) and 0.9 wt% quercetin (c) particles under different compression and expansion times; 1st compression-expansion (■), 2nd compression-expansion (●), 3rd compression-expansion (▲) and 4th compression-expansion (★)..... 176

- Figure 5.6. Surface pressure (π) versus mean area per particle (A_p) isotherms of mixtures of 0.34 wt% WPM particles plus 0.5 wt% curcumin (a), or 0.9 wt% quercetin (b) crystals. The symbols (●) are the experimentally measured points (average of 3 runs) whilst the dashed lines are the theoretical results based on ideal mixing (*i.e.*, no interactions) of WPM particles and curcumin or quercetin crystals.179
- Figure 5.7. Interfacial shear viscosity at W-O interface without polyphenol crystals (only WPM particles) [▲], with 0.14 wt% curcumin [■] and quercetin [●] crystals dispersed in purified oil with different concentrations of WPM particles in the aqueous phase after 24 h of adsorption at pH 3.0. For statistical analysis according to Tukey's test, see Appendix C, Table C5 for both curcumin and quercetin.181
- Figure 5.8. Schematic representation (not to scale) of curcumin or quercetin crystal + WPM particle-stabilized W/O emulsions, illustrating the effect of WPM particle concentration and the possible mechanism of water droplet stabilization.....183
- Figure 6.1. Viscosity (η) against shear rate ($\dot{\gamma}$) curves of soybean oil (control, ■), 0.14 wt% curcumin (●) and 0.14 wt% quercetin (▲) dispersions in soybean oil at different temperatures 25 (open symbols), 35 (closed symbols) and 50 °C (crossed symbols).197
- Figure 6.2. Viscosity (η) against shear rate ($\dot{\gamma}$) curves of 2.0 wt% WPI (a) and 2.0 wt% WPM particles (b) at different temperatures; 25 °C (■, □), 35 °C (●, ○) and 50 °C (▲, △). All the aqueous dispersions have been prepared at pH 3.0. Viscosity values are shown for ramping up (closed symbols) at shear rates from 0.1 - 100 s⁻¹ and ramping down (open symbols) at shear rates from 10² - 10⁻¹ s⁻¹.200
- Figure 6.3. Viscosity (η) against shear rate ($\dot{\gamma}$) curves of 10 wt% W/O emulsions stabilized by 0.14 wt% curcumin (a) or quercetin (b) crystals dispersed in oil + water (■, □) or 2.0 wt% WPI (●, ○) or 2.0 wt% WPM particles (▲, △) as an aqueous phase (pH 3.0) at different temperatures 25 (i), 35 (ii) and 50 (iii) °C. Viscosity values are shown for ramping up (closed symbols) at shear rates from 0.1 - 100 s⁻¹ and ramping down (open symbols) at shear rates from 10² - 10⁻¹ s⁻¹.203
- Figure 6.4. Confocal images of 10 wt% W/O Pickering emulsions stabilized by 0.14 wt% curcumin (a) and quercetin (b) crystals in the oil phase + water (i), 2.0 wt% WPI (ii) or 2.0 wt% WPM particles (iii) in the aqueous phase at pH 3.0 for fresh samples. The green brightness in the images is caused by the auto-fluorescence of curcumin (488 nm excitation) or quercetin (405 nm excitation) crystals. The red brightness is due to the WPM particles stained by Rhodamine B (568 nm excitation). The scale bar represents 20 μ m.205

- Figure 6.5. Viscosity (η) against WPM particle concentration at 0.1 s⁻¹ shear rate of 10 wt% W/O emulsions stabilized by 0.14 wt% curcumin (■) or quercetin (●) crystals dispersed in oil & WPM particles as an aqueous phase (pH 3.0) at different concentrations; 0.1, 0.5, 1.0 and 2.0 wt%. The temperature was kept constant at 25 °C.....209
- Figure 6.6. Viscosity (η) against shear rate ($\dot{\gamma}$) curves of 20 wt% W/O emulsions stabilized by curcumin (a) or quercetin (b) crystals dispersed in oil & 2.0 wt% WPM particles as an aqueous phase (pH 3.0) at different temperatures; 25 (■, □), 35 (●, ○) and 50 °C (▲, △). Viscosity values are shown for ramping up (closed symbols) at shear rates from 0.1 - 100 s⁻¹ and ramping down (open symbols) at shear rates from 10² - 10⁻¹ s⁻¹.....212
- Figure 7.1. Schematic framework of this thesis.221
- Figure 7.2. Particle size distribution plots for 0.14 wt% curcumin (a) and quercetin (b) crystals dispersed in oil under different treatments; ultra-Turrax only (9,400 rpm for 5 min) (■), ultra-Turrax (9,400 rpm for 5 min) followed by: ultrasound bath for 2 (●), 5 (▲) or 10 min (▼), heat (60 °C for 1h) (◆) or Jet homogenizer (twice at 300 bar) (▶).....226
- Figure 7.3. SEM images of 5 wt% W/O emulsions stabilized by (a) curcumin and (b) quercetin crystals at an aqueous phase of pH 3.0.227
- Figure A1. Particle size distribution of 0.14 wt% curcumin (black solid line) and 0.14 wt% quercetin (red dashed line) particles dispersed in soybean oil after passing through all stages of emulsification process (Ultra-Turrax at 9,400 rpm/ 5 min, 13,400 rpm/ 2 min and Jet homogenization for two passes, at 300 bar), respectively.....235
- Figure A2. SEM images of curcumin (a and b) and quercetin (c and d) dry powders at different magnifications: (a) and (c) at lower magnifications (250×) and (b) and (d) at higher magnification (2,000×). Scale bar is 20 μm.236
- Figure A3. Mean water droplet size distribution and corresponding visual images of W/O Pickering emulsions (10:90 wt% w:o ratio) stabilized by curcumin (a) and quercetin (b) crystals at different particle concentrations; 0.14 wt% [●] and [I] and 0.25 wt% [▲] and [II] at pH 3.0. Dashed line separates the unabsorbed particles remained into the continuous phase (≤ 1 μm) and water droplets. Samples with the same letter do not differ significantly (p > 0.05) according to Tukey's test.....238
- Figure A4. Interfacial shear viscosity at interface of Milli-Q water with purified oil [■], purified oil with 0.14 wt% curcumin particles [●] and purified oil with 0.14 wt% quercetin particles [▲]. The pH of the aqueous phase was adjusted to pH 3.0. Error bars represent standard deviation of at least two independent experiments.....238

Figure B1. Particle size distribution of 0.14 wt% curcumin in soybean oil before heating (black solid line) and after heating at 45 °C (red dashed line) particles dispersed in soybean oil, respectively. Samples with the same letter differ significantly ($p < 0.05$) according to Tukey's test.....243

Figure B2. Particle size distribution of 0.14 wt% quercetin in soybean oil before heating (black solid line) and after heating at 45 °C (red dashed line) particles dispersed in soybean oil, respectively. Samples with the same letter differ significantly ($p < 0.05$) according to Tukey's test.....243

Figure C1. Intensity distribution of 0.5 wt% WPM particles at pH 3.0 (■) and pH 7.0 (●).244

Figure C2. Droplet size distribution [(a) and (c)] and mean droplet size (d_{32}) of water droplets over time with visual images [(b) and (d)] of 10 wt% W/O emulsions stabilized by 0.14 wt% curcumin [(a) and (b)] and quercetin [(c) and (d)] crystals in the oil phase and 0.5 wt% [▲] [I], 1 wt% [□] [II] and 2 wt% [○] [III] WPM particles in the aqueous phase at pH 7.0, respectively.....247

List of Abbreviations

A-O	Air-oil interface
A-W	Air-water interface
BMI	Body mass index
CLSM	Confocal laser scanning microscopy
CNCs	Cellulose nanocrystals
CR-310	Ricinoleic acid ester
d_{32}	Sauter mean
d_{43}	De Broukere mean
DC 8500	Modified cellulose
DLS	Dynamic light scattering
DSS	Degree of surface substitution
EFSA	European Food Safety Authority
GDL	Glucono-d-lactone
HMP	High methoxyl pectin
HPC	Hydroxyl propyl cellulose
LMP	Low methoxyl pectin
MCC	Microcrystalline cellulose
MCTs	Medium chain triacylglycerols
MFC	Microfibrillated cellulose
O/W	Oil-in-water emulsion
O/W/O	Oil-in-water-in-oil emulsion
O-W	Oil-water interface
PA	Palmitoyl chloride
PGPR	Polyglycerol polyricinoleate
pI	Isoelectric point
PMT	Photomultiplier detector
PSD	Particle size distribution
PTFE	Polytetrafluoroethylene
SC	Sodium caseinate
SEM	Scanning electron microscopy
SLS	Static light scattering
SMO	Sorbitan monooleate

SO	Silicones
TS	p-toluenesulfonyl chloride
W/O	Water-in-oil emulsion
W/O/W	Water-in-oil-in-water emulsion
w:o ratio	Water to oil ratio
W-O	Water-oil interface
WPI	Whey protein isolate
WPM	Whey protein microgel
α -la	α -lactalbumin
β -lg	β -lactoglobulin

Nomenclature

A	Area
d	Diameter
D	Diffusion coefficient
d_H	Hydrodynamic diameter
D_m	Displacement
E_f	Electric field
F	Force
$f(k\alpha)$	Henry's function
g	Acceleration due to gravity
G'	Elastic (or storage) modulus
G''	Viscous (or loss) modulus
h	Height
k_b	Boltzmann constant
L	Length
L:D	Length to diameter
n_p	Number of particles
P	Partition coefficient
r	Particle radius
Re	Reynolds number
T	Temperature
t	Time
U_E	Electrophoretic mobility
v	Velocity
V	Volume
V_{Stokes}	Velocity of the droplet
$\dot{\gamma}$	Shear rate
γ	Shear strain
γ_{LV}	Liquid/vapour interfacial free energy
γ_{ow}	Oil-water free energy
γ_{po}	Particle-oil free energy
γ_{pw}	Particle-water free energy
γ_{SL}	Solid/liquid interfacial free energy

γ_{sv}	Solid/vapour interfacial free energy
γ_T	Interfacial tension
ΔA	Contact area
ΔG_d	Desorption energy
$\Delta G_{\text{formation}}$	Gibbs free energy
ΔP	Laplace pressure
ΔS_{config}	Configurational entropy
$\Delta \rho$	Density difference
ϵ_r	Dielectric constant
ζ	Zeta-potential
η	Viscosity
θ	Contact angle
λ	Wavelength
π	Surface pressure
ρ	Density
σ	Shear stress

Chapter 1

General Introduction

1.1. Research motivation

Obesity is the medical condition where a person's body fat accumulates to the extent that it could have a negative impact on their health. Obesity is usually defined as having a body mass index (BMI) of 30 or above whilst BMI between 25 and 30 is classified as 'overweight' (NHS, 2017). It is a global grand challenge that is reaching epidemic proportions worldwide, and is associated with an increased risk of cardiovascular diseases, stroke, diabetes, cancer and mortality (Adams *et al.*, 2006; Polikandrioti *et al.*, 2009). For instance, obesity levels in the UK have increased from 15% to 29% since 1993, and recent reports from NHS suggest that half of the UK's population will be considered obese by 2030 as this problem becomes more widespread (Butland *et al.*, 2007). The phenomenon of obesity has drawn the attention of the scientific communities, organizations and governments worldwide because it affects people's lives in a negative way and imposes excessive financial implications in every health system (Polikandrioti *et al.*, 2009).

Obesity has been associated with excessive consumption of calorie-dense fats present in food, and especially in margarines, butters and confectionery products. Therefore, there has been considerable emphasis on the development of such food products with reduced levels of saturated, trans-fats and total fat (Nehir El *et al.*, 2012; Wassell *et al.*, 2010). However, one of the major challenges in developing these low or no-fat products is that fats play an important role in determining the desirable textural and sensory properties of many food products (Bayarri *et al.*, 2006; Wassell *et al.*, 2010).

Fat is generally present in food products in the form of droplets dispersed in a composite food matrix. One of the most promising approach in literature has been to replace those fat droplets with non-calorific water in the form of

water-in-oil (W/O) emulsion droplets. This method enables total fat content reduction, and also allows using the aqueous phase to deliver water soluble nutrients, such as vitamins. However, the lack of stability of such W/O emulsion systems presents one of the key challenges as they are thermodynamically unstable and prone to phase separation over a short period of time. Nowadays, only chemically-synthesized emulsifiers are used to kinetically stabilize such W/O emulsion droplets, making them less appealing to consumers. This PhD work addresses this technical challenge of providing longer term stability of water droplets in an oil continuous matrix using biocompatible materials by designing novel interfaces using a combination of nature-derived polyphenol crystals (present in the oil phase) and protein or protein-based particles (present in the aqueous phase) and deciphering the stabilization mechanisms.

1.2. General insight about emulsions

Emulsions are a mixture of two or more immiscible liquids, where oil-in-water (O/W) or water-in-oil (W/O) emulsions can be formed such that one liquid is dispersed as small droplets (*i.e.*, dispersed phase) into a second liquid (*i.e.*, continuous phase). The size of the droplets can vary between 0.1 to 100 μm (Dickinson, 1992; McClements, 2015).

Mixing pure oil and water results in the formation of opaque emulsion. Over time, the formed emulsion will gradually separate into two phases through various destabilization mechanisms, such as flocculation, creaming, sedimentation, coalescence and Oswald ripening. Emulsions can be considered as thermodynamically unstable (*i.e.*, the free energy of the emulsion is greater than if the two immiscible liquids remained as separate phases) but kinetically stable (*i.e.*, the rate at which the properties of an emulsion change with time due to inter-molecular and/or inter-particle forces) systems. Emulsifiers (*i.e.*, low molecular weight surface-active agents (known as surfactants), biopolymers and/or solid particles (known as Pickering stabilizers)) are added to form a protective membrane (interfacial layer) around the surface of droplets and prevents the droplets from merging.

Emulsification occurs under mechanical agitation via mixing or homogenization.

Recently, the use of Pickering particles as stabilizers for emulsions has gained significant attention owing to their ability to adsorb irreversibly at the liquid/ liquid interface (Lam *et al.*, 2014; Xiao *et al.*, 2016). Pickering stabilization arises when particles accumulate at the water-oil (W-O) interface forming a mechanical barrier that protects the emulsion droplets against coalescence (Pickering, 1907).

1.3. Research aim

The overarching aim of this PhD project is to reduce the fat and thus, the calorific content of fat-based products by incorporating water droplets inside an oil-continuous phase, in the form of W/O emulsions, where the longer term stability will be improved due to the use of biocompatible materials as stabilizers. Extensive literature is available on stabilizing these systems with chemically-synthesized emulsifiers (*e.g.*, polyglycerol polyricinoleate (PGPR)). However, owing to the growing interests for '*clean label*' products by consumers and concerns about the presence of *E-numbers* in foods even if these *E-numbers* have approved by European Food Safety Authority (EFSA) (van Gunst *et al.*, 2019), such products tend to be less appealing. Numerous studies have reported that consumers have a negative perception of *E-numbers* because they associate them with 'chemicals in food products with a negative health effect' (Bearth *et al.*, 2014; Haen, 2014; Paans, 2013; van Gunst *et al.*, 2019). Therefore, food additives are considered as unnatural, artificial and unhealthy, resulting in more consumers rejecting foods with *E-numbers* (van Gunst *et al.*, 2019). Consequently, there is a huge driving force from food industries to replace the chemically-synthesized surfactants with some natural and biodegradable ingredients that will give a '*clean label*' on the final product. '*Clean label*' is described as "being produced free of 'chemical' additives, having easy-to-understand ingredients lists and being produced by use of traditional techniques with limited processing" (van Gunst *et al.*, 2019).

Biocompatible materials such as polyphenol crystals (e.g., curcumin, quercetin etc.) that are occurring naturally in fruits and vegetables can be good candidates for stabilizing W/O emulsions, even though, they have attracted limited research attention. A lot of work has been done on the stabilization of O/W emulsions using polyphenols/flavonoids with a successful stabilization of oil droplets due to the adsorption of polyphenols at the O-W interface (Aditya *et al.*, 2017; Duffus *et al.*, 2016; Luo *et al.*, 2012; Luo *et al.*, 2011; Marto *et al.*, 2016). However, the stabilization of W/O emulsions using these particles has not been examined yet. Polyphenols have the ability to interact with food proteins (when both are present in the aqueous phase) through hydrogen bonding, hydrophobic and ionic interactions (Andersen *et al.*, 2005; Bordenave *et al.*, 2014). However, a research question remains on how protein and polyphenol crystals would interact at the interface when polyphenol crystals are dispersed in the oil phase and protein in the aqueous phase.

Therefore, the specific objective of this PhD was to use polyphenol crystals to stabilize W/O emulsions and to identify if complexes can be formed, between proteins and polyphenol crystals at the interface when both are present in different phases, to improve the stability of the water droplets.

1.3.1. Research hypothesis & proposed stabilization mechanism

We hypothesized that polyphenol crystals act as Pickering stabilizers for W/O emulsions. Quercetin and curcumin crystals have been chosen as Pickering stabilizers because they are relatively insoluble in water. In this work, a novel way to stabilize water droplets inside an oil phase was proposed via complex formation at the interface between polyphenol crystals, dispersed in the oil phase, and whey protein isolate (WPI) or whey protein microgel (WPM) particles, dispersed in the aqueous phase, as schematically shown in Figure 1.1. We hypothesized that at an acidic aqueous phase (pH 3.0) the emulsions will be more stable. At this pH, WPI or WPM particles possess a positive charge whilst the polyphenol crystals acquire a weak negative charge as the soybean oil, where the polyphenols are dispersed, is slightly polar oil, thus the hydroxyl groups on flavonoid backbone might be ionized.

Consequently, we suggest that the complex is formed due to some electrostatic interactions and hydrogen bonding.

This mechanism is ideal to deliver both water insoluble polyphenol crystals (present in the oil phase) as well as water-soluble compounds (present in the aqueous phase) and therefore can be considered as a “dual” delivery system, as shown in Figure 1.1. This can be used in food products and especially in margarines and confectionery, to reduce the fat and the calorific content. It is also applicable to other soft matter applications such as pharmaceuticals, agricultural and personal care formulations to deliver water-soluble active ingredients.

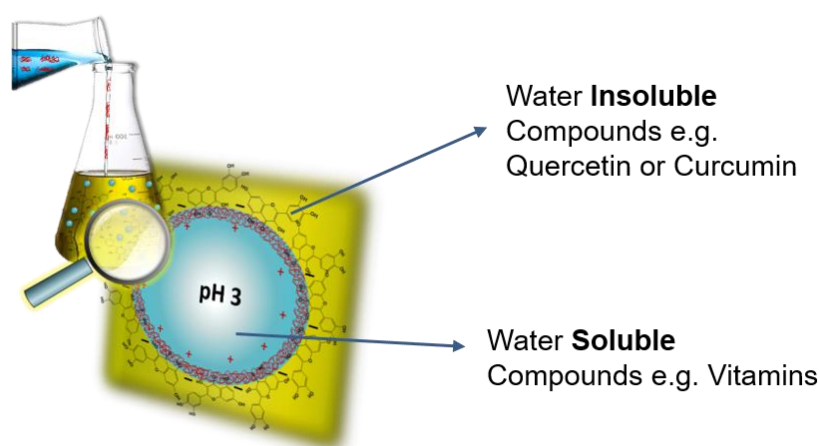


Figure 1.1. “Dual” delivery system for delivering both water insoluble polyphenol crystals, present in the oil phase, and water-soluble compounds, present in the aqueous phase, through W/O Pickering emulsions.

1.4. Rationale behind the selection of polyphenol crystals

In order to understand the structural differences between the different types of polyphenols used for stabilization of W/O droplets (curcumin and quercetin, used in this thesis), the following section includes details about the classification of polyphenols based on their structure, hydrophobicity, as well as possible interactions of polyphenols with food proteins.

1.4.1. Classification of polyphenols

Polyphenols are often characteristic of plant species or even of a particular organ or tissue of that plant and have received significant attention in recent years due to their reported biological activities and general abundance in the diet (Bordenave *et al.*, 2014). More than 8,000 phenolic structures are currently known, of which 4,000 are flavonoids (Tsao, 2010). Fruits, vegetables, leaves, seeds and other types of foods and beverages such as teas, chocolates and wines are rich sources of polyphenols (Tsao, 2010). The content of polyphenols in plant and food items depends on many environmental factors, including sun exposure, rainfall, different types of culture, fruit yield of the plant, the degree of ripeness, storage, as well as methods of culinary preparation (Marquardt *et al.*, 2014).

These compounds are classified into different groups depending on the number of phenol rings that they contain and the structural elements involved for the binding of phenol rings to one another. Thus, distinctions have been made between phenolic acids, flavonoids and the less common stilbenes and lignans, as shown in Figure 1.2. In this thesis, curcumin and quercetin were used which are classified in different groups (phenolic acids and flavonoids, respectively) due to their different structures.

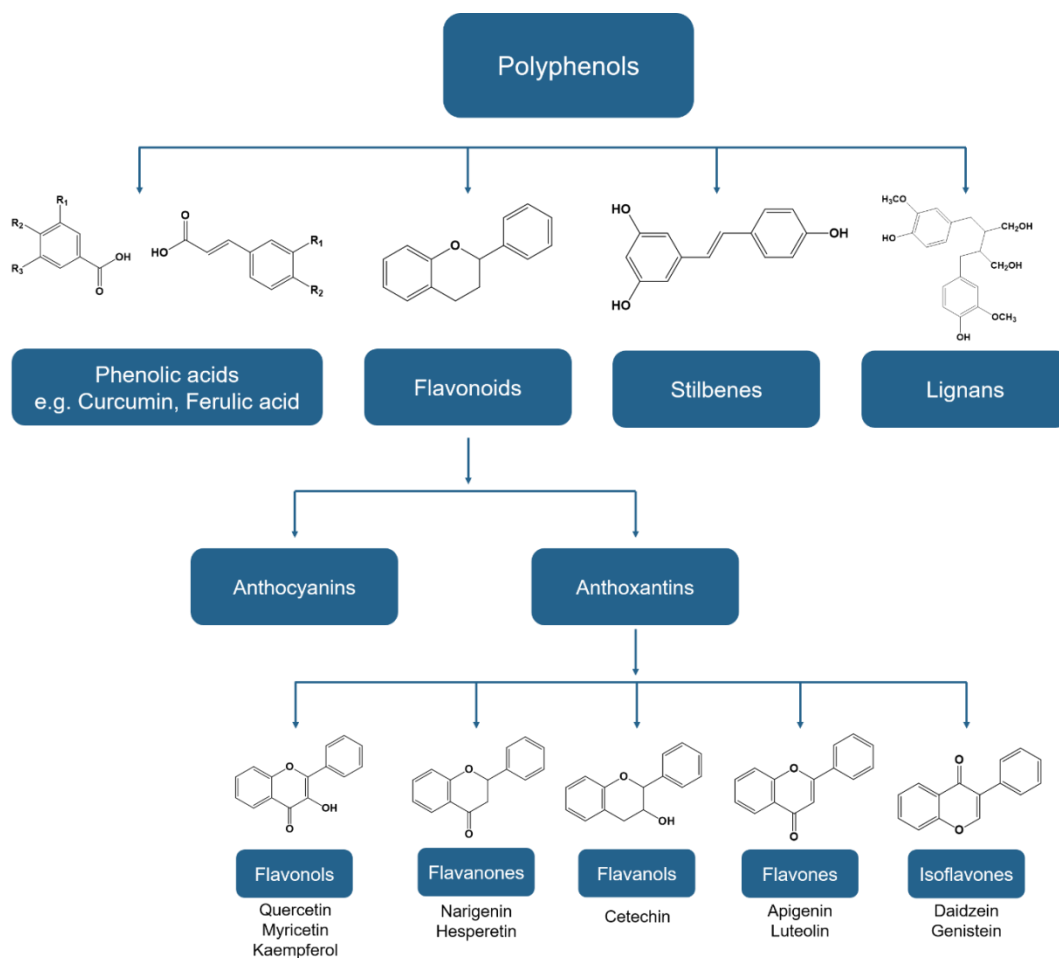


Figure 1.2. Classification of polyphenols.

Quercetin is a flavonoid characterized by its C6-C3-C6 basic backbone and is found in onions, kale, French beans, broccoli, and so forth (Formica *et al.*, 1995). Quercetin (Figure 1.3 (a)) has hydroxyl groups that impart hydrophilic characteristics, whereas the ring structures impact the hydrophobicity; thus, it can be described as an amphiphilic molecule (Luo *et al.*, 2011). The quercetin crystal structure can be described as layers of hydrogen bonded dimers. These dimers form a two-dimensional net held together via a network of hydrogen bonds with water molecules also present (Klitou *et al.*, 2019; Rossl *et al.*, 1986). Quercetin molecules adopt a more planar conformation, which allows them to pack more closely by strong π - π stacking interactions, thus resulting in a higher relative stability (Klitou *et al.*, 2019). Thus, quercetin molecules can pack in a way that some of the -OH groups are not exposed to the continuous phase, potentially explaining the

apparent hydrophobic character of the crystal particle surface (Rossl *et al.*, 1986).

Curcumin, also called diferuloylmethane, is a natural low-molecular-weight polyphenolic compound found in the rhizomes of the perennial herb turmeric (*Curcuma longa*) and is classified as a phenolic acid based on its chemical structure (Sharma *et al.*, 2005). Turmeric is an ancient spice and a traditional remedy that has been used as a medicine, condiment and flavouring in records dating back to 600 BC (Pari *et al.*, 2008). Curcumin is a crystalline compound with a bright orange-yellow colour so it is used as food colorant. From a structural viewpoint, curcumin (Figure 1.3 (b)) comprises two aromatic rings with methoxyl and hydroxyl groups in the ortho- position with respect to each other. The aromatic rings are connected through seven carbons that contain two α,β -unsaturated carbonyl groups (Araiza-Calahorra *et al.*, 2018). As a result, curcumin exists in three possible forms, the α,β -unsaturated- β -diketonic tautomeric form (Figure 1.3 (bi)) and the two isomers in an equilibrating keto-enol tautomeric form (Figure 1.3 (bii)) (Payton *et al.*, 2007). The polar hydroxyl/ketone groups are expected to impact hydrophilicity, whereas the aromatic/ aliphatic parts would be expected to make the molecule more hydrophobic. In relation to the solubility properties, curcumin is soluble in alkali or in extremely acidic solvents (Rao *et al.*, 2011). It is a keto-enol tautomeric compound with a predominant keto-form in acid or neutral solutions and the enol-form is predominant in alkalis solutions with good properties as chelator of metal ions (Anand *et al.*, 2007).

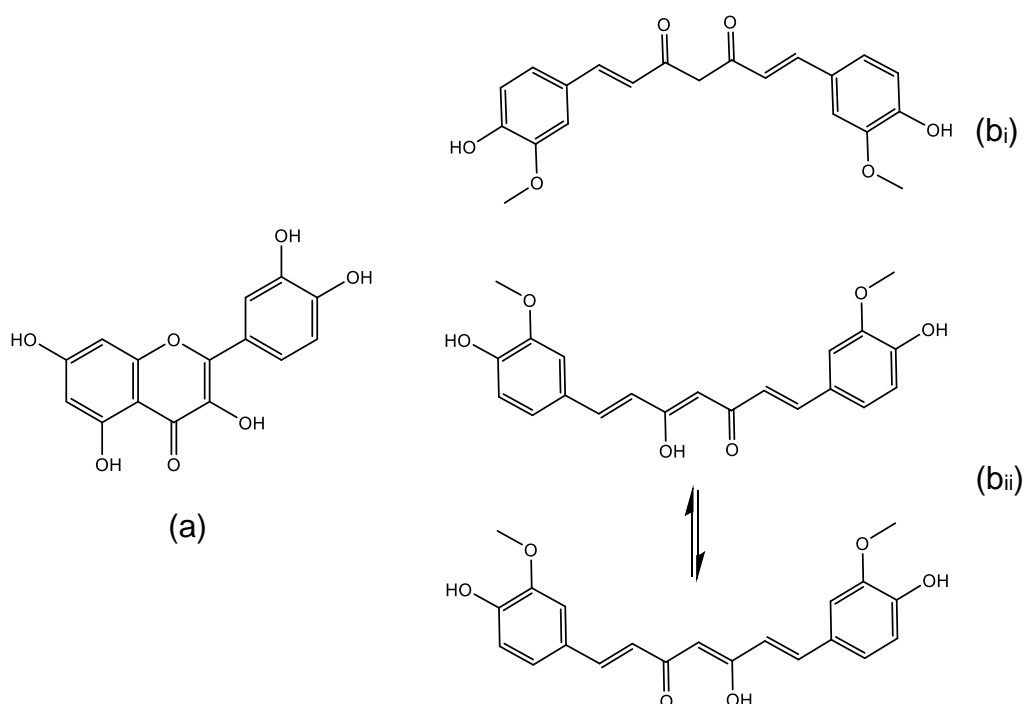


Figure 1.3. Structure of (a) quercetin molecule, (b_i) curcumin molecule in α,β -unsaturated- β -diketonic tautomeric form and (b_{ii}) two isomers of curcumin molecule in an equilibrating keto-enol tautomeric form.

Quercetin and curcumin crystals have chosen to be used in this thesis as Pickering stabilizers because they are relatively insoluble in water and have high $\log P$ values (3.29 and 2.16 for curcumin and quercetin, respectively). It was demonstrated that polyphenols with different $\log P$ values, where P is the partition coefficient between *n*-octanol and water, can act as Pickering stabilizers at the O-W interface, stabilizing O/W emulsions for several weeks without any obvious visual changes (Luo *et al.*, 2011). The $\log P$ value can be used to identify the hydrophilicity of a polyphenol molecule. However, Pickering stabilization depends on the hydrophilic/hydrophobic balance of the polyphenol crystals, not their molecules, and no simple relationship exists between $\log P$ and the ability to stabilize O/W emulsions. In addition, the maximum solubility of curcumin and quercetin in vegetable oils has been reported to be 0.02 and \sim 0.017 wt %, respectively, which suggests that these materials would be predominantly remaining as insoluble particle (crystal) form in the soybean oil (Cretu *et al.*, 2011; Roedig-Penman *et al.*, 1998).

1.4.2. Interactions of polyphenols with proteins

The phenolic nucleus of polyphenol molecules is the most favourable part for molecular (non-covalent) interactions with proteins with a defined globular tertiary structure, when both are present in the aqueous phase (Andersen *et al.*, 2005). The interactions are affected by the relative concentration of polyphenol and protein, solvent composition, temperature, ionic strength and pH (Le Bourvellec *et al.*, 2012). Many authors have suggested that polyphenol/protein interactions cause a complex formation resulting mainly from hydrophobic interactions and hydrogen bonding (Andersen *et al.*, 2005; Bordenave *et al.*, 2014; Le Bourvellec *et al.*, 2012). Hydrophobic interactions arise from the association of aromatic rings of polyphenols and hydrophobic sites of proteins, such as pyrrolidine rings of prolyl residues while hydrogen bonding occurs between the many H-acceptor sites of proteins and hydroxyl groups of the polyphenols, as shown in Figure 1.4 (Asano *et al.*, 1982; Le Bourvellec *et al.*, 2012). Ionic interactions between positively charged groups on the proteins, such as the amino acid side of lysine and arginine and negatively charged hydroxyl groups of polyphenols probably take place as well, although this has shown to have a minor distribution on the complex formation in the bulk (Figure 1.4) (Le Bourvellec *et al.*, 2012).

Polyphenol/protein interactions are dependent upon the nature of the polyphenol and protein structure. Polyphenol reactivity is influenced by the size, the conformational mobility/flexibility and the solubility of polyphenols in water (Richard *et al.*, 2006). High- molecular weight polyphenols have the ability to precipitate or interact with proteins more effectively due to the presence of more functional groups on polyphenols able to bind and form complex with the proteins (Le Bourvellec *et al.*, 2012). In addition, a greater conformational flexibility increases the capacity of interactions, whereas higher solubility of molecules in water (lower $\log P$) reduces the affinity with proteins (Le Bourvellec *et al.*, 2012). Baxter *et al.* (1997) indicated that the more hydrophobic the polyphenol is, the stronger it binds with protein.

Proteins can bind to polyphenols depending on their size, conformation, secondary/tertiary structure and amino acid composition (Le

Bourvellec *et al.*, 2012). It was demonstrated that proteins with high basic residues content (high in proline residue) are relatively large and hydrophobic with open and flexible structure which can more easily associated with polyphenols. This open and flexible conformation of proteins allows the formation of hydrophobic interactions and hydrogen bonds with polyphenols (Hagerman *et al.*, 1981). Proline residues maintain the peptide in an open extended or random coil form preventing the formation of hydrogen-bonded structures, such as α -helix (Baxter *et al.*, 1997; Murray *et al.*, 1994). Therefore, the available binding sites are maximized and the carbonyl oxygens of the peptide bonds are more exposed and available for hydrogen bonding than those of a compactly folded protein (Murray *et al.*, 1994; Williamson, 1994). In addition, the type of protein (especially milk proteins such as casein or whey) play an important role in the complex formation due to the presence of different amino acid groups in their structure that are able to bind to different polyphenols. It was noticed that the interactions between low molecular weight phenolic compounds (quercetin, vanillin, gallic acid, caffeic acid etc.) and whey protein were more prominent than with casein protein. This may be due to the presence of more sulphur amino acid groups (cysteine) in whey protein rather than casein, leading to the formation of stronger complexes via a quinone mediated mechanism including thiol groups (Hassan *et al.*, 2013). Therefore, whey proteins are more likely to bind with low molecular weight phenolic compounds whilst casein proteins prefer to bind with highly polymerized polyphenols (Ye *et al.*, 2013). Riihimaki *et al.* (2008) investigated the binding effect of different phenolic compounds, such as flavonols and isoflavonols to β -lactoglobulin (β -lg), when they are present in the aqueous phase. They showed that polyphenols formed complexes with β -lg that were stable under acidic conditions, indicating that phenolic compounds probably bind to the exterior of β -lg instead of the calyx. Moreover, it was identified that phenolic compounds withstand in solution with β -lg under basic conditions showing that β -lg might protect the phenolic compounds when exposed to high pH values (Riihimaki *et al.*, 2008). Hence, interfacial complex formation between polyphenols and whey proteins or whey protein microgel particles has been investigated in this thesis as a new strategy for stabilization of W/O emulsion droplets.

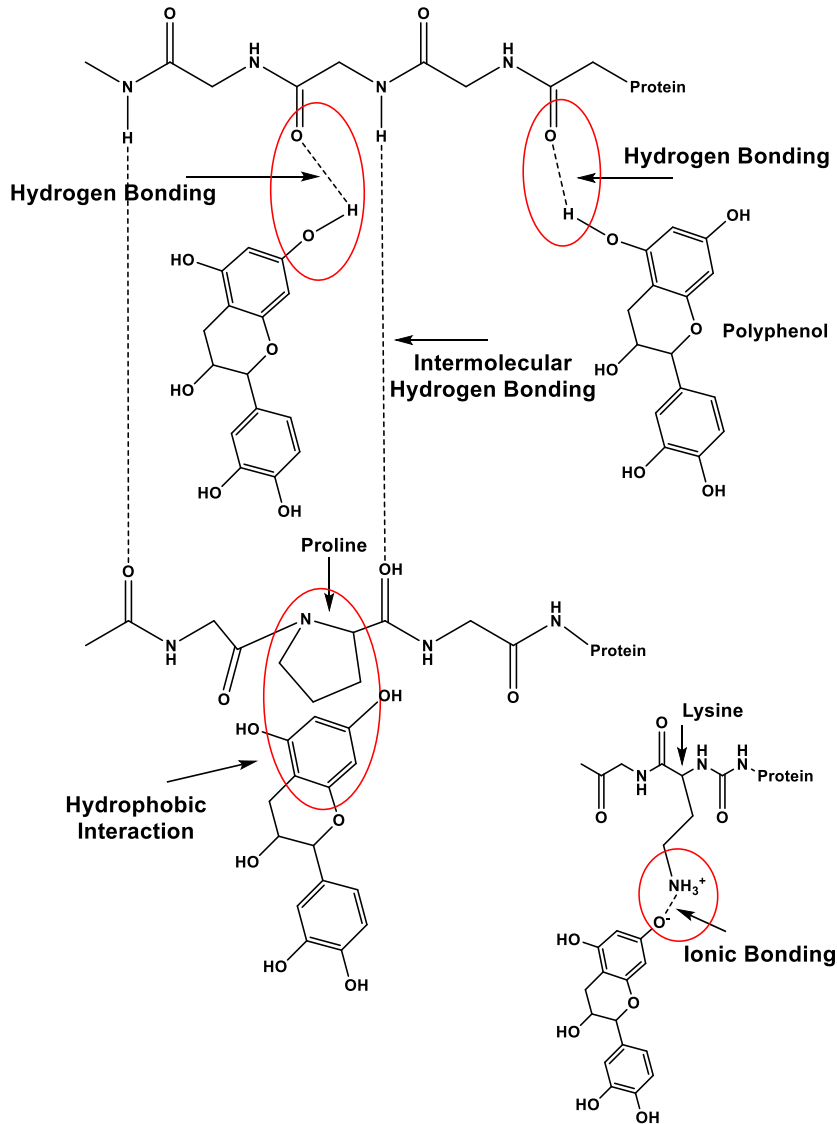


Figure 1.4. Mechanism of interactions between proteins and polyphenols.

1.5. Rationale behind the selection of biopolymers and their derivatives

Biopolymers (proteins and polysaccharides) play a key role in controlling the stability and rheology of food colloids and thus the shelf-life of most food products. Proteins are polymers of amino acids, whereas, polysaccharides are polymers of monosaccharides. Proteins are considered as effective emulsifying agents because they are surface-active; and, due to the presence of different amino acids groups (that can be charged), they can impart excellent colloidal stability to emulsion droplets by a combination of electrostatic and steric mechanisms (Dickinson, 2008).

1.5.1. Whey protein isolate

Whey protein isolate (WPI) was the biopolymer chosen for this thesis because it has extensively studied and characterized and much is known about its physicochemical properties. In addition, it has shown that low molecular weight phenolic compounds predominantly bind with whey protein (when both are present in the aqueous phase) due to the interactions between the phenolic nucleus of the polyphenols and the sulphur amino acid groups (cysteine) present in the whey protein structure. Therefore, this biopolymer was used in this thesis to test if interactions are still formed between polyphenol crystals (curcumin and quercetin) and protein, when both polyphenol crystals and WPI are present at the interface from different phases.

In general WPI can be described as having a compact globular conformation, a fact which confers many unique functional properties. It is surface active and able to form strong viscoelastic adsorbed layers at the interface on its own, when adsorbed from an aqueous to a more hydrophobic phase. Once adsorbed at the interface, it unfolds and rearranges its secondary and tertiary structure to exposed hydrophobic residues to the hydrophobic phase (MacRitchie, 1978). The high concentration of protein at the interface leads to aggregation and formation of interactions (Wilde *et al.*, 2004). The mechanical properties of the adsorbed layer influence the stability of emulsions which depends on the structure of the adsorbed protein and the strength of the interactions between them (Wilde *et al.*, 2004).

WPI is a mixture of proteins with numerous functional properties and is of a considerable importance to the food industry. The main proteins it contains are α -lactalbumin (α -la) and β -lactoglobulin (β -lg), which represent ca. 70% of the total whey protein and are responsible for its main functional properties (Cayot *et al.*, 1997). β -Lactoglobulin is a globular protein with a polypeptide chain of 162 residues stabilized by two disulfide cross-links and also contains an internal free sulfhydryl group which is sensitive to interfacial denaturation and heat treatment (Cayot *et al.*, 1997; Rodríguez Patino *et al.*, 1999). The monomeric molecular mass is 18.3 kDa. At pH 5-8, β -lactoglobulin exists as a dimer but at pH 3-5 the dimers associate to form octomers (Cayot

et al., 1997). α -Lactalbumin is a smaller protein with 123 amino acid residues and four disulfide bridges and a molecular mass of 14.2 kDa. It has a relatively low content of organized secondary structure for a globular protein and therefore has great molecular flexibility (Cayot *et al.*, 1997). The conformation and physicochemical properties of both proteins naturally depends on the environmental conditions such as salt, pH and temperature treatments (Cayot *et al.*, 1997).

1.5.2. Whey protein microgel particles

Following the same principles for the selection of WPI as the main biopolymer, whey protein microgel (WPM) particles were prepared and used to investigate if the interactions between the two biocompatible particles (polyphenol particles and protein-based particles (WPM particles)) at the interface are still formed.

WPM particles have chosen for this study because they can be formed through a physical modification of the WPI. They acquire different physicochemical properties from WPI, especially when they adsorb at the interface. WPM particles generally fall in the 100 to 1000 nm diameter size range and they possess particle-like characteristics due to their porous internal structure, which is able to hold a considerable quantity of water. They are used as stabilizing agents due to their deformability, surface activity, reversible swelling behaviour and responsiveness to pH and temperature (Dickinson, 2015; Murray, 2019).

Protein microgels are soft colloidal particles that can be produced by using a top-down technique of forming a physically cross-linked heat-set hydrogel in the first stage. Then microgel particles are produced by breaking them down under high shear forces using a homogenizer (Araiza-Calahorra *et al.*, 2019). Whey protein microgel (WPM) particles result from controlled shearing of a heat-set gel formed via the disulfide bonding between β -lactoglobulin and α -lactalbumin molecules as well as between the same proteins (Nicolai *et al.*, 2011; Schmitt *et al.*, 2010). Upon heat denaturation at 90 °C, the unfolded whey proteins expose hydrophobic residues and thiol groups and start to aggregate. The initial quick formation of small primary

aggregates is followed by fractal aggregation, which leads to the formation of larger particles that are primarily held together by hydrophobic and hydrogen bonds (Nicolai *et al.*, 2011; Schmitt *et al.*, 2010). Subsequently, intra-particle disulfide bonds are formed, leading to covalent stabilization of the structure (Dickinson, 2017). A combination of steric and electrostatic repulsion confers good colloidal stability to these microgels in aqueous dispersions (Dickinson, 2017).

1.6. Rationale behind the selection of characterization techniques

To understand the microstructures and the physicochemical characteristics of the polyphenol crystal dispersions in oil, WPI and WPM particle dispersions in the aqueous phase and their corresponding emulsions, a comprehensive suite of bulk and interfacial techniques were employed as discussed in the next section.

1.6.1. Interfacial tension

Interfacial tension (γ_T) is a concept of fundamental importance in colloid science, describing phenomena such as the formation, shape and stability of liquid drops. Determination of the interfacial tension allows to draw indirect inferences regarding the chemical composition of fluid interfaces and the adsorption and desorption of surface active materials (Berry *et al.*, 2015). In this thesis, pendant drop method was used to measure any changes of the interfacial tension in the presence of WPI and/or polyphenol crystals in water and oil phases, respectively.

Drop shape techniques (pendant drop tensiometry) are widely used for interfacial tension measurements, where the measurement consists of a fluid droplet suspended from a needle. Generally, the shape of the pendant drop depends on the balance between the gravity and the surface tension. The surface tension tends to make the drop spherical, because this shape minimizes the contact area between the liquid and its surroundings, whereas gravity deforms it, *i.e.*, gravity tends to elongate the drop (Saad *et al.*, 2011). The equilibrium shape that is adopted by a droplet is determined by its volume,

density and interfacial tension (McClements, 2015). The interfacial forces acting between the two fluids are calculated using the Young-Laplace equation (1.1):

$$\Delta P = \gamma_T \left(\frac{1}{R_1} + \frac{1}{R_2} \right) \quad (1.1)$$

where, R_1 and R_2 are the principal radii of curvature; $\Delta P \equiv P_{in} - P_{out}$ is the Laplace pressure across the interface; and γ_T is the interfacial tension.

In this thesis, pendant drop method was used instead of Du Nouy ring method since it is a more accurate method where the interfacial tension is measured based on the shape of the drop using a specific software. On the other hand, Du Nouy ring method is based on pulling a ring, with a well defined geometry, of the surface of liquids and measuring the pull force. The main disadvantage of this method is that a correction factor is required in order to calculate the 'true' interfacial tension of the system. This is happening due to the fact that the ring pulls a meniscus above the surface of liquid during the measurement. The portion of the liquid pulled above the surface contribute force to the force sensor used to measure surface tension (Kruss GmbH, 2004). Therefore, the resultant surface tension needs to be corrected to compensate that extra force in order to measure the 'true' interfacial tension. The error in surface tension due to not making the proper correction for this effect may be as large as 7%, causing a further increase in the reported interfacial tension (Kruss GmbH, 2004).

1.6.2. Contact angle and wettability

In this thesis, contact angle measurements were used to measure the hydrophilic/hydrophobic character of the polyphenol particles, and identify their wettability (the tendency of one liquid to spread on a solid surface) in aqueous and oil phases. The most suitable method to measure the angle is the static sessile drop method where the angle formed between the solid/liquid interface and liquid/vapour interface is measured using a microscope optical system or, with high-resolution cameras and software to capture and analyse the contact angle (θ) using the Young's equation:

$$\gamma_{SV} = \gamma_{SL} + \gamma_{LV} \cos(\theta) \quad (1.2)$$

where γ_{SV} , γ_{SL} and γ_{LV} are the solid/vapour, solid/liquid and liquid/vapour interfacial free energy.

If θ of an aqueous drop on a solid substrate (made by compressed particles) is smaller than 90° , the particles are hydrophilic and stabilize an O/W emulsion (Figure 1.5 (a)). However, if θ is generally greater than 90° , the particles are hydrophobic and stabilize a W/O emulsion (Figure 1.5 (b)). Particles wetted equally by oil and water have contact angle of exactly 90° .

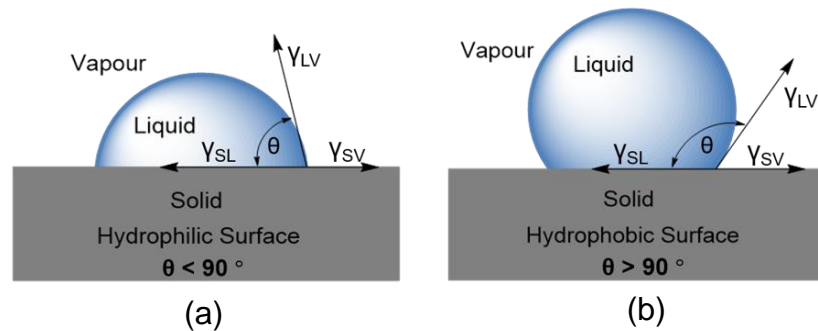


Figure 1.5. Contact angle (θ) of an aqueous drop on a solid (particle) substrate; (a) θ is smaller than 90° indicating hydrophilic particles and (b) θ is bigger than 90° indicating hydrophobic particles.

1.6.3. Static light scattering

The size of polyphenol crystals and emulsion droplets was measured via static light scattering (SLS). SLS is used to measure the size of particles or emulsion droplets in the range between 100 nm to 1 mm. The technique is based on the angular variation (θ) in the intensity of the scattered light as the laser beam passes through a dispersed sample. Large particles scatter light at small angle whereas, small particles scatter light at a larger angle as shown in Figure 1.6. The angular scattering intensity pattern is then converted into a particle size distribution using the 'Mie theory', assuming that the particles are homogeneous spheres and the refractive index of both the particles and dispersion medium are known.

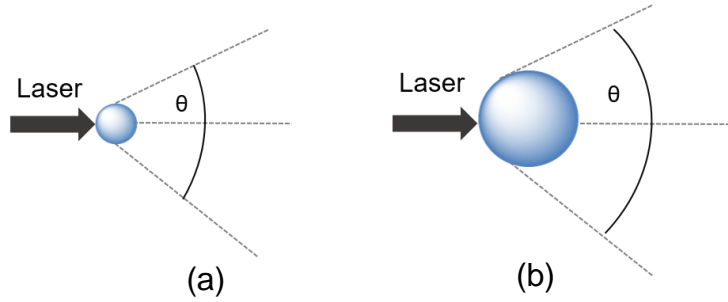


Figure 1.6. An illustration of different scattering patterns displayed a small (a) vs big (b) particle as illuminated by a laser beam.

The mean diameter of the measured particle size is usually expressed as d_{32} (also known as Sauter mean) and d_{43} (also called as the De Broukere mean) (Horiba scientific, 2012). The d_{32} refers to the surface area mean and is more sensitive to the presence of fine particles, whereas, the d_{43} refers to the volume of the particle and is more sensitive to large particles (Malvern Instruments Ltd, 2015; McClements, 2015). These two means can be calculated using the equations (1.3) and (1.4):

$$d_{32} = \frac{\sum n_i A_i d_i}{\sum n_i A_i} \quad (1.3)$$

$$d_{43} = \frac{\sum n_i V_i d_i}{\sum n_i V_i} \quad (1.4)$$

where n_i is the number of particles, A_i is the particle surface area, V_i is the particle volume, d_i is the diameter of the i^{th} particles.

In this thesis, a Hydro SM small-volume wet sample dispersion unit (Mastersizer, Malvern Instruments, UK) was utilized where soybean oil was used as the continuous phase. The size of the polyphenol crystals in oil and water droplets were measured.

1.6.4. Dynamic light scattering

The size of WPM particles at different pH values was measured using dynamic light scattering (DLS). DLS is a common method to measure the size of particles below the submicron region (*i.e.*, between 1 nm to 1 μm), illuminated via a laser beam. It primarily measures the Brownian motion of particles in solution that arises due to the successive collisions by the solvent molecules that surround them, and relates this motion to the size of particles

(Stetefeld *et al.*, 2016). Smaller particles will have a faster Brownian motion than larger ones which tend to sediment due to gravity (Jose *et al.*, 2019). Therefore, the motion of particles depends on their size, temperature, and solvent viscosity. The size of the particles affects the fluctuation rate of the scattered light intensity (Nobbmann *et al.*, 2007). For instance, a fast fluctuation rate is obtained from small particles that have rapid Brownian motion. The hydrodynamic diameter of the particle (d_H) is then calculated using the Stokes-Einstein equation (1.5), which defines the velocity of the Brownian motion as the translational diffusion coefficient (D):

$$d_H = \frac{k_b T}{3\pi\eta D} \quad (1.5)$$

where k_b is the Boltzmann constant, T is the temperature and η is the viscosity of the medium. The particle size distribution can be calculated by the autocorrelation function of the instrument's software and then fitted to obtain the average particle diameter, the z-average, defined as the intensity-weighted mean diameter (Malvern Instruments Ltd, 2004).

In this thesis, scattering information were detected using 173° detection optics, known as backscattering. Using this method, the incident beam does not have to travel through the entire sample meaning that multiple scattering, where light from one particle is itself scattered by other particles, is minimized. The effect of contaminants, such as dust particles within the dispersant, is also reduced by using backscatter detection since they mainly scatter light in the forward direction (Malvern Instruments Ltd, 2004).

1.6.5. Zeta-potential (ζ -potential)

A key characteristic of emulsions and particles is their surface charge, which allows to examine their electrostatic stability and response to changes with pH and ionic strength. In this thesis, the ζ -potential of the polyphenol particles, WPI and WPM particles was analysed at an aqueous phase of pH 3.0 and 7.0 to give indirect indication of their net surface charges. In addition, the mobility of the polyphenol crystals dispersed in the oil phase was measured using a special cell (dip cell (ZEN 1002), Zetasizer, Malvern, UK) in order to get an indication of their charge in the oil phase.

When a charged particle is dispersed into a solvent, an adsorbed double layer develops on its surface, as shown in Figure 1.7 which illustrates the double layer model on a negative charged particle. The inner layer consists of counter-ions (in this case positive ions) which are strongly attracted to the negatively charged particle, forming the “stern layer”. Beyond the “stern layer”, counter-ions are less strongly associated to the particle and form the “diffuse layer”. The “stern layer” and “diffuse layer” are usually known as “double layer”. The composition of this diffuse layer is dynamic and varies depending on a variety of factors, *e.g.*, pH, ionic strength, concentration etc. When an electric field is applied to such dispersion, the charged particles move towards the oppositely charged electrode (electrophoresis). Within this diffuse layer there is a hypothetical plane, which acts as the interface between the moving particles and the layer of dispersant around it while electrophoresis. This plane is the characteristic “slipping/shear plane” and ζ -potential is the potential at this particle-fluid interface, which indicates the potential stability of an emulsion (Bhattacharjee, 2016). For instance, emulsion droplets with a large positive or negative ζ -potential ($> +$ or $- 30$ mV) will repel each other via electrostatic repulsion, limiting flocculation and coalescence (Malvern Instruments Ltd, 2004). However, a change in pH or ionic strength will affect the ζ -potential and potentially destabilise the emulsion.

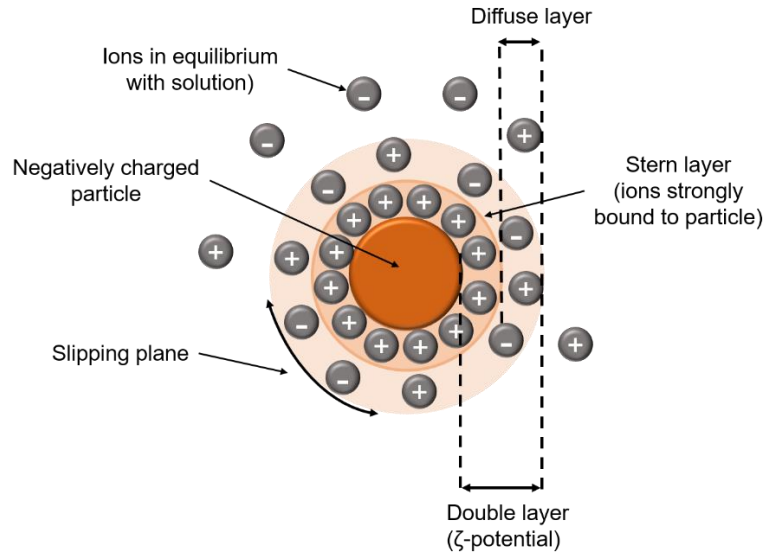


Figure 1.7. Schematic representation of a negatively charged particles and the presence of its ions at the "stern layer", "diffuse layer" and "slipping plane".

The ζ -potential of particles is measured via electrophoresis. The sample is injected into a capillary cell comprised of two oppositely charged electrodes, of distance 6 cm. Under an applied electric field ($50 < E_f < 150$ V), particles in equilibrium with the dispersion media move (at a constant velocity) towards the oppositely charge electrode. The velocity of the particles (v_p) is referred to their electrophoretic mobility (U_E) and is expressed by the following equation:

$$U_E = \frac{v_p}{E_f} \quad (1.6)$$

Therefore, the electrophoretic mobility is dependent on the strength of the electric field (E_f), the dielectric constant (ϵ_r), the viscosity (η) of the medium and the ζ -potential of the particles. The strength of an electric field can be calculated from equation 1.7:

$$E_f = \frac{\text{applied voltage}}{\text{distance between electrodes}} \quad (1.7)$$

Hence, at a voltage of 150 V the electric field is calculated to be around 25 V cm^{-1} .

The electrophoretic mobility is related to ζ -potential via Henry equation in which the ζ -potential is directly proportional to the electrophoretic mobility as shown in equation (1.8):

$$U_E = \frac{2\zeta\epsilon_r f(\kappa a)}{3\eta} \quad (1.8)$$

where ϵ_r is the dielectric constant, ζ is the ζ -potential, η is the viscosity of the dispersed media, and $f(k_a)$ is the Henry's function; $f(k_a) = 1.5$ for dispersion in polar media based on the Smoluchowski approximation. The Smoluchowski approximation is based on the assumption that the double layer thickness is smaller than the mean particle radius (*i.e.*, thin double layer). For particles in a non-polar media with a thick double layer, the Hückel approximation should be used instead, where $f(k_a) = 1$.

1.6.6. Microscopy across length scales

The morphology and surface of particles and emulsion droplets were studied using different types of microscopy (*i.e.*, optical, confocal and electron microscope) relying on different physical principles.

1.6.6.1. Light microscopy

Light microscopy is the most basic method to examine the surface of the particles and emulsions by reflected light. In this thesis, light microscopy was used to characterize the shape of the polyphenol crystals dispersed into the oil phase.

Optical microscope uses reflected light to image the surface of a sample. The wide-field illumination employed by the optical microscope leads to the uniform illumination of the focus plane but also of the plane above and below the focus plane. Therefore, only thin and relatively transparent samples can be imaged (Auty, 2013). The resolution of an optical microscope is governed by the wavelength of the light source (which can be as low as 200 nm) and the objective. However, due to the design and manufacturing of certain microscopes as well as the Brownian motion of small particles, objects smaller than 1 μm are hardly detectable. Another limitation of the optical

microscope is the limited contrast between different components in a sample due to their similar refractive indices (McClements, 2015).

1.6.6.2. Confocal laser scanning microscopy

Confocal laser scanning microscopy (CLSM) is used as a fluorescence microstructural technique that can help to generate two-dimensional images. In this thesis, CLSM was used to identify the shape and size of polyphenol crystals dispersed into the oil phase as well as to recognize the position of these polyphenol crystals at the W-O interface of the water droplets.

This microscope allows the illumination of the whole sample by scanning one or more focused laser beams where the emitted light in the sample is detected by a photomultiplier detector which transforms the light signal into live data images using a computer software (Auty, 2013). CLSM has a capability to generate two-dimensional images of structures without the need of complicated preparation method and able to distinguish between two or more components using fluorescent dyes (Auty, 2013). The incident light can be absorbed by fluorophores incorporated to the sample and emitted at different wavelengths. The dyes can be covalently or non-covalently bound to the sample. The maximum resolution obtained with CLSM is around 200 nm (Auty, 2013).

In this PhD, curcumin and quercetin crystals were used where both of them are auto-fluorescent meaning that their shape and position at the W-O interface were identified without the addition of an extra dye. Auto-fluorescence from the particles was excited using 488 and 405 nm wavelength lasers for curcumin and quercetin crystals, respectively. In addition, Rhodamine B was used to screen the WPI or WPM particles present in the aqueous phase and specify their location into the water droplets. The emission fluorescent light was detected at wavelengths of 525, 460 and 580 nm for curcumin, quercetin and Rhodamine B, respectively.

1.6.6.3. Scanning electron microscopy

Scanning electron microscopy (SEM) is one of the most common electron microscopy technique used to visualize features as small as 3–20

nm, where electron beams are used instead of optical beams (McClements, 2015). The electron beam is focused on the surface of a specimen, some energy is absorbed by the sample and generates secondary electrons, which upon leaving the sample are recorded by a detector and an image is produced using computer software. SEM provides topological surface information about the sample over a relatively large area. In conventional SEM, samples are placed in a vacuum, thus the aqueous phase needs to be removed by drying or evaporation. For non-conductive materials, samples need to be sputter coated with a conductive metal, such as platinum or gold, to enhance the intensity signal of the secondary electron generated by the bombardment of electron. The metal coating prevents some charge build-up which otherwise can cause thermal damage to the sample and image distortion. Additionally, the samples need to be placed under high vacuum to avoid obstruction and contamination by other particles, resulting in poor image quality. The main disadvantage of the high vacuum is the need to remove the aqueous phase to avoid any interference. Hence, extensive drying or evaporation of the sample is required which might disrupt its structure, shape and size causing artefacts (McClements, 2015). Cryo-SEM can overcome the need to extensively dry aqueous samples. Here, samples are cryogenically treated by rapidly freezing the sample with liquid nitrogen, to replace the water with amorphous ice crystals which can minimize the artefacts or loss of structure during the imaging process (Cosgrove, 2010). The sample is then sublimated and coated with a conductive metal to be imaged in a similar manner than with a conventional SEM (JEOL Ltd, 2011).

In this thesis, SEM was used to identify the shape and size of polyphenol crystals dispersed into the oil phase. Cryo-SEM was used to recognize the position of these polyphenol crystals at the W-O interface of the water droplets. During the cryo-SEM analysis, the sample was rapidly plunged into liquid ethane bath instead of liquid nitrogen to freeze the sample quicker and prevent the frozen water from forming cubic ice, which absorbs the electron beam, obscuring the sample. The reasons that liquid ethane is considered as a quicker method to freeze the sample instead of immersing it into the liquid nitrogen are (Russo *et al.*, 2016):

1. the melting point of liquid ethane (- 183 °C) is slightly above the boiling point of liquid nitrogen (- 196 °C) and
2. the liquid ethane has higher heat capacity (53 J K⁻¹ mol⁻¹) than liquid nitrogen (29 J K⁻¹ mol⁻¹).

1.6.7. Langmuir trough experiments

The response of the film of adsorbed materials to expansion and compression of the interface, using a Langmuir trough experiment, is a key factor determining the ease of formation and stability of a multitude of colloidal systems (Murray, 1997). In this thesis, monolayer (Langmuir trough) experiment was used to provide evidences of strengthening of the film due to the synergistic particle-particle complex formation at the interface between polyphenol crystals and WPM particles.

A Langmuir trough consists of a container that holds the liquid to be analysed, a moveable barrier that is capable of changing the area of the A-W interface, and a Wilhelmy plate, which is used to measure the surface tension at the A-W interface. The surface-active solute to be analysed is spread across the surface of the liquid. The interfacial area is then decreased in a controlled fashion using a motor to drive the moveable barrier, and the surface pressure (π) is measured as a function of interfacial area (A). The resulting π - A plot depends on the interfacial characteristics of the individual surface-active solute, as well as on the sign, magnitude, and range of solute–solute interactions at the interface.

Figure 1.8 shows a schematic of a π - A plot for a model surface-active solute. The π - A plot is divided into different regimes depending on the strength of the solute–solute interactions during compression. At high interfacial areas, the solute molecules are far apart and do not interact with each other, and therefore, the surface pressure is mainly determined by the interfacial characteristics of the individual molecules. This regime is usually called the “gas” phase (Figure 1.8 (a)), because each solute molecule acts independently of its neighbours (McClements, 2015). As the interfacial area is decreased, the interfacial concentration of the solute molecules increases, and solute–solute interactions begin to occur, which leads to an increase in

the surface pressure. The solute molecules are still far apart and are able to move freely and so this regime is referred to as the “liquid” phase (Figure 1.8 (b)). When the interfacial area is decreased further, the solute molecules become so closely packed together that there is a strong repulsive force between them, which leads to a steep increase in the surface pressure (McClements, 2015). This regime is usually referred to as the “solid” phase (Figure 1.8 (c)), because the solute molecules are densely packed and have low mobility. The interfacial area where the surface pressure increases dramatically can provide valuable information about the packing of the surface-active molecules within the interfacial layer at saturation, for example, the area per solute molecule (Lyklema, 2005; Murray, 1997; Xu *et al.*, 2007). However, any further compression cause aggregation of particles and collapse of the monolayer film (Figure 1.8 (d)).

The surface pressure is simply defined as a change of the surface tension between pure liquid (water)/vapour and the one with an adsorbed film as shown by the equation (1.9):

$$\pi = \gamma_{LV} - \gamma \quad (1.9)$$

where γ_{LV} and γ refer to the surface tension of liquid/vapour before compression and surface tension of an adsorbed film after compression, respectively.

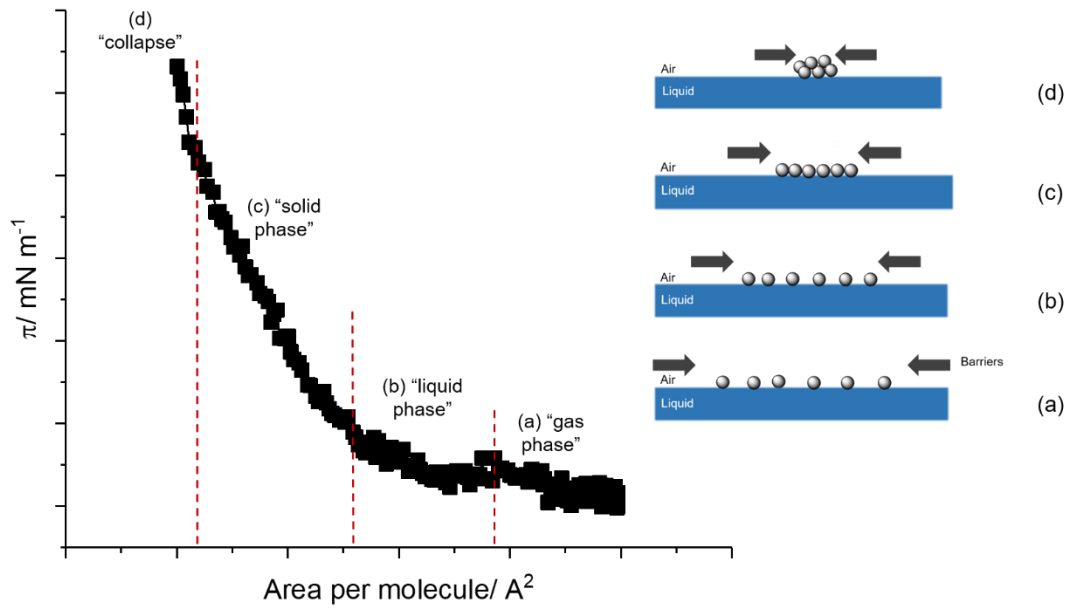


Figure 1.8. Schematic representation of surface pressure (π) versus area per molecule (A) plot of a surface-active molecule. The π - A plot is divided to different regimes (gas, liquid, solid and collapse) during compression, depending on the strength of the solute-solute interactions.

1.6.8. Rheology

Rheology is used to describe and assess the deformation and flow behaviour of materials. In this thesis, the viscosity of the polyphenol crystal dispersions, WPI and WPM particle solutions and W/O emulsions stabilized by polyphenol crystals with or without WPI or WPM particles in the aqueous phase were studied. These results will give information to understand how the particles or emulsions behave under different shear rates and temperatures.

Fluids flow at different speeds and solids can be deformed to a certain extent. A specific force is applied to a material and the resulting flow and/or deformation of the material is measured, as shown in Figure 1.9. The rheological properties of a material are then established by analysing the relationship between the applied force and the resultant flow or deformation. Shear stress (σ), shear strain (γ) and shear rate ($\dot{\gamma}$) were used to describe this deformation. Shear stress (equation (1.10)) is defined as the amount of force (F) per unit area (A), shear strain (equation (1.11)) is the displacement of the material due to stress, whilst shear rate (equation (1.12)) is the rate at which shear progresses (Mezger, 2014).

$$\text{Shear stress: } \sigma = \frac{F}{A} \quad (1.10)$$

$$\text{Shear strain: } \gamma = \frac{D_m}{h} \quad (1.11)$$

$$\text{Shear rate: } \dot{\gamma} = \frac{v}{h} \quad (1.12)$$

where D_m is the displacement, h is the height and v is the velocity obtained from: $v = \frac{D_m}{t}$ with t representing time.

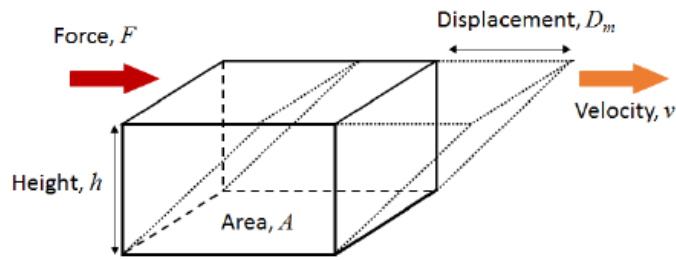


Figure 1.9. Relationship between the force and velocity of an applied stress on the displacement of a material (Mezger, 2014).

In this thesis, the rheological characterization was achieved by using a cone and plate geometry, where the cone has a slight angle ($\sim 4^\circ$), which resulted in a uniform shear stress across the sample (Gunasekaran *et al.*, 2002).

The flow behaviour of liquids, such as colloidal dispersions, is commonly characterized via viscosity measurements, where shearing induces the sample to flow due to the re-arrangement and deformation of the sample's structure. The viscosity is defined as the flow resistance given by a flowing sample. Depending on the flowing behaviour of samples, these can be classed as Newtonian or non-Newtonian fluids. For ideal Newtonian fluids, viscosity (η) is defined as the ratio between shear stress (σ) and shear rate ($\dot{\gamma}$) as shown in the equation (1.13).

$$\eta = \frac{\sigma}{\dot{\gamma}} \quad (1.13)$$

In Newtonian fluids, the viscosity of the sample is independent to the shear rate at a constant temperature (Figure 1.10). Typically, Newtonian fluids are composed of low molecular weight molecules, such as water, sugar

solutions (e.g., corn syrup) and milk. Samples with higher molecular weight molecules will show non-Newtonian behaviour, where the viscosity of the sample depends on the shear rate. The behaviour of non-Newtonian fluids can be classed as shear-thinning (pseudoplastic behaviour) or shear-thickening (dilatant behaviour) (Figure 1.10). Shear-thinning samples are commonly found in food such as polymer dispersion (e.g., ketchup, whipped cream, salad dressing). Under shear, the polymers deform and re-arrange in the direction of the flow, leading to a decrease in viscosity with increasing shear rate. Shear-thickening samples are less commonly found in food, although starch granule dispersions (e.g., corn starch) are one example. In this case, the viscosity of the sample increases with increasing shear rate due to the flocculation or compression of the dispersed particles (Mezger, 2014).

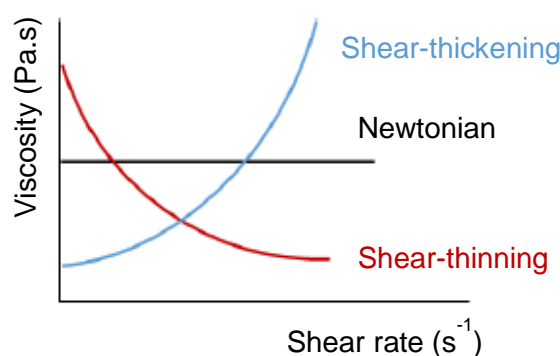


Figure 1.10. Comparison of viscosity functions of Newtonian and non-Newtonian fluids.

1.6.9. Interfacial shear viscosity

Interfacial shear viscosity is a useful way of monitoring the formation and structure of the adsorbed films (Burke *et al.*, 2014; Murray, 2002; Murray *et al.*, 1996). For this thesis, interfacial shear viscometer was used to give information about how the interfaces generated by polyphenols in presence and/or absence of proteins or protein-based microgel particles can be related to the aspects of the formation and stability of emulsions.

Interfacial rheology has been defined as ‘the study of the mechanical and flow properties of adsorbed layers at the interfaces’ (Murray *et al.*, 1996). In general, interfacial rheology describes the relationship between the

deformation of an interface and the stresses exerted on it. Shear interfacial rheological methods involve inducing shear in the adsorbed film without changing the area (Pelipenko *et al.*, 2012). These methods provide information on the structures formed at the interface.

A two-dimensional Couette type viscometer was used to measure the interfacial shear viscosity and the principle of measurement is shown in Figure 1.11. A thin torsion wire was attached to the spindle of a biconical disc. The dish was rotated at fixed, constant speed and the disc moved depending on the interfacial shear viscosity of the film. The torsion of the wire opposed the movement of the disc and equilibrium was met at the point where the rotation of the disc that is driven from the interfacial shear viscosity was equal to the resistance due to the torsion of the wire. The disc deflection was measured using a laser light beam source, a mirror and a scale. The laser light beam was directed to a mirror that is attached firmly to the disc. It was then reflected to the scale. A camera was used to record the deflection.

The constant shear rate apparent interfacial viscosity, η_i , is given by the following equation:

$$\eta_i = \frac{g_f}{\omega} K(\theta - \theta_o) \quad (1.14)$$

where K is the torsion constant of the wire, θ is the equilibrium deflection of the disc in the presence of the film, θ_o is the equilibrium deflection in the absence of the film, that is, due to the bulk drag of the sub-phase on the disc, g_f is the geometric factor, and ω is the angular velocity of the disc. A fixed value of $\omega = 1.27 \times 10^{-3} \text{ rad s}^{-1}$ was used.

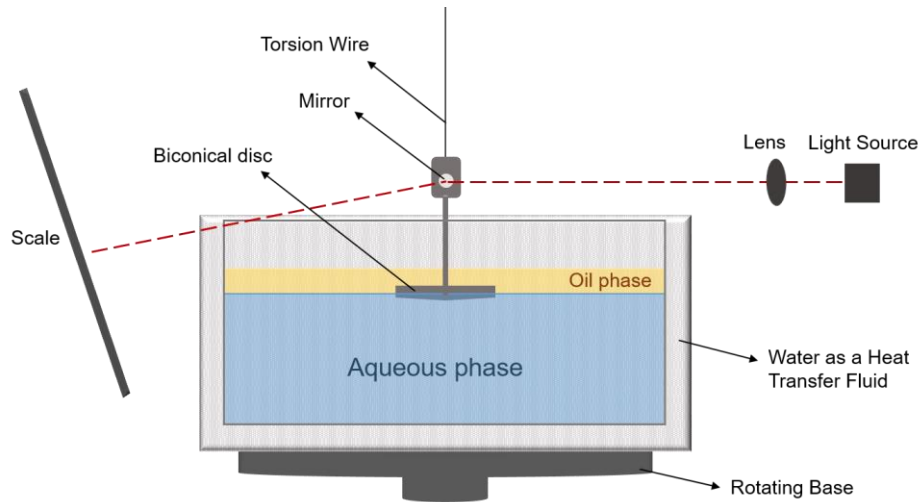


Figure 1.11. Schematic representation of interfacial shear viscometer.

1.7. Outline of the thesis

This thesis includes a further literature review and research studies starting with the characterization of polyphenols particles as Pickering stabilizers to the design of the W/O emulsions and improvement of their stability over time through interfacial complex formation with proteins and protein-based microgels. Finally, it includes the process ability of these emulsions stabilized by either of these interfaces to give indication of the stability of these emulsions during manufacturing of real-life applications. The outline of each chapter is highlighted in Figure 1.12.

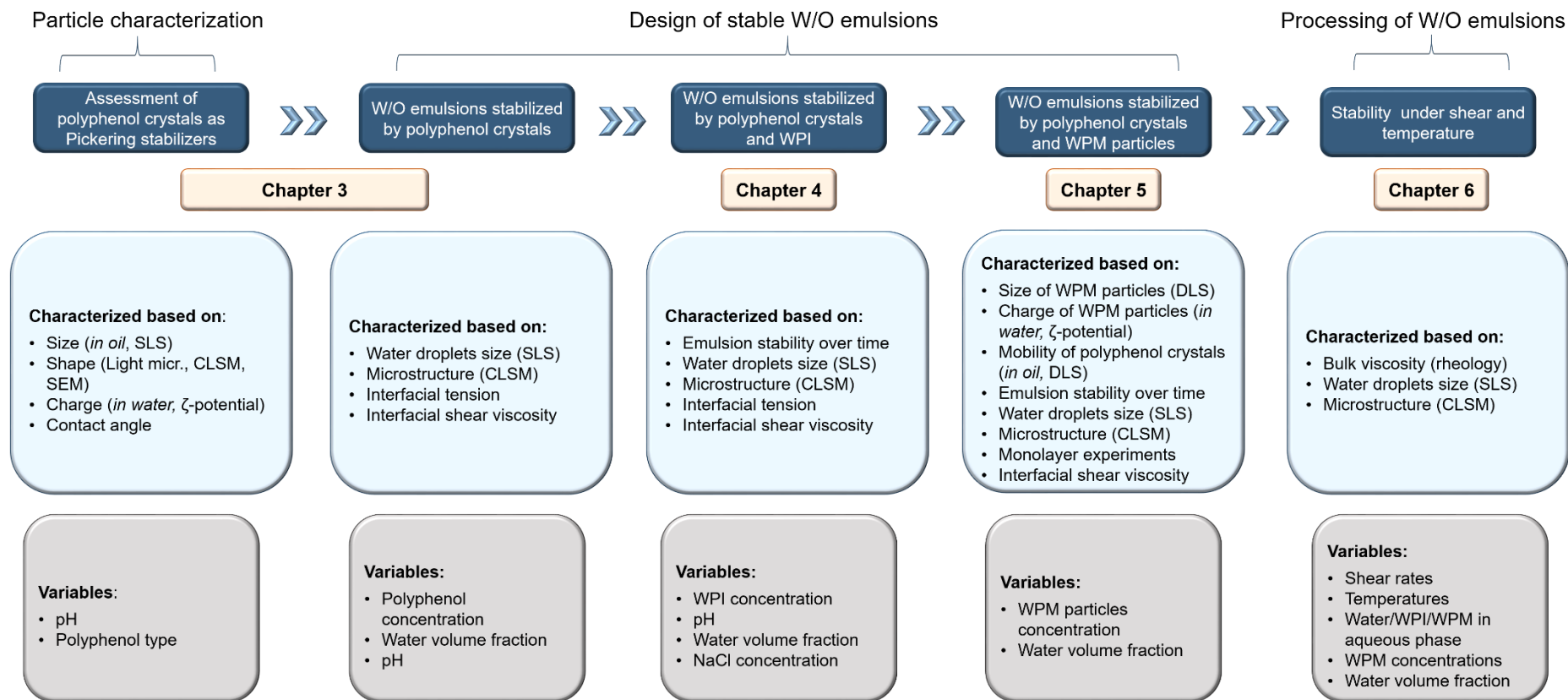


Figure 1.12. Schematic framework of this thesis.

Chapter 2 – *Water-in-oil emulsions stabilized by surfactants, proteins and particles: A literature review*

This chapter includes a literature review giving an overview of the key parameters behind emulsions formation, stability and instability phenomenon of W/O emulsions. The recent advances in designing W/O emulsions stabilized by surfactants, biopolymer, particles or combinations of these different stabilizers were also examined. The knowledge gaps in the literature on both stabilization and processing aspects were clearly highlighted to identify the aims of the thesis.

Chapter 3 – *Water-in-oil Pickering emulsions stabilized by water-insoluble polyphenol crystals*

The aim of this study was to assess the polyphenol crystals (curcumin and quercetin) as Pickering stabilizers in terms of their size, shape, hydrophilicity/hydrophobicity and charge (in water). The next step was to design W/O emulsions with these Pickering stabilizers, evaluate their size, and measure the interfacial shear viscosity. This chapter was published to the peer-reviewed journal, *Langmuir*.

Chapter 4 – *Water-in-oil Pickering emulsions stabilized by an interfacial complex of water-insoluble polyphenol crystals and protein*

Work in this chapter focussed on a unique W/O stabilization mechanism via complex formation at the interface between polyphenol crystals (curcumin and quercetin) and whey protein isolate (WPI). The stability of the corresponding W/O emulsion droplets was evaluated as a function of different WPI concentrations, water volume fractions, pH values and interfacial shear viscosity. This unique interfacial complex was patented (WO/2019/008059/A1) and the chapter was published to the peer-reviewed journal, *Journal of Colloids and Interface Science*.

Chapter 5 – *Water-in-Oil Pickering Emulsions Stabilized by Synergistic Particle-Particle Interactions*

In this chapter, a W/O 'double Pickering stabilization' via an interfacial complexation between polyphenol crystals and whey protein microgel (WPM) particles was demonstrated. This mechanism of stabilization used to improve the stability of W/O emulsions and increase the water volume fraction up to 20 wt%. The stability of the corresponding W/O emulsion droplets was evaluated as a function of different WPM particle concentrations, water volume fractions, ζ -potential measurements, monolayer experiments and interfacial shear viscosity. This chapter was published to the peer-reviewed journal, *Langmuir*.

Chapter 6 – *Shear and temperature stability of water-in-oil emulsions co-stabilized by polyphenol crystals- protein complex*

This chapter involves the characterization of the stability of W/O emulsions stabilized by curcumin or quercetin crystals dispersed in the oil phase, with or without the presence of WPI or WPM particles in the aqueous phase. Characterization was undertaken using controlled rheological tests (shear rates and temperatures) combined with particle sizing and confocal laser scanning microscopy. This chapter has been submitted to the peer-reviewed journal, *Journal of Food Engineering*.

Chapter 7 – *Conclusion and future studies*

This chapter includes a general summary and discussion of the main results as well as conclusions in relation to the principal research problem and areas for future studies.

References

- Adams, K. F., Schatzkin, A., Harris, T. B., Kipnis, V., Mouw, T., Ballard-Barbash, R., . . . Leitzmann, M. F. (2006). Overweight, obesity, and mortality in a large prospective cohort of persons 50 to 71 years old. *New England Journal of Medicine*, *355*(8), 763-778.
- Aditya, N., Hamilton, I. E., & Norton, I. T. (2017). Amorphous nano-curcumin stabilized oil in water emulsion: Physico chemical characterization. *Food chemistry*, *224*, 191-200.
- Anand, P., Kunnumakkara, A. B., Newman, R. A., & Aggarwal, B. B. (2007). Bioavailability of curcumin: problems and promises. *Molecular pharmaceutics*, *4*(6), 807-818.
- Andersen, O. M., & Markham, K. R. (2005). *Flavonoids: chemistry, biochemistry and applications*: CRC press.
- Araiza-Calahorra, A., Akhtar, M., & Sarkar, A. (2018). Recent advances in emulsion-based delivery approaches for curcumin: From encapsulation to bioaccessibility. *Trends in Food Science Technology*, *71*, 155-169.
- Araiza-Calahorra, A., & Sarkar, A. (2019). Pickering emulsion stabilized by protein nanogel particles for delivery of curcumin: Effects of pH and ionic strength on curcumin retention. *Food Structure*, *21*, 100113.
- Asano, K., Shinagawa, K., & Hashimoto, N. (1982). Characterization of haze-forming proteins of beer and their roles in chill haze formation. *Journal of the American Society of Brewing Chemists*, *40*(4), 147-154.
- Auty, M. (2013). Confocal microscopy: principles and applications to food microstructures. In *Food microstructures* (pp. 96-P98): Elsevier.
- Baxter, N. J., Lilley, T. H., Haslam, E., & Williamson, M. P. (1997). Multiple interactions between polyphenols and a salivary proline-rich protein repeat result in complexation and precipitation. *Biochemistry*, *36*(18), 5566-5577.
- Bayarri, S., Taylor, A. J., & Hort, J. (2006). The role of fat in flavor perception: effect of partition and viscosity in model emulsions. *Journal of agricultural food chemistry*, *54*(23), 8862-8868.
- Bearth, A., Cousin, M.-E., & Siegrist, M. (2014). The consumer's perception of artificial food additives: Influences on acceptance, risk and benefit perceptions. *Food Quality Preference*, *38*, 14-23.
- Berry, J. D., Neeson, M. J., Dagastine, R. R., Chan, D. Y., & Tabor, R. F. (2015). Measurement of surface and interfacial tension using pendant drop tensiometry. *Journal of colloid interface science*, *454*, 226-237.
- Bhattacharjee, S. (2016). DLS and zeta potential—what they are and what they are not? *Journal of Controlled Release*, *235*, 337-351.
- Bordenave, N., Hamaker, B. R., & Ferruzzi, M. G. (2014). Nature and consequences of non-covalent interactions between flavonoids and macronutrients in foods. *Food function*, *5*(1), 18-34.

- Burke, J., Cox, A., Petkov, J., & Murray, B. S. (2014). Interfacial rheology and stability of air bubbles stabilized by mixtures of hydrophobin and β -casein. *Food Hydrocolloids*, 34, 119-127.
- Butland, B., Jebb, S., Kopelman, P., McPherson, K., Thomas, S., Mardell, J., & Parry, V. (2007). *Tackling obesities: future choices-project report* (Vol. 10): Department of Innovation, Universities and Skills London.
- Cayot, P., & Lorient, D. (1997). Structure-function relationships of whey proteins. *FOOD SCIENCE TECHNOLOGY-NEW YORK-MARCEL DEKKER*, 225-256.
- Cosgrove, T. (2010). *Colloid science: principles, methods and applications*: John Wiley & Sons.
- Cretu, R., Dima, C., Bahrim, G., & Dima, S. (2011). Improved solubilization of curcumin with a microemulsification formulation. *The Annals of the University of Dunarea De Jos of Galati. Fascicle VI. Food Technology*, 35(2), 46.
- Dickinson, E. (1992). *Introduction to food colloids*: Oxford University Press.
- Dickinson, E. (2008). Interfacial structure and stability of food emulsions as affected by protein-polysaccharide interactions. *Soft Matter*, 4(5), 932-942.
- Dickinson, E. (2015). Microgels—an alternative colloidal ingredient for stabilization of food emulsions. *Trends in Food Science Technology*, 43(2), 178-188.
- Dickinson, E. (2017). Biopolymer-based particles as stabilizing agents for emulsions and foams. *Food Hydrocolloids*, 68, 219-231.
- Duffus, L. J., Norton, J. E., Smith, P., Norton, I. T., & Spyropoulos, F. (2016). A comparative study on the capacity of a range of food-grade particles to form stable O/W and W/O Pickering emulsions. *Journal of colloid interface science*, 473, 9-21.
- Formica, J., & Regelson, W. (1995). Review of the biology of quercetin and related bioflavonoids. *Food chemical toxicology*, 33(12), 1061-1080.
- Gunasekaran, S., & Ak, M. M. (2002). *Fundamental Rheological Methods*: CRC Press.
- Haen, D. (2014). The paradox of E-numbers: ethical, aesthetic, and cultural concerns in the Dutch discourse on food additives. *Journal of agricultural environmental ethics*, 27(1), 27-42.
- Hagerman, A. E., & Butler, L. G. (1981). The specificity of proanthocyanidin-protein interactions. *Journal of Biological Chemistry*, 256(9), 4494-4497.
- Hassan, Z., El Din, H. M. F., Ali, A., Mehanna, N. S., & El-Messery, T. (2013). Interaction of some low molecular weight phenolics with milk proteins. *World Applied Sciences Journal*, 23(2), 182-187.
- Horiba scientific. (2012). *A guidebook to particle size analysis*. Irvine, USA: Horiba Instruments, Inc.
- JEOL Ltd. (2011). Introducing Cryo Scanning Electron Microscopy. *JEOL Application Data Sheet, SEM, SM-B-004-00E*.

- Jose, N., Deshmukh, G. P., & Ravindra, M. R. (2019). Dynamic Light Scattering: Advantages and Applications. *ACTA SCIENTIFIC NUTRITIONAL HEALTH*, 3(3), 50-52.
- Klitou, P., Rosbottom, I., & Simone, E. (2019). Synthonic modelling of quercetin and its hydrates: explaining crystallization behaviour in terms of molecular conformation and crystal packing. *Crystal Growth Design*.
- Kruss GmbH. (2004). Force tensiometry with ring and plate. Retrieved from https://www.kruss-scientific.com/fileadmin/user_upload/website/literature/kruss-tn308-en.pdf
- Lam, S., Velikov, K. P., & Velev, O. D. (2014). Pickering stabilization of foams and emulsions with particles of biological origin. *Current Opinion in Colloid Interface Science*, 19(5), 490-500.
- Le Bourvellec, C., & Renard, C. (2012). Interactions between polyphenols and macromolecules: quantification methods and mechanisms. *Critical reviews in food science nutrition*, 52(3), 213-248.
- Luo, Z., Murray, B. S., Ross, A.-L., Povey, M. J., Morgan, M. R., & Day, A. J. (2012). Effects of pH on the ability of flavonoids to act as Pickering emulsion stabilizers. *Colloids Surfaces B: Biointerfaces*, 92, 84-90.
- Luo, Z., Murray, B. S., Yusoff, A., Morgan, M. R., Povey, M. J., & Day, A. J. (2011). Particle-stabilizing effects of flavonoids at the oil– water interface. *Journal of agricultural food chemistry*, 59(6), 2636-2645.
- Lyklema, J. (2005). *Fundamentals of interface and colloid science: soft colloids* (Vol. 5): Elsevier.
- MacRitchie, F. (1978). Proteins at interfaces. In *Advances in protein chemistry* (Vol. 32, pp. 283-326): Elsevier.
- Malvern Instruments Ltd. (2004). *Zetasizer Nano Series User Manual*. Worcestershire, UK: Malvern Instruments Ltd.
- Malvern Instruments Ltd. (2015). A basic guide to particle characterization. *Malvern Instruments Ltd*.
- Marquardt, K. C., & Watson, R. R. (2014). Polyphenols and public health. In *Polyphenols in Human Health and Disease* (pp. 9-15): Elsevier.
- Marto, J., Gouveia, L., Chiari, B., Paiva, A., Isaac, V., Pinto, P., . . . Ribeiro, H. (2016). The green generation of sunscreens: Using coffee industrial sub-products. *Industrial Crops Products*, 80, 93-100.
- McClements, D. J. (2015). *Food emulsions: principles, practices, and techniques*: CRC press.
- Mezger, T. G. (2014). *The rheology handbook : for users of rotational and oscillatory rheometers* (4th edition. ed.). Hanover: Vincentz Network.
- Murray, B. S. (1997). Equilibrium and dynamic surface pressure-area measurements on protein films at air-water and oil-water interfaces. *Colloids Surfaces A: Physicochemical Engineering Aspects*, 125(1), 73-83.
- Murray, B. S. (2002). Interfacial rheology of food emulsifiers and proteins. *Current Opinion in Colloid Interface Science*, 7(5-6), 426-431.

- Murray, B. S. (2019). Pickering emulsions for food and drinks. *Current Opinion in Food Science*.
- Murray, B. S., & Dickinson, E. (1996). Interfacial rheology and the dynamic properties of adsorbed films of food proteins and surfactants. *Food Science Technology International, Tokyo*, 2(3), 131-145.
- Murray, N. J., Williamson, M. P., Lilley, T. H., & Haslam, E. (1994). Study of the interaction between salivary proline-rich proteins and a polyphenol by 1H-NMR spectroscopy. *European journal of biochemistry*, 219(3), 923-935.
- Nehir El, S., & Simsek, S. (2012). Food technological applications for optimal nutrition: an overview of opportunities for the food industry. *Comprehensive Reviews in Food Science Food Safety*, 11(1), 2-12.
- NHS. (2017, 22 January 2019). Health Survey for England 2017 [NS]. Retrieved from <https://digital.nhs.uk/data-and-information/publications/statistical/health-survey-for-england/2017>
- Nicolai, T., Britten, M., & Schmitt, C. (2011). β -Lactoglobulin and WPI aggregates: formation, structure and applications. *Food Hydrocolloids*, 25(8), 1945-1962.
- Nobbmann, U., Connah, M., Fish, B., Varley, P., Gee, C., Mulot, S., . . . Sheng, F. (2007). Dynamic light scattering as a relative tool for assessing the molecular integrity and stability of monoclonal antibodies. *Biotechnology Genetic Engineering Reviews*, 24(1), 117-128.
- Paans, E. (2013). *Investigating Consumers' Avoidance of E-numbers*: Paans.
- Pari, L., Tewas, D., & Eckel, J. (2008). Role of curcumin in health and disease. *Archives of physiology biochemistry*, 114(2), 127-149.
- Payton, F., Sandusky, P., & Alworth, W. L. (2007). NMR study of the solution structure of curcumin. *Journal of natural products*, 70(2), 143-146.
- Pelipenko, J., Kristl, J., Rošic, R., Baumgartner, S., & Kocbek, P. (2012). Interfacial rheology: an overview of measuring techniques and its role in dispersions and electrospinning. *Acta Pharmaceutica*, 62(2), 123-140.
- Pickering, S. U. (1907). Cxcvi.—emulsions. *Journal of the Chemical Society, Transactions*, 91, 2001-2021.
- Polikandrioti, M., & Stefanou, E. (2009). Obesity disease. *Health science journal*, 3(3).
- Rao, E. V., & Sudheer, P. (2011). Revisiting curcumin chemistry part I: A new strategy for the synthesis of curcuminoids. *Indian journal of pharmaceutical sciences*, 73(3), 262.
- Richard, T., Lefeuvre, D., Descendit, A., Quideau, S., & Monti, J. (2006). Recognition characters in peptide–polyphenol complex formation. *Biochimica et Biophysica Acta -General Subjects*, 1760(6), 951-958.
- Riihimaki, L. H., Vainio, M. J., Heikura, J. M., Valkonen, K. H., Virtanen, V. T., & Vuorela, P. M. (2008). Binding of phenolic compounds and their

- derivatives to bovine and reindeer β -lactoglobulin. *Journal of agricultural food chemistry*, 56(17), 7721-7729.
- Rodríguez Patino, J. M., Rodríguez Niño, M. R., & Sánchez, C. C. (1999). Adsorption of whey protein isolate at the oil– water interface as a function of processing conditions: A rheokinetic study. *Journal of agricultural food chemistry*, 47(6), 2241-2248.
- Roedig-Penman, A., & Gordon, M. H. (1998). Antioxidant properties of myricetin and quercetin in oil and emulsions. *Journal of the American Oil Chemists' Society*, 75(2), 169-180.
- Rossl, M., Rickles, L. F., & Halpin, W. A. (1986). The crystal and molecular structure of quercetin: A biologically active and naturally occurring flavonoid. *Bioorganic Chemistry*, 14(1), 55-69.
- Russo, C. J., Scotcher, S., & Kyte, M. (2016). A precision cryostat design for manual and semi-automated cryo-plunge instruments. *Review of Scientific Instruments*, 87(11), 114302.
- Saad, S. M., Policova, Z., & Neumann, A. W. (2011). Design and accuracy of pendant drop methods for surface tension measurement. *Colloids Surfaces A: Physicochemical Engineering Aspects*, 384(1-3), 442-452.
- Schmitt, C., Moitzi, C., Bovay, C., Rouvet, M., Bovetto, L., Donato, L., . . . Stradner, A. (2010). Internal structure and colloidal behaviour of covalent whey protein microgels obtained by heat treatment. *Soft Matter*, 6(19), 4876-4884.
- Sharma, R., Gescher, A., & Steward, W. (2005). Curcumin: the story so far. *European journal of cancer*, 41(13), 1955-1968.
- Stetefeld, J., McKenna, S. A., & Patel, T. R. (2016). Dynamic light scattering: a practical guide and applications in biomedical sciences. *Biophysical reviews*, 8(4), 409-427.
- Tsao, R. (2010). Chemistry and biochemistry of dietary polyphenols. *Nutrients*, 2(12), 1231-1246.
- van Gunst, A., & Roodenburg, A. J. (2019). Consumer Distrust about E-numbers: A Qualitative Study among Food Experts. *Foods*, 8(5), 178.
- Wassell, P., Bonwick, G., Smith, C. J., Almiron-Roig, E., & Young, N. W. (2010). Towards a multidisciplinary approach to structuring in reduced saturated fat-based systems—a review. *International journal of food science technology*, 45(4), 642-655.
- Wilde, P., Mackie, A., Husband, F., Gunning, P., & Morris, V. (2004). Proteins and emulsifiers at liquid interfaces. *Advances in Colloid Interface Science*, 108, 63-71.
- Williamson, M. P. (1994). The structure and function of proline-rich regions in proteins. *Biochemical journal*, 297(Pt 2), 249.
- Xiao, J., Li, Y., & Huang, Q. (2016). Recent advances on food-grade particles stabilized Pickering emulsions: Fabrication, characterization and research trends. *Trends in Food Science Technology*, 55, 48-60.

- Xu, R., Dickinson, E., & Murray, B. S. (2007). Morphological changes in adsorbed protein films at the air– water interface subjected to large area variations, as observed by Brewster angle microscopy. *Langmuir*, 23(9), 5005-5013.
- Ye, J., Fan, F., Xu, X., & Liang, Y. (2013). Interactions of black and green tea polyphenols with whole milk. *Food research international*, 53(1), 449-455.

Chapter 2

Water-in-oil emulsions stabilized by surfactants, proteins and particles: A literature review

Abstract

Considering the global rise of obesity and food-linked cardiovascular diseases, food industries are often challenged to produce low fat or fat-free products. To address such challenges, incorporation of water in the form of water-in-oil (W/O) emulsions to replace fat has gained significant research attention. This review aims to provide comprehensive insights on stabilization of W/O emulsions with clear focus on interfacial design with surfactants, biopolymers, particles and/or a combination thereof that have been researched in the last 20 years. Particular emphasis has been given to Pickering stabilization of water droplets stabilized by non-bio-derived as well as bio-derived particles with or without the addition of surfactants or biopolymers that allows long term kinetic stabilization of W/O emulsions against coalescence. In addition, the stability of W/O emulsions under processing conditions are also briefly discussed. Although extensive work has been done on non-bio-derived and non-biodegradable particles, rare attention has been given to biocompatible particles, proteins and a combination thereof to stabilize water-droplets for longer periods during ambient storage as well as processing conditions.

2.1. Introduction

A number of food-linked chronic diseases have been associated with the overconsumption of calorie-dense total fat, saturated fats, and trans-fatty acids, such as obesity, coronary heart disease, diabetes and hypertension (Abete *et al.*, 2011; Cotton *et al.*, 2007; Dhaka *et al.*, 2011). Therefore, there has been considerable emphasis on the development of lipid-based food products with reduced levels of saturated, trans-fats and total fat (Nehir El *et al.*, 2012; Wassell *et al.*, 2010). One of the major challenges in developing

these products is that fats play an important role in determining the desirable textural and sensory properties of many food products (Bayarri *et al.*, 2006; Wassell *et al.*, 2010). In many instances, the food industry has been unable to produce reduced fat products that consumers find pleasurable. Fat has some important functions in the sensory characteristics of food products. It influences the: (a) appearance (*e.g.*, gloss, colour, translucency, surface uniformity, and crystallization); (b) texture (*e.g.*, viscosity, elasticity, and hardness); (c) flavour (*e.g.*, intensity of flavour, flavour release, flavour profile and flavour development); and (d) mouthfeel (*e.g.*, meltability, creaminess, lubricity, thickness, and degree of mouth-coating) of the final product (Roller *et al.*, 1996). Food scientists have attempted to identify or design “fat-replacers” that can mimic all of the different roles that fat plays in determining a products’ functional and sensorial properties (McClements *et al.*, 1998).

The major approaches that have been used in literature to develop reduced-fat emulsion products are as follows:

- (a) *Fat mimetics*. These are ingredients that have distinctly different chemical structures to triacylglycerols and usually consist of carbohydrates and/or proteins, such as starch granules and whey protein microparticles. These products have diverse functional properties, and have showed limited success in mimicking some of the characteristic physicochemical properties of fat, such as mouthfeel, viscosity, and appearance (Lucca *et al.*, 1994; McClements *et al.*, 1998).
- (b) *Fat substitutes*. They are substances that look and feel like fat and have physical and thermal properties similar to fat. They are often called fat substitutes as they can, theoretically, replace all or part of the fat in a food. Included in this category are emulsifiers, medium chain triacylglycerols (MCTs) and structured lipids. However, they are either indigestible to humans and often not seen as ‘*clean label*’ by consumers (Lucca *et al.*, 1994; McClements *et al.*, 1998).
- (c) *Aeration*. Aeration is another approach whereby air under high pressure is forced through a fat matrix so that the air forms numbers of

bubbles resulting in a foam in which the gas forms the discontinuous phase dispersed in the continuous fat phase (Venkata Ramana *et al.*, 2013). In general, replacing fat with bubbles may impart a unique texture and distinctive in-mouth sensory properties as compared full-fat product (Campbell *et al.*, 1999; Venkata Ramana *et al.*, 2013).

- (d) *Water*. Last but not the latest, the most promising approach to replace fat is adding non-calorific water in the form of water-in-oil (W/O) emulsion droplets to mimic fat droplets in a fatty product. This method enables total fat content reduction, and also allows incorporation of water soluble nutrients and flavourings in the aqueous phase. Although this appears to be the most promising approach in theory, lack of stability of the emulsion systems presents one of the key challenges since W/O emulsions are thermodynamically unstable and prone to phase separation over time (see § 2.2).

In this review, we therefore examine the recent advances in designing W/O emulsions as an approach to reduce the fat, and thus the calorific content of fat continuous products. The review especially emphasizes on the stabilizers (*e.g.*, surfactants, biopolymer and/or particles) used on the last 20 years to stabilize W/O emulsions. Also, combinations of these different stabilizers are elaborated. We first discuss the theory behind emulsion formation, followed by covering the instability phenomenon of W/O emulsions. Then we focus on comparing the stability of emulsions stabilized by surfactants, biopolymers, particles and a combination thereof. We then highlight the gaps in the literature on both stabilization and processing aspects to clearly identify the areas where future studies need to be conducted. The literature search was conducted using three key search engines: Web of Science, ScienceDirect and PubMed. In addition, 'Google Scholar' was also used to search for publications and additional information. The initial selection of publications was made on the basis of the title of the publication, keywords, and abstract screening. After full-text analysis, articles were included in the review. In addition, reference list of each paper was carefully checked to identify any relevant previous studies and full-text screening was conducted for the same. Several excellent reviews on polymeric microgels, fat crystals or

wax-stabilized emulsions are available in the literature (Dickinson, 2010; Ghosh *et al.*, 2011a; Murray, 2019; Richtering, 2012; Rousseau, 2000; Sato *et al.*, 2011; Tang *et al.*, 2015), therefore these W/O stabilizers are not within the scope of this review. Also, this review focuses on W/O emulsions and does not include any specific discussion of multiple emulsions (*e.g.*, water-in-oil-in-water (W/O/W) or oil-in-water-in-oil (O/W/O) emulsions) or crude oil emulsions.

2.2. Emulsions characteristics

2.2.1. Definition

Emulsions play a major role in a variety of commercial applications such as chemical, agrochemical, cosmetic, pharmaceutical and in many food products (Bibette *et al.*, 1999; Mazo Rivas *et al.*, 2016). Emulsions are dispersions of two or more immiscible liquids, where oil-in-water (O/W, *e.g.*, mayonnaise, milk, cream etc.) or water-in-oil (W/O, *e.g.*, margarine, butter and spreads) emulsions can be formed such that one liquid is dispersed as small droplets (*i.e.*, dispersed phase) into a second liquid (*i.e.*, continuous phase). The size of the droplets may vary; for so-called nano-emulsions the droplets are < 100 nm whilst for macro-emulsions they are > 1 μm (Cosgrove, 2010). The process of converting two immiscible liquids into an emulsion is usually carried out by subjecting the liquids to intense mechanical agitation.

2.2.2. Thermodynamic and kinetic stability of the emulsions

Thermodynamics gives information about the driving forces for processes taking place under quiescent conditions (*i.e.*, after homogenization). Kinetics gives information about the rate at which these processes occur, *i.e.*, the time taken for the these emulsified droplets to eventually merge and separate back into two completely separate (more thermodynamically stable) phases. Emulsions can be considered as thermodynamically unstable but kinetically stable systems.

2.2.2.1. Thermodynamic stability

Emulsions are thermodynamically unstable systems because they tend to phase separate over time. The thermodynamic instability is illustrated by the free energy of a system (ΔG_f):

$$\Delta G_{formation} = \gamma_T \Delta A - |T \Delta S_{config}| \quad (2.1)$$

where $\Delta G_{formation}$ is the free energy of a system; γ_T is the interfacial tension; ΔA is the contact area between the oil and water phases; T is the temperature and ΔS_{config} is the configurational entropy of the droplets in the system.

The change in interfacial free energy term ($\gamma_T \Delta A$) is always positive, because the contact area (ΔA) increases after homogenization. On the other hand, in the absence of surfactants, biopolymers or particles at the interface, the configurational entropy term ($-|T \Delta S_{config}|$) is always negative, because the number of arrangements accessible to the droplets in the emulsified state is much greater than in the non-emulsified state (McClements, 2015). In most cases $\gamma_T \Delta A \gg -|T \Delta S_{config}|$, which means that $\Delta G_{formation}$ is positive, *i.e.*, the formation of emulsions is not spontaneous and the system is thermodynamically unstable (Tadros, 2009).

2.2.2.2. Kinetic stability

Kinetic stability arises from inter-molecular and/or inter-particle forces. It can be determined by the dynamics and interactions of the droplets in emulsion systems (McClements, 2015). The droplets experience random collisions due to Brownian motion, gravity, or applied external forces. They can also remain loosely associated with each other or fuse together after the collisions, depending upon the nature of the interactions between them (McClements, 2015). An energy barrier, known as activation energy (ΔG^*) exists in the system and prevents complete merging of the droplets into a single phase (Figure 2.1), as long as this activation energy is much larger than the thermal energy (kT) of the system (McClements, 2015). Stabilizers/emulsifiers provide this energy barrier (see § 2.4).

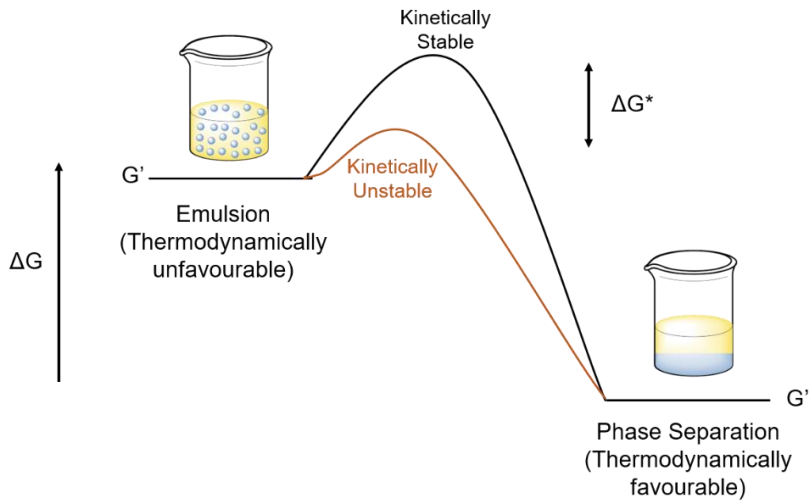


Figure 2.1. Activation energy (ΔG^*) required to form kinetically stable emulsions which prevents the phase separation arising from thermodynamically unstable systems for a certain time period.

2.2.3. Instability of W/O emulsions

The main physical mechanisms that cause destabilization of W/O emulsions are shown in Figure 2.2.

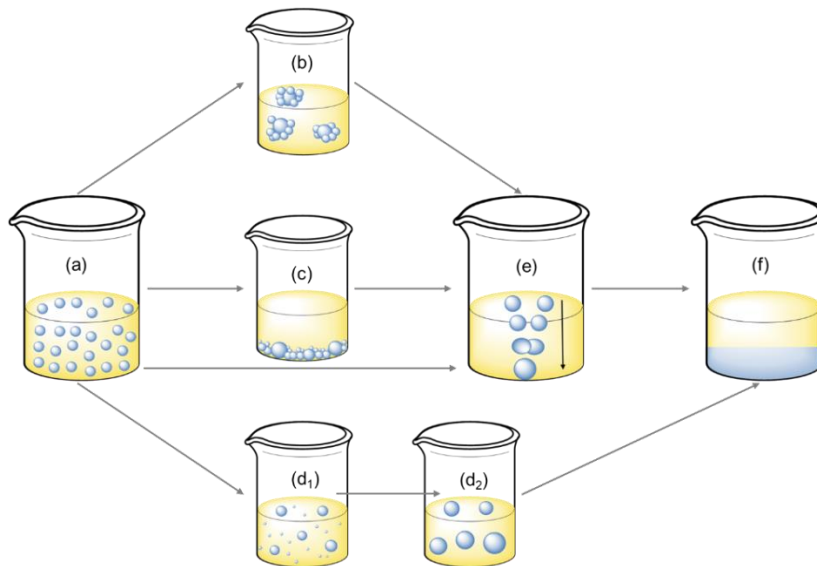


Figure 2.2. Physical emulsions destabilization mechanisms for W/O emulsions; (a) original emulsion, (b) flocculation, (c) sedimentation, (d₁-d₂) Ostwald ripening, (e) coalescence and (f) phase separation.

2.2.3.1. Flocculation

Flocculation (Figure 2.2 (b)) is generally a reversible mechanism arising from the aggregation of droplets due to the unbalanced inter-droplet attractive and repulsive forces (Killian, 2011). Flocculation occurs when the droplets stick to each other without rupture of their interfacial layers and affects the rate of droplet sedimentation. Flocculated droplets (flocs) form effectively larger droplet diameters thus increasing the sedimentation rate, especially in dilute systems. In more concentrated emulsions, the flocs provide a network that hinders the movement of other droplets, retarding the sedimentation (Killian, 2011). Flocculation can generally be retarded by changing the viscosity of the continuous phase, concentration of the droplets, concentration and coverage of the interfacial materials, droplet size, charges on the droplet surface and/or on the continuous phase and the addition of polymers or other colloidal particles to the continuous phase (Killian, 2011).

2.2.3.2. Sedimentation

Sedimentation (Figure 2.2 (c)) occurs when the dispersed phase is denser than the continuous phase, leading the dispersed phase droplets to migrate downwards to settle at the bottom of the container. If only sedimentation occurs, the droplets can generally be re-dispersed in the continuous phase through gentle mixing, *i.e.*, this is a reversible process (Killian, 2011).

Stokes' law can be used to determine the rate of gravitational sedimentation from the velocity of an isolated spherical droplet in an infinite and ideal (Newtonian) liquid medium as shown in equation (2.2) (Dickinson, 1992). If V_{Stokes} is negative the droplet will move downwards and sediment.

$$V_{Stokes} = -\frac{2gr^2(\rho_2-\rho_1)}{9\eta} \quad (2.2)$$

where V_{Stokes} is the velocity of the droplet, g is the acceleration due to gravity, r is the radius of the droplet, ρ_1 and ρ_2 are the densities of the continuous phase and dispersed phase, respectively, and η is the shear viscosity of the continuous phase.

From equation (2.2), sedimentation can obviously be prevented by reducing the droplet size, increasing the viscosity of the continuous phase (for example by adding appropriate polymers or reducing the density difference between the two phases) (McClements, 2015).

2.2.3.3. Coalescence

Coalescence (Figure 2.2 (e)) is the irreversible merging of two or more emulsion droplets to form a larger single droplet (Dickinson, 1992). It occurs when droplets are close to each other, sometimes after an extended time period, for example in a sedimentation layer or in some flocculated state. Coalescence results from film thinning and rupture of the interfacial layer around each droplet (Dickinson, 1992). Coalescence can be delayed by decreasing the 'contact' time between droplets and increasing the mechanical or electrostatic properties of the interfacial films surrounding the droplets (*e.g.*, by adding a stabilizer/ emulsifier, see § 2.2.4).

2.2.3.4. Ostwald ripening

In Ostwald ripening (Figure 2.2 ($d_1 - d_2$)), droplets grow at the expense of smaller ones in a polydisperse system due to mass transport of dispersed phase from one droplet to another via the continuous phase (Dickinson, 1992). The resulting system has fewer but larger droplets, increasing the rate of sedimentation (McClements, 2015). Ostwald ripening is ultimately due to an increase in solubility with decreasing particle size, due to the increase in Laplace pressure within more highly curved objects. Thus, a higher concentration of dispersed phase molecules develops around small droplets compared to larger ones and the dispersed phase molecules therefore diffuse to the larger ones because of this concentration gradient. Thus smaller droplets shrink and larger ones grow, leading to an overall net increase in the mean droplet size with time (McClements, 2015).

Ostwald ripening can be difficult to distinguish from coalescence because both processes lead to an increase in the average droplet size (Urbina-Villalba *et al.*, 2009). However, coalescence usually leads to a bimodal distribution (heterogeneous coalescence), whereas Ostwald ripening leads to a monomodal distribution where the cube of the mean particle diameter

increasing linearly with time (Kabalnov, 2001). The process can be controlled by decreasing the solubility of the dispersed phase in the continuous phase (by adding small ions into the aqueous phase, *e.g.*, salt), reducing the interfacial tension (*e.g.*, by adding stabilizers/ emulsifiers, see § 2.2.4) or increasing the thickness of the interfacial layer (*e.g.*, by adding Pickering particles, see § 2.2.4) (Dickinson, 1992; McClements, 2015).

2.2.4. Stabilizers/ Emulsifiers

In order to prepare kinetically stable emulsions, a stabilizer or emulsifier, is added to protect the newly formed droplets against the different destabilization mechanisms (Dickinson, 1992). A stabilizer tends to maintain the physicochemical state of a foodstuff by maintaining a homogenous dispersion of two or more immiscible substances (they mainly act as thickening agents, enhancing the viscosity of the continuous phase) (Borreani *et al.*, 2019). On the other hand, an emulsifier tends to form or maintain a homogenous mixture of two or more immiscible phases (Borreani *et al.*, 2019). An emulsifier forms a protective interfacial layer when it adsorbs to the surface of droplets, preventing the droplets from merging together. There is a variety of emulsifiers for stabilizing W/O emulsions, as indicated below and shown in Figure 2.3:

- a) Low molecular weight surface active agents, known as surfactants (*e.g.*, polyglycerol polyricinoleate (PGPR), sorbitan monooleate, lecithin);
- b) biopolymers (*e.g.*, proteins, polysaccharides);
- c) insoluble particles (*e.g.*, hydrophobic silica particles, modified starch particles, modified cellulose particles etc.);
- d) combinations of the above.

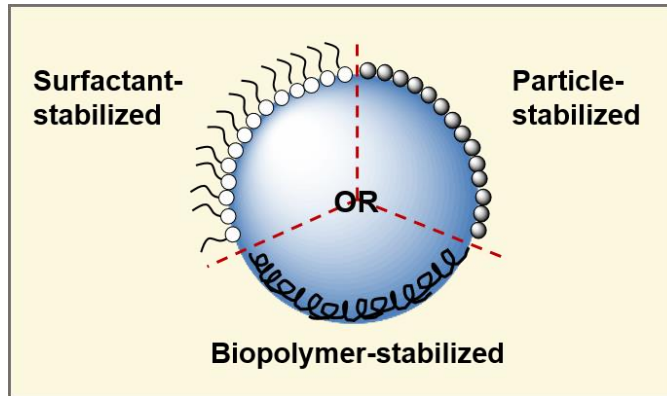


Figure 2.3. Schematic diagram of a W/O emulsion droplet showing different interfacial stabilization by surfactant, biopolymers or particles.

2.3. Emulsification parameters influencing the stability of W/O emulsions

To maintain a homogeneous and stable emulsion over a long time period, some of the parameters must be taken into account during the emulsification procedure:

- (a) *Emulsification process.* The aim of emulsification is usually to obtain small droplets with droplet size being an important characteristic of the stability of emulsions. Many laboratory devices have been used, such as high-speed mixers, colloid mills, ultrasound generators, high-pressure homogenizers and micro-fluidizers as shown in Table 2.1. Depending on the type of apparatus, it's mechanical configuration (e.g., valve design), and the viscosity of the continuous phase, droplet disruption occurs via laminar shear forces or turbulent shear forces (Iqbal *et al.*, 2013a; Scherze *et al.*, 2006). The Reynolds number (Re) is an important dimensionless number in fluid dynamics, which is the relative magnitude of the inertial forces and viscous forces, as shown in the equation (2.3) (Goodarzi *et al.*, 2019; Tadros, 2009). Inertial forces are the forces due to the momentum of the fluid. Thus, the denser a fluid is, and the higher its velocity, the more inertia (momentum) it has (Goodarzi *et al.*, 2019). Viscous forces are the frictional shear forces due to the relative motion of the different layers in a flowing fluid, resulting in different velocities for different layers,

which are directly related to the dynamic pressure and shearing stresses (Goodarzi *et al.*, 2019).

$$Re = \frac{\text{inertia forces}}{\text{viscous forces}} = \frac{vl\rho}{\eta} \quad (2.3)$$

where v is the linear liquid velocity, ρ is the liquid density, η is the viscosity and l is the characteristic length that is given by the diameter of flow through a cylindrical tube and by twice the slit width in a narrow slit. Based on the value of this dimensionless number, the flow regime can be identified. At low Reynolds number values, the viscous forces are greater than the inertial forces and the flow regime is laminar (Goodarzi *et al.*, 2019; Tadros, 2009). When the viscous forces are dominated by the inertial forces, the turbulent flow occurs as seen in high pressure homogenizers and micro-fluidizers (Goodarzi *et al.*, 2019; Tadros, 2009).

Table 2.1. Summary of homogenizers that have been used in literature to prepare W/O emulsions and their physicochemical characteristics (applied energy (Tadros, 2013) and size of droplets (Dickinson, 1992; McClements, 2015)) .

Homogenizer Type	Applied energy	Size of droplets/ μm	References
High-speed mixer	Medium	2 – 10	Ahuja <i>et al.</i> (2018); Almeida <i>et al.</i> (2017); Andresen <i>et al.</i> (2007); Bhatti <i>et al.</i> (2017); Binks <i>et al.</i> (2001); Brugger <i>et al.</i> (2008); Clausse <i>et al.</i> (2018); Destribats <i>et al.</i> (2011); Drelich <i>et al.</i> (2010); Dridi <i>et al.</i> (2016); Duffus <i>et al.</i> (2016); Golemanov <i>et al.</i> (2006); Gould <i>et al.</i> (2016); Guo <i>et al.</i> (2017); Khalid <i>et al.</i> (2013); Lif <i>et al.</i> (2010); Márquez <i>et al.</i> (2010); Masalova <i>et al.</i> (2013); Midmore (1999); Nazari <i>et al.</i> (2019); Nesterenko <i>et al.</i> (2014); Opawale <i>et al.</i> (1998); Pan <i>et al.</i> (2002); Pang <i>et al.</i> (2018); Pimentel-Moral <i>et al.</i> (2018); Politova <i>et al.</i> (2017); Rabelo <i>et al.</i> (2018); Rutkevičius <i>et al.</i> (2018); Sacca <i>et al.</i> (2008); Santini <i>et al.</i> (2014); Skelhon <i>et al.</i> (2012); Tshilumbu <i>et al.</i> (2015); Ushikubo <i>et al.</i> (2014); Venkataramani <i>et al.</i> (2016); Wardhono <i>et al.</i> (2014); Xhanari <i>et al.</i> (2011); Yan <i>et al.</i> (2001)
Colloid mill	High	1 – 2	Wolf <i>et al.</i> (2013)
Ultrasound generator	Medium - High	< 1	Hu <i>et al.</i> (2015); Macedo Fernandes Barros <i>et al.</i> (2018); Rein <i>et al.</i> (2012); Scherze <i>et al.</i> (2006)
High pressure homogenizer	High	> 0.1	Gülseren <i>et al.</i> (2014); Iqbal <i>et al.</i> (2012, 2013b, 2013c); Iqbal <i>et al.</i> (2019a, 2019b); Knoth <i>et al.</i> (2005a, 2005b); Massel <i>et al.</i> (2015); Scherze <i>et al.</i> (2006); Surh <i>et al.</i> (2007); Wang <i>et al.</i> (2016)
Micro- fluidizer	High	< 0.1	Chen <i>et al.</i> (2016); Yi <i>et al.</i> (2014)

- (b) *Emulsification time.* Increasing the time of the emulsification can result in formation of smaller droplets. However, extended mixing time can cause an increase in the size of the water droplets because the input energy (during emulsification) may raise the temperature of the system (Iqbal *et al.*, 2013a). It has been also shown by Nazari *et al.* (2019) that by increasing stirring time (from 1.5 to 2.5 hrs) at a constant speed (900 rpm), the droplet size increased from 45 to 72 nm on the emulsions stabilized by PGPR or Span 80, due to increased droplet-droplet collisions resulting in enhanced coalescence rate (which may lead to phase separation).
- (c) *Emulsification shear rate.* Increasing the emulsification shear rate (speed) smaller water droplets can be formed. The bulk viscosity of W/O emulsion system may also increase with the increase of the homogenization shear rate (Iqbal *et al.*, 2013a). This is attributed to generation of large number of smaller droplets resulting in an increased viscosity (Almeida *et al.*, 2017). It has been shown by Khalid *et al.* (2013) that by increasing stirring speed from 5,000 to 15,000 rpm, the droplet size decreased from 3 to 2 μm on the emulsions stabilized by ricinoleic acid ester (CR-310). Also, Almeida *et al.* (2017) showed that by increasing stirring speed (from 10,000 to 20,000 rpm) for the emulsification of W/O emulsions stabilized by Span 80 and Tween 80 (and mineral oil as continuous phase), a decrease on the average water droplet size was observed.
- (d) *Temperature.* Physical properties are strongly affected by temperature. For instance, the interfacial characteristics of oil and water, and emulsifying agent solubility are dependent on the thermodynamic conditions, particularly temperature (Goodarzi *et al.*, 2019). One important factor that is influenced by temperature is viscosity. At higher temperatures, the viscosity of the continuous oil phase decreases, accelerating the demulsification process and water droplet collisions. Saito *et al.* (1970) and Brown *et al.* (1965) showed that above 40 °C, the emulsions were not stable due to the increase of the thermal motion

of the molecules of the oil continuous phase (e.g., fatty acids, triglycerides etc.) which reduced its viscosity.

- (e) *Emulsifier concentration.* The emulsifier molecules/particles are adsorbed at the W-O interface during the emulsification process resulting in a decrease in surface tension. Hence, smaller and higher number of water droplets are obtained (Almeida *et al.*, 2017). However, above a certain concentration of emulsifier, the system is saturated and no more adsorption at the droplet surface takes place. The non-adsorbed emulsifiers remain into the continuous phase strengthening the tendency of flocculation (Iqbal *et al.*, 2013a).
- (f) *Water volume fraction.* Depending on the concentration of the emulsifier present in the continuous phase, a maximum water volume fraction can be stabilized. Above this fraction, there is a high tendency for the emulsions to coalesce (due to not enough emulsifier to cover the W-O interface) or cause inversion (from W/O to O/W emulsions) (Iqbal *et al.*, 2013a). For example, Nazari *et al.* (2019) showed that by increasing the water volume fraction from 10 to 50 vol%, the water droplet size (stabilized by PGPR) also increased (from 53 to 722 nm) because there was not enough surfactant to cover the interface, leading to coalescence.

A summary of literature on using surfactants, biopolymers or particles for stabilizing W/O emulsions is shown in Table 2.2, which is discussed in sections 2.4, 2.5 and 2.6.

Table 2.2. Summary of surfactants, biopolymers or particles (bio-derived and non-bio-derived) used for stabilizing W/O emulsions.

Type	Emulsifier	Emulsifier concentration/ wt%	Water volume fraction/ vol%	References
Surfactants	PGPR	0.2 – 10	10 – 50	Chen <i>et al.</i> (2016); Dridi <i>et al.</i> (2016); Killian <i>et al.</i> (2012); Knoth <i>et al.</i> (2005a); Márquez <i>et al.</i> (2010); Nazari <i>et al.</i> (2019); Ushikubo <i>et al.</i> (2014); Wolf <i>et al.</i> (2013)
	Span 20, 80, 85	0.001 – 12	10 – 50	Almeida <i>et al.</i> (2017); Koneva <i>et al.</i> (2017); Koroleva <i>et al.</i> (2003); Nazari <i>et al.</i> (2019); Opawale <i>et al.</i> (1998); Pimentel-Moral <i>et al.</i> (2018); Politova <i>et al.</i> (2017); Ushikubo <i>et al.</i> (2014)
	Lecithin	0.1 – 6	30 – 40	Chen <i>et al.</i> (2016); Killian <i>et al.</i> (2012); Knoth <i>et al.</i> (2005a); Pan <i>et al.</i> (2002); Ushikubo <i>et al.</i> (2014)
	Ricinoleic acid ester (CR- 310)	1 – 5	10 – 30	Bhatti <i>et al.</i> (2017); Khalid <i>et al.</i> (2013); Rabelo <i>et al.</i> (2018)
Biopolymers & Surfactants	Proteins & PGPR or Lecithin	0.5 – 8	2 – 40	Gülseren <i>et al.</i> (2012); Iqbal <i>et al.</i> (2012, 2013b, 2013c); Iqbal <i>et al.</i> (2019a); Knoth <i>et al.</i> (2005b); Scherze <i>et al.</i> (2006); Surh <i>et al.</i> (2007); Wang <i>et al.</i> (2016); Yi <i>et al.</i> (2014)
	Polysaccharides & PGPR or Lecithin	2.5 – 16	30 – 80	Clausse <i>et al.</i> (2018); Gülseren <i>et al.</i> (2014); Iqbal <i>et al.</i> (2019a, 2019b); Knoth <i>et al.</i> (2005b); Massel <i>et al.</i> (2015); Scherze <i>et al.</i> (2006); Wardhono <i>et al.</i> (2014)

Particles	Non-Bio-derived	Silica	0.4 – 8	20 – 60	Ahuja <i>et al.</i> (2018); Drelich <i>et al.</i> (2010); Macedo Fernandes Barros <i>et al.</i> (2018); Masalova <i>et al.</i> (2013); Midmore (1999); Nesterenko <i>et al.</i> (2014); Pichot <i>et al.</i> (2012); Sacca <i>et al.</i> (2008); Santini <i>et al.</i> (2014); Skelhon <i>et al.</i> (2012); Tshilumbu <i>et al.</i> (2015); Venkataramani <i>et al.</i> (2016); Yan <i>et al.</i> (2001); Zhao <i>et al.</i> (2019) ^{*,**}
		Latex	1.5 – 6	20 – 50	Binks <i>et al.</i> (2001); Golemanov <i>et al.</i> (2006); Yan <i>et al.</i> (2001)
	Bio-derived	Cellulose	$3.8 \times 10^3 - 3$	20 - 89	Andresen <i>et al.</i> (2007); Duffus <i>et al.</i> (2016); Guo <i>et al.</i> (2017); Hu <i>et al.</i> (2015); Lee <i>et al.</i> (2014); Lif <i>et al.</i> (2010); Pang <i>et al.</i> (2018); Rein <i>et al.</i> (2012); Xhanari <i>et al.</i> (2011) *
		Lignin	8	50	Gould <i>et al.</i> (2016)
		Zein	2.5	10 – 30	Rutkevičius <i>et al.</i> (2018)
		Starch	0.5 – 2	50	Zhai <i>et al.</i> (2019)
		Sunflower oleosomes	0.5	10	Karefyllakis <i>et al.</i> (2019)

* = In some articles, surfactant were used in combination with the particles.

** = In some articles, biopolymers were used in combination with the particles.

2.4. Stabilization of W/O emulsions by surface active agents (surfactants)

2.4.1. Definition & characteristics

Surface active agents, known as surfactants, are used to generate W/O emulsions because they have the ability to lower the surface tension at the W-O interface (Opawale *et al.*, 1998; Ushikubo *et al.*, 2014). A surfactant is a low-molecular weight emulsifier with an amphiphilic character having both polar (hydrophilic “head”) and non-polar (hydrophobic “tail”) parts (Dickinson, 1992). The characteristics of a particular surfactant depend on the nature of its head and tail groups. The head group may be anionic, cationic, amphoteric (both positive and negative electrical charge), or non-ionic. The tail group usually consists of one or more hydrocarbon chains, having between 10 and 20 carbon atoms per chain. Surfactant tails may be saturated or unsaturated, linear or branched, aliphatic and/or aromatic. The main low molecular weight surfactants used for W/O emulsion stabilization are polyglycerol polyricinoleate (PGPR), lecithin and sorbitan fatty acid esters.

2.4.2. W/O emulsions stabilized by low molecular weight surfactants

A number of studies have been undertaken using surfactants such as PGPR, lecithin and sorbitan fatty acid ester (*e.g.*, Span 20, 80 and 83) to stabilize W/O emulsions as shown in Table 2.2. PGPR and lecithin were mainly used to stabilize water droplets (up to 30 wt%) in soybean oil (Killian *et al.*, 2012). PGPR-stabilized droplets were significantly smaller and more stable than the ones stabilized by lecithin, with the latter showing evidence of flocculation immediately after emulsification (Killian *et al.*, 2012). This was attributed to the ability of PGPR to form elastic interfaces that slows down the rate of coalescence between droplets. The properties of lecithin-stabilized W/O emulsions were strongly dependent on the lipid type used as continuous phase. Emulsions containing sunflower or olive oil produced smaller water droplets characterized by aggregates, due to the high content of long-chain

triacylglycerol present in the oils (Knoth *et al.*, 2005a). On the other hand, MCT oil (used as continuous phase) led to the formation of larger water droplets with a lower bulk viscosity compared to that of sunflower and olive oil emulsions (Knoth *et al.*, 2005a).

Similar work has been done by Ushikubo *et al.* (2014) where the stability of W/O emulsions (30 - 40 vol% water) was evaluated in the presence of different surfactants (PGPR, lecithin and Span 80) and different oils as the continuous phase (soybean oil and hexadecane). Emulsions with higher kinetic stability (> 14 days) and smaller water droplets ($d_{43} \sim 1 - 4 \mu\text{m}$) were observed in the systems containing soybean oil and PGPR or hexadecane with Span 80 (Ushikubo *et al.*, 2014). The molecular structure of both oil and emulsifier were important to define the emulsion stability, where better chemical affinity of the hydrophobic moieties of the emulsifier and the oil led to more stable water droplets (Ushikubo *et al.*, 2014).

Addition of salt (NaCl, CaCl₂ or other calcium salts up to 0.25 M) was essential to achieve coalescence-stable emulsions prepared with PGPR. The addition of electrolytes to the dispersed phase was shown to lower the rate of Ostwald ripening and hinder the increase in size of the water droplets with time (Koroleva *et al.*, 2003; Wolf *et al.*, 2013). However, this coalescence stable system was not seen in the emulsions stabilized by lecithin where coalescence of water droplets and phase separation was observed (Scherze *et al.*, 2006). Addition of salt in the aqueous phase resulted in an increase on the surface active impurities from the commercial vegetable oil to the interface due to the ability of salt to bind with the fatty acids present in the oil, reducing the interfacial tension. However, lecithin-stabilized W/O emulsions are sensitive to the presence of other surface active substances and adsorption of impurities can favour interfacial film breakdown and contribute to the rapid coalescence of water droplets (Scherze *et al.*, 2006).

The interfacial rheological film strength is an important contributor to W/O emulsion stability, since film strength and emulsion stability followed the same trends (Opawale *et al.*, 1998). Electrolytes were shown to change the hydrophilicity/hydrophobic balance and the hydration conditions of the

surfactants by depletion of the hydration shell around the polar head groups of surfactant molecules (Kawashima *et al.*, 1992). With an increase in the hydrophobicity of the surfactant and hydrophobic interactions, a relatively rigid surfactant molecule layer would be formed (Kawashima *et al.*, 1992). In addition Márquez *et al.* (2010) explained that the stabilizing effect of salt (up to 1000 mg Ca/ 100 g aqueous phase) in the emulsions containing PGPR (up to 1 wt%) was attributed to the diminution of the water droplets size ($d_{43} = 6$ and $1 \mu\text{m}$ for no added salt and added salt emulsions, respectively) and decrease of the attractive forces between water droplets (Márquez *et al.*, 2010). According to Israelachvili (2015), the attractive forces (by van der Waals interactions) between two water droplets in the oil continuous phase (e.g., mineral oil) is at minimum when the refractive indices and/or the dielectric constants of the two phases are matched. Increasing the electrolyte concentration, increases the detachment of the water phase, and thus decreases the refractive index difference between oil and water phases. Thus, the addition of salt into the water phase would decrease the attractive forces between water droplets, reducing the collision frequency. In this way, calcium salt would allow the production of W/O emulsions with higher stability to coalescence (Márquez *et al.*, 2010).

2.5. W/O emulsions stabilized by biopolymers

2.5.1. Definition & characteristics

Proteins and polysaccharides are biopolymers that are used to stabilize emulsions in food products. Proteins are polymers of amino acids, whereas, polysaccharides are polymers of monosaccharides. A biopolymer can be incorporated into the surface of an emulsion in two ways depending on whether the biopolymer is surface active (most proteins) or non-surface active (most polysaccharides) (Dickinson, 2011). Therefore, they associated with the interfacial region either:

- (a) by adsorption directly to the interface during droplet formation and stabilization, or

(b) through interactions with a biopolymer layer which is already located at the interface (Dickinson, 2011).

All proteins contain both hydrophilic and hydrophobic regions along their backbones (Dickinson, 2003) whereas only limited number of natural polysaccharides have non-polar side chains attached to their polar backbones (McClements, 2015). Some polysaccharide chains that are largely hydrophilic may contain small amounts of protein 'impurities' that impart surface activity (Osano *et al.*, 2010). Therefore, the driving force for adsorption of these amphiphilic biopolymers to interfaces is the hydrophobic effect (McClements, 2015). The hydrophobic effect arises from the tendency of non-polar groups to accumulate away from water, when the biopolymer is dispersed in an aqueous phase. Once a biopolymer is adsorbed at an interface, it undergoes structural rearrangement where the non-polar groups are more closely associated with the oil phase and the hydrophilic groups are located in the aqueous phase. Adsorption also reduces the contact area between the oil and water molecules at the interface, lowering the interfacial tension (McClements, 2015).

Random-coil biopolymers (*e.g.*, polypeptides) are fairly flexible molecules and can, thus, rearrange their structures rapidly at the O-W interface. On the other hand, globular biopolymers (*e.g.*, proteins) are more rigid molecules and, hence, rearrange their structures more slowly at the interface. They unfold at an interface and usually expose amino acids that were originally located in the hydrophobic interior of the molecule, leading to enhanced interactions with neighbouring protein molecules through hydrophobic attraction or disulphide bond formation (Tcholakova *et al.*, 2006). Consequently, globular biopolymers tend to form relatively compact films at interfaces with high viscoelasticity (McClements, 2015).

2.5.2. Biopolymer & surfactant-stabilized W/O emulsions

There has been not a single study using a biopolymer alone as a sole emulsifier for W/O emulsions, so combinations of biopolymers and surfactants have been discussed in this review. Increasing the viscosity of the aqueous

phase has also been proposed to improve W/O emulsion stability that are already stabilized by a surfactant. The incorporation of a thickening or gelling polymer (e.g., xanthan, gelatine, WPI, sodium caseinate, pectin, lactoferrin, β -lactoglobulin, glucono-d-lactone (GDL)) within the dispersed aqueous phase has been proposed as a way of improving the long-term stability of W/O emulsions stabilized by surfactants such as PGPR, especially if the added polymer forms a network throughout the internal water droplet or a gel-like layer at the inner W-O interface either by cross-linking with enzyme or calcium ions or by thermal processing (Table 2.2) (Gülseren *et al.*, 2012, 2014; Iqbal *et al.*, 2012, 2013c; Surh *et al.*, 2007; Wang *et al.*, 2016; Zhu *et al.*, 2015).

Drop shape tensiometry studies have demonstrated that β -lactoglobulin and sodium caseinate can further decrease the interfacial tension of an interface loaded with PGPR, and that the viscoelastic properties of β -lactoglobulin covered interface are affected by the presence of PGPR in the oil phase (Gülseren *et al.*, 2012). It was identified that PGPR interacts with the hydrophobic moieties of the protein, causing changes in the viscoelastic properties of the interface; its presence dominates the elastic properties of the interfacial film, even at fairly low concentrations (up to 0.1 and 0.008 wt% of protein and PGPR, respectively) (Gülseren *et al.*, 2012). These results demonstrated that there were synergistic effects between the hydrophobic emulsifier and protein molecules in the water phase (Gülseren *et al.*, 2012).

An irreversible liquid-to-solid transition was undertaken when the WPI presented into the aqueous phase of W/O emulsions stabilized by PGPR (in soybean oil phase) and when the emulsion was heated above the thermal denaturation temperature of WPI (Iqbal *et al.*, 2012; Surh *et al.*, 2007). This caused protein gelation into the aqueous phase where protein microspheres were formed into the oil phase. Aggregation of microsphere into the aqueous phase formed a three-dimensional network at high aqueous phase contents (> 30 wt%) (Iqbal *et al.*, 2012). The materials formed exhibited a non-ideal plastic behaviour: they were solid-like at low stresses, fluid-like (shear-thinning) at intermediate stresses, and became disrupted at high stresses (shear rate $\sim 20 \text{ s}^{-1}$) (Iqbal *et al.*, 2012). In another study, W/O emulsions were

prepared with phosphatidylcholine depleted lecithin in sunflower oil and sodium caseinate (SC), whey protein isolate (WPI), gelatine and/or xanthan incorporated into the aqueous phase (Knoth *et al.*, 2005b). Emulsions were more stable and smaller in size when they contained WPI with xanthan in the aqueous phase ($d_{43} \sim 1 - 2 \mu\text{m}$) than those without any biopolymer into the aqueous phase ($d_{43} \sim 3 - 5 \mu\text{m}$). In contrast, the addition of gelatine or SC resulted in an increase in water droplet size ($d_{43} \sim 10 - 20 \mu\text{m}$) and rapid sedimentation of the dispersed water phase. WPI and xanthan presented to the aqueous phase, increased the viscosity of the water phase while not induced a strong reduction in interfacial tension nor a negative interaction with lecithin at the interface (Knoth *et al.*, 2005b). However, adding unfolded proteins (gelatine, SC) with high surface activity to the water phase caused an increased instability of the W/O emulsion with fractionated lecithin (Knoth *et al.*, 2005b). Addition of gelatine or SC led to a drastic increase in water droplet size due to the rapid adsorption of gelatine or SC at the interface, thus, lecithin was not able to completely displace gelatine or SC from the droplet surface and form a uniform layer at the interface.

In a different study, casein dispersions containing glucono-d-lactone (GDL) and soybean oil with PGPR were homogenized to form W/O emulsions (Wang *et al.*, 2016). GDL was hydrolysed to gluconic acid inside the aqueous phase, causing a gradual reduction on the pH value. When the pH reached the isoelectric point of casein ($pI = 4.6$), gelation of the inner aqueous phase was occurred (Wang *et al.*, 2016). The GDL-induced casein gels in the inner aqueous phase provided higher resistance to destabilization than the non-gelled W/O emulsions. In addition, the size of the emulsions formulated by the gelled aqueous phase and 2% PGPR was even smaller ($\sim 649 \text{ nm}$) after 90 days of storage than emulsions with 6% PGPR in the absence of the gelled aqueous phase ($\sim 1128 \text{ nm}$, after 90 days) (Wang *et al.*, 2016). Pectin was used, as well, as a gelling agent into the aqueous phase (& PGPR in the oil phase) to increase the stability of the aqueous droplets by creating interacting films with polysaccharides at the W-O interface. It was demonstrated that the presence of high methoxyl (HMP) or low methoxyl pectin (LMP) in the aqueous phase of PGPR-stabilized emulsion caused the formation of smaller

water droplets (~ 305 and 317 nm for HPM and LMP, respectively) and more stable emulsions than the same PGPR stabilized emulsion without pectin (~ 440 nm) (Massel *et al.*, 2015).

2.6. Stabilization of W/O emulsions by particles (Pickering stabilization)

2.6.1. Definition & characteristics

The term Pickering stabilization is used for finely divided insoluble solid particles that stabilize emulsions preventing coalescence and film drainage (Pickering, 1907; Tambe *et al.*, 1994). Finkle *et al.* (1923) stated that in an emulsion containing solid particles, the liquids which wet the solid less than the other liquid is the dispersed phase. This type of stabilization involves either the adsorption of discrete solid particles at the interface or the sintering of crystals at the interface (Ngai *et al.*, 2014). Solid particles unable to reside at the interface remain in the continuous phase to form a network in the bulk continuous phase due to van der Waals interactions (Ghosh *et al.*, 2011b). This network prevents water droplet collision, reducing the risk of coalescence, hence the term network stabilization attracted a significant attention in the literature (Ngai *et al.*, 2014). An effective Pickering stabilization can be achieved when the average size of adsorbed particles is at least an order of magnitude smaller than the emulsion droplet size (Dickinson, 2012). Depending on the size and wetting angle (see § 2.6.2.) which the particles enclose with a W-O interface, the energy of attachment may exceed 10^6 kT, as shown in equation (2.4) below, and thus particle adsorption is virtually irreversible (Binks, 2002). This high detachment forces is the reason for the increased stability of particle-stabilized emulsions compared to conventional surfactant-stabilized systems. Example of food emulsions stabilized by Pickering stabilization is margarine, which contains fat crystals (Dickinson, 1992; Ngai *et al.*, 2014).

The permanence of the particle-surface binding arises from the high free energy of spontaneous desorption (ΔG_d) compared with the thermal energy (Dickinson, 2012):

$$\Delta G_d = \pi r^2 \gamma_{ow} (1 \pm \cos(\theta))^2 \quad (2.4)$$

where γ_{ow} is the interfacial tension between the oil and aqueous phases; θ is the particle contact angle (the sign inside the bracket is negative if the particle are removed into the aqueous phase and positive if removed into the oil phase); and r is the particle radius. Therefore, the ΔG_d is related to the interfacial tension (γ_{ow}) and the size of the solid particles. As soon as a spherical particle is attached to the W-O interface with contact angle not too close to 0 or 180°, it can be considered as being irreversibly adsorbed because the value of ΔG_d can be 1000s of kT. Therefore there is a huge energy barrier for droplet shrinkage or coalescence, and the emulsions are very stable (Luo *et al.*, 2011). Adsorption is stronger when the contact angle is 90°, which corresponds to a maximum stability of emulsions in most instances.

2.6.2. Wettability

The contact angle (θ) describes the wettability of a spherical particle at the interface, thus, it is used to identify whether the particle resides in water or oil phase (Binks, 2002). If θ , measured into the aqueous phase, is smaller than 90° then a larger fraction of the particle surface resides in aqueous than in the non-polar phase, *i.e.*, the particle is hydrophilic and stabilizes an O/W emulsion. However, if θ is generally greater than 90°, the particle resides more in oil phase, the particle is hydrophobic and stabilizes a W/O emulsion. Particles wetted equally by oil and water have contact angle exactly 90° (Binks, 2002). The three-phase contact angle is related to the balance of surface free energies at the particle-water (γ_{pw}), particle-oil (γ_{po}) and oil-water (γ_{ow}) interfaces (Figure 2.4) and is expressed by the classic Young's equation (equation (2.5)) (Binks *et al.*, 2006; Dickinson, 2012).

$$\cos(\theta) = \frac{(\gamma_{po} - \gamma_{pw})}{\gamma_{ow}} \quad (2.5)$$

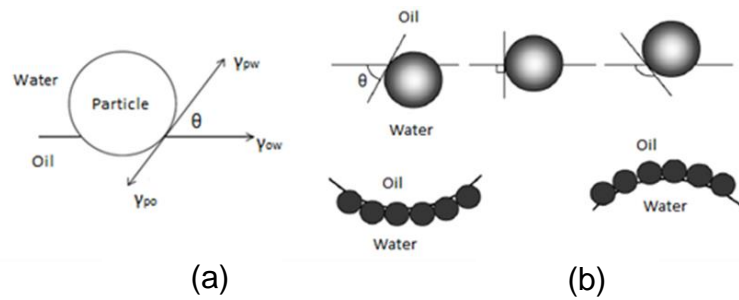


Figure 2.4. (a) The three-phase contact angle is related to the balance of surface free energies at the particle-water, particle-oil and water-oil interfaces. (b) Hydrophilic particle ($\gamma_{po} > \gamma_{pw}$) with contact angle smaller than 90° form O/W emulsions (left). Hydrophobic particles ($\gamma_{po} < \gamma_{pw}$) with contact angle bigger than 90° form W/O emulsions (right).

2.6.3. Macroscopic configurations and stabilization mechanisms

For particle-stabilized emulsions, several configurations may exist that would prevent droplet coalescence and promote droplet stability (Binks *et al.*, 2006). Most often extensive coverage of droplets by particles occurs, where droplets are surrounded by two layers of particles as shown in Figure 2.5 (a). Coalescence is then prevented when droplets approach each other, due to the presence of two layers of particles. Another possible configuration is shown in Figure 2.5 (b). It involves the formation of a single layer of particles between interfaces shared by two adjacent emulsion droplets and is called "bridged" Pickering stabilization, which usually occurs in presence of limited amount of particles. In order to avoid collision with this type of configuration, particles need to have an interfacial position with the majority portion of the particle in the continuous phase (Binks *et al.*, 2006). The final possible configuration of particle-stabilized emulsions is the formation of a three-dimensional network of particles between emulsion droplets. It exists when an excess of particles is presented in the continuous phase and a dense layer of particles is still presented at the droplet surface as shown in Figure 2.5 (c).

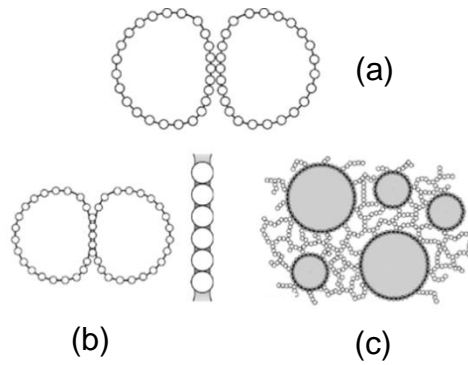


Figure 2.5. Possible configurations of particles in solid-stabilized emulsions (Binks *et al.*, 2006).

Some important mechanisms that contribute to the prevention of coalescence in the configurations discussed above are shown in Figure 2.6. Firstly, steric hindrance prevents particle displacement and lateral movement from the interface (Figure 2.6 (i) and (ii)). The lateral displacement is responsible for emulsion stability only when the surface concentration of particles is sufficiently high at the interface (Binks *et al.*, 2006). Additionally, the stability of the thin film of continuous phase formed between the emulsion droplets is influenced by the maximum capillary pressure, preventing the film thinning (Figure 2.6 (iii)), and the rheological properties of the interfacial film, affecting film drainage (Figure 2.6 (iv)). These stabilization mechanisms are dependent on the properties of the particles and emulsion systems (Binks *et al.*, 2006).

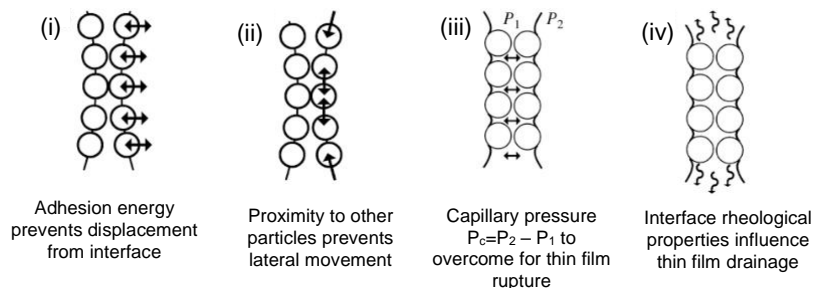


Figure 2.6. Possible mechanisms responsible for stability of particles in solid-stabilized emulsions (Binks *et al.*, 2006).

2.6.4. Particle-stabilized W/O emulsions

Mostly, synthetic particles, such as hydrophobic silica, polystyrene latex, modified biopolymers, such as, cellulose, lignin, starch, zein, and so forth, have been used in the literature to stabilize W/O emulsions (see Table 2.2). In the next section, W/O emulsions stabilized by non-bio-derived and bio-derived particles will be discussed as well as those stabilized by a combination of particles and surfactants/ biopolymers.

2.6.4.1 Non-bio-derived particles

a) Silica particles

Hydrophobic silica has attracted significant research attention due to its high three-phase contact angle (up to 96°) which renders it to stabilize W/O emulsion (Yan *et al.*, 2001). Fumed silica particles became hydrophobic after their surface silanols are replaced by silane or siloxane hydrophobic agents. It was found that the stability and the type of emulsions formed, were dependent on the hydrophobicity (contact angle) of the particles in the continuous phase, as shown in Figure 2.7 (Yan *et al.*, 2001). When hydrophilic particles (Sample #1, $\theta = 0^\circ$ and #2, $\theta = 60^\circ$, Figure 2.7) were used, no W/O emulsions formed, and most of the particles remained into the water phase (Yan *et al.*, 2001). When the particles were more hydrophobic (Samples #3, $\theta = 67^\circ$ and #4, $\theta = 75^\circ$, Figure 2.7), all the water in the system became dispersed into toluene to form very stable W/O emulsions, with water droplets diameter as small as $2\ \mu\text{m}$ (Yan *et al.*, 2001). When the hydrophobicity of the particles was further increased (Samples #5, $\theta = 86^\circ$ and #6, $\theta = 96^\circ$, Figure 2.7), not all the water in the system could be emulsified, and the emulsions formed were not as stable as those of Samples #3 or #4 (Figure 2.7) (Yan *et al.*, 2001). From the results presented above, it is clear that the ability of particles to stabilize W/O emulsions is related to the degree of hydrophobicity.

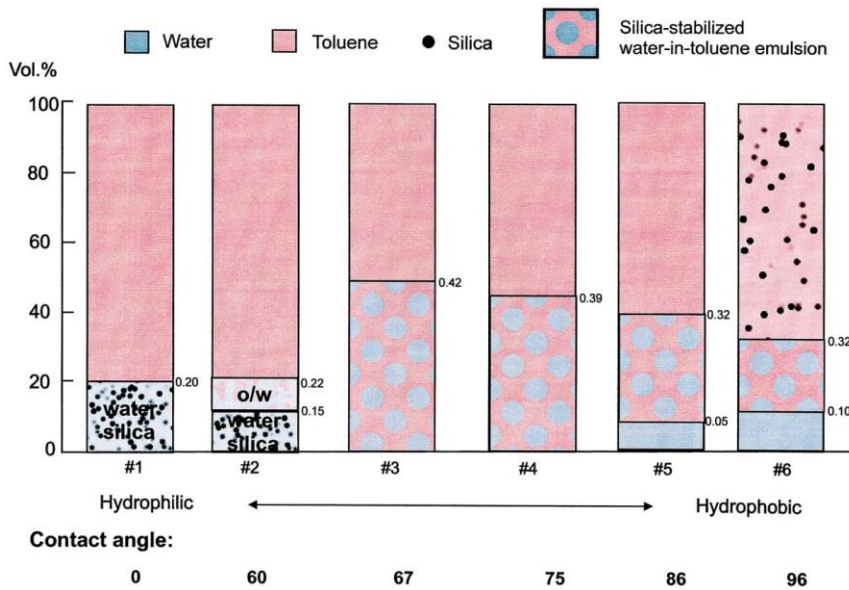


Figure 2.7. Preparation of water-in-toluene emulsions stabilized by silica nanospheres with different contact angles (volume fraction of water: 0.20, silica concentration: 5 kg m^{-3}) (Yan *et al.*, 2001).

When dispersed in oil, such silica particles are often partially flocculated (Masalova *et al.*, 2013; Midmore, 1999; Nesterenko *et al.*, 2014; Yan *et al.*, 2001). Solid hydrophobic silica particles efficiently stabilize emulsion droplets (30 wt% water) by forming a three-dimensional network in the continuous oil phase and preventing droplet coalescence. However, no interfacial tension reduction was observed at the W-O interface in the presence of silica particles (Drelich *et al.*, 2010). Addition of surfactant (Span 80 or sorbitan monooleate (SMO) in oil phase) in particle-stabilized W/O emulsion showed a decreased in the interfacial tension, indicating the existence of interactions between particles and emulsifier at the interface (Drelich *et al.*, 2010; Masalova *et al.*, 2013; Nesterenko *et al.*, 2014; Tshilumbu *et al.*, 2015). The presence of closely packed aggregates around the large droplets in emulsions stabilized by small amount of surfactant (0.1 wt%) and silica particles (1.8 wt%) showed an improvement on the stability for up to 21 days without any indication of phase separation (Nesterenko *et al.*, 2014). However, emulsions prepared solely by silica particles showed a 15% oil separation after 21 days and they were bigger in size ($\sim 13 \mu\text{m}$) comparing those in the presence of surfactant ($\sim 4 \mu\text{m}$), probably due to the ability of surfactant molecules to adsorb onto the particles' surface prior the emulsification. It was found that the stability

enhancement was more pronounced at low surfactant concentrations, when particles start to dominate over surfactants forming a three-dimensional network into the oil continuous phase (Masalova *et al.*, 2013; Nesterenko *et al.*, 2014).

Highly stable silica stabilized W/O emulsions (60 vol% water) have been prepared by incorporating hydroxyl propyl cellulose (HPC) in the dispersed aqueous phase (Midmore, 1999). Addition of strong acid or alkali in the aqueous phase caused gelation of the HPC and flocculation to the system due to acid- or alkali-catalysed cleavage of surface siloxane groups, resulting in an increase in silanol groups and thereby hydrogen bonding (Midmore, 1999). Similar work has been done by Skelhon *et al.* (2012) who used hydrophobic fumed silica particles (in oil phase) in combination with chitosan (low and medium molecular weight (75 - 85%) into the aqueous phase) under acidic conditions (pH 3.2 – 3.8) to prepare W/O emulsions. Adsorption of the positively charged chitosan onto the surface of the negatively charged silica particles (due to electrostatic attraction) influenced the particle's wettability making it an effective Pickering stabilizer (Skelhon *et al.*, 2012). It was identified that as the concentration of silica particles increased (0.6 to 5.3 wt%), at constant concentration of chitosan (1 wt%), a continuous network of colloidal flocs was formed, which effectively renders the emulsion into a quiescent state, where the sedimentation of water droplets reduced due to the formation of solid like matrix. In addition, the viscosity of the system increased from 690 mPa·s to ~ 2000 mPa·s when the chitosan concentration increased from 0 to 1 wt%. Zhao *et al.* (2019) identified that combining silicones (SO), modified silicones (DC8500) and starch in the dispersed phase, high internal phase emulsions were prepared with up to 83 vol% water and were stable for more than 6 months. Without the addition of starch in the aqueous phase, the water content in stable emulsions could only be raised up to 20 wt% (Zhao *et al.*, 2019). Therefore, food-grade starch enhanced both water content and stability of emulsion when added at low concentration (Zhao *et al.*, 2019).

b) Latex particles

Organic latex particles, which are probably the most widespread type of monodisperse colloids, have found a relative narrow range of application as emulsifiers. The reason seems to be that, under normal conditions, latex particles (initially dispersed in water) do not adsorb well at the W-O interface. Latex particles tend to be hydrophobic, even though they are synthesized and dispersed in water due to the ionisable surface sulfate groups, and can stabilize W/O emulsions (Binks *et al.*, 2001). This fact opposes the empirical Bancroft rule, which states that “in order to have a stable emulsion, the emulsifier must have a relative dispersibility in the continuous phase” (Tsabet *et al.*, 2015). This rule works very well for surfactant-stabilized emulsions which has been shown that when the surfactant is dissolved in the dispersed phase, it efficiently suppresses the surface (Gibbs) elasticity of the adsorption monolayer (Traykov *et al.*, 1977a; Traykov *et al.*, 1977b). However, in the case of Pickering emulsions, the stability is ensured by the formation of a dense (shell-like) particle adsorption layer, irrespective of from where these particles originate.

Emulsions formed with cyclohexane and either “hydrophilic” aldehyde/sulfate particles or “hydrophobic” sulfate latex particles (dispersed in the water phase) formed stable W/O emulsions over a wide range of salt concentrations (10^{-3} – 1 M) and water volume fractions ($\phi_w = 0.2$ – 0.9). Such emulsions were stable for over 6 months with no sign of coalescence. Increasing the water volume fraction (from $\phi_w = 0.1$ to 0.8), a transition from a non-flocculated to a flocculated system was observed, as predicted theoretically for charged water droplets in oil (Albers *et al.*, 1959; Binks *et al.*, 2001). Due to the large number of water droplets at higher water volume fraction, the energy barrier was lowered and the stability against flocculation was reduced. Such considerations lead to the prediction that, for a fixed Debye length, W/O emulsions of low water volume fraction were stable to flocculation whilst flocculation was enhanced continuously with increasing volume fraction (Albers *et al.*, 1959).

2.6.4.2 Bio-derived particles

A lot of studies have been done on stabilizing W/O emulsions using bio-derived particles however most of these particles have received a sort of chemical treatment or complex formation with other chemicals in order to become more hydrophobic and increase their potential for W/O stabilization.

a) Modified cellulose

Cellulose is the most abundant biopolymer in Nature. It is biodegradable and renewable, and can be manufactured by sustainable technology, and possesses some very interesting chemical and physical properties (Moon *et al.*, 2011; Siró *et al.*, 2010). In the native state, cellulose consists of long chains of poly- β -(1 \rightarrow 4)-D-glucosyl residues (Andresen *et al.*, 2007). During biosynthesis, these chains aggregate to form microfibrils, which are long, thread-like, highly crystalline bundles of molecules stabilized laterally by intermolecular hydrogen bonds. The production of nanoscale cellulose fibers and their application in composite materials has gained increasing attention due to their high strength and stiffness combined with low weight, biodegradability and renewability (Siró *et al.*, 2010).

In 1986, Oza *et al.* (1986) presented the first scientific study of microcrystalline cellulose (MCC)-stabilized Pickering emulsions. The authors proposed that, in addition to their "active" role at the interface, the MCC particles form a three-dimensional network structure in the continuous phase of O/W emulsions, which provides further retardation of coalescence through entrapment of emulsion droplets (Oza *et al.*, 1986). Due to the hydrophilic nature of the cellulose molecules, the fibrils and microfibrils are better wetted by water than oil, and, thus, tend to stabilize water-continuous emulsions. However, preparation of hydrophobic modified microfibrillated cellulose (MFC), through silylation with different surface substitutions (DSS of 0.6, 0.9 and 1.1), caused the formation of a contact angle $> 90^\circ$, which stabilized W/O emulsions (Andresen *et al.*, 2006; Andresen *et al.*, 2007). The contact angles of modified MFC were 132, 146 and 97° for DSS of 0.6, 0.9 and 1.1. The

stability against sedimentation increased with increasing MFC concentration, due to an increase in the viscosity of the continuous oil-phase. At fixed concentration and toluene:water ratio (7:3 ratio), the smallest drops were achieved with MFC of moderate hydrophobicity (DSS 0.6) (Andresen *et al.*, 2007). Consequently, these emulsions also displayed the highest stability against sedimentation. Upon increasing the hydrophobicity of the MFC (from DSS 0.6 to 1.1), an increase in the average drop size was observed (from 50 to 200 μm) (Andresen *et al.*, 2007).

Guo *et al.* (2017) prepared a novel W/O Pickering emulsifier through the fabrication of cellulose nanocrystals (CNCs) by substituting some of the CNC hydroxyl groups with alkyl groups (via a chemical reaction with n-octadecyl isocyanate). Alkyl-intercalated CNCs with different particle lengths (77 – 84 nm) failed to stabilize W/O emulsions, if hydroxyl groups were fully substituted with alkyl groups but alkyl-intercalated CNCs with intermediate degrees of substitution possessed a good emulsifying capacity (Guo *et al.*, 2017). Results showed that alkyl-intercalated CNCs with different degrees of substitution gave similar interfacial tensions, possessed similar molecular arrangement of internal intercalated alkyls, but exhibited different contact angles ranging between 124 - 147°. Increasing degree of substitution gave larger contact angles and increasing ease of dispersibility in the oil phase (Guo *et al.*, 2017).

b) Lignin and modified-starch particles

Lignin is also an extremely abundant terrestrial biopolymer, accounting for approximately 30% of the organic carbon in the biosphere (Boerjan *et al.*, 2003). It is characterized by its highly branched heterogeneous structure built from cross-linking various phenolic residues (Gould *et al.*, 2016). Lignin is crucial for structural integrity of the cell wall, stiffness and strength of the stem. In addition, lignin acts as a waterproof coating to the cell wall, enabling transport of water and solutes through the vascular system, and plays a role in protecting plants against pathogens (Boerjan *et al.*, 2003). Ground coffee waste is rich in lignin and has been investigated as a potential Pickering stabilizer. Hydrothermal treatment of lignin, adapted from the bioenergy field,

has been used to generate lignin particle capable of stabilizing W/O emulsions (Gould *et al.*, 2016). The hydrothermal treatment caused relocation of the lignin component present in the cell walls of the coffee particles, onto the particle surface in the form of droplets, thereby increasing the surface hydrophobicity of the particles (Gould *et al.*, 2016). Emulsions stabilized by lignin particles (8 wt%) showed an intermediate stage coalescence – termed arrested coalescence (Gould *et al.*, 2016). However, the W/O emulsions were not analysed further because the large size of the water droplets stabilized by hydrothermally treated waste coffee particles were not desirable in food products due to their predictable instability towards shear and mixing processes (Gould *et al.*, 2016). More work is needed to improve the properties of lignin particles in order to be able to adsorb easily at the W-O interface and stabilize W/O emulsions for long time period.

Starch is a natural, renewable, and biodegradable polymer produced by many plants as a source of stored energy (Le Corre *et al.*, 2010). It is one of the most abundant biomass material in Nature. It is found in plant roots, stalks, seeds, and staple crops such as rice, corn, wheat, tapioca, and potato (Le Corre *et al.*, 2010). Starch consist of two types of molecules: amylose (linear polymer of α -D-glucose units linked by α -1,4 glycosidic linkages) and amylopectin (branched polymer of α -D-glucose units linked by α -1,4 and α -1,6 glycosidic linkages) (Singh *et al.*, 2010). Corn starch was successively esterified by p-toluenesulfonyl chloride (TS) and palmitoyl chloride (PA) (Zhai *et al.*, 2019) and used as a W/O emulsifier. The palmitoyl groups imparted sufficient hydrophobicity to the resultant starch-mixed ester to avoid the aggregation and collapse of the nanoparticles in ethyl acetate. If the starch was modified only by PA, no stable W/O emulsions would be obtained, probably because the particles would be too hydrophobic to remain at the interface. TS was introduced into the starch backbone so that some degree of hydrophobicity may be incorporated, coupled with the relatively hydrophilic tosylate groups (Zhai *et al.*, 2019). The obtained starch-based nanoparticles were hydrophobic, ~ 150 nm in size and used as a Pickering emulsifier to stabilize water-ethyl acetate emulsions. The average size of the water droplets were ~ 34 μ m when the nanoparticle concentration was 0.5 wt%, and

decreased to ~ 10 μm with an increased in the nanoparticle concentration to 2 wt% (at a water volume fraction below 50 wt%). Therefore, the stability of the emulsions increased with increasing concentration of starch-based nanoparticles (Zhai *et al.*, 2019).

c) Modified-zein particles

The storage proteins of maize seeds are alcohol-soluble proteins that are collectively known as zein (Matsushima *et al.*, 1997). Their only known function is to store nitrogen for the developing seed (Matsushima *et al.*, 1997). Zein is one of the few hydrophobic, water insoluble biopolymers which have been approved for oral use by Food and Drug Administration (Patel *et al.*, 2014). The hydrophobicity of zein is attributed to the high percentage of non-polar amino acids (Leucine, Alanine and Pro-line), which together makes up more than 50% of its total amino acid content (Patel *et al.*, 2014). Rutkevičius *et al.* (2018) investigated the ability of zein particles (~ 180 nm) to stabilize oil continuous emulsions. It was found that zein colloidal particle dispersions in water at pH 4.0 emulsified with soybean oil produced W/O emulsions with water content \leq 30 vol% (stable for 1 hr) and water droplets size of ~ 100 μm (Rutkevičius *et al.*, 2018). Zein particles formed networks within water droplets as observed from cryo-SEM images (Figure 2.8), improving the stability of the emulsions. The use of particle dispersion of a pH = 6.5 (zein's isoelectric point) prior to emulsification, destabilized the suspension due to lower electrostatic repulsion, which lead to particle aggregation with sizes $>$ 6 μm and emulsions were stable only for few minutes (Rutkevičius *et al.*, 2018). Addition of lecithin into the oil phase (prior to emulsification) enhanced the hydrophobic character of zein particles and improved the stability of W/O emulsions (1 day) increasing as well the dispersed water content to 40 vol% (Rutkevičius *et al.*, 2018). However, more work is needed to improve the stability of W/O emulsions stabilized by zein particles.

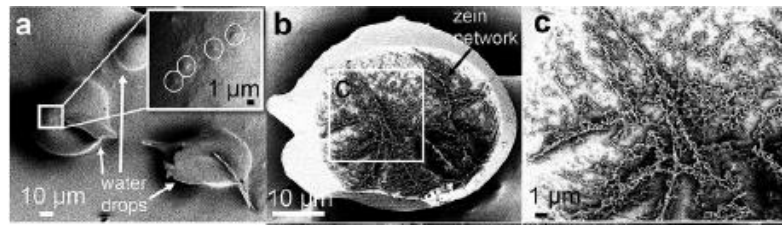


Figure 2.8. Cryo-SEM images of W/O emulsions with 20 vol% water. (a) Water droplets in oil with zein particles circled in the inset on one of the droplet surface; one droplet is cut-open during freeze-fracture. (b - c) A network of zein particles observed within the etched core of the water droplets (Rutkevičius *et al.*, 2018).

2.7. Rheological properties of W/O emulsions

Rheology plays an important role in food manufacture, *i.e.*, design of handling systems, quality control and evaluation of sensory stimuli associated with oral and non-oral evaluation of viscosity (Rao, 2010). The rheology of food emulsions is fundamental to their properties and often related to their stability (Gallegos *et al.*, 2004). In general, emulsion stability depends on droplet size distribution, rheology of the continuous phase and inter-particle interactions, temperature and water volume fraction. All these factors are strongly influenced by processing conditions, such as energy input during emulsification, residence time, application of thermal treatments, mixing efficiency, etc. (Gallegos *et al.*, 2004). Emulsions for industrial application are compositionally and structurally complex materials which can exhibit a wide range of different rheological behaviours, ranging from low-viscosity fluids (*e.g.*, milk and fruit juices) to hard solids (*e.g.*, butter or margarine) (McClements, 2015). Table 2.3 shows a summary of processing experiments (shear rate scanning experiment, frequency sweep experiment and temperature scanning experiment) for W/O emulsions stabilized by surfactants, biopolymers or particles.

Rheological studies on W/O emulsions stabilized by surfactants (Span 80) generally showed a non-Newtonian shear-thinning behaviour with dynamic viscosities (η) much higher ($\sim 1 - 8$ Pa·s) than pure oil (~ 0.14 mPa·s) (Almeida *et al.*, 2017). It was reported that by increasing the surfactant

concentration (0.25 - 3 wt%) present in the continuous phase, the bulk emulsion viscosity also increased (from 1 to 8 Pa·s), since surfactant-free molecules act as oil thickeners (Almeida *et al.*, 2017; Leal-Calderon *et al.*, 2007). Similar results were observed at W/O systems stabilised by particles (silica particles) and surfactants (Span 80), both present into the continuous phase (Nesterenko *et al.*, 2014). Silica particles alone in W/O emulsions, behave like a thickening agent due to the formation of a three-dimensional network in the continuous phase with a $\eta \approx 8 \text{ Pa}\cdot\text{s}$ (1 s^{-1}). However, addition of small amount of Span 80 (up to 0.1 wt%) in the bulk phase caused an increased in the η ($10 \text{ Pa}\cdot\text{s}$ at 1 s^{-1}) of the system due to the adsorption of the surfactant molecules on the particle surface (Nesterenko *et al.*, 2014). All samples showed a shear-thinning behaviour as the shear rate increased from 1 to 100 s^{-1} , where the gel-like structure was broken and droplets moved away from each other without showing any coalescence or phase separation. An increased of the bulk η of the W/O emulsion system was observed due to the addition of biopolymers, such as proteins or polysaccharides, into the aqueous phase showing an improvement of the stability of these emulsions. Addition of pectin into the aqueous phase of emulsions stabilized by PGPR (8 wt%) exhibited a significant improvement of the bulk η of the system (0.14 and 0.22 Pa·s for samples without and with pectin, respectively) (Massel *et al.*, 2015).

The type of oil also plays a significant effect on the rheological properties of W/O emulsions. Lecithin-stabilized W/O emulsions containing sunflower or olive oil formed small water droplets characterized by aggregates, and an increased viscosity with strong shear-thinning flow behaviour (Knoth *et al.*, 2005a). However, the application of MCT oil as continuous phase led to the formation of larger water droplets and emulsions with lower bulk viscosity which decreased only slightly with increasing shear rate ($0.1 - 500 \text{ s}^{-1}$) compared to the emulsions with sunflower and olive oil (Knoth *et al.*, 2005a). Emulsions prepared with high viscosity oils (sunflower or olive oil) showed an improvement of the stability and prevention of sedimentation of water droplets due to the presence of long-chain triacylglycerols in the continuous phase.

Temperature is another very important parameter to control the stability and rheological properties of W/O emulsions and a lot of studies have been undertaken to test the temperature effect during shearing of the emulsions (see Table 2.3). PGPR-stabilized emulsions containing three different types of polysaccharides (pectin, k-carrageenan or starch) in the aqueous phase (pH 3.5) showed different gelation properties before and after heating (Iqbal *et al.*, 2019b). Such behaviour can be attributed that thermal treatment increased the thickening and gelling properties of polysaccharides in emulsions, which leads to more elastic characteristics due to the creation of junction zones by polymer-polymer interlinked chains at acidic pH during heating and cooling phases. Similar results were observed by Iqbal *et al.* (2012) and Iqbal *et al.* (2013b), who identified that samples containing PGPR in the oil phase and WPI in the aqueous phase showed a solid-like behaviour at low shear rates and a fluid-like behaviour at high shear rates, using a temperature treatment from 30 to 90 °C.

Wardhono *et al.* (2014) measured the viscosity of W/O emulsions at different water volume fractions ($\phi = 60 - 80$ vol%) stabilized by PGPR with carboxymethyl cellulose (CMC) with glycerol dissolved in the aqueous phase. All the samples showed shear-thinning behaviour (at shear rates = 0.1 – 1000 s⁻¹) and the initial viscosity (at 0.1 s⁻¹) increased as the water volume fraction increased (the η of emulsions with $\phi = 60$ and 80 vol% was 10 and 10⁴ Pa·s, respectively) (Wardhono *et al.*, 2014). This increased on the η of emulsions containing 80 vol% water was due to the increase of the interactions between the water droplets that causing flocculation. During shearing, the apparent viscosity decreased due to the deformation or disruption of the droplet flocs present into the samples.

Table 2.3. Summary of processing experiments for W/O emulsions stabilized by surfactants, biopolymers or particles.

Emulsion stabilized by	References		
	Shear rate scanning	Frequency sweep experiment	Temperature scanning experiment
Surfactant	Almeida <i>et al.</i> (2017); Knoth <i>et al.</i> (2005a)	Almeida <i>et al.</i> (2017)	
Surfactant & Biopolymer	Iqbal <i>et al.</i> (2012, 2013b, 2013c); Iqbal <i>et al.</i> (2019a, 2019b); Knoth <i>et al.</i> (2005b); Massel <i>et al.</i> (2015)	Iqbal <i>et al.</i> (2012, 2013b, 2013c); Iqbal <i>et al.</i> (2019a, 2019b)	Iqbal <i>et al.</i> (2013b, 2013c); Iqbal <i>et al.</i> (2019a, 2019b); Knoth <i>et al.</i> (2005b)
Particles	Ahuja <i>et al.</i> (2018); Drelich <i>et al.</i> (2010); Gould <i>et al.</i> (2016); Nesterenko <i>et al.</i> (2014)	Midmore (1999); Nesterenko <i>et al.</i> (2014); Tshilumbu <i>et al.</i> (2015); Zhao <i>et al.</i> (2019)	

2.8. Conclusion

Food industries have given considerable emphasis on the development of lipid based food products with reduced levels of saturated, trans-fats and total fat, in order to prevent the global increase of obesity and food-linked cardiovascular diseases. However, one of the major challenges in developing these products is that fats play an important role in determining the desirable textural and sensory properties of many food products and it is very difficult to replace it. To address such challenges, incorporation of water in the form of water-in-oil (W/O) emulsions to replace fat has gained significant research attention. This review provided comprehensive insights on stabilization of W/O emulsions with clear focus on interfacial design with surfactants, biopolymers, particles and/or a combination thereof. Particular emphasis has been given to Pickering stabilization of water droplets stabilized by non-bio-derived as well as bio-derived particles with or without the addition of surfactants or biopolymers that allows long term kinetic stabilization of W/O emulsions against coalescence. In addition, the stability of W/O emulsions under processing conditions was also briefly discussed. Although extensive work has been done on non-bio-derived and non-biodegradable particles, attention

has been rarely given to biocompatible particles, proteins and a combination thereof to stabilize water-droplets for longer periods during ambient storage as well as processing conditions. Further work is needed on the stabilization of W/O emulsions using Pickering stabilizers which are natural, biodegradable and derived from renewable resource ingredients, *i.e.*, that can give a '*clean label*' on the final product and improve the stabilization of water droplets for the required period of time.

The following chapter (**Chapter 3**) will focus on assessing the ability of natural and biodegradable particles, such as polyphenol crystals, to act as Pickering stabilizers at the W-O interface and stabilize W/O emulsions. Additionally, these W/O emulsions stabilized by polyphenol crystals will be studied as a function of different polyphenol concentrations, pH values and water volume fractions.

References

- Abete, I., Goyenechea, E., Zulet, M., & Martinez, J. (2011). Obesity and metabolic syndrome: potential benefit from specific nutritional components. *Nutrition, metabolism cardiovascular diseases*, 21, B1-B15.
- Ahuja, A., Iqbal, A., Iqbal, M., Lee, J. W., & Morris, J. F. (2018). Rheology of hydrate-forming emulsions stabilized by surfactant and hydrophobic silica nanoparticles. *Energy fuels*, 32(5), 5877-5884.
- Albers, W., & Overbeek, J. T. G. (1959). Stability of emulsions of water in oil: II. Charge as a factor of stabilization against flocculation. *Journal of Colloid Science*, 14(5), 510-518.
- Almeida, M., Charin, R., Nele, M., & Tavares, F. (2017). Stability studies of high-stable water-in-oil model emulsions. *Journal of Dispersion Science Technology*, 38(1), 82-88.
- Andresen, M., Johansson, L.-S., Tanem, B. S., & Stenius, P. (2006). Properties and characterization of hydrophobized microfibrillated cellulose. *Cellulose*, 13(6), 665-677.
- Andresen, M., & Stenius, P. (2007). Water-in-oil emulsions stabilized by hydrophobized microfibrillated cellulose. *Journal of Dispersion Science Technology*, 28(6), 837-844.
- Bayarri, S., Taylor, A. J., & Hort, J. (2006). The role of fat in flavor perception: effect of partition and viscosity in model emulsions. *Journal of agricultural food chemistry*, 54(23), 8862-8868.

- Bhatti, H. S., Khalid, N., Uemura, K., Nakajima, M., & Kobayashi, I. (2017). Formulation and characterization of food grade water-in-oil emulsions encapsulating mixture of essential amino acids. *European journal of lipid science technology*, 119(6), 1600202.
- Bibette, J., Calderon, F. L., & Poulin, P. (1999). Emulsions: basic principles. *Reports on Progress in Physics*, 62(6), 969.
- Binks, B., & Lumsdon, S. (2001). Pickering emulsions stabilized by monodisperse latex particles: effects of particle size. *Langmuir*, 17(15), 4540-4547.
- Binks, B. P. (2002). Particles as surfactants—similarities and differences. *Current opinion in colloid & interface science*, 7(1-2), 21-41.
- Binks, B. P., & Horozov, T. S. (2006). *Colloidal particles at liquid interfaces*: Cambridge University Press.
- Boerjan, W., Ralph, J., & Baucher, M. (2003). Lignin biosynthesis. *Annual review of plant biology*, 54(1), 519-546.
- Borreani, J., Leonardi, C., Moraga, G., Quiles, A., & Hernando, I. (2019). How do Different Types of Emulsifiers/Stabilizers Affect the In Vitro Intestinal Digestion of O/W Emulsions? *Food biophysics*, 1-13.
- Brown, A., & Hanson, C. (1965). Effect of oscillating electric fields on coalescence in liquid+ liquid systems. *Transactions of the Faraday Society*, 61, 1754-1760.
- Brugger, B., Rosen, B. A., & Richtering, W. (2008). Microgels as stimuli-responsive stabilizers for emulsions. *Langmuir*, 24(21), 12202-12208.
- Campbell, G. M., & Mougeot, E. (1999). Creation and characterisation of aerated food products. *Trends in Food Science Technology*, 10(9), 283-296.
- Chen, B., Rao, J., Ding, Y., McClements, D. J., & Decker, E. A. (2016). Lipid oxidation in base algae oil and water-in-algae oil emulsion: Impact of natural antioxidants and emulsifiers. *Food research international*, 85, 162-169.
- Clausse, D., Lanoisellé, J. L., Pezron, I., & Saleh, K. (2018). Formulation of a water-in-oil emulsion encapsulating polysaccharides to improve the efficiency of spraying of plant protection products. *Colloids Surfaces A: Physicochemical Engineering Aspects*, 536, 96-103.
- Cosgrove, T. (2010). *Colloid science: principles, methods and applications*: John Wiley & Sons.
- Cotton, J. R., Burley, V. J., Weststrate, J. A., & Blundell, J. E. (2007). Dietary fat and appetite: similarities and differences in the satiating effect of meals supplemented with either fat or carbohydrate. *Journal of human nutrition dietetics: the official journal of the British Dietetic Association*, 20(3), 186-199.
- Destribats, M., Lapeyre, V., Sellier, E., Leal-Calderon, F., Schmitt, V., & Ravaine, V. (2011). Water-in-oil emulsions stabilized by water-

- dispersible poly (N-isopropylacrylamide) microgels: Understanding anti-Finkle behavior. *Langmuir*, 27(23), 14096-14107.
- Dhaka, V., Gulia, N., Ahlawat, K. S., & Khatkar, B. S. (2011). Trans fats—sources, health risks and alternative approach-A review. *Journal of food science technology*, 48(5), 534-541.
- Dickinson, E. (1992). *An introduction to food colloids*. Oxford ; New York: Oxford University Press.
- Dickinson, E. (2003). Hydrocolloids at interfaces and the influence on the properties of dispersed systems. *Food Hydrocolloids*, 17(1), 25-39.
- Dickinson, E. (2010). Food emulsions and foams: stabilization by particles. *Current Opinion in Colloid Interface Science*, 15(1-2), 40-49.
- Dickinson, E. (2011). Mixed biopolymers at interfaces: competitive adsorption and multilayer structures. *Food Hydrocolloids*, 25(8), 1966-1983.
- Dickinson, E. (2012). Use of nanoparticles and microparticles in the formation and stabilization of food emulsions. *Trends in Food Science & Technology*, 24(1), 4-12.
- Drelich, A., Gomez, F., Clause, D., & Pezron, I. (2010). Evolution of water-in-oil emulsions stabilized with solid particles: Influence of added emulsifier. *Colloids Surfaces A: Physicochemical Engineering Aspects*, 365(1-3), 171-177.
- Dridi, W., Essafi, W., Gargouri, M., Leal-Calderon, F., & Cansell, M. (2016). Influence of formulation on the oxidative stability of water-in-oil emulsions. *Food Chemistry*, 202, 205-211.
- Duffus, L. J., Norton, J. E., Smith, P., Norton, I. T., & Spyropoulos, F. (2016). A comparative study on the capacity of a range of food-grade particles to form stable O/W and W/O Pickering emulsions. *Journal of colloid interface science*, 473, 9-21.
- Finkle, P., Draper, H. D., & Hildebrand, J. H. (1923). The theory of emulsification¹. *Journal of the American Chemical Society*, 45(12), 2780-2788.
- Gallegos, C., Franco, J. M., & Partal, P. (2004). Rheology of food dispersions. *Rheology reviews*, 1, 19-65.
- Ghosh, S., & Rousseau, D. (2011a). Fat crystals and water-in-oil emulsion stability. *Current Opinion in Colloid Interface Science*, 16(5), 421-431.
- Ghosh, S., Tran, T., & Rousseau, D. (2011b). Comparison of Pickering and network stabilization in water-in-oil emulsions. *Langmuir*, 27(11), 6589-6597.
- Golemanov, K., Tcholakova, S., Kralchevsky, P., Ananthapadmanabhan, K., & Lips, A. (2006). Latex-particle-stabilized emulsions of anti-Bancroft type. *Langmuir*, 22(11), 4968-4977.
- Goodarzi, F., & Zendehboudi, S. (2019). A comprehensive review on emulsions and emulsion stability in chemical and energy industries. *The Canadian Journal of Chemical Engineering*, 97(1), 281-309.

- Gould, J., Garcia-Garcia, G., & Wolf, B. (2016). Pickering particles prepared from food waste. *Materials*, 9(9), 791.
- Gülseren, İ., & Corredig, M. (2012). Interactions at the interface between hydrophobic and hydrophilic emulsifiers: Polyglycerol polyricinoleate (PGPR) and milk proteins, studied by drop shape tensiometry. *Food Hydrocolloids*, 29(1), 193-198.
- Gülseren, İ., & Corredig, M. (2014). Interactions between polyglycerol polyricinoleate (PGPR) and pectins at the oil–water interface and their influence on the stability of water-in-oil emulsions. *Food Hydrocolloids*, 34, 154-160.
- Guo, J., Du, W., Gao, Y., Cao, Y., & Yin, Y. (2017). Cellulose nanocrystals as water-in-oil Pickering emulsifiers via intercalative modification. *Colloids Surfaces A: Physicochemical Engineering Aspects*, 529, 634-642.
- Hu, Z., Ballinger, S., Pelton, R., & Cranston, E. D. (2015). Surfactant-enhanced cellulose nanocrystal Pickering emulsions. *Journal of colloid interface science*, 439, 139-148.
- Iqbal, S., Baloch, M. K., Hameed, G., & Bano, A. (2013a). Impact of various parameters over the stability of water-in-vegetable oil emulsion. *Journal of Dispersion Science Technology*, 34(11), 1618-1628.
- Iqbal, S., Hameed, G., Baloch, M. K., & McClements, D. J. (2012). Formation of semi-solid lipid phases by aggregation of protein microspheres in water-in-oil emulsions. *Food research international*, 48(2), 544-550.
- Iqbal, S., Hameed, G., Baloch, M. K., & McClements, D. J. (2013b). Structuring lipids by aggregation of acidic protein microspheres in W/O emulsions. *LWT-Food Science Technology*, 51(1), 16-22.
- Iqbal, S., Hameed, G., Baloch, M. K., & McClements, D. J. (2013c). Structuring of lipid phases using controlled heteroaggregation of protein microspheres in water-in-oil emulsions. *Journal of food engineering*, 115(3), 314-321.
- Iqbal, S., Xu, Z., Huang, H., & Chen, X. D. (2019a). Controlling the rheological properties of oil phases using controlled protein-polysaccharide aggregation and heteroaggregation in water-in-oil emulsions. *Food Hydrocolloids*, 96, 278-287.
- Iqbal, S., Xu, Z., Huang, H., & Chen, X. D. (2019b). Structuring of water-in-oil emulsions using controlled aggregation of polysaccharide in aqueous phases. *Journal of food engineering*, 258, 34-44.
- Israelachvili, J. N. (2015). *Intermolecular and surface forces*: Academic press.
- Kabalnov, A. (2001). Ostwald ripening and related phenomena. *Journal of Dispersion Science Technology*, 22(1), 1-12.
- Karefyllakis, D., Van Der Goot, A. J., & Nikiforidis, C. V. (2019). The behaviour of sunflower oleosomes at the interfaces. *Soft Matter*, 15(23), 4639-4646.

- Kawashima, Y., Hino, T., Takeuchi, H., & Niwa, T. (1992). Stabilization of water/oil/water multiple emulsion with hypertonic inner aqueous phase. *Chemical pharmaceutical bulletin*, 40(5), 1240-1246.
- Khalid, N., Kobayashi, I., Neves, M. A., Uemura, K., & Nakajima, M. (2013). Preparation and characterization of water-in-oil emulsions loaded with high concentration of l-ascorbic acid. *LWT-Food Science Technology*, 51(2), 448-454.
- Killian, L. A., & Coupland, J. N. (2012). Manufacture and application of water-in-oil emulsions to induce the aggregation of sucrose crystals in oil: a model for melt-resistant chocolate. *Food biophysics*, 7(2), 124-131.
- Killian, L. B. A. (2011). *Development of water-in-oil emulsions for application to model chocolate products*. (Master of Science), The Pennsylvania State University,
- Knoth, A., Scherze, I., & Muschiolik, G. (2005a). Effect of lipid type on water-in-oil-emulsions stabilized by phosphatidylcholine-depleted lecithin and polyglycerol polyricinoleate. *European journal of lipid science technology*, 107(12), 857-863.
- Knoth, A., Scherze, I., & Muschiolik, G. (2005b). Stability of water-in-oil-emulsions containing phosphatidylcholine-depleted lecithin. *Food Hydrocolloids*, 19(3), 635-640.
- Koneva, A., Safonova, E., Kondrakhina, P., Vovk, M., Lezov, A., Chernyshev, Y. S., & Smirnova, N. (2017). Effect of water content on structural and phase behavior of water-in-oil (n-decane) microemulsion system stabilized by mixed nonionic surfactants SPAN 80/TWEEN 80. *Colloids Surfaces A: Physicochemical Engineering Aspects*, 518, 273-282.
- Koroleva, M. Y., & Yurtov, E. (2003). Effect of ionic strength of dispersed phase on Ostwald ripening in water-in-oil emulsions. *Colloid Journal*, 65(1), 40-43.
- Le Corre, D., Bras, J., & Dufresne, A. (2010). Starch nanoparticles: a review. *Biomacromolecules*, 11(5), 1139-1153.
- Leal-Calderon, F., Schmitt, V., & Bibette, J. (2007). *Emulsion science: basic principles*: Springer Science & Business Media.
- Lee, K.-Y., Blaker, J. J., Murakami, R., Heng, J. Y., & Bismarck, A. (2014). Phase behavior of medium and high internal phase water-in-oil emulsions stabilized solely by hydrophobized bacterial cellulose nanofibrils. *Langmuir*, 30(2), 452-460.
- Lif, A., Stenstad, P., Syverud, K., Nydén, M., & Holmberg, K. (2010). Fischer-Tropsch diesel emulsions stabilised by microfibrillated cellulose and nonionic surfactants. *Journal of colloid interface science*, 352(2), 585-592.
- Lucca, P. A., & Tepper, B. J. (1994). Fat replacers and the functionality of fat in foods. 5(1), 12-19.

- Luo, Z., Murray, B. S., Yusoff, A., Morgan, M. R., Povey, M. J., & Day, A. J. (2011). Particle-stabilizing effects of flavonoids at the oil– water interface. *Journal of agricultural and food chemistry*, *59*(6), 2636-2645.
- Macedo Fernandes Barros, F., Chassenieux, C., Nicolai, T., de Souza Lima, M. M., & Benyahia, L. (2018). Effect of the hydrophobicity of fumed silica particles and the nature of oil on the structure and rheological behavior of Pickering emulsions. *Journal of Dispersion Science Technology*, 1-10.
- Márquez, A. L., Medrano, A., Panizzolo, L. A., & Wagner, J. R. (2010). Effect of calcium salts and surfactant concentration on the stability of water-in-oil (w/o) emulsions prepared with polyglycerol polyricinoleate. *Journal of colloid interface science*, *341*(1), 101-108.
- Masalova, I., & Kharatyan, E. (2013). Effect of silica particles on stability of highly concentrated water-in-oil emulsions with non-ionic surfactant. *Colloid Journal*, *75*(1), 95-102.
- Massel, V., Alexander, M., & Corredig, M. (2015). The colloidal behavior of pectin containing water in oil emulsions as a function of emulsifier concentration. *Food biophysics*, *10*(1), 57-65.
- Matsushima, N., Danno, G.-i., Takezawa, H., & Izumi, Y. (1997). Three-dimensional structure of maize α -zein proteins studied by small-angle X-ray scattering. *Biochimica et Biophysica Acta -Protein Structure Molecular Enzymology*, *1339*(1), 14-22.
- Mazo Rivas, J. C., Schneider, Y., & Rohm, H. (2016). Effect of emulsifier type on physicochemical properties of water-in-oil emulsions for confectionery applications. *International Journal of Food Science Technology*, *51*(4), 1026-1033.
- McClements, D. J. (2015). *Food emulsions: principles, practices, and techniques*: CRC press.
- McClements, D. J., & Demetriades, K. (1998). An integrated approach to the development of reduced-fat food emulsions. *Critical Reviews in Food Science Nutrition, metabolism cardiovascular diseases*, *38*(6), 511-536.
- Midmore, B. (1999). Effect of aqueous phase composition on the properties of a silica-stabilized W/O emulsion. *Journal of colloid interface science*, *213*(2), 352-359.
- Moon, R. J., Martini, A., Nairn, J., Simonsen, J., & Youngblood, J. (2011). Cellulose nanomaterials review: structure, properties and nanocomposites. *Chemical Society Reviews*, *40*(7), 3941-3994.
- Murray, B. S. (2019). Microgels at fluid-fluid interfaces for food and drinks. *Advances in colloid interface science*, 101990.
- Nazari, M., Mehrnia, M. A., Jooyandeh, H., & Barzegar, H. (2019). Preparation and characterization of water in sesame oil microemulsion by spontaneous method. *Journal of Food Process Engineering*, e13032.

- Nehir El, S., & Simsek, S. (2012). Food technological applications for optimal nutrition: an overview of opportunities for the food industry. *Comprehensive Reviews in Food Science Food Safety*, 11(1), 2-12.
- Nesterenko, A., Drelich, A., Lu, H., Clause, D., & Pezron, I. (2014). Influence of a mixed particle/surfactant emulsifier system on water-in-oil emulsion stability. *Colloids Surfaces A: Physicochemical Engineering Aspects*, 457, 49-57.
- Ngai, T., & Bon, S. A. (2014). *Particle-stabilized emulsions and colloids: formation and applications*: Royal Society of Chemistry.
- Opawale, F. O., & Burgess, D. J. (1998). Influence of interfacial properties of lipophilic surfactants on water-in-oil emulsion stability. *Journal of colloid interface science*, 197(1), 142-150.
- Osano, J., Matia-Merino, L., Hosseini-Parvar, S., Golding, M., & Goh, K. (2010). Adsorption properties of basil (*Ocimum basilicum* L.) seed gum. *USM R & D*, 18(113), e117.
- Oza, K. P., & Frank, S. G. (1986). Microcrystalline cellulose stabilized emulsions. *Journal of dispersion science and technology*, 7(5), 543-561.
- Pan, L., Tomás, M., & Añón, M. (2002). Effect of sunflower lecithins on the stability of water-in-oil and oil-in-water emulsions. *Journal of surfactants detergents*, 5(2), 135-143.
- Pang, B., Liu, H., Liu, P., Peng, X., & Zhang, K. (2018). Water-in-oil Pickering emulsions stabilized by stearylated microcrystalline cellulose. *Journal of colloid interface science*, 513, 629-637.
- Patel, A. R., & Velikov, K. P. (2014). Zein as a source of functional colloidal nano- and microstructures. *Current Opinion in Colloid Interface Science*, 19(5), 450-458.
- Pichot, R., Spyropoulos, F., & Norton, I. (2012). Competitive adsorption of surfactants and hydrophilic silica particles at the oil-water interface: interfacial tension and contact angle studies. *Journal of colloid interface science*, 377(1), 396-405.
- Pickering, S. U. (1907). Cxcvi.—emulsions. *Journal of the Chemical Society, Transactions*, 91, 2001-2021.
- Pimentel-Moral, S., Rodríguez-Pérez, C., Segura-Carretero, A., & Martínez-Férez, A. (2018). Development and stability evaluation of water-in-edible oils emulsions formulated with the incorporation of hydrophilic *Hibiscus sabdariffa* extract. *Food chemistry*, 260, 200-207.
- Politova, N. I., Tcholakova, S., Tsibranska, S., Denkov, N. D., & Muelheims, K. J. C. (2017). Coalescence stability of water-in-oil drops: Effects of drop size and surfactant concentration. *Colloids Surfaces A: Physicochemical Engineering Aspects*, 531, 32-39.
- Rabelo, C. A., Taarji, N., Khalid, N., Kobayashi, I., Nakajima, M., & Neves, M. A. (2018). Formulation and characterization of water-in-oil

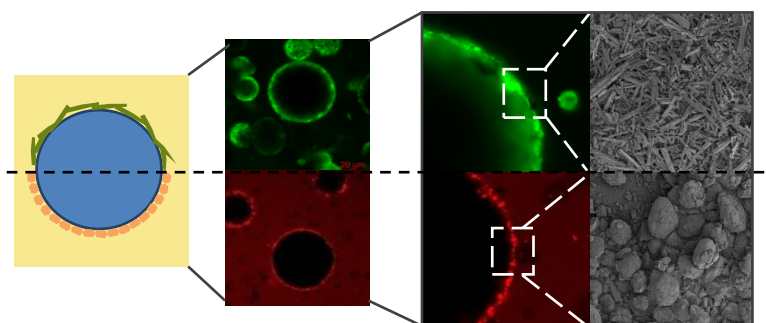
- nanoemulsions loaded with açai berry anthocyanins: insights of degradation kinetics and stability evaluation of anthocyanins and nanoemulsions. *Food research international*, 106, 542-548.
- Rao, M. A. (2010). *Rheology of fluid and semisolid foods: principles and applications*: Springer Science & Business Media.
- Rein, D. M., Khalfin, R., & Cohen, Y. (2012). Cellulose as a novel amphiphilic coating for oil-in-water and water-in-oil dispersions. *Journal of colloid interface science*, 386(1), 456-463.
- Richtering, W. (2012). Responsive emulsions stabilized by stimuli-sensitive microgels: emulsions with special non-Pickering properties. *Langmuir*, 28(50), 17218-17229.
- Roller, S., & Jones, S. A. (1996). *Handbook of fat replacers*: CRC Press.
- Rousseau, D. (2000). Fat crystals and emulsion stability—a review. *Food research international*, 33(1), 3-14.
- Rutkevičius, M., Allred, S., Velev, O. D., & Velikov, K. P. (2018). Stabilization of oil continuous emulsions with colloidal particles from water-insoluble plant proteins. *Food Hydrocolloids*, 82, 89-95.
- Sacca, L., Drelich, A., Gomez, F., Pezron, I., & Clause, D. (2008). Composition ripening in mixed water-in-oil emulsions stabilized with solid particles. *Journal of Dispersion Science Technology*, 29(7), 948-952.
- Saito, H., & Shinoda, K. (1970). The stability of W/O type emulsions as a function of temperature and of the hydrophilic chain length of the emulsifier. *Journal of colloid interface science*, 32(4), 647-651.
- Santini, E., Guzmán, E., Ferrari, M., & Liggieri, L. (2014). Emulsions stabilized by the interaction of silica nanoparticles and palmitic acid at the water–hexane interface. *Colloids Surfaces A: Physicochemical Engineering Aspects*, 460, 333-341.
- Sato, K., & Ueno, S. (2011). Crystallization, transformation and microstructures of polymorphic fats in colloidal dispersion states. *Current Opinion in Colloid Interface Science*, 16(5), 384-390.
- Scherze, I., Knoth, A., & Muschiolik, G. (2006). Effect of emulsification method on the properties of lecithin-and PGPR-stabilized water-in-oil-emulsions. *Journal of dispersion science and technology*, 27(4), 427-434.
- Singh, J., Dartois, A., & Kaur, L. (2010). Starch digestibility in food matrix: a review. *Trends in Food Science Technology*, 21(4), 168-180.
- Siró, I., & Plackett, D. (2010). Microfibrillated cellulose and new nanocomposite materials: a review. *Cellulose*, 17(3), 459-494.
- Skelhon, T. S., Grossiord, N., Morgan, A. R., & Bon, S. A. (2012). Quiescent water-in-oil Pickering emulsions as a route toward healthier fruit juice infused chocolate confectionary. *Journal of Materials Chemistry*, 22(36), 19289-19295.

- Surh, J., Vladisavljević, G. T., Mun, S., & McClements, D. J. (2007). Preparation and characterization of water/oil and water/oil/water emulsions containing biopolymer-gelled water droplets. *Journal of agricultural food chemistry*, 55(1), 175-184.
- Tadros, T. F. (2009). *Emulsion science and technology: a general introduction*: Wiley Online Library.
- Tadros, T. F. (2013). *Emulsion formation and stability*: John Wiley & Sons.
- Tambe, D. E., & Sharma, M. M. (1994). The effect of colloidal particles on fluid-fluid interfacial properties and emulsion stability. *Advances in colloid interface science*, 52, 1-63.
- Tang, J., Quinlan, P. J., & Tam, K. C. (2015). Stimuli-responsive Pickering emulsions: recent advances and potential applications. *Soft Matter*, 11(18), 3512-3529.
- Tcholakova, S., Denkov, N. D., Ivanov, I. B., & Campbell, B. (2006). Coalescence stability of emulsions containing globular milk proteins. *Advances in Colloid and Interface Science*, 123, 259-293.
- Traykov, T., & Ivanov, I. (1977a). Hydrodynamics of thin liquid films. Effect of surfactants on the velocity of thinning of emulsion films. *International Journal of Multiphase Flow*, 3(5), 471-483.
- Traykov, T., Manev, E., & Ivanov, I. (1977b). Hydrodynamics of thin liquid films. Experimental investigation of the effect of surfactants on the drainage of emulsion films. *International Journal of Multiphase Flow*, 3(5), 485-494.
- Tsabet, É., & Fradette, L. (2015). Effect of the properties of oil, particles, and water on the production of Pickering emulsions. *Chemical Engineering Research Design*, 97, 9-17.
- Tshilumbu, N. N., & Masalova, I. (2015). Stabilization of highly concentrated emulsions with oversaturated dispersed phase: effect of surfactant/particle ratio. *Chemical Engineering Research Design*, 102, 216-233.
- Urbina-Villalba, G., Forgiarini, A., Rahn, K., & Lozsán, A. (2009). Influence of flocculation and coalescence on the evolution of the average radius of an O/W emulsion. Is a linear slope of R^3 vs. t an unmistakable signature of Ostwald ripening? *Physical Chemistry Chemical Physics*, 11(47), 11184-11195.
- Ushikubo, F., & Cunha, R. (2014). Stability mechanisms of liquid water-in-oil emulsions. *Food Hydrocolloids*, 34, 145-153.
- Venkata Ramana, S., & Serbescu, A. (2013).
- Venkataramani, D., Smay, J., & Aichele, C. (2016). Transient stability of surfactant and solid stabilized water-in-oil emulsions. *Colloids Surfaces A: Physicochemical Engineering Aspects*, 490, 84-90.
- Wang, P., Cui, N., Luo, J., Zhang, H., Guo, H., Wen, P., & Ren, F. (2016). Stable water-in-oil emulsions formulated with polyglycerol

- polyricinoleate and glucono- δ -lactone-induced casein gels. *Food Hydrocolloids*, 57, 217-220.
- Wardhono, E. Y., Zafimahova-Ratisbonne, A., Lanoiselle, J. L., Saleh, K., & Clause, D. (2014). Optimization of the formulation of water in oil emulsions entrapping polysaccharide by increasing the amount of water and the stability. *The Canadian Journal of Chemical Engineering*, 92(7), 1189-1196.
- Wassell, P., Bonwick, G., Smith, C. J., Almiron-Roig, E., & Young, N. W. (2010). Towards a multidisciplinary approach to structuring in reduced saturated fat-based systems—a review. *International journal of food science technology*, 45(4), 642-655.
- Wolf, F., Koehler, K., & Schuchmann, H. P. (2013). Stabilization of water droplets in oil with PGPR for use in oral and dermal applications. *Journal of Food Process Engineering*, 36(3), 276-283.
- Xhanari, K., Syverud, K., & Stenius, P. (2011). Emulsions stabilized by microfibrillated cellulose: the effect of hydrophobization, concentration and o/w ratio. *Journal of Dispersion Science Technology*, 32(3), 447-452.
- Yan, N., Gray, M. R., & Masliyah, J. H. (2001). On water-in-oil emulsions stabilized by fine solids. *Colloids Surfaces A: Physicochemical Engineering Aspects*, 193(1-3), 97-107.
- Yi, J., Zhu, Z., McClements, D. J., & Decker, E. A. (2014). Influence of aqueous phase emulsifiers on lipid oxidation in water-in-walnut oil emulsions. *Journal of agricultural food chemistry*, 62(9), 2104-2111.
- Zhai, K., Pei, X., Wang, C., Deng, Y., Tan, Y., Bai, Y., . . . Wang, P. (2019). Water-in-oil Pickering emulsion polymerization of N-isopropyl acrylamide using starch-based nanoparticles as emulsifier. *International journal of biological macromolecules*, 131, 1032-1037.
- Zhao, Q., Jiang, L., Lian, Z., Khoshdel, E., Schumm, S., Huang, J., & Zhang, Q. (2019). High internal phase water-in-oil emulsions stabilized by food-grade starch. *Journal of colloid interface science*, 534, 542-548.
- Zhu, Q., Li, J., Liu, H., Saito, M., Tatsumi, E., & Yin, L. (2015). Development of stable water-in-oil emulsions using polyglycerol polyricinoleate and whey protein isolate and the impact on the quality of bittern-tofu. *Journal of Dispersion Science Technology*, 36(11), 1548-1555.

Chapter 3

Water-in-Oil Pickering Emulsions Stabilized by Water-Insoluble Polyphenol Crystals ¹



Abstract

In recent years, there has been a resurgence of interest in Pickering emulsions due to recognition of the unique high steric stabilization provided by particles at interfaces. This interest is particularly keen for water-in-oil (W/O) emulsions due to the limited range of suitable Pickering stabilizers available. We demonstrate for the first time that W/O emulsions can be stabilized by using crystals from naturally occurring polyphenols (curcumin or quercetin particles). The particles were assessed based on their size, microstructure, contact angle, interfacial tension and ζ -potential measurements in an attempt to predict the way that they act as Pickering stabilizers. Static light scattering results and microstructural analysis at various length scales (optical, confocal laser scanning and scanning electron microscopy) confirmed that quercetin particles have a nearly perfect crystalline rod shape with high aspect ratio, *i.e.*, the ratio of length to diameter (L:D) was

¹ Published as: Zembyla, M., Murray, B.S., & Sarkar, A. (2018). Water-in-Oil Pickering Emulsions Stabilized by Water-Insoluble Polyphenol Crystals. *Langmuir*, 34 (34), 10001-10011. DOI: [10.1021/acs.langmuir.8b01438](https://doi.org/10.1021/acs.langmuir.8b01438)

ca 2.5:1 – 7:1. On the other hand, curcumin particles ($d_{32} = 0.2 \mu\text{m}$) had a polyhedral shape. Droplet sizing and confocal laser scanning microscopy revealed that there was an optimum concentration (0.14 and 0.25 wt% for quercetin and curcumin, respectively) where smaller water droplets were formed ($d_{32} \sim 6 \mu\text{m}$). Interfacial shear viscosity (η_i) measurements confirmed that a stronger film was formed at the interface with quercetin particles ($\eta_i \approx 340 \text{ mN s m}^{-1}$) rather than with curcumin particles ($\eta_i \approx 22 \text{ mN s m}^{-1}$) possibly due to the difference in shape and size of the two crystals. This study provides new insights on creation of Pickering W/O emulsions with polyphenol crystals and may lead to various soft matter applications where Pickering stabilization using biocompatible particles is a necessity.

3.1. Introduction

Water-in-oil (W/O) emulsions are widely used for different soft matter applications in food, pharmaceutical, personal care, agriculture etc. Recently, the use of Pickering particles as stabilizers for emulsions has gained significant attention owing to their ability to adsorb irreversibly at the liquid-liquid interface (Lam *et al.*, 2014; Xiao *et al.*, 2016). Pickering stabilization arises when particles accumulate at the water-oil (W-O) interface forming a mechanical (steric) barrier that protects the emulsion droplets against coalescence (Pickering, 1907). Effective Pickering stabilization is achieved when the average size of the adsorbed particles is at least an order of magnitude smaller than the emulsion droplet size (Dickinson, 2012; Sarkar *et al.*, 2016).

The size of the particles dispersed in the continuous phase is an important parameter that determines the Pickering functionality. Simple geometrical consideration can be used to estimate the minimum amount of surface active particles required for adequate surface coverage in order to form stable emulsions (Luo *et al.*, 2011). The particle contact angle (θ) represents the wettability of a particle at the interface identifying whether the particle preferentially resides in the water or oil phase (Binks, 2002). If θ measured in the aqueous phase, is smaller than 90° , a larger fraction of the

particle surface will reside in the aqueous rather than in the non-polar phase, *i.e.*, the particle is more hydrophilic and will tend to stabilize an O/W emulsion. However, if θ is greater than 90° , the particle will reside more in the oil phase, *i.e.*, the particle is more hydrophobic and will stabilize W/O emulsions. Maximum adsorption occurs when particles are wetted equally by oil and water and have contact angle exactly 90° (Binks, 2002; Binks *et al.*, 2000). The stability of Pickering emulsions is usually inversely proportional to particle size; smaller particles will give a higher packing efficiency, and therefore a more homogeneous layer at the interface preventing coalescence (Aveyard *et al.*, 2003; Hunter *et al.*, 2008). Particle size also has a direct effect on the energy of desorption (ΔG_d), and if adsorption occurs, smaller particles provide lower ΔG_d , according to the equation 3.1 as follows:

$$\Delta G_d = \pi r^2 \gamma_{ow} (1 \pm |\cos(\theta)|)^2 \quad (3.1)$$

where γ_{ow} is the interfacial tension between the oil and water phases; $|\cos(\theta)|$ is the modulus of $\cos(\theta)$; θ is the particle contact angle (the sign inside the bracket is negative if the particles are removed into the water phase and positive if removed into the oil phase); and r is the particle radius, *i.e.*, assumed spherical. Thus, smaller particles can more easily detach from the W-O interface than larger ones (Aveyard *et al.*, 2003). However, it should be noted that even particles with just a few 10s of nm in radius can have ΔG_d of several 1000 $k_B T$ at 298 K (Sarkar *et al.*, 2016). Note, that this assumes that the particles are perfectly spherical and thus, equation 3.1 is rarely directly applicable in real systems. Non-spherical particles of the same volume and of the same material as spherical particles will have a greater specific surface area and therefore higher desorption energies than the equivalent spherical particles (Binks *et al.*, 2006).

Mostly synthetic particles have been used in literature to stabilize W/O emulsions, such as hydrophobic silica, modified cellulose, polystyrene latex, microgels from cross-linked poly(N-isopropylacrylamide)-co-methacrylic acid etc (Binks *et al.*, 2001; Brugger *et al.*, 2008; Kim *et al.*, 2004; Midmore, 1999; Rein *et al.*, 2012; Skelhon *et al.*, 2012). Therefore, there is an enormous opportunity to identify a new class of particles for stabilization of W/O

emulsions where the particles are based on natural, biodegradable and renewable-resource ingredients that are immediately suitable for soft matter applications (food, pharmaceuticals, cosmetics, agrochemicals etc.), where biocompatibility is a key requirement. In this regard, polyphenol crystals would be promising biocompatible Pickering stabilizers. Polyphenol molecules are characteristics of particular plant species and even particular organs or tissues of that plant and have received significant attention in recent years due to their reported biological activities and widespread occurrence in the diet (Bordenave *et al.*, 2014). Fruits, vegetables, leaves, seeds and other types of foods and beverages such as teas, chocolates and wines are rich sources of polyphenols (Tsao, 2010).

Luo *et al.* (2011) suggested for the first time that polyphenol crystals may adsorbed at the liquid-liquid interface. The authors identified that some common polyphenols can act as stabilizers of O/W emulsions through their adsorption as water-insoluble particles to the surface of oil droplets. It was demonstrated that polyphenols with different $\log P$ values, where P is the partition coefficient between n-octanol and water, can act as Pickering stabilizers at the W-O interface, stabilizing emulsions for several weeks without any obvious visual changes (Luo *et al.*, 2011). The $\log P$ value can be used to identify the hydrophilicity of a polyphenol molecule. However, Pickering stabilization depends upon the hydrophilic/ hydrophobic balance of the *particles*, not their molecules and no simple relationship seemed to exist between $\log P$ and ability to stabilize the O/W emulsions. More importantly, here, the ability of polyphenol crystals to stabilize W/O emulsions apparently still remains uninvestigated.

In this study quercetin and curcumin particles were investigated for their potential to act as Pickering stabilizers for W/O emulsions due to their widespread availability, 'clean label' feature and biocompatibility. Curcumin is a natural low-molecular-weight polyphenolic compound found in the rhizomes of the perennial herb turmeric (*Curcuma longa*) (Sharma *et al.*, 2005). From a structural viewpoint, curcumin (Figure 3.1 (a)) is comprised of two aromatic rings with methoxyl and hydroxyl groups in the ortho- position with respect to

each other (Araiza-Calahorra *et al.*, 2018). The aromatic rings are connected through seven carbons that contain two α,β -unsaturated carbonyl groups (Araiza-Calahorra *et al.*, 2018). As a result, curcumin exists in three possible forms, two isomers in an equilibrating keto-enol tautomeric form, and the α,β -diketonic tautomeric form (Payton *et al.*, 2007). The polar hydroxyl/ ketone groups are expected to impact hydrophilicity whilst the aromatic/ aliphatic parts would be expected to make the molecule more hydrophobic. Quercetin is a flavonoid characterized by its C6-C3-C6 basic backbone, found in onions, kale, French beans, broccoli etc. (Formica *et al.*, 1995). Quercetin (Figure 3.1 (b)) has hydroxyl groups that impart hydrophilic characteristics whilst the ring structures impact the hydrophobicity; thus it can be described as amphiphilic molecule (Luo *et al.*, 2011). Both curcumin and quercetin are relatively insoluble in water with relatively high $\log P$ values of 3.29 and 2.16, respectively, and also appear to be relatively insoluble in vegetable oils. The maximum solubility of curcumin and quercetin in vegetable oils have been reported to be 0.02 wt% and ~0.017 wt%, respectively, which suggests that these materials would have been predominantly in their insoluble particle (crystal) form in the soybean oil (Cretu *et al.*, 2011; Roedig-Penman *et al.*, 1998). Firstly, the interfacial properties of these particles dispersed in oil were investigated in terms of their size, wettability and interfacial behaviour to assess their potential as Pickering stabilizers. Secondly, the characteristics of W/O emulsions stabilized by curcumin or quercetin particles were evaluated using a range of complimentary physical and microstructural techniques at different pH values. To our knowledge, the present study is the first report of use of polyphenol crystals to stabilize W/O emulsions.

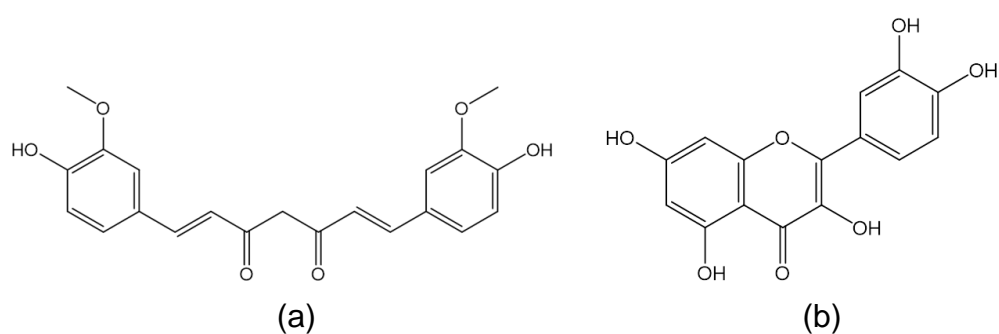


Figure 3.1. Structure of curcumin (a) and quercetin (b) molecules.

3.2. Material and methods

3.2.1. Materials

Curcumin (orange-yellow powder) from turmeric rhizome (95 wt% total curcuminoid content) was obtained from Alfa Aesar (UK). Quercetin ($\geq 95\%$) in the form of yellow crystalline solid was purchased from Cayman Chemicals (USA). Both polyphenols were used without further purification. Soybean oil (KTC Edibles, UK) was purchased from a local store. Aluminium oxide, 99 %, extra pure was used for soybean oil purification in some experiments and was purchased from Acros Organics (Belgium). Water purified by treatment with Milli-Q apparatus (Millipore, Bedford, UK) with a resistivity not less than $18\text{ M}\Omega\text{ cm}^{-1}$ was used for the preparation of the emulsions. A few drops of hydrochloric acid (0.1 M HCl) or sodium hydroxide (0.1 M NaOH) were used to adjust the pH of the emulsions. Sodium azide was purchased from Sigma-Aldrich (USA).

3.2.2. Contact angle and wettability

The hydrophilic/ hydrophobic character of the polyphenol crystals was evaluated in terms of their wettability. The wettability measurements were carried out at $25\text{ }^{\circ}\text{C}$ using OCA25 drop-shape tensiometer (DataPhysics Instruments, Germany) fitted with a micro-syringe and a high speed camera. Compressed discs of the particulate materials were prepared by placing 0.3 g curcumin or quercetin crystals between the plates of a hydraulic bench press (Clarke, UK) using a 1.54 cm diameter die under a weight of 6 tonnes for 30 s. Static contact angles were measured using the sessile drop method. Water or oil droplets ($3\text{ }\mu\text{L}$) were produced using a straight needle of 0.52 mm outer diameter and 0.26 mm internal diameter, to form a sessile drop onto the compressed particle disc surfaces. A video camera was used to record the droplet behaviour. The droplet contour was fitted using the SCA software and the contact angles between the particle substrate and the water (θ_w) or oil droplet (θ_o) was measured. All measurements were carried out in triplicate and error bars represent the standard deviations.

3.2.3. Interfacial tension

Interfacial tension (γ_T) measurements were performed between the soybean oil with or without the presence of polyphenol crystals and Milli-Q water (pH 3.0) using the pendant drop method in a Dataphysics OCA tensiometer (DataPhysics Instruments, Germany). The apparatus includes an experimental cell, an optical system for the illumination and the visualization of the drop shape and a data acquisition system. An upward bended needle was used to immerse a drop of a lower density liquid into a higher density one. Thus, a drop of soybean oil or oil suspension (0.14 wt% curcumin or quercetin dispersed in soybean oil) was formed at the tip of the needle and suspended in the cuvette containing Milli-Q water, at pH 3.0. The contour of the drop extracted by the SCA 20 software was fitted to Young-Laplace equation to obtain γ_T . All measurements were carried out in triplicate and error bars represent the standard deviations.

3.2.4. Preparation of oil dispersions and W/O emulsions

Curcumin or quercetin dispersions were prepared by dispersing these polyphenol crystals in the continuous phase (soybean oil) using an Ultra-Turrax T25 mixer (Janke & Kunkel, IKA-Labortechnik) with a 13 mm mixer head (S25N- 10 G) operating at 9,400 rpm for 5 min. The aqueous phase was Milli-Q water at pH 3.0. The pH of the water was adjusted by adding few drops of 0.1 M HCl and 0.02 wt% sodium azide was added into the aqueous phase as a preservative. Coarse emulsions were prepared by homogenizing 5 wt% of the aqueous phase with 95 wt% oil phase using an Ultra-Turrax mixer for 2 min at 13,400 rpm. Fine emulsions were prepared by passing the coarse emulsions through a high pressure Leeds Jet homogenizer (Burgaud *et al.*, 1990), twice, operated at 300 bar. The initial temperature of the particle dispersion was 21 °C. The temperature of the dispersion was 23 and 26 °C after Ultra-Turrax mixing at 9,400 rpm/ 5 min and 13,400 rpm/ 2 min, respectively. The temperature of the particle dispersion after passing through the Jet homogenizer (two passes) was 33 – 34 °C. These slight temperature increases were too low to have any significant impact on the solubility of the particles. Immediately after preparation, emulsions were sealed in a 25 ml

cylindrical tubes (internal diameter = 17 mm) and stored at room temperature in a dark place.

3.2.5. Particle and emulsion droplet size measurements

Particle and emulsion droplet size distributions were measured using static light scattering (SLS) via a Mastersizer Hydro SM small volume wet sample dispersion unit (Malvern Instruments, UK). Average droplet size was monitored via the Sauter mean diameter, d_{32} , or volume mean diameter, d_{43} , defined by:

$$d_{ab} = \frac{\sum n_i d_i^a}{\sum n_i d_i^b} \quad (3.2)$$

where n_i is the number of the droplets of diameter d_i .

Refractive indices of 1.42, 1.82 and 1.47 for curcumin, quercetin and soybean oil were used, respectively, for particle size measurements. For water droplet size measurements, refractive indices of 1.33 and 1.47 were used, for water and soybean oil, respectively. Absorption coefficient of 0.01, 0.1 and 0.01 for curcumin, quercetin and water, were used, respectively. All measurements were made at room temperature on at least three different samples.

3.2.6. ζ -Potential measurements

The ζ -potential measurements of curcumin and quercetin dispersions in water at pH 3.0 and 7.0 values were performed using a Nanoseries ZS instrument (Zetasizer Nano-ZS, Malvern Instruments, Worcestershire, UK). The instrument software was used to convert the electrophoretic mobility into ζ -potential values using the Smoluchowski assumption (see equation 3.3). Polyphenol dispersions were prepared by mixing the polyphenol crystals (0.14 wt%) with water at pH 3.0 or 7.0, via an Ultra-Turrax mixer operating at 9,400 rpm for 5 min. The pH of freshly prepared suspensions was adjusted at pH 3.0 and 7.0 using 0.1 M HCl or NaOH. Three readings of ζ -potential were made per sample.

The ζ -potential was calculated from the measured electrophoretic mobility (U_E) using the Henry equation (Niknafs, 2011):

$$U_E = \frac{2\varepsilon_r\zeta f(ka)}{3\eta} \quad (3.3)$$

where ε_r is the dielectric constant, ζ is the ζ -potential, η is the viscosity of the dispersed media, and $f(k_a)$ is the Henry's function; $f(k_a) = 1.5$ for dispersion in polar media based on the Smoluchowski approximation. The Smoluchowski approximation is based on the assumption that the double layer thickness is smaller than the mean particle radius (*i.e.*, thin double layer). It should be noted that although in the W/O emulsions the particles were dispersed in the oil, we cannot use this equipment for measuring ζ -potential in such non-aqueous systems. However, it was expected that the ζ -potential measured in the aqueous phase might provide some insights into the behaviour of the crystals when partially wetted by water at the W-O interface.

3.2.7. Optical microscopy

A drop of the curcumin or quercetin dispersion (0.14 wt%) was placed on a microscope slide and then covered with a cover slip (0.17 mm thickness). The size and shape of the polyphenol crystals were observed using a LCD digital microscope (PentaView, Celestron, USA). The samples were scanned at room temperature (25 ± 1 °C) using 20 \times /0.4 objective lenses.

3.2.8. Scanning electron microscopy (SEM)

Particle morphology of the curcumin and quercetin crystals was imaged using SEM (Nova NanoSEM450, FEI, USA). Curcumin or quercetin dispersions were prepared as described above and filtered through 0.20 or 0.45 μm filter papers, respectively. The particles on the filter paper were left overnight in a vacuum oven at 25 °C. Then, they were coated with iridium (4 nm) and analysed using a 2 keV beam to prevent damage to the sample.

3.2.9. Confocal laser scanning microscopy (CLSM)

The microstructure of the W/O emulsion droplets was observed using a confocal microscope (Zeiss LSM700 inverted, Germany). The emulsions

were gently agitated before analysis to ensure a homogeneous sample was observed. Approximately, 80 μL of samples were placed into a laboratory-made well slide and a cover slip (0.17 mm thickness) was placed on top, ensuring that there was no air gap (or bubbles) trapped between the sample and coverslip. The samples were scanned at room temperature (25 ± 1 °C) using 20 \times /0.5 objective lens. Auto-fluorescence from the particles was excited using 488 and 405 nm lasers for curcumin and quercetin crystals, respectively.

3.2.10. Interfacial shear viscosity (η_i)

A two dimensional Couette-type interfacial viscometer (Murray, 2002; Sarkar *et al.*, 2017) was operated in a constant shear-rate mode. A stainless steel biconical disc (radius 15.0 mm) was suspended from a thin torsion wire with its edge in the plane of the W-O interface of the solution contained within a cylindrical glass dish (radius 72.5 mm). For these measurements, 0.14 wt% curcumin and quercetin particles were dispersed in purified or non-purified oil using the Ultra-Turrax mixer at 9,400 rpm for 5 min. For the experiments with purified oil, the oil was purified with aluminium oxide to eliminate free fatty acids and surface active impurities that may affect the measurements. A mixture of oil and aluminium oxide in proportion 2:1 w/w was stirred for 3 h and centrifuged at 4,000 rpm for 30 min.

The constant shear rate apparent interfacial viscosity, η_i , is given by the following equation:

$$\eta_i = \frac{g_f}{\omega} K(\theta - \theta_o) \quad (3.4)$$

where K is the torsion constant of the wire; θ is the equilibrium deflection of the disc in the presence of the film; θ_o is the equilibrium deflection in the absence of the film, *i.e.*, due to the bulk drag of the sub-phase on the disc; g_f is the geometric factor and ω is the angular velocity of the dish. A fixed value of $\omega = 1.27 \times 10^{-3}$ rad s⁻¹ was used.

3.2.11. Statistical analysis

Significant differences between samples were determined by one-way ANOVA and multiple comparison test with Tukey's adjustment performed using SPSS software (IBM, SPSS statistics) and the level of confidence was 95 %.

3.3. Results and discussion

3.3.1. Assessment of polyphenol crystals as Pickering stabilizers

3.3.1.1. Size and shape of curcumin and quercetin crystals dispersed in oil

In this study, the size of curcumin and quercetin crystals dispersed in soybean oil was measured after treatment with the Ultra-Turrax mixer at 9,400 rpm for 5 min as shown in Figure 3.2. The particle size distribution shows that curcumin particles were polydispersed with d_{32} and d_{43} values of 0.2 and 20.5 μm , respectively. In comparison, quercetin particles were more monodispersed with d_{32} and d_{43} values of 5.9 and 14.9 μm , respectively. The size of particles passed through all the stages of homogenization process (Ultra Turrax 9,400 rpm/ 5 min, 13,400 rpm/ 2 min and Jet homogenizer, two passes, at 300 bar) are shown in Appendix A, Figure A1 and Table A1. The Jet homogenizer produced a slight milling effect but this appeared to predominantly affect the larger crystals or their aggregates ($> 10 \mu\text{m}$). The overall particle distributions, which were quite broad, still remained largely in the micrometer range and were comparable with Figure 3.2, although Figure 3.2 also shows that the curcumin part of the distribution extends to smaller sizes than for quercetin.

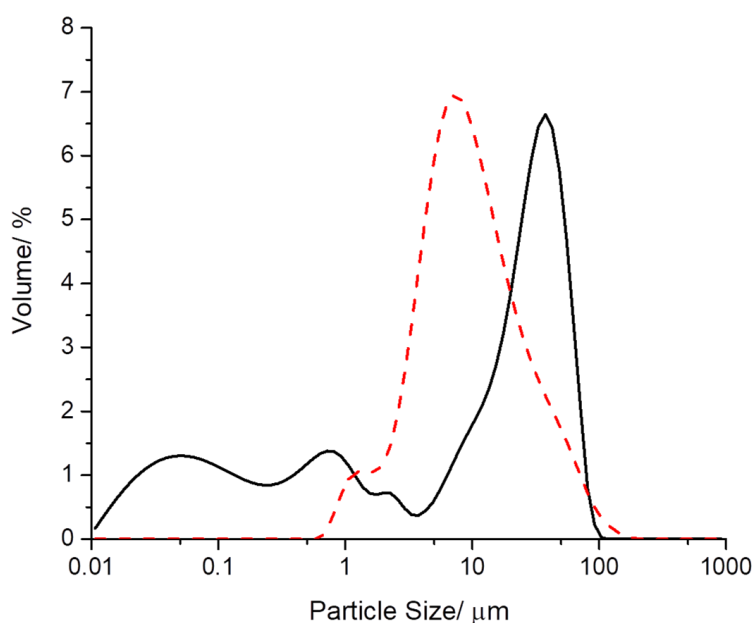


Figure 3.2. Particle size distribution of curcumin (black solid line, 0.14 wt%) and quercetin (red dashed line, 0.14 wt%) particles dispersed in soybean oil, respectively.

The microstructure of curcumin (Figure 3.3) and quercetin (Figure 3.4) dispersions in soybean oil was observed using optical microscopy, CLSM and SEM at different magnifications. Curcumin particles appeared to have a rather polyhedral shape, whilst quercetin particles had a nearly perfect microcrystalline structure with a rod-shape. The results from the size distribution plots measured using the Mastersizer (Figure 3.2) can be confirmed from the figures of curcumin (Figures 3.3 (a), 3.3 (b) and 3.3 (c)) and quercetin (Figures 3.4 (a), 3.4 (b) and 3.4 (c)) particles at lower magnification. For curcumin particles there was a range of different sizes (0.5 – 15 µm) however for quercetin the particles had a length of 5 – 35 µm and a ratio of length to diameter (L:D) of around 2.5:1 – 7:1. At higher magnification for both curcumin (Figure 3 (d)) and quercetin (Figure 4 (d)) particles, it was clear that the particles were aggregates of smaller particles, probably due to the filtration used on the preparation procedure. The microstructure of curcumin and quercetin powders was observed using SEM at different magnifications (see Appendix A, Figure A2). It can be observed that the shape of the crystals in powdered form was very similar to that of the ones dispersed in oil (Figure 3.3 (c - d) and 3.4 (c - d), for curcumin and quercetin,

respectively) indicating that there was no change of the crystal habit when they were passed through the stages of emulsification process.

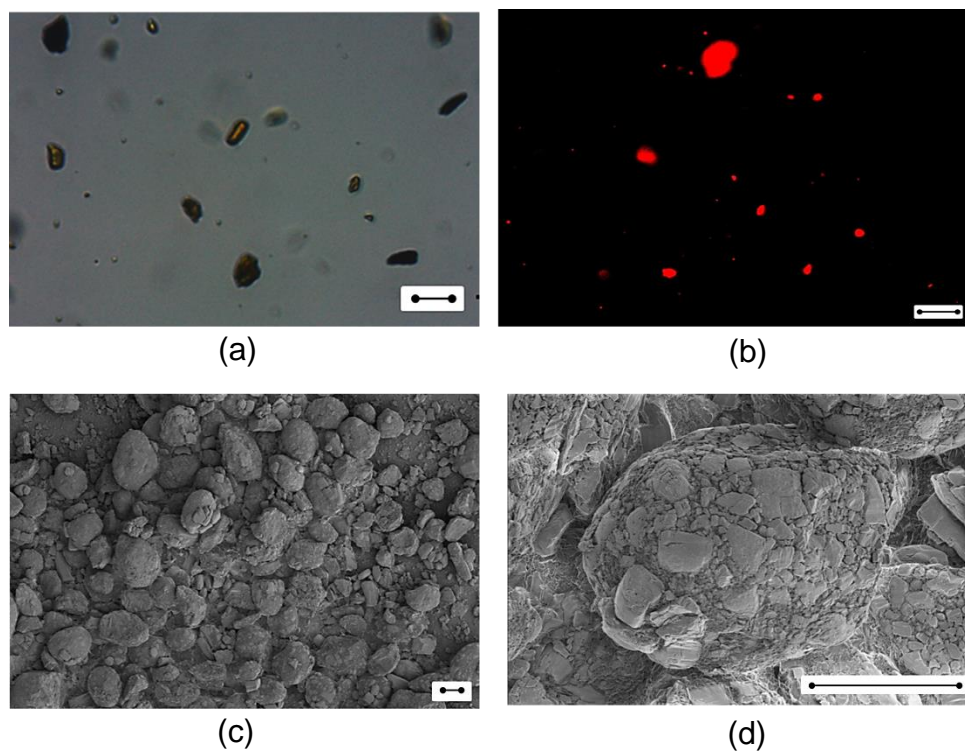


Figure 3.3. Microstructure of curcumin dispersion (0.14 wt%) in soybean oil at various length scales: (a) optical microscopy, (b) CLSM at 488 nm excitation, (c) SEM at lower magnification (250 \times) and (d) SEM at higher magnification (2,000 \times). Scale bar is 20 μm .

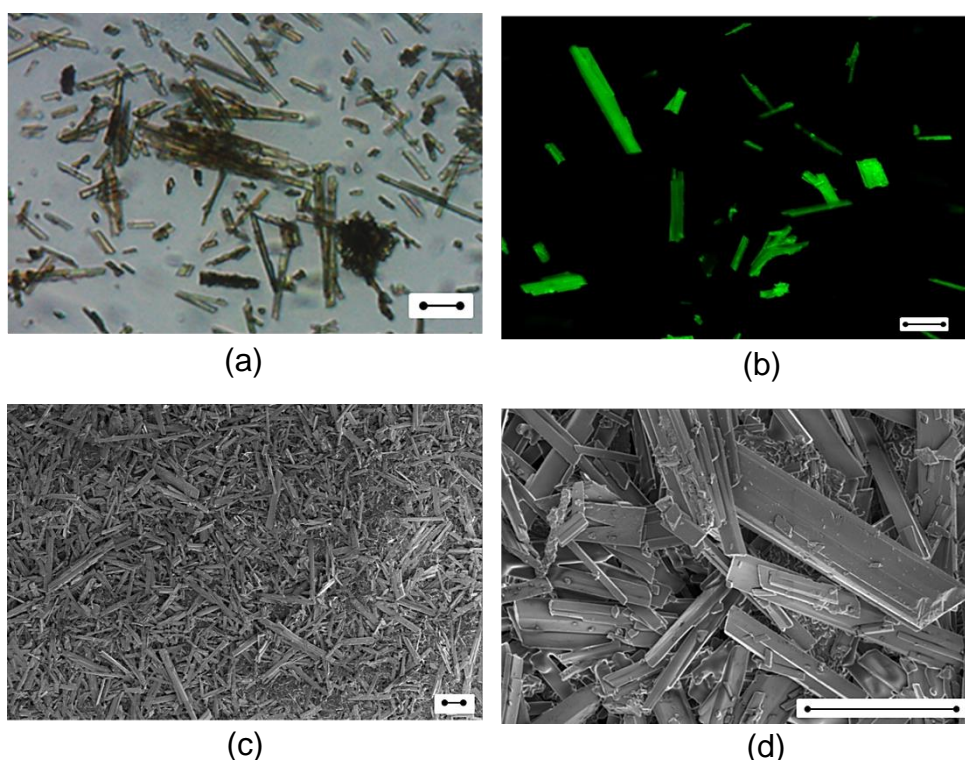


Figure 3.4. Microstructure of quercetin dispersion (0.14 wt%) in soybean oil at various length scales: (a) optical microscopy, (b) CLSM at 405 nm excitation, (c) SEM at lower magnification (250 \times) and (d) SEM at higher magnification (2,000 \times). Scale bar is 20 μ m.

3.3.1.2. Contact angle and wettability of polyphenol particles

The hydrophilic/ hydrophobic character of particles can be identified via their wettability (the tendency of one liquid to spread on a solid surface) in aqueous and oil phases (Aveyard *et al.*, 2003). When the contact angle of a water droplet, θ_w , significantly exceeds the contact angle of an oil droplet, θ_o , the particles can be categorized as hydrophobic, *i.e.*, they are preferentially wetted by oil and will tend to stabilize W/O rather than O/W emulsions (Duffus *et al.*, 2016).

In this study, both curcumin and quercetin particles had θ_w values exceeding their θ_o values, indicating that both possess a hydrophobic character as shown in Table 3.1. For curcumin particles, θ_w at pH 3.0 was significantly larger than that at pH 7.0. This agrees with Tønnesen *et al.* (2002) that the curcumin molecule is hydrophobic with a very low water solubility (11 ng/ ml at 25 $^{\circ}$ C), due to its aliphatic chains (Balasubramanian, 2006).

Quercetin particles had a lower θ_w than curcumin, probably due to the presence of more –OH groups on their backbone and the formation of hydrogen bonds with water molecules. Quercetin crystal structure can be described as layers of hydrogen bond dimers. These dimers form a 2-dimensional net connected through a hydrogen bonding network with water molecules present in the quercetin (Rossi *et al.*, 1986). Therefore, quercetin molecules can pack in a way that some of the –OH groups are not exposed to the continuous phase, giving a hydrophobic nature to the particle surface. It can be observed that the different pH values did not affect the contact angle on the quercetin particles as much as for curcumin. The same effect was observed for oil phase.

From these values we estimate the three-phase contact angle (θ) of the polyphenol particles at the W-O interface via Young's equation (see Table 3.1), using measured values of 70.8, 32.5 and 26.4 mN/ m for 0.14 wt% curcumin in oil and 71.5, 33.4 and 26.4 mN/ m for 0.14 wt% quercetin in oil for the A-W, A-O and W-O interfacial tensions, respectively (see Appendix A, Table A2). Note the A-W tensions were measured after contacting the oil phase with water and were very close to the value for pure water (72.0 mN/ m), suggesting little solubilisation of surface active components from the oil into the aqueous phase. Similarly, the W-O tension value measured for purified soybean oil without polyphenols was ~32 mN/ m (see Appendix A, Table A3), only slightly higher than the value of ~26 mN/ m measured in the presence of curcumin or quercetin (in non-purified oil, see Appendix A, Table A3), suggesting limited solubilisation of the polyphenol crystals in the oil and their molecular adsorption at the W-O interface. The calculated θ values are 175 and 116° for curcumin at pH 3.0 and 7.0, respectively, and 81 and 79° for quercetin at pH 3.0 and 7.0, respectively. Although one should view these values with some caution, since components from the oil could still adsorb to the surfaces of the crystals and affect their microscopic contact angles, it is interesting to apply these values to equation (3.1) and calculate possible ΔG_d . Assuming a spherical particle of radius 0.1 μm , one obtains values of 8.0×10^5 and 4.2×10^5 $\text{k}_\text{B}\text{T}$ for curcumin at pH 3.0 and 7.0, respectively, and 2.7×10^5 and 2.9×10^5 $\text{k}_\text{B}\text{T}$ for quercetin at pH 3.0 and 7.0, respectively. Note that

for $r = 1 \mu\text{m}$ (closer to the size of the majority of the particles observed) all these values would be $100\times$ higher, confirming that there is a very strong driving force for the crystals to get trapped at the interface. The θ and ΔG_d calculations therefore confirm the above discussion of the relative hydrophobicities of the crystals based on just their water/solid and oil/solid contact angles (in Table 3.1). The relatively small lowering of the O-W interfacial tension in the presence of the particles is also another characteristic of Pickering stabilization (see Appendix A, Table A3) (Al-Rossies *et al.*, 2010; Melle *et al.*, 2005).

Table 3.1. Measured contact angles of water droplets (pH 3.0 and 7.0) on polyphenol crystals in air (θ_w) and oil droplets on polyphenol crystals in air (θ_o). Also shown is the calculated three-phase contact angle (θ) at the W-O interface in the aqueous phase (pH 3.0 and 7.0). Samples with the same letter do not differ significantly ($p > 0.05$) according to Tukey's test.

Contact angle at the polyphenol, water or oil and air interface/ °				Three-phase contact angle/ °	
Particle type	Aqueous phase (θ_w)		Oil phase (θ_o)	Aqueous phase (θ)	
	pH 3.0	pH 7.0		pH 3.0	pH 7.0
Curcumin	85.6 ± 0.4	73.4 ± 1.2	11.9 ± 2.0	175.3 ± 1.0	115.7 ± 2.1
Quercetin	60.2 ± 0.7 ^a	59.4 ± 0.4 ^a	19.8 ± 0.5	80.9 ± 2.1 ^b	79.1 ± 1.4 ^b

3.3.1.3. ζ - Potential Measurements

The surface charge and therefore the ζ -potential of particles is frequently pH dependent and can potentially affect particle dispersion/aggregation (Duffus *et al.*, 2016). It was not possible to measure ζ -potential of particles dispersed in soybean oil. Therefore, in order to predict how the particles might behave when they adsorb at the W-O interface, the ζ -potential of those particles dispersed in the aqueous phase was measured, since this might have some relevance to the behaviour of the particles when partially

wetted by water at the W-O interface. Table 3.2 shows the ζ -potential of curcumin and quercetin particles dispersed in water at pH 3.0 and 7.0. The curcumin particles had a positive charge at pH 3.0 but at pH 7.0, they became strongly anionic. Under alkaline conditions, curcumin can be dissolved sparsely in water as the acidic phenolic group in curcumin donates its H⁺ ion, forming the phenolate ion enabling dissolution (Araiza-Calahorra *et al.*, 2018). On the other hand, quercetin had negative charge at both pH values and rose from -26.2 to -48.1 mV. The C₇-OH on the quercetin nucleus also behaves as a polyprotic acid undergoing dissociation at alkaline conditions (> pH 7.0) by imparting a negative charge (Luo *et al.*, 2012). As particles become more highly charged they are likely to be less hydrophobic and less surface active (Luo *et al.*, 2012). Thus, the ζ -potential results predict that both curcumin and quercetin would be more surface active at the lower pH. Most notably, curcumin at pH 3.0 is predicted as the most hydrophobic from the above contact angle measurements, which agrees with the lowest absolute magnitude of ζ -potential in contact with water and also with the population of crystals in the lower size range observed in Figure 3.2. In other words, curcumin is more easily dispersed in the oil phase (as also noted in the confocal observations discussed below).

Table 3.2. ζ -potential (mV) of curcumin and quercetin particles (0.14 wt%) dispersed in the aqueous phase at pH 3.0 and 7.0. Samples with * do not differ significantly ($p > 0.05$) according to Tukey's test.

Particle type	pH 3.0	pH 7.0
Curcumin	12.0 ± 2.2	- 47.6 ± 2.4*
Quercetin	- 26.2 ± 1.2	- 48.1 ± 1.2*

3.3.2. W/O emulsions

3.3.2.1. Effect of particle concentration and pH on the stability of W/O Pickering emulsion droplets

Water droplet size distributions of the particle-stabilized W/O emulsions are shown at different concentrations of particles (0.06 – 1.5 wt%) in Figures

3.5 (a) and 3.5 (b). In this case, the aqueous phase was adjusted to pH 3.0. Emulsions prepared at 0.06 wt% of either curcumin or quercetin particles were not as stable as those with higher concentrations of particles; they tended to coalesce and the size of the water droplets increased dramatically within 3 days. On the other hand, the size of emulsion droplets prepared at higher concentrations of particles (> 0.14 wt%) did not change significantly after 7 days although some particle sedimentation was observed. The lack of stability of emulsions at 0.06 wt% of particles suggests incomplete droplet surface coverage by the limited quantity of particles available, leading to coalescence. In the size distribution plots for both sets of emulsions (Figures 3.5 (a) and 3.5 (b)), smaller peaks were observed ($\leq 1 \mu\text{m}$), probably due to the non-adsorbed particles remaining in the continuous phase, since the static light scattering technique cannot distinguish between emulsion droplets and polyphenol particles as scattering centers (Atarés *et al.*, 2012). These peaks were more obvious in the curcumin-stabilized emulsions, perhaps indicating that curcumin particles were less completely adsorbed at the interface. This was also observed in confocal images of emulsions (see later). In addition, significant particle sedimentation was observed especially at highest concentrations (0.5 and 1.5 wt%) for both curcumin and quercetin. Higher water volume fraction (10:90 wt% w:o ratio) was tested. The results showed that for both curcumin and quercetin particles the size of the water droplets was significantly bigger (20 – 24 μm) (see Appendix A, Figure A3) comparing the size of the water droplets (7 – 9 μm) at lower volume fraction (5:95 wt% w:o ratio, Figure 3.6). In addition, fewer peaks were observed at $\leq 1 \mu\text{m}$ region, indicating that more crystals were absorbed at the interface.

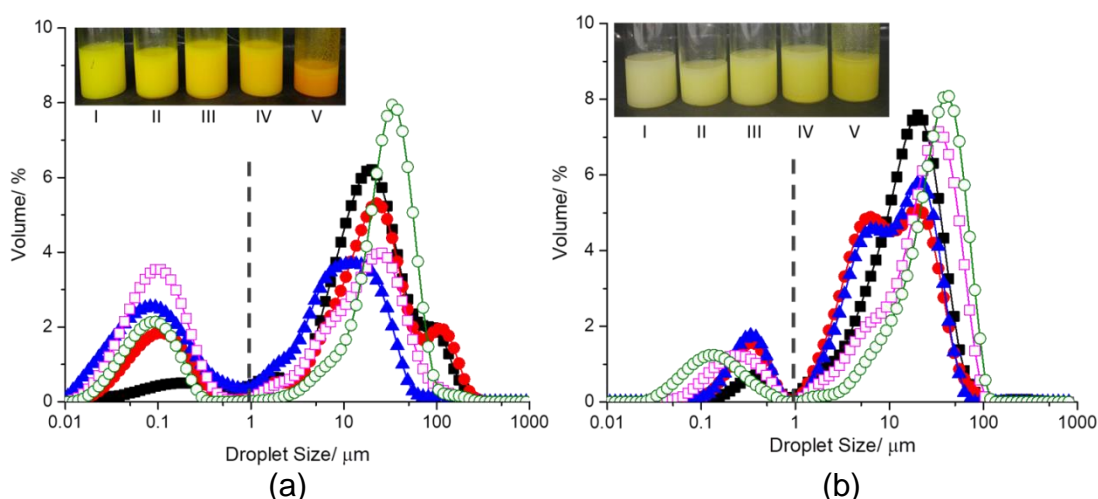


Figure 3.5. Mean water droplet size distributions and corresponding visual images of W/O Pickering emulsions (5:95 wt% w:o ratio) stabilized by curcumin (a) and quercetin (b) crystals at different particle concentrations; 0.06 wt% [■] and [I], 0.14 wt% [●] and [II], 0.25 wt% [▲] and [III], 0.5 wt% [□] and [IV], 1.5 wt% [○] and [V] curcumin or quercetin particles at pH 3.0. Dashed line separates the unabsorbed particles remained into the continuous phase ($\leq 1 \mu\text{m}$) and water droplets.

As discussed above, some smaller peaks ($\leq 1 \mu\text{m}$) were observed in the size distribution plots (Figures 3.5 (a) and 3.5 (b)) for both curcumin and quercetin particles due to the presence of free particles in the continuous phase (the peaks were separated by a dashed line). Therefore the actual water droplets size can be identified from the peaks above $1 \mu\text{m}$ for both particle stabilizers and are shown in Figure 3.6 (the d_{32} values were recalculated for water droplets ($> 1 \mu\text{m}$) for both systems). Smaller water droplets were identified at particle concentrations of 0.14 and 0.25 wt% for quercetin and curcumin, respectively. At particle concentration below 0.25 wt% for curcumin and 0.14 wt% of quercetin; there were not enough particles to fully cover the water droplets. However, at the concentrations indicated above (0.25 wt% for curcumin and 0.14 wt% of quercetin), there was maximum surface coverage and minimum d_{32} values were observed. By increasing the concentration of polyphenol particles above 0.25 wt%, the d_{32} value started to increase. This reflects the competition between particle adsorption at the interface and particle aggregation in the oil phase as the particle concentration increased. At a very high concentration of particles (1.5 wt%), aggregation mechanism in the bulk oil phase appeared to dominate,

depleting the particles that could have contributed to the stabilization of the water droplets, otherwise.

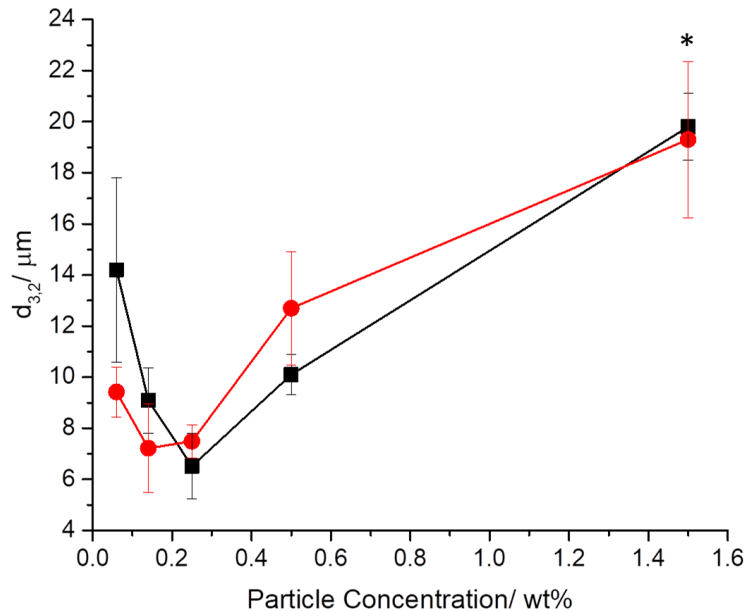


Figure 3.6. Mean droplet size of water droplets (d_{32}) stabilized by curcumin [■] or quercetin [●] particles at different concentrations; 0.06, 0.14, 0.25, 0.5 and 1.5 wt%. The pH of the aqueous phase was adjusted to pH 3.0. Error bars represent standard deviation of at least three independent experiments. Samples with * do not differ significantly ($p > 0.05$) according to Tukey's test.

W/O Pickering emulsions were also prepared at pH 7.0. Droplet size distributions for both curcumin and quercetin emulsions (Figure 3.7 (a) and 3.7 (b)) show very similar trends at all particle concentrations with no significant change in the mean size. However, for all the systems, the size of the water droplets increased significantly within 3 days indicating unstable emulsions. In addition, as observed at pH 3.0, some smaller peaks below 1 μm were seen for both particles (the peaks were separated by a dashed line and the d_{32} values were re-calculated for water droplets as above). However, the peaks in curcumin-stabilized emulsions were much larger than those in quercetin, again indicating that curcumin was not efficiently adsorbed to the interface at pH 7.0.

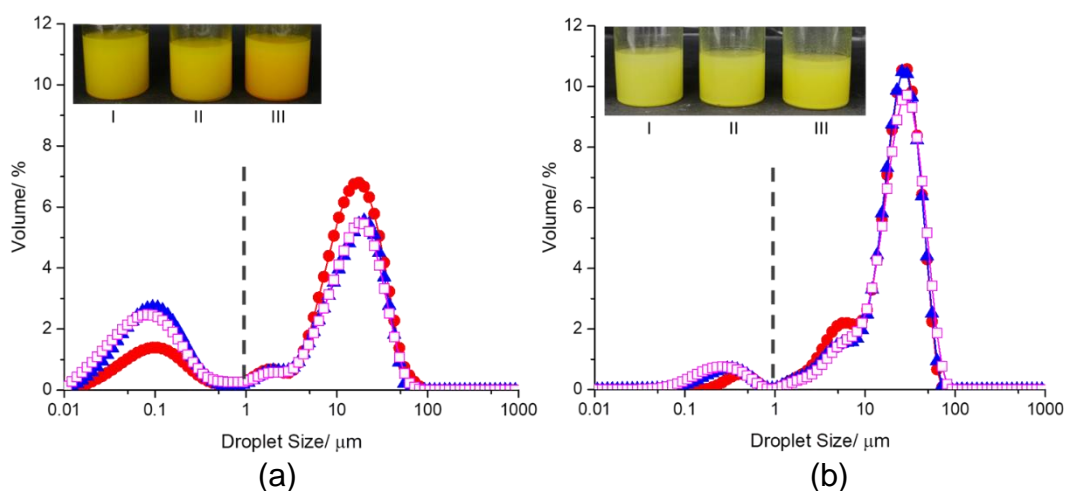


Figure 3.7. Mean water droplet size distributions and corresponding visual images of W/O Pickering emulsions (5:95 wt% w:o ratio) stabilized by curcumin (a) and quercetin (b) crystals at different particle concentrations; 0.14 wt% [●] and [I], 0.25 wt% [▲] and [II] and 0.5 wt% [◻] and [III] curcumin or quercetin particles at pH 7.0. Dashed line separates the unabsorbed particles remained into the continuous phase ($\leq 1 \mu\text{m}$) and water droplets.

Figures 3.8 (a) and 3.8 (b) compare the calculated mean droplet sizes (*i.e.*, $> 1 \mu\text{m}$) at different particle concentrations and different pH values. For curcumin-stabilized emulsions with an aqueous phase of pH 7.0, the mean size of the water droplets was similar at all curcumin concentrations; $d_{32} = 9 - 10 \mu\text{m}$. Similarly, quercetin-stabilized emulsions at pH 7.0 were similar in size at all concentrations; $d_{32} = 12.5 - 14.5 \mu\text{m}$. Water droplets stabilized by quercetin particles at pH 7.0 were larger than those at pH 3.0 at concentrations of 0.06 and 0.14 wt%. Interestingly, at 0.5 wt% for both particles, the size of water droplets did not vary much on changing the pH. The ζ -potential measurements suggested both types of particles would have a greater (negative) charge on attaching water at pH 7.0, which may reduce particle surface activity and increase inter-particle repulsion, explaining the decreases in emulsifying capability.

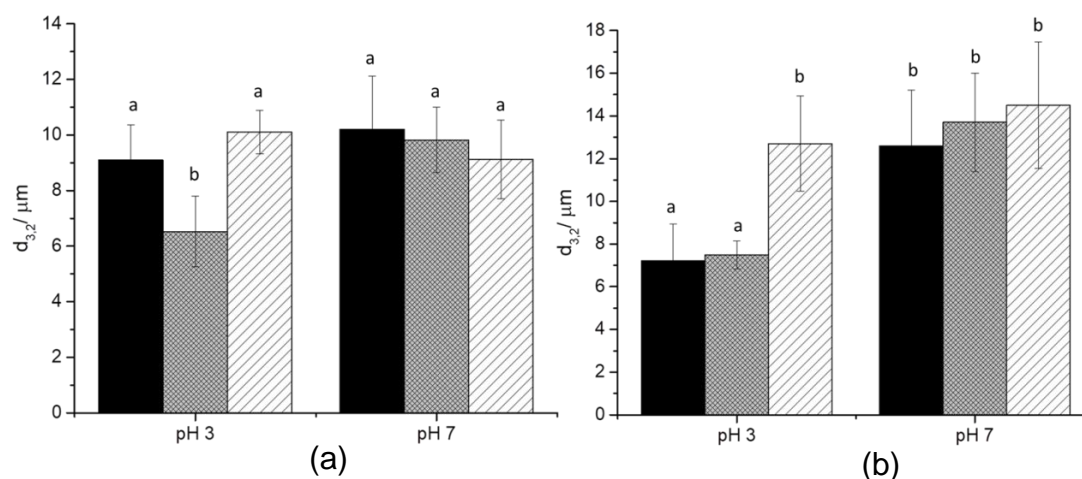


Figure 3.8. Mean droplet size (d_{32}) of the W/O Pickering emulsions versus pH for curcumin (a) and quercetin (b) at different particle concentrations; 0.14 wt% [black], 0.25 wt% [gray] and 0.5 wt% [white]. Error bars represent standard deviation of at least three independent experiments. Bars with the same letter do not differ significantly ($p > 0.05$) according to Tukey's test for each polyphenol crystal at the two different pH values used.

Confocal images of emulsions in Figures 3.9 and 3.10 show how water droplets were surrounded by a dense layer of curcumin (red) or quercetin (green) particles, confirming the preferential location of the polyphenol crystals at the W-O interface. The brightness in the images was due to the auto-fluorescence of polyphenol particles. Furthermore, some droplets appeared to be not completely spherical, which is another indication of Pickering stabilization (Dickinson, 2010). For curcumin-stabilized emulsions some small particles appeared in the oil continuous phase, agreeing with the results from the light scattering (Figure 3.5 (a) and 3.7 (a) at pH 3.0 and 7.0, respectively) and macroscopic observations of the emulsions, that a significant amount of curcumin particles remained unabsorbed, *i.e.*, dispersed in the oil phase. This agrees with the predictions of the contact angle measurements and calculated ΔG_d discussed above, plus the particle size distributions in Figure 3.2. Curcumin is more hydrophobic and more compatible with the oil than quercetin, whilst larger crystals of either should have a very large energy barrier to detach from the interface.

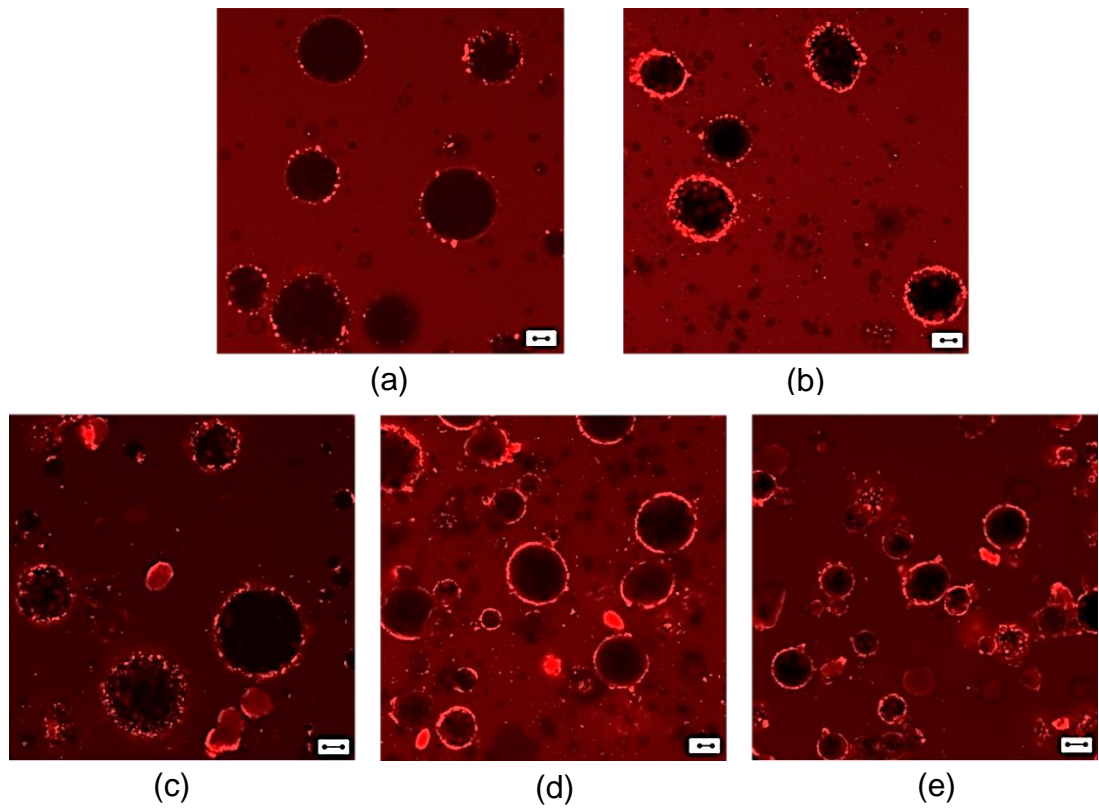


Figure 3.9. Confocal images of W/O Pickering emulsions (5:95 wt% w:o ratio) stabilized by curcumin (red) particles at different concentrations; 0.06 (a), 0.14 (b), 0.25 (c), 0.5 (d) and 1.5 wt% (e). The pH of the aqueous phase was adjusted to pH 3.0. The scale bar is equal with 20 μm . The brightness in the images is caused by auto-fluorescence of curcumin particles (488 nm excitation).

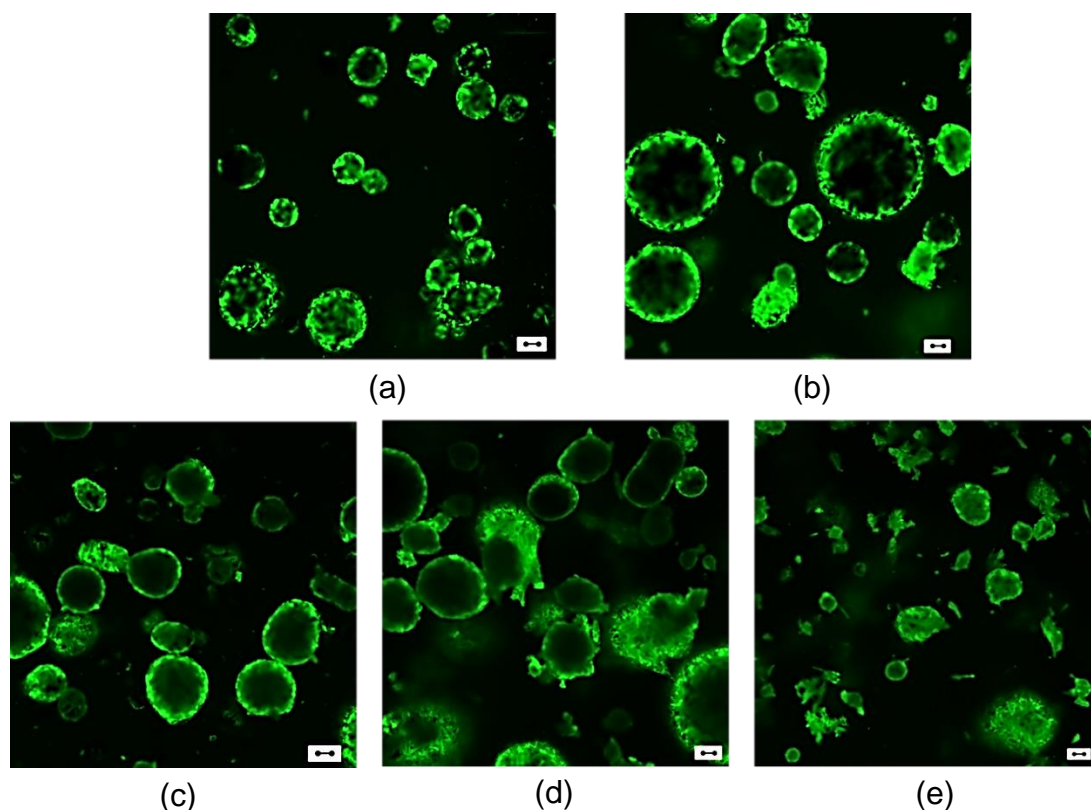


Figure 3.10. Confocal images of W/O Pickering emulsions (5:95 wt% w:o ratio) stabilized by quercetin (green) particles at different concentrations; 0.06 (a), 0.14 (b), 0.25 (c), 0.5 (d) and 1.5 wt% (e). The pH of the aqueous phase was adjusted to pH 3.0. The scale bar is equal with 20 μm . The brightness in the images is caused by auto-fluorescence of quercetin particles (405 nm excitation).

To further verify the claim that the curcumin or quercetin-stabilized systems were Pickering emulsions, images were collected at different depths of focus on a single large droplet as shown in Figures 3.11 and 3.12. The presence of a continuous bright ring at the W-O interface demonstrates even more clearly that water droplets were covered by curcumin or quercetin particles. Moreover, the size and shape of particles at the interface were assessed by zooming in to a specific region. Quercetin particles had their rod-like shape and formed a denser layer at the interface whilst curcumin particles had their polyhedral shape, in agreement with the images of the particles in oil observed previously (Figure 3.3 and 3.4, respectively).

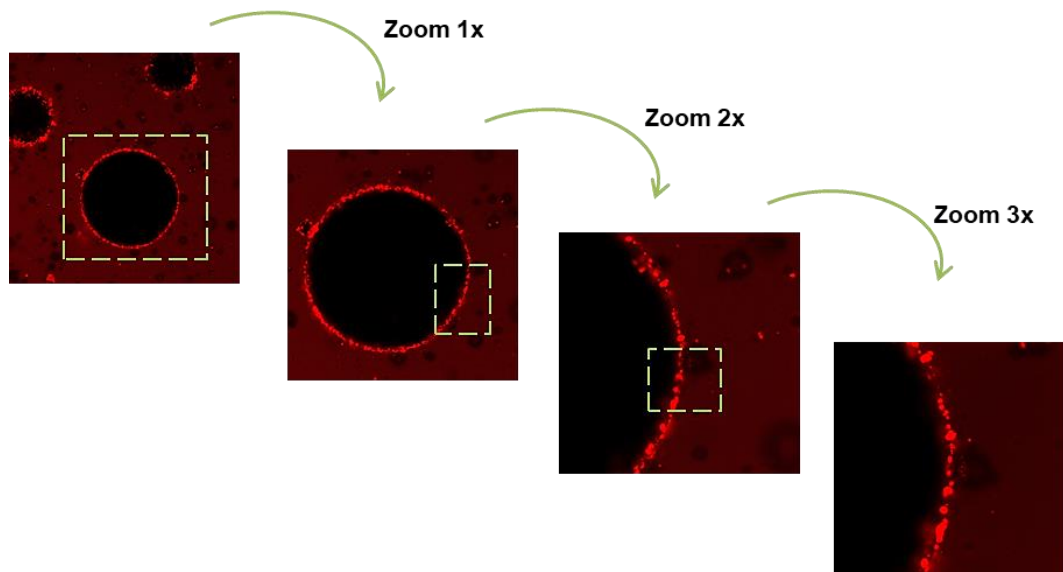


Figure 3.11. Confocal images of W/O Pickering emulsions stabilized by 0.14 wt% curcumin particles. The arrows indicate the sequence of images collected at depths of focus in order to visualize the particles at the W-O interface. The brightness in the image is caused by auto-fluorescence of the curcumin particles (488 nm excitation).

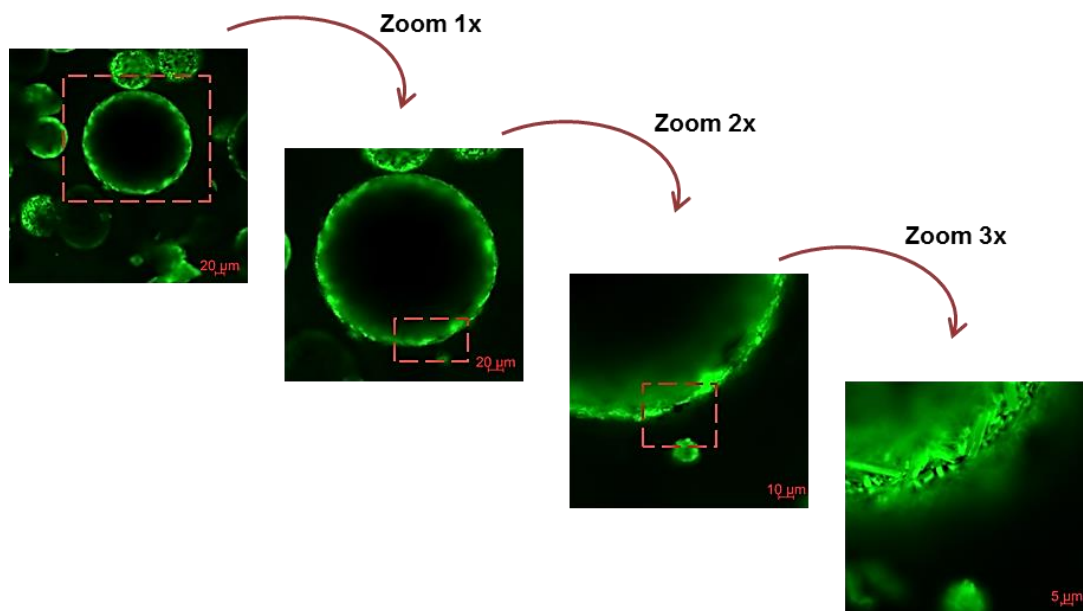


Figure 3.12. Confocal images of W/O Pickering emulsions stabilized by 0.14 wt% quercetin particles. The arrows indicate the sequence of images collected at depths of focus in order to visualize the particles at the W-O interface. The brightness in the image is caused by auto-fluorescence of the quercetin particles (405 nm excitation).

3.3.2.2. Interfacial shear viscosity

Interfacial shear viscosity (η_i) is a useful way of monitoring the formation and structuring of adsorbed films (Burke *et al.*, 2014). It gives information about structural and compositional changes within adsorbed layers, and how the surface behaviour can be related to aspects of the formation and stability of emulsions (Murray, 2002; Murray *et al.*, 1996). Figure 3.13 shows the effect of the presence of curcumin or quercetin particles dispersed in non-purified oil on the mean values of interfacial shear viscosity. A control experiment with non-purified oil and Milli-Q water (pH 3.0) was performed but η_i was equal with 0 mN s m⁻¹ even after 24 h. Thus, addition of curcumin or quercetin particles at 0.14 wt% caused an increase in η_i . In the presence of curcumin particles the rate of growth of η_i was very slow at the beginning of the experiment (*i.e.*, up to at least \approx 7 h of adsorption) but after 24 h η_i had increased to 22 mN s m⁻¹. In contrast, in the presence of quercetin particles at the same concentration, η_i rose significantly right at the beginning of the experiment and was still increasing even after 24 h of adsorption ($>$ 338 mN s m⁻¹). This suggests stronger accumulation of quercetin particles at the interface and/or stronger interactions between the particles at the interface than with curcumin particles. This might be attributed to the larger aspect ratio of the quercetin particles giving higher desorption energy per unit mass and allowing more efficient packing at the interface (Figure 3.10). The curcumin particles were much smaller ($d_{32} = 0.2 \mu\text{m}$) and polyhedral in shape, giving lower desorption energy per unit mass whilst at the same time less efficient particle packing at the interface (Figure 3.9). On the other hand, since both curcumin and quercetin particles are denser than oil, the curcumin particles will also take longer to fall and settle at the interface in the interfacial shear viscosity experiment.

Fat crystals and mono- and di-glycerides that are present in vegetable oils can influence the interfacial rheology of adsorbed particle films (Murray, 2002). Based on the literature; the co-adsorption of mono and di-glycerides tends to destroy high values of η_i of particle films because they tend to be more surface active than particles and displace them completely (Murray,

2002). For this reason, soybean oil was purified using aluminum oxide in order to remove any surface active components that may affect the interfacial shear viscosity results. Experiments with curcumin and quercetin particles dispersed in purified oil are shown in Appendix A, Figure A4. The same trends were observed in purified oil as with non-purified oil (Figure 3.13), indicating that the surface active materials in the oil did not affect the interfacial viscosity significantly.

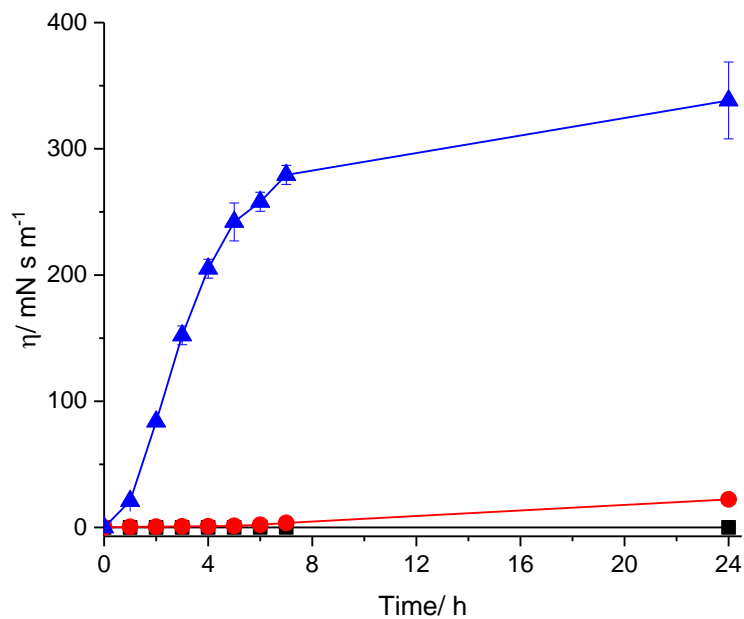


Figure 3.13. Interfacial shear viscosity at interface of Milli-Q water with non-purified oil [■], non-purified oil with 0.14 wt% curcumin particles [●] and non-purified oil with 0.14 wt% quercetin particles [▲]. The pH of the aqueous phase was adjusted to pH 3.0. Error bars represent standard deviation of at least two independent experiments.

3.4. Conclusion

We have demonstrated for the first time that W/O emulsions can be stabilized with curcumin or quercetin particles, which were both sufficiently hydrophobic according to contact angle measurements. Microstructural evaluation at various length scales revealed that quercetin particles had a rod shape and larger aspect ratio than curcumin particles, the latter having a polyhedral shape. Neither particle dispersions significantly suppressed the interfacial tension again indicating a Pickering stabilization mechanism.

When preparing W/O particle-stabilized emulsions, a low concentration of particles (0.06 wt%) was not able to cover the water droplets fully, whereas at much higher concentration (0.5 and 1.5 wt%), significant proportion of particles still remained unabsorbed leading to aggregation of water droplets and particle sedimentation. An optimum concentration of particles with the smallest water droplets and fewer free particles in the continuous phase was identified at 0.14 and 0.25 wt% for quercetin and curcumin, respectively. Increasing the pH of the aqueous phase from pH 3.0 to pH 7.0 gave more coarse emulsions, possibly related to an increase in magnitude of the ζ -potential (more negative) of the particle surface when in contact with water. Interfacial shear viscosity results also show stronger film formation at the interface due to stronger interactions between quercetin particles, possibly due to their larger size and higher aspect ratio. Therefore, we suggest that particle stabilization of W/O emulsions may be imparted by biocompatible polyphenol crystals of appropriate size, shape, charge and wettability. As such, this work should have broad implications in the rational design of stable W/O or double emulsions for various soft matter applications, such as food, pharmaceuticals, personal care, agriculture etc., plus have implications for the behaviour of such polyphenol crystals in food processing and even their digestion.

As it was discussed in **Chapter 1**, polyphenols have the ability to interact with proteins and form complexes when both are present into the aqueous phase. Hence, in the next chapter (**Chapter 4**), the ability of polyphenols to form complexes with proteins at the W-O interface, even if polyphenols and proteins are present in different phases, will be evaluated. Therefore, W/O emulsions stabilized by polyphenol crystals, present in the oil phase, and whey protein isolate (WPI), present in the aqueous phase, will be formed. This interfacial complexation between polyphenol crystals and WPI will be extensively studied and the stability of the corresponding W/O emulsion droplets will be evaluated as a function of different WPI concentrations, pH values, water volume fractions and different NaCl concentrations in the aqueous phase.

References

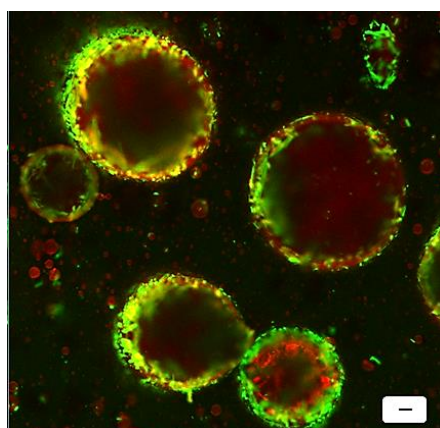
- Al-Rossies, A. A. S., Al-Anazi, B. D., & Paiaman, A. M. (2010). Effect of pH-values on the contact angle and interfacial tension. *Nafta*, *61*, 181-186.
- Araiza-Calahorra, A., Akhtar, M., & Sarkar, A. (2018). Recent advances in emulsion-based delivery approaches for curcumin: From encapsulation to bioaccessibility. *Trends in Food Science & Technology*, *71*, 155-169.
- Atarés, L., Marshall, L. J., Akhtar, M., & Murray, B. S. (2012). Structure and oxidative stability of oil in water emulsions as affected by rutin and homogenization procedure. *Food Chemistry*, *134*(3), 1418-1424.
- Aveyard, R., Binks, B. P., & Clint, J. H. (2003). Emulsions stabilised solely by colloidal particles. *Advances in Colloid and Interface Science*, *100*, 503-546.
- Balasubramanian, K. (2006). Molecular orbital basis for yellow curry spice curcumin's prevention of Alzheimer's disease. *Journal of agricultural and food chemistry*, *54*(10), 3512-3520. doi:10.1021/jf0603533
- Binks, B., & Lumsdon, S. (2001). Pickering emulsions stabilized by monodisperse latex particles: effects of particle size. *Langmuir*, *17*(15), 4540-4547.
- Binks, B. P. (2002). Particles as surfactants—similarities and differences. *Current opinion in colloid & interface science*, *7*(1-2), 21-41.
- Binks, B. P., & Horozov, T. S. (2006). *Colloidal particles at liquid interfaces*: Cambridge University Press.
- Binks, B. P., & Lumsdon, S. (2000). Influence of particle wettability on the type and stability of surfactant-free emulsions. *Langmuir*, *16*(23), 8622-8631.
- Bordenave, N., Hamaker, B. R., & Ferruzzi, M. G. (2014). Nature and consequences of non-covalent interactions between flavonoids and macronutrients in foods. *Food & function*, *5*(1), 18-34.
- Brugger, B., Rosen, B. A., & Richtering, W. (2008). Microgels as stimuli-responsive stabilizers for emulsions. *Langmuir*, *24*(21), 12202-12208.
- Burgaud, I., Dickinson, E., & Nelson, P. (1990). An improved high-pressure homogenizer for making fine emulsions on a small scale. *International journal of food science & technology*, *25*(1), 39-46.
- Burke, J., Cox, A., Petkov, J., & Murray, B. S. (2014). Interfacial rheology and stability of air bubbles stabilized by mixtures of hydrophobin and β -casein. *Food Hydrocolloids*, *34*, 119-127.
- Cretu, R., Dima, C., Bahrim, G., & Dima, S. (2011). Improved solubilization of curcumin with a microemulsification formulation. *The Annals of the University of Dunarea De Jos of Galati. Fascicle VI. Food Technology*, *35*(2), 46.
- Dickinson, E. (2010). Food emulsions and foams: Stabilization by particles. *Current Opinion in Colloid & Interface Science*, *15*(1), 40-49.

- Dickinson, E. (2012). Use of nanoparticles and microparticles in the formation and stabilization of food emulsions. *Trends in Food Science & Technology*, 24(1), 4-12.
- Duffus, L. J., Norton, J. E., Smith, P., Norton, I. T., & Spyropoulos, F. (2016). A comparative study on the capacity of a range of food-grade particles to form stable O/W and W/O Pickering emulsions. *Journal of colloid interface science*, 473, 9-21.
- Formica, J., & Regelson, W. (1995). Review of the biology of quercetin and related bioflavonoids. *Food and chemical toxicology*, 33(12), 1061-1080.
- Hunter, T. N., Pugh, R. J., Franks, G. V., & Jameson, G. J. (2008). The role of particles in stabilising foams and emulsions. *Advances in Colloid and Interface Science*, 137(2), 57-81.
- Kim, J.-H., Kim, S.-I., Kyong, K.-Y., Lee, E.-J., & Yoon, M.-S. (2004). Effect of aqueous phase composition on the stability of a silica-stabilized water-in-oil emulsion. *Journal of the Society of Cosmetic Scientists of Korea*, 30(3), 353-359.
- Lam, S., Velikov, K. P., & Velev, O. D. (2014). Pickering stabilization of foams and emulsions with particles of biological origin. *Current Opinion in Colloid & Interface Science*, 19(5), 490-500.
- Luo, Z., Murray, B. S., Ross, A.-L., Povey, M. J. W., Morgan, M. R. A., & Day, A. J. (2012). Effects of pH on the ability of flavonoids to act as Pickering emulsion stabilizers. *Colloids and Surfaces B: Biointerfaces*, 92, 84-90.
- Luo, Z., Murray, B. S., Yusoff, A., Morgan, M. R., Povey, M. J., & Day, A. J. (2011). Particle-stabilizing effects of flavonoids at the oil-water interface. *Journal of agricultural and food chemistry*, 59(6), 2636-2645.
- Melle, S., Lask, M., & Fuller, G. G. (2005). Pickering emulsions with controllable stability. *Langmuir*, 21(6), 2158-2162. doi:10.1021/la047691n
- Midmore, B. (1999). Effect of aqueous phase composition on the properties of a silica-stabilized W/O emulsion. *Journal of colloid and interface science*, 213(2), 352-359.
- Murray, B. S. (2002). Interfacial rheology of food emulsifiers and proteins. *Current Opinion in Colloid & Interface Science*, 7(5-6), 426-431.
- Murray, B. S., & Dickinson, E. (1996). Interfacial rheology and the dynamic properties of adsorbed films of food proteins and surfactants. *Food Science and Technology International, Tokyo*, 2(3), 131-145. doi:10.3136/fsti9596t9798.2.131
- Niknafs, N. (2011). *Mechanistic understanding of emulsion formation during processing*. University of Birmingham,
- Payton, F., Sandusky, P., & Alworth, W. L. (2007). NMR study of the solution structure of curcumin. *Journal of natural products*, 70(2), 143-146.

- Pickering, S. U. (1907). Cxcvi.—emulsions. *Journal of the Chemical Society, Transactions*, 91, 2001-2021.
- Rein, D. M., Khalfin, R., & Cohen, Y. (2012). Cellulose as a novel amphiphilic coating for oil-in-water and water-in-oil dispersions. *Journal of colloid and interface science*, 386(1), 456-463.
- Roedig-Penman, A., & Gordon, M. H. (1998). Antioxidant properties of myricetin and quercetin in oil and emulsions. *Journal of the American Oil Chemists' Society*, 75(2), 169-180.
- Rossi, M., Rickles, L. F., & Halpin, W. A. (1986). The crystal and molecular structure of quercetin: A biologically active and naturally occurring flavonoid. *Bioorganic Chemistry*, 14(1), 55-69.
- Sarkar, A., Murray, B., Holmes, M., Ettelaie, R., Abdalla, A., & Yang, X. (2016). In vitro digestion of Pickering emulsions stabilized by soft whey protein microgel particles: influence of thermal treatment. *Soft Matter*, 12(15), 3558-3569.
- Sarkar, A., Zhang, S., Murray, B., Russell, J. A., & Boxal, S. (2017). Modulating in vitro gastric digestion of emulsions using composite whey protein-cellulose nanocrystal interfaces. *Colloids and Surfaces B: Biointerfaces*, 158, 137-146.
- Sharma, R., Gescher, A., & Steward, W. (2005). Curcumin: the story so far. *European journal of cancer*, 41(13), 1955-1968.
- Skelhon, T. S., Grossiord, N., Morgan, A. R., & Bon, S. A. (2012). Quiescent water-in-oil Pickering emulsions as a route toward healthier fruit juice infused chocolate confectionary. *Journal of Materials Chemistry*, 22(36), 19289-19295.
- Tønnesen, H. H., Másson, M., & Loftsson, T. (2002). Studies of curcumin and curcuminoids. XXVII. Cyclodextrin complexation: solubility, chemical and photochemical stability. *International Journal of Pharmaceutics*, 244(1), 127-135.
- Tsao, R. (2010). Chemistry and biochemistry of dietary polyphenols. *Nutrients*, 2(12), 1231-1246.
- Xiao, J., Li, Y., & Huang, Q. (2016). Recent advances on food-grade particles stabilized Pickering emulsions: Fabrication, characterization and research trends. *Trends in Food Science & Technology*, 55, 48-60.

Chapter 4

Water-in-Oil Pickering Emulsions Stabilized by an Interfacial Complex of Water-Insoluble Polyphenol Crystals and Protein ²



Abstract

Long-term stabilization of water-in-oil (W/O) emulsions remains a particularly challenging problem in colloid science. Recent studies have shown that polyphenols act as Pickering stabilizers at the water-oil interface. In this work, we propose a novel way to stabilize water droplets via interfacial complex formation. It was observed that polyphenol crystals (curcumin or quercetin) absorb at the interface and provide stabilization of water droplets for several days; however, formation of a polyphenol- whey protein (WPI) complex at the water-oil (W-O) interface revealed a pronounced improvement in the stabilization. The mechanism of complex formation was tested by subjecting the systems to different environmental conditions, such as pH, ionic strength and temperature. The evidence suggests that the complex is probably

² Published as: Zembyla, M., Murray, B.S., Radford, S. J., & Sarkar, A. (2019). Water-in-oil Pickering emulsions stabilized by an interfacial complex of water-insoluble polyphenol crystals and protein. *Journal of Colloid and Interface Science*, 548, 88-99. DOI: [10.1016/j.jcis.2019.04.010](https://doi.org/10.1016/j.jcis.2019.04.010)

stabilized by electrostatic attraction between the oppositely-charged polyphenol particles and protein at the interface, although hydrogen bonding between the two components may also contribute. The resulting stable water droplets have a Sauter mean diameter (d_{32}) of approximately ~ 22 and ~ 27 μm for curcumin and quercetin systems, respectively. Emulsions were more stable at pH 3.0 than at pH 7.0, due to either weaker complex formation at pH 7.0 and/or chemical degradation of the polyphenols at this more alkaline pH. Interfacial shear viscosity measurements confirmed that there was strong interfacial complex formation with aqueous WPI concentrations of ~ 0.5 wt%.

4.1. Introduction

In many water-in-oil (W/O) emulsion systems (e.g., in food, pharmaceuticals, cosmetics, agriculture etc.), adsorbed solid particles can provide kinetic stability to the dispersed phase (Ghosh *et al.*, 2011). Such solid particles are known as 'Pickering' particles and create a steric barrier between adjacent water droplets, thereby hindering coalescence (Ghosh *et al.*, 2011). The use of Pickering particles as stabilizers for W/O emulsions is gaining significant attention owing to their ability to adsorb irreversibly at the interface and the lack of alternative, 'clean label' W/O emulsifiers (Dickinson, 2010; Zembyla *et al.*, 2018). Particularly, there is a huge driving force from food and pharmaceutical industries to replace the chemically-synthesized surfactants (e.g., PGPR) with some natural, biodegradable and affordable materials.

Combination of particles, biopolymers and/or surfactants have been reported in literature to stabilize W/O emulsions, however, the research in this area is very limited. Midmore (1999) prepared W/O emulsions using hydrophobic silica particles in the oil phase and hydroxypropyl cellulose into the aqueous phase. It was found that the addition of hydroxypropyl cellulose allowed silica particles to adsorb more readily at the interface owing to the presence of hydrophobically modified cellulose in the aqueous phase (Midmore, 1999). Skelhon *et al.* (2012) used fumed silica particles (dispersed in the oil phase) and positively charged chitosan in the aqueous phase under acidic conditions to stabilize W/O emulsions. They have observed that the

addition of chitosan in the system promoted the silica to adsorb favourably onto the droplet surface due to electrostatic interactions between the oppositely charged chitosan and silica particles (Skelhon *et al.*, 2012). In addition, Rutkevičius *et al.* (2018) studied the stabilization of W/O emulsions through the addition of zein particles present in the aqueous phase and lecithin in the oil phase, where the latter promoted adsorption of zein particles to the interface (Rutkevičius *et al.*, 2018).

In our previous work, we have shown the ability of polyphenol crystals to stabilize water droplets via the Pickering mechanism (Zembyla *et al.*, 2018). Water-insoluble curcumin and quercetin crystals were proven to be hydrophobic, based on their three-phase contact angle measurements. Neither of these particle dispersions suppressed the interfacial tension significantly, indicating a Pickering stabilization mechanism. Micro-structural evaluation at various length scales revealed that quercetin crystals had a more rod-like shape than curcumin crystals, the latter being smaller and having a more polyhedral shape. The differences in the shape and size of the polyphenols were reflected in the Pickering stabilization efficiency of the two materials, perhaps explaining why other workers (Duffus *et al.*, 2016) were apparently not able to stabilize W/O emulsions as effectively with different polyphenols. Curcumin and quercetin particles at 0.14 wt% imparted stability to coalescence of W/O emulsions for several days of storage, but the size (up to 6 μm) of the droplets resulted in significant sedimentation of both droplets and particles over this time period (Zembyla *et al.*, 2018), most probably due to the large size range of the stabilizing particles, making efficient coverage of small water droplets difficult. Thus, although polyphenol crystals show potential as W/O emulsion stabilizers, improvements are required to extend the kinetic stability of such emulsions. In this paper we describe a novel strategy based on complex formation between polyphenols and protein at the interface where a patent has been recently filed on this technology (Murray *et al.*, 2019). This novel mechanism uses natural materials, such as polyphenol crystal and proteins to stabilize water droplets in the oil phase allowing a '*clean label*' emulsifier in the final product.

Curcumin is a natural low-molecular weight polyphenolic compound found in the rhizomes of the perennial herb turmeric (*Curcuma longa*) (Sharma *et al.*, 2005). It possesses two phenolic -OH groups and an α,β -unsaturated- β -diketone moiety in its chemical structure (Araiza-Calahorra *et al.*, 2018; Majhi *et al.*, 2010). The polar hydroxyl/ketone groups are expected to impart hydrophilicity whilst the aromatic/aliphatic parts would be expected to make the molecule more hydrophobic. Quercetin is one of the most abundant flavonoids present in fruits and vegetables - particularly onions, kale, French beans, broccoli, etc. (Wach *et al.*, 2007). It is characterized by its C6-C3-C6 basic backbone (Formica *et al.*, 1995). Quercetin has hydroxyl groups that impart hydrophilic characteristics and ring structures that impart hydrophobicity (Luo *et al.*, 2011). The quercetin crystal structure can be described as layers of hydrogen bonded dimers. These dimers form a two-dimensional net held together via a network of hydrogen bonds with water molecules also present (Rossi *et al.*, 1986). Thus, quercetin molecules can pack in a way that some of the -OH groups are not exposed to the continuous phase, potentially explaining apparent hydrophobic character of the crystal particle surface. Polyphenols have the ability to interact with proteins via hydrogen bonding, hydrophobic and ionic interactions (Bordenave *et al.*, 2014; Dangles *et al.*, 2006). However, the way proteins adsorbing from the aqueous side of a W-O interface might interact with polyphenol crystals adsorbing from the oil side of the interface has not been explored to date.

In this work, we provide evidences that the addition of protein to the aqueous phase of W/O emulsions can give significant improvement to their stability. Whey protein isolate (WPI) was the protein chosen, due to its surface activity (in water) and its ability to form strong viscoelastic adsorbed layers at the interface on its own, when adsorbed from an aqueous phase to a more hydrophobic phase. WPI is a mixture of proteins with numerous functional properties and is of a considerable importance to the food industry. The main proteins it contains are α -lactalbumin and β -lactoglobulin, which represent ca. 70% of the total whey protein and are responsible for its main functional properties (Cayot *et al.*, 1997). β -Lactoglobulin is a globular protein with a polypeptide chain of 162 residues stabilized by two disulfide cross-links and

also contains an internal free sulfhydryl group which is sensitive to interfacial denaturation and heat treatment (Cayot *et al.*, 1997; Rodríguez Patino *et al.*, 1999). The monomeric molecular mass is 18.3 kDa. At pH 5.0 – 8.0, β -lactoglobulin exists as a dimer but at pH 3.0 – 5.0 the dimers associate to form octomers (Cayot *et al.*, 1997). α -Lactalbumin is a smaller protein with 123 amino acid residues and four disulfide bridges and a molecular mass of 14.2 kDa. It has a relatively low content of organized secondary structure for a globular protein and therefore has great molecular flexibility (Cayot *et al.*, 1997). The conformation and physicochemical properties of both proteins naturally depends on the environmental conditions such as salt, pH and temperature treatments (Cayot *et al.*, 1997).

In this work, we show a unique stabilization mechanism of water droplets in oil via complex formation at the interface between polyphenol crystals (*i.e.*, curcumin and quercetin) and WPI. It is hypothesized that polyphenol crystals in the continuous (oil) phase and WPI in the aqueous phase form complexes at the W-O interface via attractive electrostatic interactions and/or hydrogen bonding. The stability of the corresponding W/O emulsion droplets was evaluated as a function of different WPI concentrations and pH values and the mechanism of the interfacial interactions was probed by subjecting the systems to different ionic strengths and temperatures whilst using a range of complimentary physical and microstructural techniques.

4.2. Material and methods

4.2.1. Materials

Curcumin (orange-yellow powder) from turmeric rhizome (96 % total curcuminoid content) was obtained from Alfa Aesar (UK). Quercetin (≥ 95 %) in the form of a yellow crystalline solid was purchased from Cayman Chemicals (USA). Both polyphenols were used without further purification. Soybean oil (KTC Edibles, UK) was purchased from a local store. Aluminium oxide, (99 %, extra pure) was used for soybean oil purification in some experiments and was purchased from Acros Organics (Belgium). Whey protein isolate (WPI) containing 96.5 % protein was obtained from Fonterra

(New Zealand). Water, purified by treatment with a Milli-Q apparatus (Millipore, Bedford, UK), with a resistivity not less than $18 \text{ M}\Omega \text{ cm}^{-1}$, was used for the preparation of the emulsions. A few drops of hydrochloric acid (0.1 M HCl) or sodium hydroxide (0.1 M NaOH) were used to adjust the pH of the emulsions. Sodium azide and Rhodamine B were purchased from Sigma-Aldrich (USA).

4.2.2. Preparation of W/O emulsions

Curcumin or quercetin dispersions were prepared by dispersing the polyphenol crystals (0.14 wt%) in the continuous phase (soybean oil) using an Ultra-Turrax T25 mixer (Janke & Kunkel, IKA-Labortechnik) with a 13 mm mixer head (S25N- 10G) operating at 9,400 rpm for 5 min. The aqueous phase was prepared without or with WPI (0.05 - 4 wt%). The WPI (4 wt%) was dissolved in aqueous phase for at least 2 h at room temperature to ensure complete hydration. The WPI solution was then diluted to the desired WPI concentration and 0.02 wt% sodium azide was added as a preservative. The pH of the aqueous phase was adjusted to 3.0 or 7.0, depending on the experiment, by adding few drops of 0.1 M HCl or NaOH. Coarse W/O emulsions were prepared by homogenizing 5, 10 or 20 wt% of this aqueous phase with soybean oil in an Ultra-Turrax mixer for 2 min at 13,400 rpm. Fine emulsions were prepared by passing the coarse emulsions through a high pressure Leeds Jet Homogenizer, twice, operated at 300 bar. The initial temperature of the particle dispersion was 21 °C. The temperatures of the dispersions were 23 and 26 °C after Ultra-Turrax mixing at 9,400 rpm for 5 min and 13,400 rpm for 2 min, respectively. The temperature of the particle dispersion after passing through the Jet homogenizer (two passes at 300 bar) was 33 – 34 °C. Note that these slight temperature increases were too low to have any significant impact on solubility of the particles or the proteins (Zembyla *et al.*, 2018). Immediately after preparation, emulsions were sealed in 25 mL cylindrical tubes (internal diameter = 17 mm) and stored at room temperature in a dark place.

4.2.3. Particle size measurements

The particle size distributions (*PSD*) of emulsions were measured using static light scattering (SLS) via a Mastersizer Hydro SM small volume wet sample dispersion unit (Malvern Instruments, UK). Average droplet size was monitored via the Sauter mean diameter, d_{32} , or volume mean diameter, d_{43} , defined by:

$$d_{ab} = \frac{\sum n_i d_i^a}{\sum n_i d_i^b} \quad (4.1)$$

where n_i is the number of the droplets of diameter d_i .

For water droplet size measurements, refractive indices of 1.33 and 1.47 were used, for water and soybean oil, respectively. Absorption coefficients of 0.01, 0.1 and 0.01 for curcumin, quercetin and water, were used, respectively. All measurements were made at room temperature on at least three different samples.

4.2.4. Confocal laser scanning microscopy (CLSM)

The microstructure of the W/O emulsions was observed using a confocal microscope (Zeiss LSM700 inverted, Germany). The emulsions were prepared as before but were deliberately not passed through the Leeds Jet homogenizer in order to maximize their size because with larger droplets it was easier to discern the absorbed layers of polyphenols and WPI at the interface. Approximately, 80 μ L of sample were placed into a laboratory-made well slide and a cover slip (0.17 mm thickness) was placed on top, ensuring that there was no air gap (or bubbles) trapped between the sample and coverslip. The samples were scanned at room temperature (25 ± 1 °C) using a 20 \times /0.5 objective lens. Auto-fluorescence from the particles was excited using 488 and 405 nm lasers for curcumin and quercetin crystals, respectively. Rhodamine B was used as a dye for whey protein and was excited using 545 nm lasers. The emission fluorescent light was detected at 525, 460 and 580 nm for curcumin, quercetin and Rhodamine B, respectively.

4.2.5. Interfacial tension

Interfacial tension (γ_T) measurements were performed using soybean oil, with or without the presence of polyphenol crystals and for Milli-Q water in the absence or presence of 0.5 wt% WPI (pH 3.0), using the pendant drop method in a Dataphysics OCA tensiometer (DataPhysics Instruments, Germany). The apparatus includes an experimental cell, an optical system for the illumination and the visualization of the drop shape and a data acquisition system. An upward bended needle was used to immerse a drop of the lower density liquid (oil) into the higher density one (water). Thus, a drop of soybean oil or polyphenol suspension in oil (0.14 wt% curcumin or quercetin) was formed at the tip of the needle and suspended in the cuvette containing Milli-Q water with or without 0.5 wt% WPI, at pH 3.0. The contour of the drop was extracted by the SCA 22 software and fitted to the Young-Laplace equation to obtain γ_T . All measurements were carried out in triplicate and error bars represent the standard deviations.

4.2.6. Interfacial shear viscosity (η_i)

A two dimensional Couette-type interfacial viscometer, described in detail elsewhere (Murray, 2002; Sarkar *et al.*, 2017) was operated in a constant shear-rate mode to measure interfacial viscosity. Briefly, a stainless steel biconical disc (radius 15.0 mm) was suspended from a thin torsion wire with its edge in the plane of the W-O interface of the solution contained within a cylindrical glass dish (radius 72.5 mm). The constant shear rate apparent interfacial viscosity, η_i , is given by the following equation:

$$\eta_i = \frac{g_f}{\omega} K(\theta - \theta_o) \quad (4.2)$$

where K is the torsion constant of the wire; θ is the equilibrium deflection of the disc in the presence of the film; θ_o is the equilibrium deflection in the absence of the film, *i.e.*, due to the bulk drag of the sub-phase on the disc; g_f is the geometric factor and ω is the angular velocity of the dish. A fixed value of $\omega = 1.27 \times 10^{-3} \text{ rad s}^{-1}$ was used, which aids comparison with measurements made on many other systems at the same shear rate.

For these measurements, 0.14 wt% curcumin or quercetin particles were dispersed in purified soybean oil using the Ultra-Turrax mixer at 9,400 rpm for 5 min. The oil was purified with aluminium oxide to eliminate free fatty acids and surface active impurities that may affect the measurements. A mixture of oil and aluminium oxide in proportion 2:1 w/w was stirred for 3 h and centrifuged at 4,000 rpm for 30 min. For the experiments with salt, the aqueous phase consisted of 0.5 wt% WPI dispersed in 0.001, 0.01 or 0.1 M NaCl at pH 3.0. For the experiments with thermal treatment, the systems were prepared as before but η_i was measured at 45 °C for 3 h and then the system was left to cool down overnight, at 25 °C and the η_i was measured again, at this temperature.

4.2.7. Optical microscopy

Curcumin or quercetin dispersions (0.14 wt%) were heated at 45 °C under continuous stirring at 20 - 40 rpm using mixer (IKA 2830001 Compact Mixer, UK) for 30 min. A drop of each dispersion was placed on a microscope slide at (25 °C) before the heating, during the heating (to 45 °C) and after it had cooled back down to 25 °C (after 1 h). The slide was covered with a cover slip (0.17 mm thickness). The size and shape of the polyphenol crystals were observed using an LCD digital microscope (PentaView, Celestron, USA) using a 20×/0.4 objective lens.

4.2.8. Statistical analysis

Significant differences between samples were determined by one-way ANOVA and multiple comparison test with Tukey's adjustment performed using SPSS software (IBM, SPSS statistics) and the level of confidence was 95 %.

4.3. Results and discussion

4.3.1. Stability measurements of W/O Pickering emulsions

4.3.1.1. Aqueous phase at pH 3.0

The main component of WPI, β -lactoglobulin, undergoes significant changes on adsorption, in terms of unfolding of its globular conformation (Jiménez-Flores *et al.*, 2005; Rodríguez Patino *et al.*, 1999; Sarkar *et al.*, 2016). WPI acquires a positive charge (ζ -potential = +34 mV) at pH 3.0, whilst as the pH increases it becomes more negatively charged (*e.g.*, ζ -potential = -34 mV at pH 7.0) (Lam *et al.*, 2015). The isoelectric point (pI) of WPI is at around pH 5.0 (Lam *et al.*, 2015). It has been shown previously that at pH 3.0 curcumin crystals *dispersed in water* had a low positive ζ -potential (+12 mV), whilst quercetin had a distinct negative charge (ζ -potential = -26 mV) (Zembyla *et al.*, 2018). Both crystals *dispersed in water* had similar negative ζ -potentials at pH 7.0 (-48 mV) (Zembyla *et al.*, 2018). Therefore, at pH 3.0, there is a possibility of electrostatic attraction between the negatively-charged quercetin crystals wetted by water from the oil side of the interface and the positively-charged WPI adsorbing from the aqueous side of the interface. For curcumin, weaker electrostatic attraction might take place at pH 3.0, noting that proteins are polyampholytes and that WPI will bear some negatively-charged patches even at pH 3.0, whilst its net charge is still positive.

The *PSD* of the fine emulsions, prepared at pH 3.0 with 0.14 wt% curcumin or quercetin dispersed in the oil phase plus varying concentrations of WPI in the aqueous phase, are shown in Figures 4.1 (a) and 4.1 (c), respectively. Some smaller peaks ($\leq 1 \mu\text{m}$) were observed in the *PSDs* for both curcumin and quercetin particles because of the presence of free particles in the continuous phase (the peaks are separated by the dashed line). Thus, the *PSD* of the water droplets is more correctly identified by the distribution $> 1 \mu\text{m}$ for both systems and these are shown in Figure 4.1 (b) and 4.1 (d). The d_{32} values for the water droplets (*i.e.*, $> 1 \mu\text{m}$) were recalculated from this cut of the total *PSDs* for both systems. For both curcumin- or quercetin-stabilized emulsions, the mean size (d_{32}) of the water

droplets with 0 and 0.05 wt% WPI was smaller (~ 12 and $20 \mu\text{m}$ for curcumin and quercetin, respectively) than the d_{32} for the systems containing a higher concentration of WPI (0.5, 1, 2 and 4 wt%), at ~ 22 and $27 \mu\text{m}$ for curcumin and quercetin, respectively. However, over time (see Figures 4.1 (b) and 4.1 (d)), the d_{32} of emulsions with 0 and 0.05 wt% WPI in the aqueous phase increased significantly ($p < 0.05$, see Appendix B, Table B1 and Table B2) and phase separation occurred within 24 h. On the other hand, d_{32} of the emulsions with 0.5, 1, 2 and 4 wt% WPI was stable ($p > 0.05$, see Appendix B, Table B1 and Table B2), for more than 3 weeks. Sedimentation of particles and/or water droplets was observed, but no coalescence or obvious phase separation of a clear water layer was seen. From these visual observations, plus the changes in mean particle size, it is suggested that the presence of ≥ 0.5 wt% WPI, improved significantly the stability of the emulsions, suggesting some synergistic interaction of WPI and polyphenol crystals at the W-O interface. Our previous work has shown that the dispersion and emulsification conditions had negligible effect on the size distributions of the polyphenol crystals themselves.

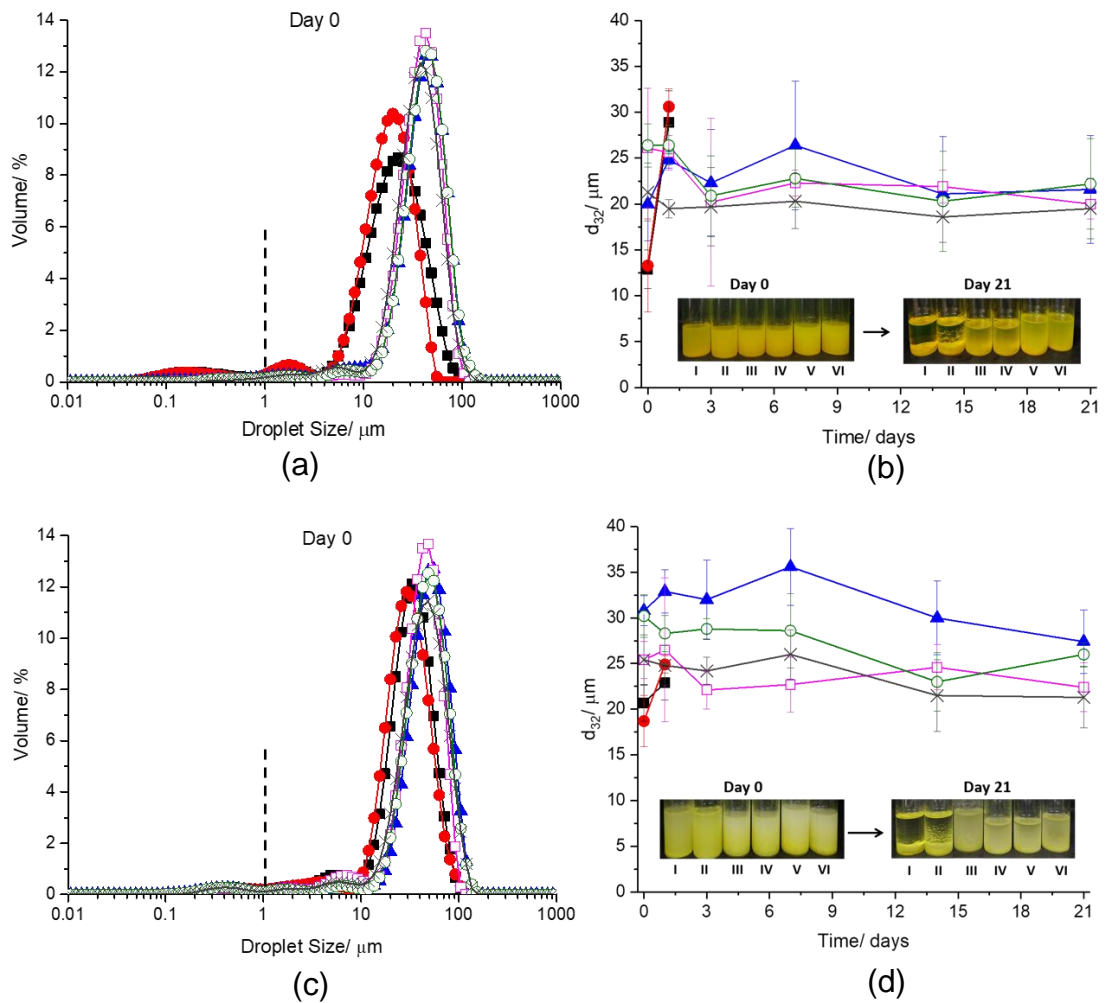


Figure 4.1. PSD [(a) and (c)] and mean particle size (d_{32}) of water droplets over time with visual images [(b) and (d)] of 5 wt% W/O emulsions stabilized by 0.14 wt% curcumin [(a) and (b)] and quercetin [(c) and (d)] particles containing 0 wt% [■] [I], 0.05 wt% [●] [II], 0.5 wt% [▲] [III], 1 wt% [□] [IV], 2 wt% [○] [V] and 4 wt% [×] [VI] WPI in the aqueous phase at pH 3.0, respectively. For statistical analysis according to Tukey's test see Appendix B, Table B1 and Table B2 for curcumin and quercetin, respectively.

Confocal images of the emulsions stabilized by curcumin or quercetin plus WPI are shown in Figures 4.2 (a) and 4.2 (b), respectively, demonstrating that water droplets were surrounded by a dense layer of polyphenol particles (green), confirming their preferential location at the W-O interface. The green brightness of the image is due to the auto-fluorescence of polyphenol particles. Rhodamine B (red) was used to visualize the position of protein and so the intensity of the red colour indicates a higher concentration of WPI on

the inside of the droplets at the W-O interface, as expected. Thus, both polyphenol crystals and WPI appeared to be in close proximity at the interface. Note the size of the water droplets in these images does not reflect the size measured using the Mastersizer because these emulsions were prepared without passing through the Jet homogenizer, as mentioned above, in order to deliberately have larger water droplets and make it easier to visualize the location of the two types of surface active material at the W-O interface.

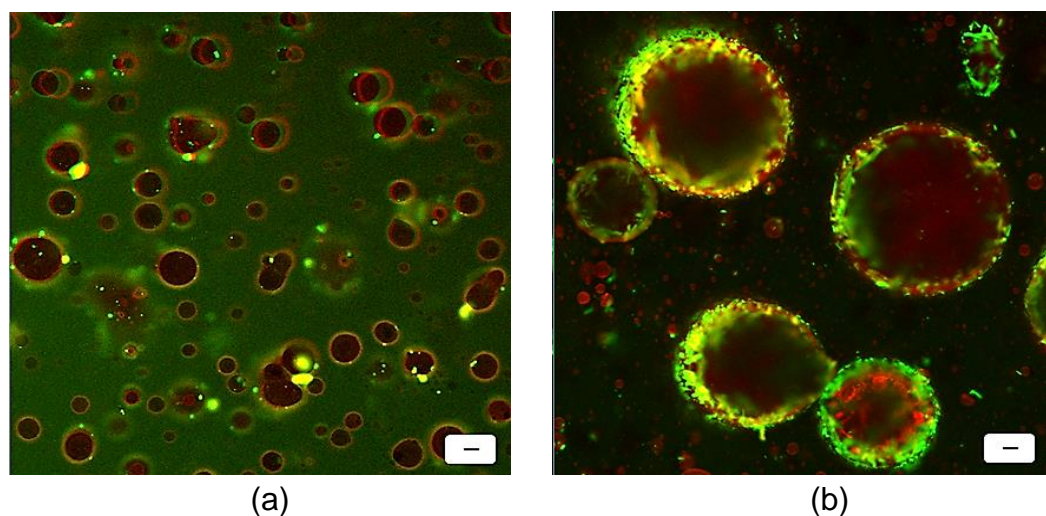


Figure 4.2. Confocal images of 5 wt% W/O Pickering emulsions stabilized by 0.14 wt% curcumin (a) and quercetin (b) crystals with 0.5 wt% WPI in the aqueous phase, at pH 3.0. The green brightness in the images is caused by auto-fluorescence of curcumin (488 nm excitation) or quercetin (405 nm excitation) crystals. The red brightness is due to WPI stained by Rhodamine B (568 nm excitation). The scale bar represents 20 μm .

To further understand the interfacial stabilization mechanism, the interfacial tension (γ_T) was measured, at pH 3.0, and the results are shown in Table 4.1. Firstly, γ_T was measured between soybean oil and the aqueous phase (in the absence of particles) as a control. The equilibrium γ_T for this system was $26.2 \pm 0.5 \text{ mN m}^{-1}$. The value of γ_T did not alter significantly on the addition of curcumin or quercetin particles in the oil phase, indicating Pickering stabilization (Zembyla *et al.*, 2018). However, upon addition of 0.5 wt% WPI (to the aqueous phase) there was a significant decrease in γ_T ($p <$

0.05), presumably due to WPI adsorption, *i.e.*, irrespective of whether polyphenol crystals also adsorbed from the other (oil) side of the interface.

Table 4.1. Interfacial tension (γ_{if}) data, with or without the presence of curcumin or quercetin particles (0.14 wt%) and WPI (0.5 wt%), between the soybean oil and aqueous phases. Samples with the same letter do not differ significantly ($p > 0.05$) according to Tukey's test.

Oil Phase	Aqueous Phase (pH 3.0)	γ_{if} mN m ⁻¹
Soybean Oil	Milli-Q Water	26.2 ± 0.5 ^a
Curcumin	Milli-Q Water	25.4 ± 0.3 ^a
Quercetin	Milli-Q Water	25.8 ± 0.4 ^a
Curcumin	WPI solution (0.5 wt%)	17.1 ± 0.7 ^b
Quercetin	WPI solution (0.5 wt%)	18.0 ± 0.6 ^b

These results support the idea that WPI and polyphenols adsorb together at the W-O interface at pH 3.0. This co-adsorption may explain the improvement in stability of the emulsions at pH 3.0, but to test whether such improvement was due to electrostatic complex formation between them, experiments were also conducted at pH 7.0, where both crystals and protein have the same (negative) sign of charge, which should inhibit such complex formation.

4.3.1.2. Aqueous phase at pH 7.0

Similar to the behaviour at pH 3.0, freshly prepared W/O emulsions stabilized by curcumin or quercetin (Figures 4.3 (a) and 4.3 (c)) at pH 7.0, with 0 and 0.05 wt% WPI, had smaller initial droplet sizes, but their size increased ($p < 0.05$, see Appendix B, Table B3 and Table B4) and gross phase separation occurred within 1 day. The emulsions with 0.5, 1, 2 and 4 wt% WPI had similar d_{32} compared to those prepared at pH 3.0 (Figure 4.1 (a) and 4.1 (c)) but the emulsions at pH 7.0 were not as stable as at pH 3.0. Emulsions prepared with quercetin + WPI (≥ 0.5 wt%) showed sedimentation and some degree of phase separation within 7 days (Figure 4.3 (d)) whereas those with

curcumin crystals took 2 weeks to show phase separation (Figure 4.3 (b)). Therefore, in both cases the emulsions at pH 7.0 were not as stable as the corresponding emulsions at pH 3.0, with an obvious water layer appearing on the bottom of the samples. As observed at pH 3.0, some smaller peaks below 1 μm were seen for both particles (the peaks were separated by a dashed line, and the d_{32} values were recalculated for water droplets as above (Figures 4.3 (b) and 4.3 (d))). In addition, the *PSD* of the emulsions with both curcumin and quercetin crystals + ≥ 0.5 wt% WPI had a second peak at larger particle sizes (between 1 and 10 μm - see Figure 4.3 (c)) at pH 7.0, unlike those at pH 3.0. From the confocal images (Figure 4.4), one can clearly observe considerably greater aggregation of polyphenol particles at pH 7.0 compared to at pH 3.0 (Figure 4.2). Much of the extra aggregation at pH 7.0 seemed to occur at the interface, appearing to 'stick' droplets together. Therefore, the peaks at larger sizes at pH 7.0 probably represent these mixed polyphenol + droplet aggregates. Such flocculation might be attributed to particle aggregation in the continuous phase with consequently less coverage of the W-O interface, *i.e.*, less primary particle coverage of the interface. In any case, the results suggest that if electrostatic complex formation contributes to emulsion stability, it is less effective at pH 7.0, where both protein and polyphenols have the same (negative) sign of charge.

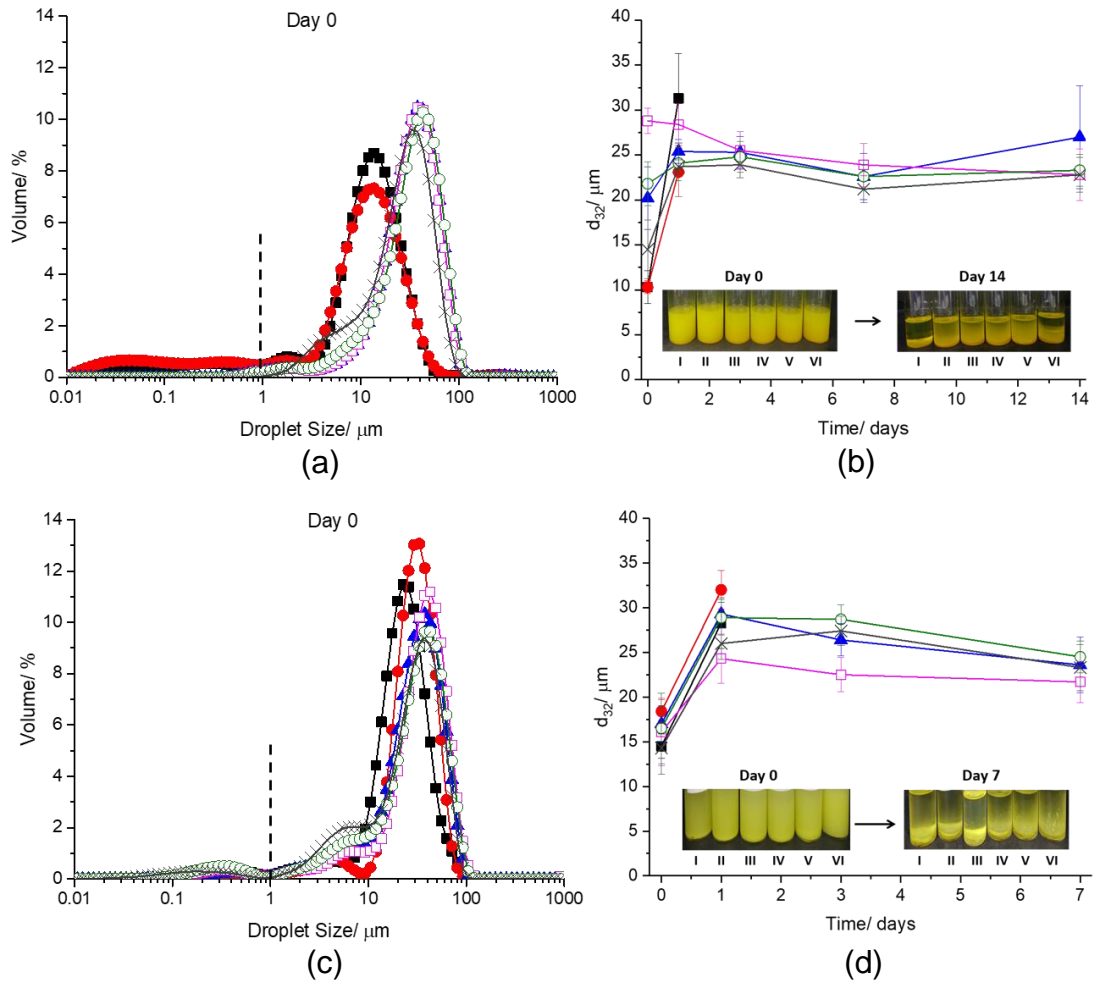


Figure 4.3. PSD [(a) and (c)] and mean particle (d_{32}) size of water droplets over time with visual images [(b) and (d)] of 5 wt% W/O emulsions stabilized by 0.14 wt% curcumin [(a) and (b)] and quercetin [(c) and (d)] particles containing 0 wt% [■] [I], 0.05 wt% [●] [II], 0.5 wt% [▲] [III], 1 wt% [□] [IV], 2 wt% [○] [V] and 4 wt% [×] [VI] WPI in the aqueous phase at pH 7.0, respectively. For statistical analysis according to Tukey's test see Appendix B, Table B3 and Table B4 for curcumin and quercetin, respectively.

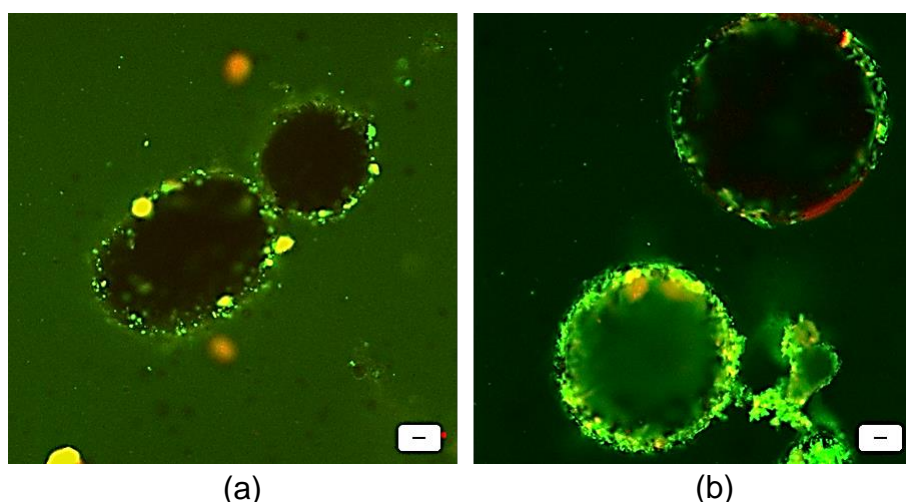


Figure 4.4. Confocal images of 5 wt% W/O Pickering emulsions stabilized by 0.14 wt% curcumin (a) and quercetin (b) crystals with 0.5 wt% WPI in the aqueous phase at pH 7.0. The green brightness in the images is caused by auto-fluorescence of curcumin (488 nm excitation) or quercetin (405 nm excitation) crystals. The red brightness is due to WPI stained by Rhodamine B (568 nm excitation). The scale bar represents 20 μm .

4.3.2. Effect of increase in volume fraction of water droplets

Higher water:oil ratios (10 and 20 wt% water) were tested at pH 3.0 for 0.14 wt% curcumin or quercetin crystals + 0.5 wt% WPI as Pickering stabilizers, since this WPI concentration seemed to be the minimum required to give enhanced stability to 5 wt% W/O emulsions and emulsions were more stable for both polyphenol crystals at this lower pH. As observed previously, some smaller peaks below 1 μm were seen for both particle types (the peaks are separated by a dashed line and the d_{32} values were recalculated for water droplets, as above (Figures 4.3 (b) and 4.3 (d))). Figure 4.5 shows that with curcumin the initial d_{32} increased slightly from ~ 20 to ~ 25 μm ($p > 0.05$) as the wt% water was increased from 5 to 20 wt%, whilst with quercetin d_{32} decreased from ~ 30 to ~ 22 μm as the wt% water increased from 5 to 20 wt% ($p < 0.05$). However, both curcumin- and quercetin-stabilized emulsions containing 10 or 20 wt% water showed an obvious water layer at the bottom of the samples after 1 day and the systems had completely phase separated after 3 days. This suggests that at these higher water volume fractions there were not enough polyphenol crystals or WPI to fully cover the interface. The d_{32} of the 5 wt% W/O emulsion stabilized by curcumin was slightly lower than

that for the corresponding emulsions stabilized by quercetin and this is probably due to the smaller size of the curcumin crystals ($d_{32} = 0.2$ and $6 \mu\text{m}$ for curcumin and quercetin in oil, respectively), which also had a lower aspect ratio (Zembyla *et al.*, 2018). This would lead to more densely packed and even multilayers of curcumin particles at the interface forming smaller water droplets. At 10 and 20 wt% water there is more interface to cover and so both crystal types will be more evenly spread at the interface, which probably explains why there was relative little difference in the mean droplet size for the two systems at these higher water droplet concentrations.

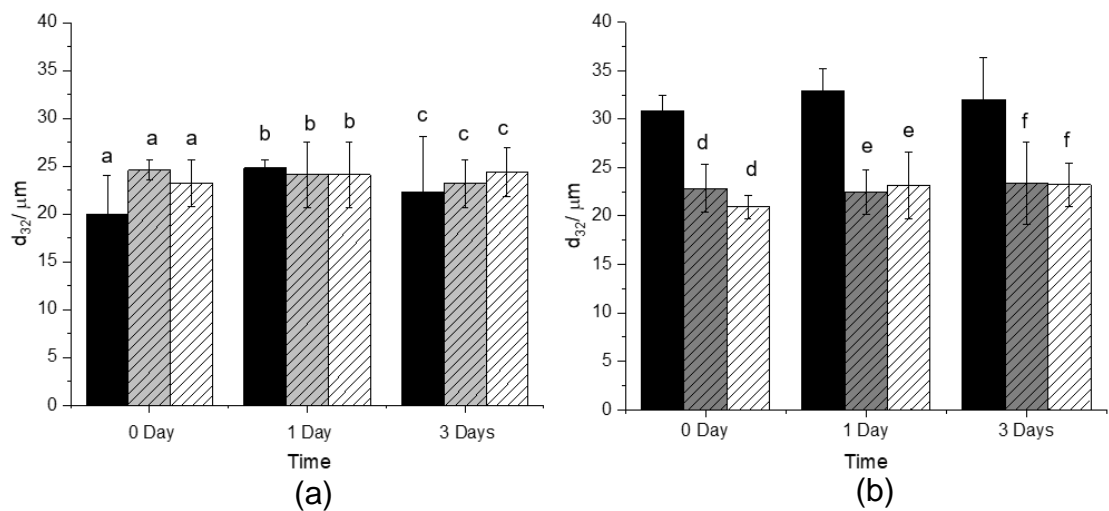
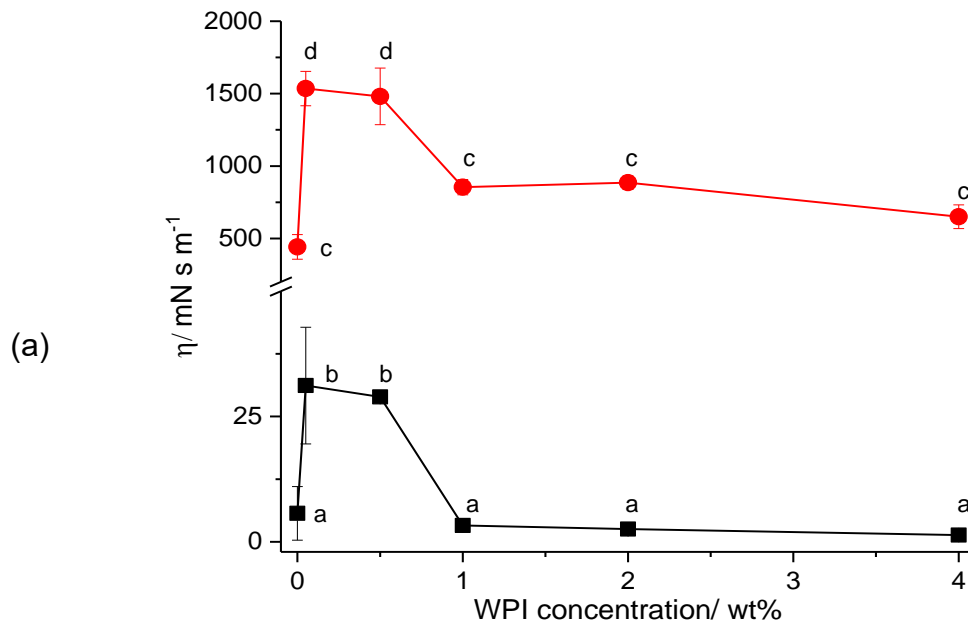


Figure 4.5. Mean size of water droplets (d_{32}) over time of W/O emulsions containing 5 wt% (black), 10 wt% (grey) and 20 wt% (white) water stabilized by 0.14 wt% curcumin (a) and quercetin (b) particles at 0.5 wt% WPI in the aqueous phase at pH 3.0, respectively. Samples with the same letter do not differ significantly ($p > 0.05$) according to Tukey's test.

4.3.3. Interfacial shear viscosity

In order to test more directly for evidence of interfacial complex formation, measurements of interfacial shear viscosity (η_i) were undertaken. Interfacial shear viscosity is a particularly sensitive method for monitoring the formation and structuring of adsorbed films (Burke *et al.*, 2014). It can give insight into structural and compositional changes within adsorbed layers, and how interfacial properties can be related to aspects of the formation and stability of emulsions (Murray, 2002; Murray *et al.*, 1996). Fat crystals and mono- and di- glycerides that are present in vegetable oils can influence the

interfacial rheology of adsorbed particle films (Murray, 2002). The co-adsorption of mono and di-glycerides tends to destroy high values of η_i of particle films because they tend to be more surface active than particles and displace them from the interface (Murray, 2002). For this reason, experiments were first performed with soybean oil purified via aluminium oxide (as described in the Methods section) in order to remove any such low molecular weight surface active components. Figures 4.6 (a) and 4.6 (b) show the values of interfacial shear viscosity after 24 h in the presence of 0.14 wt% curcumin or quercetin particles dispersed in the oil with different concentrations of WPI in the aqueous phase, at pH 3.0 and 7.0. A control experiment with purified oil (*i.e.*, containing no polyphenol crystals) and Milli-Q water (at pH 3.0 and 7.0) was performed but $\eta_i = 0 \text{ mN s m}^{-1}$ even after 24 h (results not shown). Addition of 0.5 wt% WPI (pH 3.0) to the aqueous phase (but with only purified oil as the continuous phase) also did not show a significant increase in η_i even after 24 h (maximum of 4.5 mN s m^{-1}).



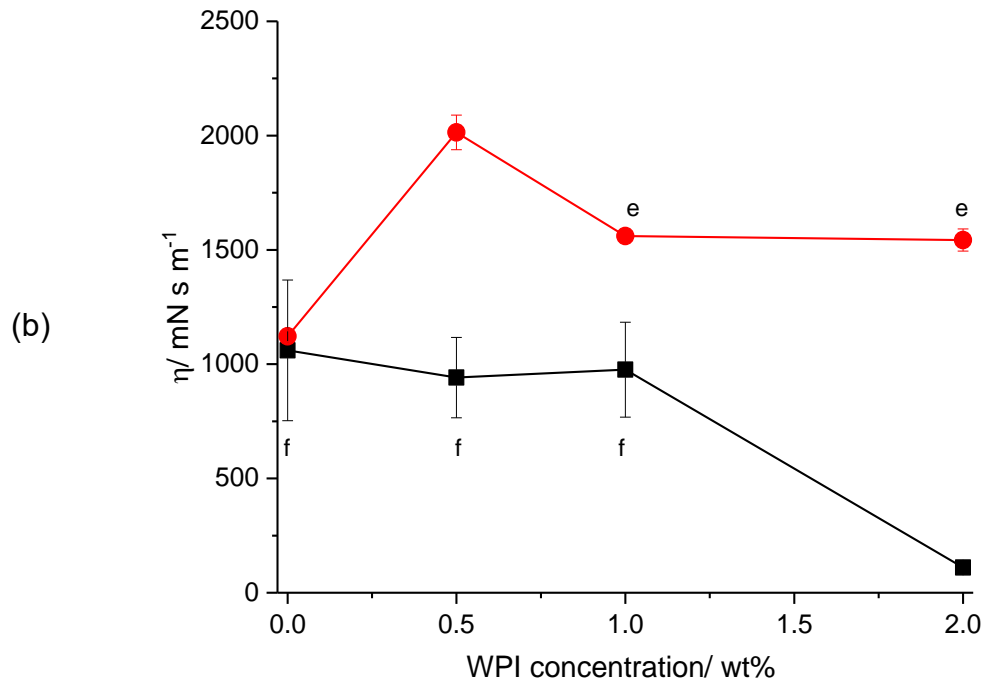


Figure 4.6. Interfacial shear viscosity at W-O interface of 0.14 wt% curcumin [■] and quercetin [●] particles dispersed in purified oil with different concentrations of WPI in the aqueous phase after 24 h of adsorption at pH 3.0 (a) and pH 7.0 (b), respectively. Samples with the same letter do not differ significantly ($p > 0.05$) according to Tukey's test for each polyphenol + WPI system at each pH value.

As seen in Figure 4.6 (a), for both curcumin and quercetin the trend of η_i (24 h) versus WPI concentration at pH 3.0 was very similar. Below 0.5 wt% WPI, there was a significant increase ($p < 0.05$) of η_i , whereas above 0.5 wt% WPI, η_i decreased ($p < 0.05$). Such behaviour is typical – at low concentrations of protein the particles and protein co-adsorb at the interface and so are able to form complexes, which often forms much stronger films than proteins on their own. For example, such behaviour in η_i has been observed previously for WPI + cellulose particles, where electrostatic complexation between the protein and particles resulted in a significantly stronger interfacial film than the protein alone (Sarkar *et al.*, 2017). At higher concentrations of WPI, protein adsorption tends to dominate over the particle adsorption, and so η_i values decrease to those more similar of pure protein films (Figures 4.6 (a) and 4.6 (b)).

Curcumin particles gave lower η_i at all concentrations of WPI at pH 3.0 (Figure 4.6 (a)) compared to quercetin, suggesting stronger accumulation of quercetin particles at the interface. This could be due to the larger aspect ratio of the quercetin particles compared to those of curcumin, which were smaller in size and therefore would also require more time to settle at the interface (Zembyla *et al.*, 2018). On the other hand, this might also be due to stronger interactions between quercetin and WPI when the protein was present, noting again that quercetin (in water) has net negative charge whereas WPI net charge is positive at pH 3.0, as discussed above.

The η_i results with quercetin at pH 7.0 (Figure 4.6 (b)) were fairly constant across the WPI concentration range, but all higher than at pH 3.0. This may explain why the emulsions at pH 3.0 (Figure 4.1) were more stable than at pH 7.0 (Figure 4.3). The results with curcumin at pH 7.0 (Figure 4.6 (b)) were similar to at pH 3.0 in that values of η_i increased initially and then decreased with increase in WPI concentration. However, the values at pH 7.0 were all considerably higher than at pH 3.0. The η_i of curcumin even without WPI at pH 7.0 was ca. 60x higher than at pH 3.0, indicating some other possible mechanism of strengthening of the adsorbed film. It is widely known that curcumin is more stable in acidic emulsions, existing in its enolic structure, but it is very unstable at higher pH values (Kharat *et al.*, 2017). Oxidative and hydrolytic degradation reactions of curcumin could take place at the interface at pH \geq 7.0 (Stankovic, 2004). Some of these degradation products are more hydrophilic and therefore more likely to move into the aqueous phase (Stankovic, 2004). To restore the equilibrium, more curcumin would migrate from the oil phase to the interface and then eventually to the aqueous phase, continuing the degradation process (Stankovic, 2004). Some of the products, such as vanillin and ferulic acid, have been shown to covalently cross-link whey proteins, which might explain higher values of η_i at pH 7.0 (Houde *et al.*, 2018; Zhang *et al.*, 2014). Literature suggests that the center ring structure of quercetin at pH 7.0 is also unstable due to oxidation reactions, resulting in degradation of the ring structure (Moon *et al.*, 2008; Sokolová *et al.*, 2012). These possible changes in the chemical nature of the polyphenols at pH 7.0

therefore make it more difficult to interpret the differences in emulsion stability and η_i at pH 7.0.

Another way of testing for the electrostatic origin of complex formation at the interface is to increase the ionic strength of the aqueous phase, which will screen attraction between opposite charges on the protein and the particles (Boye *et al.*, 1995). Measurements of η_i at pH 3.0 were therefore also conducted at different salt concentrations in systems with curcumin and quercetin (+ 0.5 wt% WPI); values after 24 h as shown in Figure 4.7. It was observed that addition of a very low concentration of NaCl (0.001 M) caused a two-fold decrease in η_i for both curcumin and quercetin particles. Higher concentrations (0.01 and 0.1 M) of NaCl did not change η_i significantly further ($p > 0.05$), but the inverse dependence of the Debye screening length on the square root of the ionic strength means that the biggest change in screening length would be expected between 'zero' and 10^{-3} M salt. Therefore, it seems that at pH 3.0, electrostatic attraction between the two components is probably important in strengthening the adsorbed film and increasing emulsion stability, although it is recognized that other interactions might also take place, discussed below.

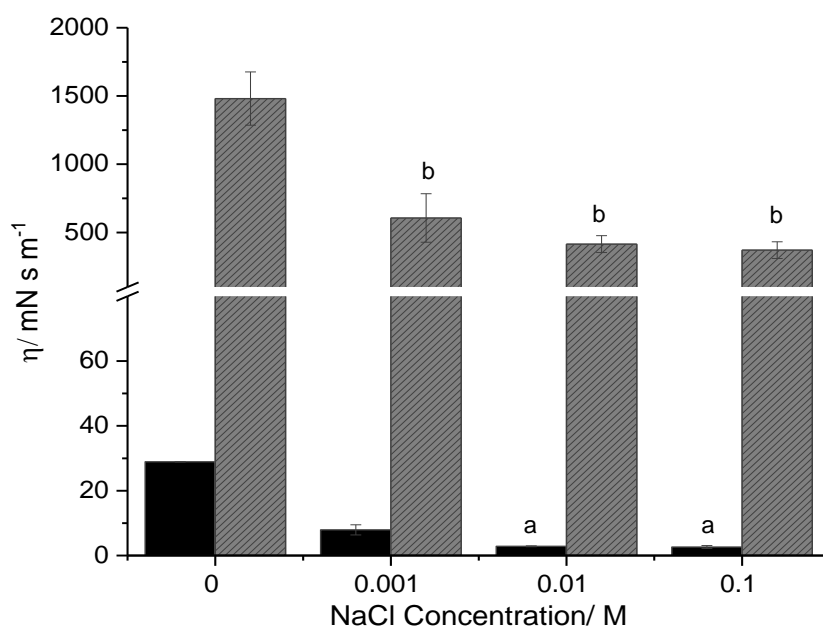
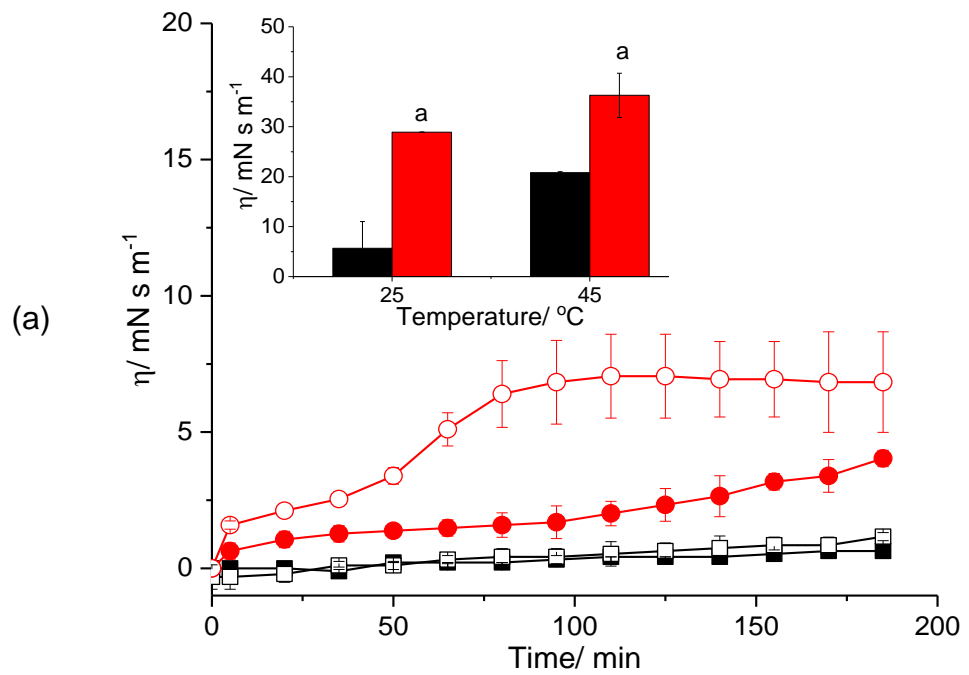


Figure 4.7. Interfacial shear viscosity at W-O interface of 0.14 wt% particles of curcumin [black] and quercetin [grey] dispersed in purified oil and 0.5 wt% WPI at different NaCl concentrations in aqueous phase at pH 3.0, after 24 h of adsorption. Samples with the same letter do not differ significantly ($p > 0.05$) according to Tukey's test.

Heat treatment at 45 °C was also used to test the nature of the interactions between polyphenols and WPI at the interface, but also because of the importance of heat processing in practical applications. The η_i of the system was measured during heating at 45 °C for 3 h and then after cooling down to 25 °C and leaving overnight (Figure 4.8). A control experiment was undertaken without any polyphenol crystals in the oil phase but with only 0.5 wt% WPI in the aqueous phase at pH 3.0. It was observed that η_i of this system increased significantly, within the first 3 h, when the system heated at 45 °C (from 0.4 to 3.0 mN s m⁻¹, results not shown) due to the formation of new covalent cross-links between the molecules, as observed previously (Murray, 2002; Murray *et al.*, 1996). However no any change in η_i was observed after 24 h for the heated system: η_i remained the same as that of the non-heated system (4.5 mN s m⁻¹, results not shown). With curcumin crystals in the oil phase (without WPI in the aqueous phase), η_i increased slightly over the first 3 h, but after 24 h η_i had increased dramatically compared to the non-heated system at 25 °C (Figure 4.8 (a)). However, η_i with quercetin crystals (without WPI) increased very quickly over the first 3 h but after 24 h,

η_i was 2x higher compared to the non-heated system at 25 °C (Figure 4.8 (b)). The larger change over the first 3 h of heating for quercetin could possibly be due to the higher temperature accelerating the adsorption and rearrangement of the larger quercetin crystals at the interface. When WPI was added into the aqueous phase, the η_i was much higher but approximately the same for both curcumin ($\sim 30 \text{ mN s m}^{-1}$, $p > 0.05$) and quercetin ($\sim 1600 \text{ mN s m}^{-1}$, $p > 0.05$) after 24 h, whether heated or not.



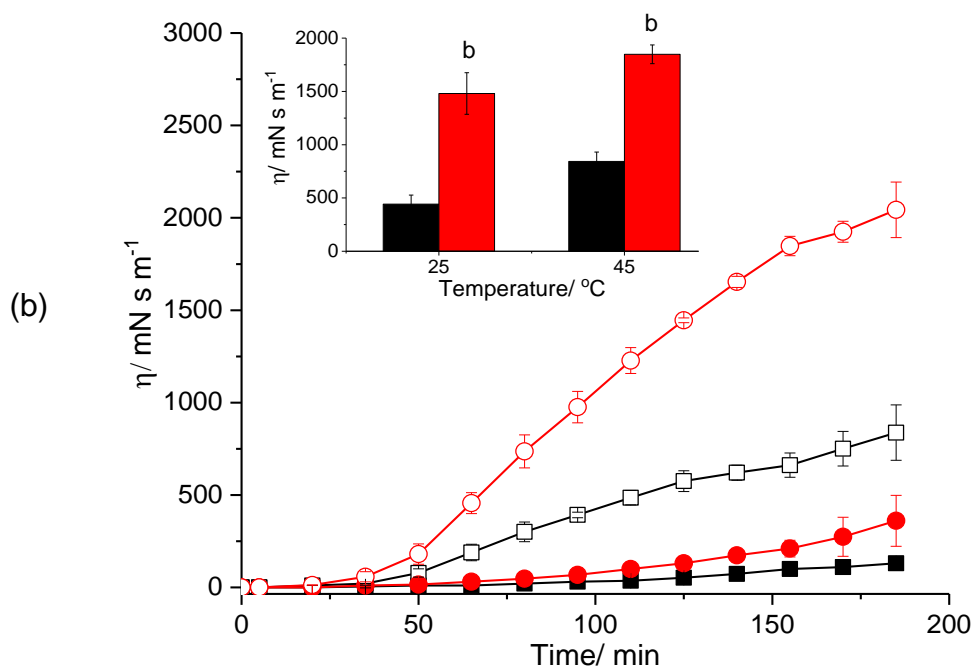


Figure 4.8. Interfacial shear viscosity at W-O interface against time of 0.14 wt% curcumin (a) and quercetin (b) particles with Milli-Q water [black], 0.5 wt% WPI in aqueous phase [red] at 25 °C [filled symbols] or 45 °C [open symbols] at pH 3.0 for the first 3 h of adsorption. The embedded graph shows the interfacial shear viscosity at 25 or 45 °C, for curcumin (a) or quercetin (b) particles with Milli-Q water [black] and 0.5 wt% WPI [red] at pH 3.0, after 24 h of adsorption. Error bars represent standard deviation of at least two independent experiments. Samples with the same letter do not differ significantly ($p > 0.05$) according to Tukey's test.

Optical images of the above systems described in Figure 4.8 were also taken at 25 °C (before heating), during heating at 45 °C and 1 h after heating (at 25 °C, shown in Figure 4.9. Curcumin crystals during heating at 45 °C (Figure 4.9 (b)) were much smaller in size than at 25 °C (before heating, Figure 4.9 (a)) but the size of quercetin crystals did not change significantly during heating. After cooling at 25 °C and 1 h later (Figure 4.9 (c)), curcumin crystals were smaller in size compared to before heating, whilst quercetin crystals showed a small increase in size (see Appendix B, Figure B1 and B2). These changes suggest Ostwald ripening of quercetin crystal size due to its increased solubility at high temperature that perhaps explains the higher η_i after heating (24 h, Figure 4.8 (b)), since larger particles (of the same contact angle properties) are adsorbed more strongly.

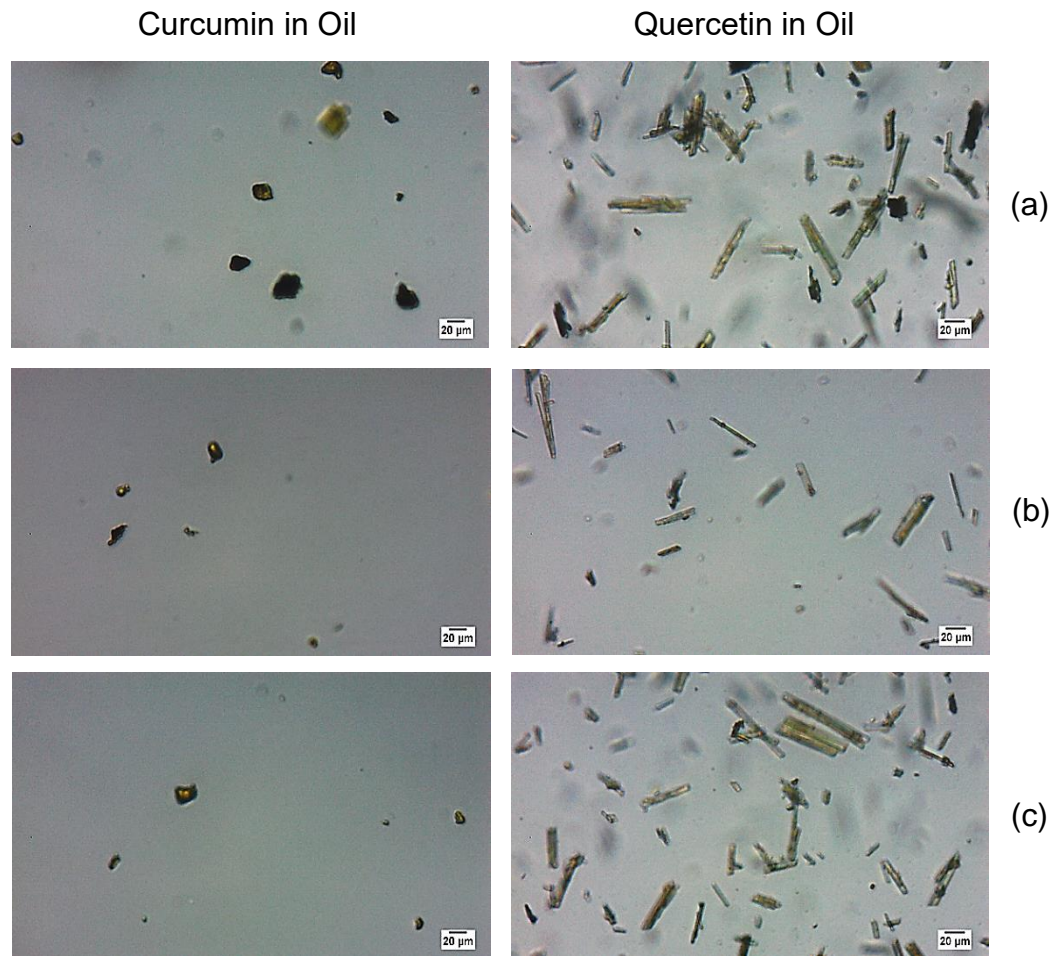


Figure 4.9. Optical microscope images of curcumin or quercetin dispersions (0.14 wt%) at 25 °C (a), during heating at 45 °C (b) and after cooling down to 25 °C (c). The scale bar represents 20 μm.

4.4. Discussion

Drawing together the results of all these experiments, a possible mechanism of complex formation between the proteins and polyphenols at the interface is schematically shown in Figure 4.10. The phenolic nucleus of polyphenols is the most favourable part for molecular (non-covalent) interactions with proteins with a defined globular tertiary structure (Dangles *et al.*, 2006). The interactions are affected by the relative concentration of polyphenol and protein, solvent composition, temperature, ionic strength and pH (Le Bourvellec *et al.*, 2012). It has been suggested by many authors that polyphenol interactions give rise to complex formation mainly via hydrophobic

interactions and hydrogen bonding (Bordenave *et al.*, 2014; Dangles *et al.*, 2006; Le Bourvellec *et al.*, 2012). Hydrophobic interactions arise from the association of aromatic rings of polyphenols and hydrophobic sites of proteins, such as the pyrrolidine rings of proline residues, plus phenolic rings tyrosine and phenylalanine, whilst hydrogen bonding can occur between the many H-acceptor sites of proteins and hydroxyl groups of the polyphenols (Asano *et al.*, 1982; Le Bourvellec *et al.*, 2012). Ionic interactions between positively charged groups on the proteins, such as the amino acid side chains of lysine and arginine and the negatively charged hydroxyl groups of polyphenols probably take place as well, although this has shown to have a minor effect on complex formation in the bulk (Le Bourvellec *et al.*, 2012).

Obviously, polyphenol-protein interactions are dependent upon the nature of the polyphenol and protein, plus how the protein structure changes on adsorption at the W-O interface (Le Bourvellec *et al.*, 2012). Polyphenol reactivity is influenced by the size, the conformational mobility/flexibility and the solubility of polyphenols in water (Richard *et al.*, 2006). Higher solubility in water (lower log *P*) reduces the affinity with proteins (Le Bourvellec *et al.*, 2012). High molecular weight polyphenols have the ability to precipitate or interact with proteins more effectively because they possess more functional groups (Le Bourvellec *et al.*, 2012), whilst greater conformational flexibility increases the capacity of interactions. Similarly, proteins with more open and flexible structures can more easily associate with polyphenols (Hagerman *et al.*, 1981): higher contents of charged or proline residues maintain the peptide in a more open conformation, inhibiting the formation of intramolecular hydrogen-bonded structures such as α -helix (Baxter *et al.*, 1997; Murray *et al.*, 1994). Available binding sites are then maximized and the carbonyl oxygen of peptide bonds are more exposed and available for hydrogen bonding than those of a compactly folded protein (Baxter *et al.*, 1997; Williamson, 1994).

Riihimaki *et al.* (2008) investigated the binding effect of different phenolic compounds, such as flavonols and isoflavonols, to the main constituent of WPI: β -lactoglobulin (β -lg). They showed the polyphenols

formed complexes with β -lg that were stable under acidic conditions, indicating that phenolic compounds probably bind to the exterior of β -lg rather than the calyx.

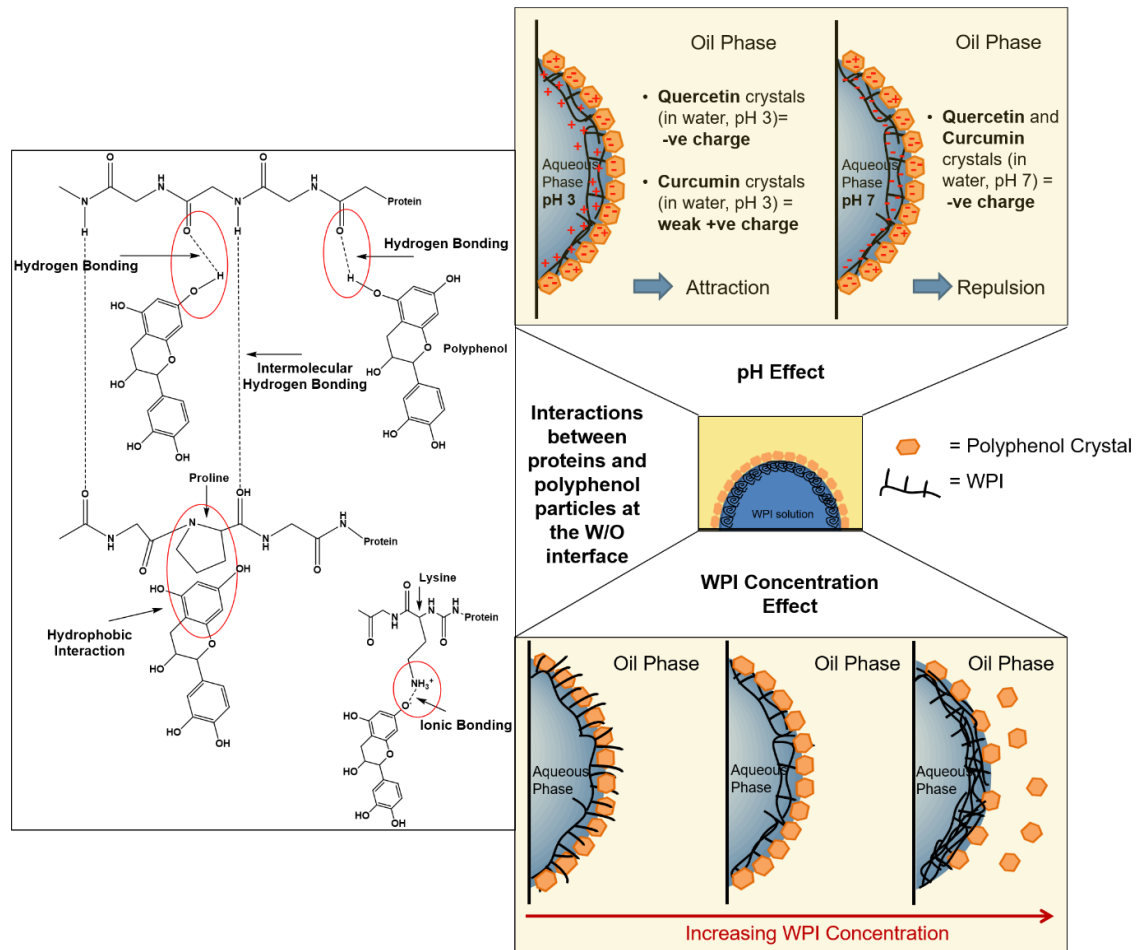


Figure 4.10. Schematic representation (not to scale) of curcumin or quercetin + WPI-stabilized W/O emulsions, illustrating the effects of pH and WPI concentration and the possible mechanisms of interaction between the proteins and polyphenols at the interface.

4.5. Conclusion

In this work, we propose a novel way to stabilize W/O emulsions via complex formation at the interface between Pickering polyphenol particles adsorbing from the oil side and biopolymers (proteins) co-adsorbing from the aqueous side of the interface, which strengthens the mechanical properties of the adsorbed film. In this case, addition of WPI protein up to 0.5 wt% gave a

significant increase in improvement in the stability of the emulsions over time. Based on the interfacial shear viscosity measurements, with and without added salt, we concluded that one of the main factors affecting complex formation and strengthening of the film is the electrostatic attraction between oppositely-charged polyphenol particles and proteins at the interface, which therefore also depends on the pH of the aqueous phase. This agrees with correspondingly more stable emulsions at pH 3.0 compared to pH 7.0, due to more disparate charges between the two stabilizers at pH 3.0, though greater chemical instability of the polyphenols at pH 7.0 may also have an influence. Higher concentrations of WPI do not improve the stability further due to protein adsorption dominating over polyphenol particle adsorption. Such particle + biopolymer interfacial complex formation could be utilized for designing W/O emulsions for a variety of soft matter applications, in foodstuffs but also more widely, where there is a lack of biocompatible Pickering particles for stabilization of aqueous droplets in an oily (non-aqueous) phase.

All these emulsions showed a good stability with only 5 wt% water. In order to further increase the water volume fraction, a physical modification of the WPI can undertake where whey protein microgel (WPM) particles will be formed and used in the aqueous phase of the emulsions. Hence, in the following chapter (**Chapter 5**), the stability of W/O emulsions prepared by 'double Pickering stabilization' between polyphenol crystals and WPM particles will be evaluated as a function of different WPM particle concentrations and water volume fractions.

References

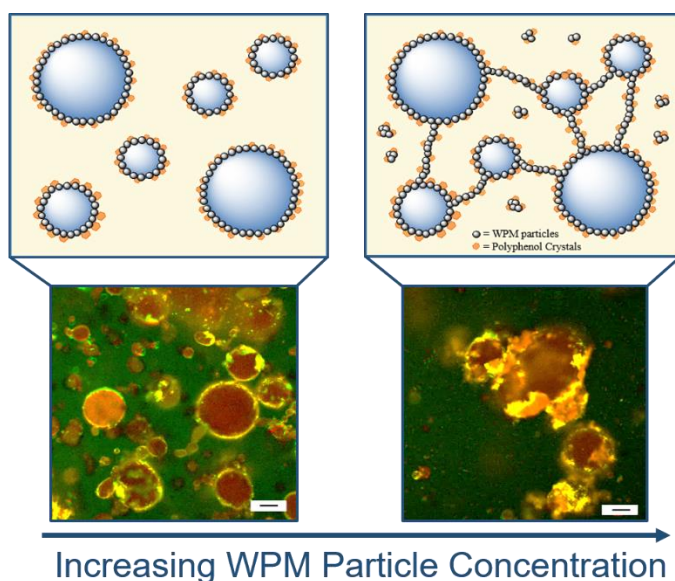
- Araiza-Calahorra, A., Akhtar, M., & Sarkar, A. (2018). Recent advances in emulsion-based delivery approaches for curcumin: From encapsulation to bioaccessibility. *Trends in Food Science & Technology*, *71*, 155-169.
- Asano, K., Shinagawa, K., & Hashimoto, N. (1982). Characterization of haze-forming proteins of beer and their roles in chill haze formation. *Journal of the American Society of Brewing Chemists*, *40*(4), 147-154.
- Baxter, N. J., Lilley, T. H., Haslam, E., & Williamson, M. P. (1997). Multiple interactions between polyphenols and a salivary proline-rich protein repeat result in complexation and precipitation. *Biochemistry*, *36*(18), 5566-5577. doi:10.1021/bi9700328
- Bordenave, N., Hamaker, B. R., & Ferruzzi, M. G. (2014). Nature and consequences of non-covalent interactions between flavonoids and macronutrients in foods. *Food & function*, *5*(1), 18-34.
- Boye, J. I., Alli, I., Ismail, A. A., Gibbs, B. F., & Konishi, Y. (1995). Factors affecting molecular characteristics of whey protein gelation. *International Dairy Journal*, *5*(4), 337-353.
- Burke, J., Cox, A., Petkov, J., & Murray, B. S. (2014). Interfacial rheology and stability of air bubbles stabilized by mixtures of hydrophobin and β -casein. *Food Hydrocolloids*, *34*, 119-127.
- Cayot, P., & Lorient, D. (1997). Structure-function relationships of whey proteins. *FOOD SCIENCE AND TECHNOLOGY-NEW YORK-MARCEL DEKKER-*, 225-256.
- Dangles, O., & Dufour, C. (2006). Flavonoid-protein interactions. *Flavonoids: chemistry, biochemistry and applications*, 443-469.
- Dickinson, E. (2010). Food emulsions and foams: stabilization by particles. *Current opinion in colloid & interface science*, *15*(1-2), 40-49.
- Duffus, L. J., Norton, J. E., Smith, P., Norton, I. T., & Spyropoulos, F. (2016). A comparative study on the capacity of a range of food-grade particles to form stable O/W and W/O Pickering emulsions. *Journal of colloid interface science*, *473*, 9-21.
- Formica, J., & Regelson, W. (1995). Review of the biology of quercetin and related bioflavonoids. *Food and chemical toxicology*, *33*(12), 1061-1080.
- Ghosh, S., & Rousseau, D. (2011). Fat crystals and water-in-oil emulsion stability. *Current opinion in colloid & interface science*, *16*(5), 421-431.
- Hagerman, A. E., & Butler, L. G. (1981). The specificity of proanthocyanidin-protein interactions. *Journal of Biological Chemistry*, *256*(9), 4494-4497.
- Houde, M., Khodaei, N., & Karboune, S. (2018). Assessment of interaction of vanillin with barley, pea and whey proteins: Binding properties and sensory characteristics. *LWT*, *91*, 133-142.

- Jiménez-Flores, R., Ye, A., & Singh, H. (2005). Interactions of whey proteins during heat treatment of oil-in-water emulsions formed with whey protein isolate and hydroxylated lecithin. *Journal of agricultural and food chemistry*, 53(10), 4213-4219.
- Kharat, M., Du, Z., Zhang, G., & McClements, D. J. (2017). Physical and chemical stability of curcumin in aqueous solutions and emulsions: Impact of pH, temperature, and molecular environment. *Journal of agricultural and food chemistry*, 65(8), 1525-1532.
- Lam, R. S., & Nickerson, M. T. (2015). The effect of pH and temperature pre-treatments on the physicochemical and emulsifying properties of whey protein isolate. *LWT-Food Science and Technology*, 60(1), 427-434.
- Le Bourvellec, C., & Renard, C. (2012). Interactions between polyphenols and macromolecules: quantification methods and mechanisms. *Critical reviews in food science and nutrition*, 52(3), 213-248.
- Luo, Z., Murray, B. S., Yusoff, A., Morgan, M. R., Povey, M. J., & Day, A. J. (2011). Particle-stabilizing effects of flavonoids at the oil-water interface. *Journal of agricultural and food chemistry*, 59(6), 2636-2645.
- Majhi, A., Rahman, G. M., Panchal, S., & Das, J. (2010). Binding of curcumin and its long chain derivatives to the activator binding domain of novel protein kinase C. *Bioorganic & medicinal chemistry*, 18(4), 1591-1598.
- Midmore, B. R. (1999). Effect of Aqueous Phase Composition on the Properties of a Silica-Stabilized W/O Emulsion. *Journal of colloid and interface science*, 213(2), 352-359.
- Moon, Y. J., Wang, L., DiCenzo, R., & Morris, M. E. (2008). Quercetin pharmacokinetics in humans. *Biopharmaceutics & drug disposition*, 29(4), 205-217.
- Murray, B. S. (2002). Interfacial rheology of food emulsifiers and proteins. *Current opinion in colloid & interface science*, 7(5-6), 426-431.
- Murray, B. S., & Dickinson, E. (1996). Interfacial rheology and the dynamic properties of adsorbed films of food proteins and surfactants. *Food Science and Technology International, Tokyo*, 2(3), 131-145.
- Murray, B. S., Zembyla, M., & Sarkar, A. (2019). Switzerland Patent No. WO/2019/008059.
<https://patentscope2.wipo.int/search/en/detail.jsf?docId=WO2019008059&tab=PCTBIBLIO>.
- Murray, N. J., Williamson, M. P., Lilley, T. H., & Haslam, E. (1994). Study of the interaction between salivary proline-rich proteins and a polyphenol by 1H-NMR spectroscopy. *European Journal of Biochemistry*, 219(3), 923-935. doi:10.1111/j.1432-1033.1994.tb18574.x
- Richard, T., Lefeuvre, D., Descendit, A., Quideau, S., & Monti, J. (2006). Recognition characters in peptide-polyphenol complex formation. *Biochimica et Biophysica Acta (BBA)-General Subjects*, 1760(6), 951-958.

- Riihimäki, L. H., Vainio, M. J., Heikura, J. M. S., Valkonen, K. H., Virtanen, V. T., & Vuorela, P. M. (2008). Binding of phenolic compounds and their derivatives to bovine and reindeer beta-lactoglobulin. *Journal of agricultural and food chemistry*, *56*(17), 7721-7729. doi:10.1021/jf801120a
- Rodríguez Patino, J. M., Rodríguez Niño, M. R., & Sánchez, C. C. (1999). Adsorption of whey protein isolate at the oil– water interface as a function of processing conditions: A rheokinetic study. *Journal of agricultural and food chemistry*, *47*(6), 2241-2248.
- Rossi, M., Rickles, L. F., & Halpin, W. A. (1986). The crystal and molecular structure of quercetin: A biologically active and naturally occurring flavonoid. *Bioorganic Chemistry*, *14*(1), 55-69.
- Rutkevičius, M., Allred, S., Velez, O. D., & Velikov, K. P. (2018). Stabilization of oil continuous emulsions with colloidal particles from water-insoluble plant proteins. *Food Hydrocolloids*, *82*, 89-95.
- Sarkar, A., & Singh, H. (2016). Emulsions and foams stabilised by milk proteins. In *Advanced dairy chemistry* (pp. 133-153): Springer.
- Sarkar, A., Zhang, S., Murray, B., Russell, J. A., & Boxal, S. (2017). Modulating in vitro gastric digestion of emulsions using composite whey protein-cellulose nanocrystal interfaces. *Colloids and Surfaces B: Biointerfaces*, *158*, 137-146.
- Sharma, R., Gescher, A., & Steward, W. (2005). Curcumin: the story so far. *European journal of cancer*, *41*(13), 1955-1968.
- Skelhon, T. S., Grossiord, N., Morgan, A. R., & Bon, S. A. F. (2012). Quiescent water-in-oil Pickering emulsions as a route toward healthier fruit juice infused chocolate confectionary. *Journal of Materials Chemistry*, *22*(36), 19289-19295. doi:10.1039/C2JM34233B
- Sokolová, R., Ramešová, Š., Degano, I., Hromadová, M., Gál, M., & Žabka, J. (2012). The oxidation of natural flavonoid quercetin. *Chemical Communications*, *48*(28), 3433-3435.
- Stankovic, I. (2004). Chemical and technical assessment curcumin. *61st jecfa*.
- Wach, A., Pyrzyńska, K., & Biesaga, M. (2007). Quercetin content in some food and herbal samples. *Food chemistry*, *100*(2), 699-704.
- Williamson, M. P. (1994). The structure and function of proline-rich regions in proteins. *Biochemical Journal*, *297*, 249-260. doi:10.1042/bj2970249
- Zembyla, M., Murray, B. S., & Sarkar, A. (2018). Water-in-Oil Pickering Emulsions Stabilized by Water-Insoluble Polyphenol Crystals. *Langmuir*, *34*, 10001-10011. doi:10.1021/acs.langmuir.8b01438
- Zhang, H., Yu, D., Sun, J., Guo, H., Ding, Q., Liu, R., & Ren, F. (2014). Interaction of milk whey protein with common phenolic acids. *Journal of Molecular Structure*, *1058*, 228-233.

Chapter 5

Water-in-Oil Pickering Emulsions Stabilized by Synergistic Particle-Particle Interactions ³



Abstract

Here, we report a novel 'double Pickering stabilization' of water-in-oil (W/O) emulsions, where complex formation at the interface between Pickering polyphenol particles adsorbing from the oil side and WPM (whey protein microgel) particles co-adsorbing from the aqueous side of the interface is investigated. The interfacial complex formation was strongly dependent on the concentration of WPM particles. At low WPM concentrations, both polyphenol crystals and WPM particles are present at the interface and the water droplets were stabilized through their synergistic action, whilst at higher concentrations, the WPM particles acted as 'colloidal glue' between the water droplets and polyphenol crystals, enhancing the water droplet stability for

³ Zembyla, M., Lazidis, A., Murray, B.S., & Sarkar, A. (2019). Water-in-Oil Pickering Emulsions Stabilized by Synergistic Particle-Particle Interactions. *Langmuir*, 35 (40), 13078-13089. DOI: [10.1021/acs.langmuir.9b02026](https://doi.org/10.1021/acs.langmuir.9b02026)

more than 90 days and prevented coalescence. Via this mechanism, addition of WPM particles up to 1 wt% gave a significant improvement in the stability of the W/O emulsions, allowing increasing to 20 wt% water droplet fraction. The evidence suggests that the complex was probably formed due to electrostatic attraction between oppositely-charged polyphenol Pickering particles on the oil side of the interface and WPM Pickering particles mainly on the aqueous side of the interface. Interfacial shear viscosity measurements and monolayer (Langmuir trough) experiments at the air-water interface provided further evidence of this strengthening of the film due to the synergistic particle-particle complex formation at the interface.

5.1. Introduction

The stabilization of emulsions by solid particles has gained significant attention during the last two decades due to their ability to irreversibly adsorb at the interface, providing kinetic stability to the dispersed phase (Dickinson, 2010; Zembyla *et al.*, 2018). Such solid particles are known as 'Pickering' particles and tend to hinder coalescence by virtue of their exceptionally high desorption energies that make the particles practically impossible to desorb once adsorbed (Ghosh *et al.*, 2011). Besides oil-in-water (O/W) emulsions, Pickering stabilization has gained increased research attention among colloid scientists for stabilizing water-in-oil (W/O) emulsions owing to the limited number of biocompatible water-insoluble particles being investigated to stabilize water droplets to date, such as fat crystals, polyphenol crystals etc. (Ghosh *et al.*, 2011; Zembyla *et al.*, 2019; Zembyla *et al.*, 2018).

In addition to single particle-laden interfaces, there has been growing interests in stabilizing emulsions by dual or hybrid particles. When two oppositely charged colloidal particles are used, the ability of particles to adsorb at the water-oil interface depends on mutual interactions between these two particles (Pushpam *et al.*, 2015). For an emulsion drop to be stable, sufficient packing of particles at the interface is necessary to prevent coalescence and subsequent phase separation (Pushpam *et al.*, 2015). For example, droplets have been shown to be stabilized by an electrostatic

complex of lactoferrin nanogel particle and inulin nanoparticle, where the particles form particle-particle complexes at the interface and provide better coverage and consequently more stability (Sarkar *et al.*, 2018). However, such studies are relatively rare in the W/O emulsion domain. Nallamilli *et al.* (2015); Nallamilli *et al.* (2014) stabilized W/O emulsions using a combination of silica and polystyrene particles. The silica particles were more hydrophilic and sited towards the water phase whilst polystyrene particles were more hydrophobic and protruded outward into the oil phase, located above the silica particle layer. Pushpam *et al.* (2015) also showed that oppositely charged colloids can stabilize W/O emulsions by controlling the charge ratio and the number of particles on their surfaces. In addition, they have investigated the influence of the charge ratio on the structural arrangement of particles or in the pattern formation at the emulsion interface (Pushpam *et al.*, 2015).

In our previous work, we have shown the ability of water-insoluble polyphenol crystals, such as curcumin and quercetin to stabilize water droplets via the Pickering mechanism (Zembyla *et al.*, 2018). Micro-structural evaluation at various length scales revealed that quercetin crystals had a more rod-like shape than curcumin crystals, the latter being smaller and having a more polyhedral shape (Zembyla *et al.*, 2018). It was observed that such polyphenol crystals adsorb at the interface and provide stabilization of water droplets for several days. However, formation of a hybrid polyphenol-whey protein isolate (WPI) complex at the water-oil interface revealed a pronounced improvement in the kinetic stability (Zembyla *et al.*, 2019). This complex formation was produced between the Pickering polyphenol particles adsorbing from the oil side and free molecules of biopolymer (WPI protein) co-adsorbing from the aqueous side of the interface, which strengthened the mechanical properties of the adsorbed film (Zembyla *et al.*, 2019). It was also suggested that this complex strengthening was due to electrostatic attraction between the oppositely-charged polyphenol particles and protein at the interface, although hydrogen bonding between the two components may also contribute (Zembyla *et al.*, 2019). Although the complexes stability, above 5 wt% water the emulsions still exhibit some coalescence over several weeks. Therefore, to engineer interfaces of W/O emulsions with enhanced

performance, one novel strategy would be to investigate if W/O emulsions could be stabilized by complex formation between *two* Pickering stabilizers, namely the same polyphenol particles combined with protein-based microgel particles, rather than protein molecules. To our knowledge, the use in this way of such combined biocompatible Pickering stabilizers remains uninvestigated.

Protein microgels are soft colloidal particles that can be produced by using a top-down technique of forming a physically cross-linked heat-set hydrogel in the first stage. Then microgel particles are produced by breaking the gel down under high shear forces using a homogenizer (Araiza-Calahorra *et al.*, 2019). Whey protein microgel (WPM) particles result from controlled shearing of a heat-set gel formed via the disulfide bonding between β -lactoglobulin (β -lg) and α -lactalbumin (α -la) molecules as well as between the same proteins (Nicolai *et al.*, 2011). Upon heat denaturation at 90 °C, the unfolded whey proteins expose hydrophobic residues and thiol groups and start to aggregate. The initial quick formation of small primary aggregates is followed by fractal aggregation, which leads to the formation of larger particles that are primarily held together by hydrophobic and hydrogen bonds (Nicolai *et al.*, 2011; Schmitt *et al.*, 2010). Subsequently, intra-particle disulfide bonds are formed, leading to covalent stabilization of the structure (Nicolai *et al.*, 2011; Schmitt *et al.*, 2010). A combination of steric and electrostatic repulsion confers good colloidal stability to these microgels in aqueous dispersions (Dickinson, 2017).

In this work, we show a unique stabilization mechanism for W/O emulsions, containing up to 20 wt% water, via interfacial complex formation between the same curcumin or quercetin polyphenol crystals and WPM particles. It is hypothesized that polyphenol crystals coming from the continuous (oil) phase and WPM particles in the aqueous phase form complexes at the interface via the same attractive electrostatic and/or hydrogen-bonding interactions as observed earlier for non-microgel (molecular) WPI, but in this case forming a sort of 'double Pickering stabilization'. The stability of the corresponding W/O emulsion droplets was evaluated as a function of different WPM particle concentrations and the

mechanism of the interfacial interactions was probed using a range of complimentary physical and microstructural techniques.

5.2. Material and methods

5.2.1. Materials

Curcumin (orange-yellow powder) from turmeric rhizome (96 % total curcuminoid content) was obtained from Alfa Aesar (UK). Quercetin (≥ 95 %) in the form of a yellow crystalline solid was purchased from Cayman Chemicals (USA). Both the polyphenol crystals were used without further purification. Soybean oil (KTC Edibles, UK) was purchased from a local store. Aluminium oxide, (99 %, extra pure) was used for soybean oil purification in some experiments and was purchased from Acros Organics (Belgium). Whey protein isolate (WPI) containing 96.5 % protein was obtained from Fonterra (New Zealand). Water, purified by treatment with a Milli-Q apparatus (Millipore, Bedford, UK), with a resistivity not less than $18 \text{ M}\Omega \text{ cm}^{-1}$, was used for the preparation of the emulsions. A few drops of hydrochloric acid (0.1 M HCl) or sodium hydroxide (0.1 M NaOH) were used to adjust the pH of the emulsions. n-Hexane (99 %) was obtained from Alfa Aesar (UK). Sodium azide and Rhodamine B were purchased from Sigma-Aldrich (USA).

5.2.2. Preparation of aqueous dispersion of whey protein microgel (WPM) particles

An aqueous dispersion of WPM particles was prepared based on a slight modification of the methods previously described (Murray *et al.*, 2016; Sarkar *et al.*, 2017a) via the disulfide bond mediated covalent cross-linking of WPI followed by controlled shearing. Whey protein solution (10 wt%) was prepared by dissolving WPI powder in 20 mM phosphate buffer solution at pH 7.0 for 2 h. The WPI solution was then heated at 90 °C for 30 min and cooled at room temperature for 30 min followed by storage at 4 °C overnight to form whey protein hydrogels. The gels were mixed with 20 mM phosphate buffer solution (1:1 w/w) at pH 7.0 and were pre-homogenized using a blender (HB711M, Kenwood, UK) for 3 min before homogenized, twice, through the Leeds Jet

homogenizer (University of Leeds, UK) operating at a pressure of 300 ± 20 bar. Sodium azide (0.02 wt%) was added to the final 5 wt% WPM particles stock solution.

5.2.3. Particle size measurement of WPM particles

The mean hydrodynamic diameter (d_H) of the WPM particles at pH 3.0 was measured by dynamic light scattering at 25 °C via a Malvern Zetasizer Nano-ZS instrument (Malvern Instruments, Worcestershire, UK). Assuming WPM particles to be spherical, the apparent particle diameter was calculated from the measured diffusion coefficient (D) via the Stokes- Einstein equation:

$$d_H = \frac{k_b T}{3\pi\eta D} \quad (5.1)$$

where, k_b is the Boltzmann constant, T is the temperature and η is the viscosity of the solution.

Particle sizes were measured after diluting the samples to 0.5 wt% with 20 mM phosphate buffer. The pH was adjusted to 3.0 or 7.0 by adding few drops of 0.1 M HCl or NaOH. One mL of solution was injected into a clean cuvette (PMMA, Brand Gmbh, Wertheim, Germany). The refractive index of WPM particles and the dispersion medium were set at 1.545 and 1.33, respectively. The absorbance of the protein was assumed to be 0.001. The hydrodynamic diameters (d_H) were calculated by the cumulant analysis method of the autocorrelation function from the Zetasizer software.

5.2.4. Electrophoretic mobility

The ζ -potential and electrophoretic mobilities measurements of WPM particles in the aqueous phase and polyphenol crystals dispersed into the soybean oil phase were performed using the Malvern Zetasizer Nano-ZS instrument. The WPM dispersion was diluted to 0.5 wt% using phosphate buffer solution (20 mM). The pH was adjusted to 3.0 or 7.0 by adding few drops of 0.1 M HCl or NaOH. It was then added to a folded capillary cell (Model DTS 1070, Malvern Instruments Ltd. Worcestershire, UK). Curcumin and quercetin crystals (0.14 wt%) were dispersed in the continuous phase

(soybean oil) using an Ultra-Turrax T25 mixer (Janke & Kunkel, IKA-Labortechnik) with a 13 mm mixer head (S25N- 10G) operating at 9,400 rpm for 5 min. The bigger crystals were left to sediment for 2 h at room temperature and then the top layer was added to a cuvette (Model PCS 1115, Malvern Instruments Ltd. Worcestershire, UK) where a universal 'dip' cell (Model Zen 1002, Malvern Instruments Ltd. Worcestershire, UK) was used for measuring the mobility in non-aqueous systems.

For the WPM particle dispersions, the instrument software was used to convert the electrophoretic mobility into ζ -potential values using the Smoluchowski or Hückel approximation. The ζ -potential was calculated from the measured electrophoretic mobility (U_E) using the Henry's equation:

$$U_E = \frac{2\varepsilon_r \zeta f(\kappa a)}{3\eta} \quad (5.2)$$

where ε_r is the dielectric constant of the medium, ζ is the zeta-potential, η is the viscosity of the dispersed media, and $f(k_a)$ is the Henry's function; $f(k_a) = 1.5$ for dispersion in polar media based on the Smoluchowski approximation. The Smoluchowski approximation is based on the assumption that the double layer thickness is smaller than the mean particle radius (*i.e.*, thin double layer). For particles in a non-polar media with a thick double layer, the Hückel approximation should be used instead where $f(k_a) = 1$. Hence mobilities in non-aqueous systems (relevant for curcumin or quercetin) are greatly reduced (Patel *et al.*, 2010) compared to aqueous systems (relevant for WPM) due to the lower dielectric constant of the medium and in this case the higher viscosity of the oil (57.1 ± 1.1 mPa·s (Sahasrabudhe *et al.*, 2017)).

5.2.5. Preparation of W/O emulsions

Curcumin or quercetin dispersions were prepared by dispersing the polyphenol crystals (0.14 wt%) in the continuous phase (soybean oil) using an Ultra-Turrax T25 mixer (Janke & Kunkel, IKA-Labortechnik) with a 13 mm mixer head (S25N- 10G) operating at 9,400 rpm for 5 min. The stock WPM solution (5 wt%) was diluted to the desired WPM particle concentration (0.05 – 2.0 wt%) and used as the aqueous phase. The pH of the aqueous phase

was adjusted to 3.0 or 7.0, depending on the experiment, by adding few drops of 0.1 M HCl or NaOH. Coarse W/O emulsions were prepared by homogenizing 10, 20 or 30 wt% of this aqueous phase with soybean oil in an Ultra-Turrax mixer for 2 min at 13,400 rpm. Fine emulsions were prepared by passing the coarse emulsions through a high pressure Leeds Jet Homogenizer, twice, operated at 300 ± 20 bar. The initial temperature of the particle dispersion was 21 °C. The temperatures of the dispersions were 23 and 26 °C after Ultra-Turrax mixing at 9,400 rpm for 5 min and 13,400 rpm for 2 min, respectively. The temperature of the dispersions after passing through the Jet homogenizer (two passes at 300 ± 20 bar) was 33 – 34 °C. Note that these slight temperature increases were too low to have any significant impact on solubility of the particles or the proteins (Zembyla *et al.*, 2018). Immediately after preparation, emulsions were sealed in 25 mL cylindrical tubes (internal diameter = 17 mm) and stored at room temperature in a dark place.

5.2.6. Droplet size measurement of emulsions

The particle size distributions (*PSD*) of emulsions were measured using static light scattering (SLS) via a Mastersizer Hydro SM small volume wet sample dispersion unit (Malvern Instruments, Worcestershire, UK). Average droplet size was monitored via the Sauter mean diameter, d_{32} , or volume mean diameter, d_{43} , defined by:

$$d_{ab} = \frac{\sum n_i d_i^a}{\sum n_i d_i^b} \quad (5.3)$$

where n_i is the number of the droplets of diameter d_i .

For water droplet size measurements, refractive indices of 1.33 and 1.47 were used, for water and soybean oil, respectively. Absorption coefficients of 0.01, 0.1 and 0.01 for curcumin, quercetin and water, were used, respectively. All measurements were made at room temperature on at least three different samples.

5.2.7. Confocal laser scanning microscopy (CLSM)

The microstructure of the W/O emulsions was observed using a confocal microscope (Zeiss LSM700 inverted, Germany). Approximately, 80 μL of sample were placed into a laboratory-made well slide and a cover slip (0.17 mm thickness) was placed on top, ensuring that there was no air gap (or bubbles) trapped between the sample and coverslip. The samples were scanned at room temperature (25 ± 1 °C) using a 20 \times /0.5 objective lens. Auto-fluorescence from the particles was excited using 488 and 405 nm lasers for curcumin and quercetin crystals, respectively. Rhodamine B was used as a dye for whey protein and was added before the confocal analysis in all cases. It was excited using 545 nm lasers. The emitted fluorescent light was detected at 525, 460 and 580 nm for curcumin, quercetin and Rhodamine B, respectively.

5.2.8. Langmuir trough measurements

A specialist Langmuir trough featuring a rhombic PTFE barrier, described in detail elsewhere (Murray, 1997; Murray *et al.*, 2002; Murray *et al.*, 1996b; Xu *et al.*, 2007), was used throughout this work. The surface pressure was measured by the Wilhelmy plate method, using a thoroughly cleaned, roughened mica plate (3-5 cm in length), which was suspended in the middle of the trough from a sensitive force transducer (Maywood Instruments, Basingstoke, UK). Before WPM particles or polyphenol crystals were spread, the air-water (A-W) interface was reduced rapidly to an area lower than that used in the subsequent π -A experiments. The interface was sucked clean with a vacuum line, the interface expanded and the process repeated until $\pi < 0.1$ m N m⁻¹ was obtained on compression. For spreading from organic solvent (hexane), a drop of spreading solution was slowly formed on the tip of the syringe and then the drop slowly lowered to touch the interface, the syringe tip raised, and the process repeated until all the solution had been spread. For the WPM particle experiments, 50 μL of a 0.3 wt% WPM particle suspension (in Milli-Q water, pH 3.0) were spread at the A-W interface (aqueous phase at pH 3.0). For the polyphenol crystal experiments, concentrations of 0.5 wt% curcumin or 0.9 wt% quercetin in hexane were

prepared and the mixture sonicated for 1 min using a high intensity ultrasonic probe (Sonics & Materials Inc., Newton, CT) while sparging with air. Then, 100 μL of these hexane mixtures were spread at the A-W interface (aqueous phase at pH 3.0). Spreading took 1 - 2 min and measurement of the π -A isotherm was begun 10 min after spreading, after which all the hexane had evaporated. For the experiments where both polyphenol crystals and WPM particles were spread at the interface, polyphenol suspensions in hexane were spread first (100 μL) and then the system left for 10 min to allow the solvent to evaporate before adding the WPM particle suspension (50 μL) as before. The system was then left for another 10 min to help ensure that both components were evenly dispersed throughout the interface. Films were compressed at constant low speed as described previously (Murray, 1997; Murray *et al.*, 2002; Murray *et al.*, 1996b; Xu *et al.*, 2007), such that the rate of relative change in area was practically linear at $1.5 \times 10^{-4} \text{ s}^{-1}$ for the isotherms recorded.

5.2.9. Interfacial shear viscosity (η_i)

A two dimensional Couette-type interfacial viscometer, described in detail elsewhere (Murray, 2002; Sarkar *et al.*, 2017b) was operated in a constant shear-rate mode to measure interfacial viscosity. Briefly, a stainless steel biconical disc (radius 15.0 mm) was suspended from a thin torsion wire with its edge in the plane of the W-O interface of the solution contained within a cylindrical glass dish (radius 72.5 mm). The constant shear rate apparent interfacial viscosity, η_i , is given by the following equation:

$$\eta_i = \frac{g_f}{\omega} K(\theta - \theta_o) \quad (5.4)$$

where K is the torsion constant of the wire; θ is the equilibrium deflection of the disc in the presence of the film; θ_o is the equilibrium deflection in the absence of the film, *i.e.*, due to the bulk drag of the sub-phase on the disc; g_f is the geometric factor and ω is the angular velocity of the dish. A fixed value of $\omega = 1.27 \times 10^{-3} \text{ rad s}^{-1}$ was used, which aids comparison with measurements made on many other systems at the same shear rate.

For these measurements, 0.14 wt% curcumin or quercetin particles were dispersed in purified soybean oil using the Ultra-Turrax mixer at 9,400 rpm for 5 min. The oil was purified with aluminium oxide to eliminate free fatty acids and surface active impurities that may affect the measurements. A mixture of oil and aluminium oxide in proportion 2:1 w/w was stirred for 3 h and centrifuged at 4,000 rpm for 30 min.

5.2.10. Statistical analysis

Significant differences between samples were determined by one-way ANOVA and multiple comparison test with Tukey's adjustment performed using SPSS software (IBM, SPSS statistics) and the level of confidence was 95 %.

5.3. Results and discussion

5.3.1. Characterization of aqueous dispersion of WPM particles

The particle size distribution of the WPM dispersions as determined by dynamic light scattering was monomodal (Appendix C, Figure C1) with a polydispersity index of ~ 0.3, and a mean hydrodynamic radius of ~ 90 nm at either pH 3.0 or 7.0 (Table 5.1), *i.e.*, there was no significant change in size at these pH values. The WPM particles display a polyampholyte character in line with their constituent proteins, with an isoelectric point (pI) at pH 4.7, where their overall charge is zero (Destribats *et al.*, 2014b). Below and above this pH value, WPM particles were positively and negatively charged, respectively (Table 5.1), as observed previously (Araiza-Calahorra *et al.*, 2019; Sarkar *et al.*, 2016). The particles are stable against aggregation when the ζ -potential exceeds the absolute value of 20 mV (Schmitt *et al.*, 2010). The overall charge and the colloidal stability of these particles are a result of a balance between the dissociation of carboxylic and amino groups of the whey protein side chains as a function of pH (Schmitt *et al.*, 2010).

The attachment of WPM particles to the interface must differ from that exhibited by solid particles (Murray, 2019). In Pickering emulsions, the contact angle of the solid particle surface at the O-W interface is fixed and can be

used to predict the type of the emulsion (oil-in-water or water-in-oil) and the particle adsorption strength (Binks *et al.*, 2006). However, for a microgel system the particles are deformable and porous and to think in terms of a particle contact angle is misleading (Schmidt *et al.*, 2011). Consequently, it is not easy to define properly a line of contact between the pair of immiscible liquids and the particle surface (Dickinson, 2015). Due to the conformational flexibility of its dangling chains, the location of the adsorbed microgel particle is characterized, not so much by a sharp particle-fluid interface, but rather by a continuous polymer density profile (Dickinson, 2015).

Table 5.1. Size and ζ -potential of 0.5 wt% WPM particles in the aqueous phase at pH 3.0 and 7.0.

WPM particles	pH 3.0	pH 7.0
Size/ nm	90.4 \pm 0.7	91.4 \pm 0.5
ζ -potential/ mV	+ 24.5 \pm 1.1	-24.3 \pm 0.4
Mobility/ $\mu\text{m cm V}^{-1} \text{s}^{-1}$	+ 1.9 \pm 0.1	- 1.9 \pm 0.0

5.3.2. Characterization of polyphenol particles in the oil phase

Particle charging in non-aqueous liquid suspensions has received increasing attention due to enhanced technological interest (Arts *et al.*, 1994; Rosenholm, 2018). Electric charges and surface potentials depend not only on the nature of solid particles but also on the nature of suspension liquid and on the soluble residues (potential determining ions, impurities, etc.) (Morrison, 1993; Rosenholm, 2018). Large particles are suspended more readily than the smaller ones. Therefore they tend to appear as characteristic clusters (Rosenholm, 2018). Van der Waals forces acting between the particles have been supposed to control their aggregation. However, these forces depend only slightly on the nature of the oil (Morrison, 1993).

Surface charging in non-aqueous suspensions is considered to occur through (Rosenholm, 2018):

- a) Electron transfer due to extreme Lewis type of electron acceptor (acid) – electron donor (base) interactions.
- b) Proton transfer due to extreme Brønsted type of hydrogen bond (acid–base) interactions. This is typical in the presence of moisture which results in dissociation of surface hydroxyl groups and dissolution of ions as solvated complexes.
- c) Adsorption of surface active solutes (surfactants), ion transfer of dissolved ions or presence of liquid or solid impurities.

The electrophoretic mobility results for curcumin and quercetin crystals dispersed in the oil phase are shown in the Table 5.2. Different applied voltages were tested in order to determine the most reproducible results. It was determined that at higher voltages (> 80 V), the phase plots and the mobility results were more reproducible (results are not shown) and the results at an applied voltage of 150 V are shown in Table 5.2. Partly due to the very high viscosity (57.1 ± 1.1 mPa·s (Sahasrabudhe *et al.*, 2017)) of the soybean oil, the mobility of the particles is expected to be low. Both polyphenol crystals showed a small negative mobility value indicating the presence of some negative charge at the particle surface when they are dispersed in the oil. This validates the hypothesis of attractive electrostatic interactions at the W-O interfaces between the slightly anionic polyphenol crystals in the oil and cationic WPM particles in the aqueous phase at pH 3.0 (Table 5.1) (Zembyla *et al.*, 2019). Since converting mobilities to ζ -potentials in non-polar media (Arts *et al.*, 1994; Morrison, 1993) can be complicated, involving lot of unknowns, we have chosen not to do this conversion, since the main objective of this experiment was to confirm the sign (negative or positive) of any charge on the particles.

Table 5.2. Mobility of 0.14 wt% polyphenol crystals in the oil phase (at 150 V).

Crystals in oil	Curcumin	Quercetin
Mobility/ $\mu\text{m cm V}^{-1} \text{s}^{-1}$	-0.0031 ± 0.0009	-0.0035 ± 0.0002

5.3.3. W/O Pickering emulsions stabilized by WPM-polyphenol crystal complexes

5.3.3.1. Stability of W/O emulsions as a function of WPM particle concentration

The particle size distribution (PSD) of W/O emulsions prepared at pH 3.0 with 0.14 wt% curcumin or quercetin crystals dispersed in the oil phase plus different concentrations of WPM particles in the aqueous phase, are shown in Figures 5.1 (a) and 5.1 (b), respectively. A small peak below 1 μm was observed in all the emulsions, most likely due to some WPM aggregates or WPM-polyphenol particle complexes dispersed into the bulk oil phase by the very high shear fields. The initial size (d_{32} values) of the water droplets stabilized by curcumin crystals decreased from 23 to 20 μm as the concentration of WPM particles increased from 0.05 wt% to 2.0 wt%, respectively. Over time, the d_{32} values of curcumin systems containing 0.05 and 0.1 wt% WPM particles increased significantly (from ~ 22 to ~ 32 μm , $p < 0.05$, see Appendix C, Table C1) as shown in Figure 5.1 (b), and the emulsions with curcumin + 0.05 wt% WPM particles formed even bigger water droplets, with a clear water layer being observed after 21 days. On the other hand, the size of the water droplets containing 0.1, 0.5, 1.0 and 2.0 wt% WPM particles was stable ($p > 0.05$, see Appendix C, Figure C1), for more than 90 days (Figure 5.1 (b)). The d_{32} values of the systems containing quercetin were stable (~ 20 μm) for all the concentrations of WPM particles for more than 21 days, except for the lowest WPM concentration (0.05 wt%), where the size of the water droplets increased significantly ($p < 0.05$, see Appendix C, Table C2) and they phase separated within 2 weeks (Figure 5.1 (d)). The emulsions containing quercetin + 0.1 and 0.5 wt% WPM particles were stable for 21 days whereas those with 1.0 and 2.0 wt% WPM particles were stable for more than 90 days ($p > 0.05$, see Appendix C, Table C2) and no clear water layer observed after this time. The curcumin systems were even stable for > 90 days at WPM concentrations > 0.1 wt%, probably due to the smaller size ($d_{32} \sim 0.2$ μm) (Zembyla *et al.*, 2018) and lower aspect ratio of the curcumin crystals, allowing greater coverage of the interface (as observed in the confocal images Figure 5.2 (a)) as noted previously (Zembyla *et al.*, 2019;

Zembyla *et al.*, 2018). The quercetin crystals have a more rod-like shape and larger mean size ($d_{32} \sim 5.9 \mu\text{m}$) (Zembyla *et al.*, 2018).

The sizes of the water droplets for both the curcumin and quercetin systems with WPM particles, though stable, were apparently larger than those obtained in our previous work with just the polyphenols (Zembyla *et al.*, 2018), though it should be remembered that the light scattering technique used cannot distinguish between water droplets, polyphenol crystals, WPM particles or their aggregates as scattering centers (Atarés *et al.*, 2012). Although the apparent larger droplet size suggests the WPM particles inhibited the stabilization by the polyphenols, or caused the water droplets to aggregate more, in the previous work (Zembyla *et al.*, 2018) with just polyphenols the water fraction in the emulsions was only 5 wt%, whereas here with WPM particles 10 wt% water was stabilized.

Emulsions were also prepared at pH 7.0 but as previously discussed (Zembyla *et al.*, 2019) at this pH value the polyphenol crystals tend to degrade chemically and the emulsion stability was significantly impaired (see Appendix C, Figure C2). In any case, the results suggest that if electrostatic complex formation contributes to emulsion stability, it will be less effective at pH 7.0 because both WPM particles and the polyphenols would have the same (negative) sign of charge (Tables 5.1 and 5.2) (Zembyla *et al.*, 2019).

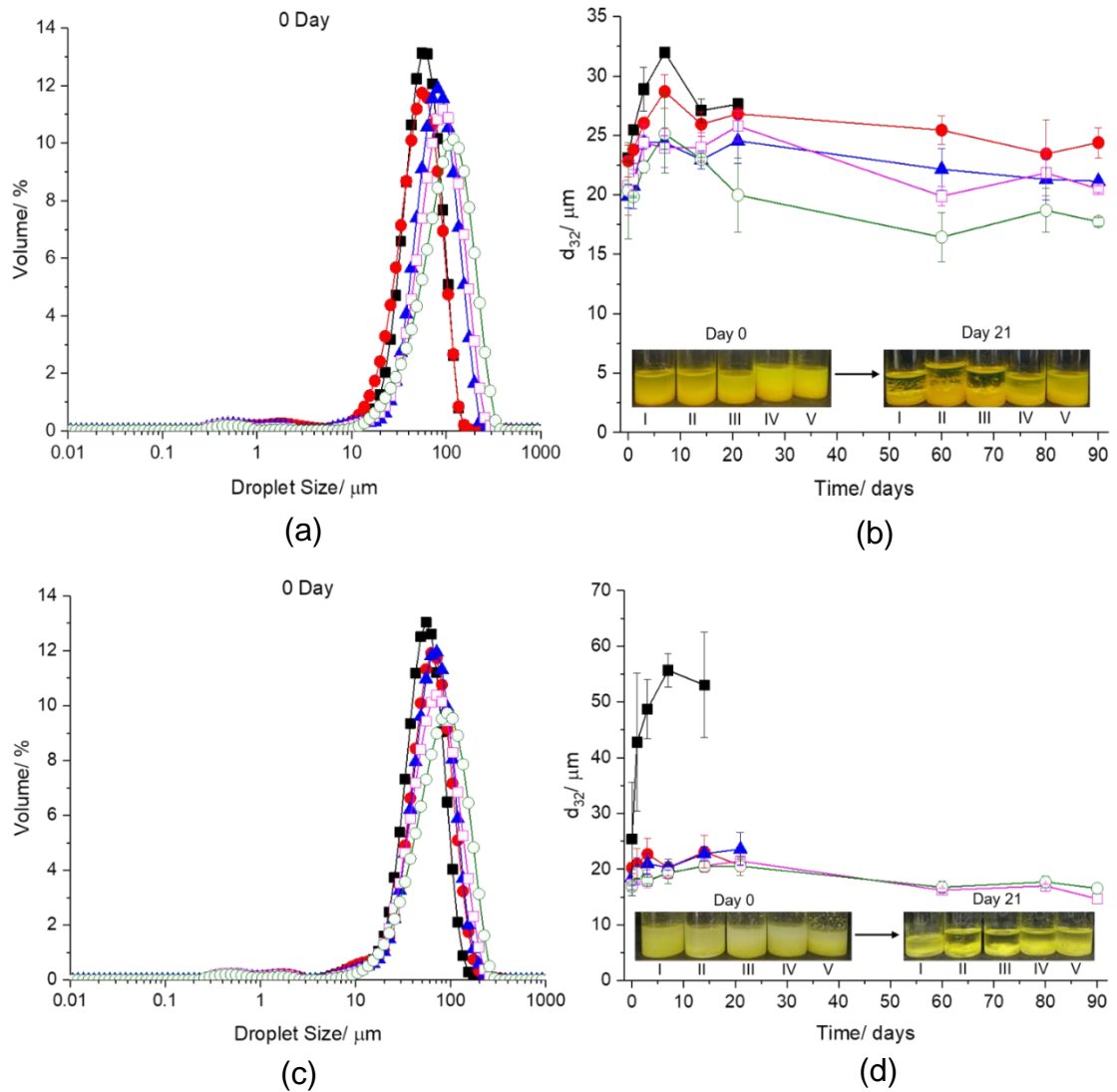


Figure 5.1. Droplet size distribution [(a) and (c)] and mean droplet size (d_{32}) of water droplets over time with visual images [(b) and (d)] of 10 wt% W/O emulsions stabilized by 0.14 wt% curcumin [(a) and (b)] and quercetin [(c) and (d)] crystals in the oil phase and 0.05 wt% [■] [I], 0.1 wt% [●] [II], 0.5 wt% [▲] [III], 1.0 wt% [□] [IV] and 2.0 wt% [○] [V] WPM particles in the aqueous phase at pH 3.0, respectively. For statistical analysis according to Tukey’s test, see Appendix C, Table C1 and Table C2 for curcumin and quercetin, respectively.

Confocal images of fresh emulsions stabilized by polyphenol crystals dispersed in the oil plus different concentrations of WPM particles dispersed in the aqueous phase are shown in Figure 5.2. The green brightness in the images is due to the auto-fluorescence of the polyphenol particles. Rhodamine B (red) was used to visualize the WPM particles. As one might expect, the intensity of red colour within the spherical water droplets indicates

that the WPM particles preferred to be in the water phase. In line with the emulsion results indicating higher stability at higher WPM particle concentration (Figure 5.2), the intensity of red colour at the W-O interface increased with increasing WPM particle concentration (Figure 5.2 (a)). In the curcumin system with low concentrations of WPM particles (< 0.1 wt%), the WPM particles and crystals formed a very uniform layer around the water droplets. With quercetin even at WPM particle concentrations > 0.1 wt%, the adsorbed layer was less uniform, with some droplets apparently having far less than complete coverage, with increasing tendency for the droplets to aggregate, e.g., Figure 5.2 (bii). As the concentration of WPM particles increased (> 0.1 wt%) in both systems, there was an increased tendency for the whole system to aggregate, with WPM particles seemingly aggregated at the interface of individual droplets and between interfaces, *i.e.*, causing flocculation of the water droplets. The polyphenol crystals seemed to be mixed in with these aggregates. In other words, as the concentration of WPM particles increased, there was increased tendency for microgels to become shared between droplets.

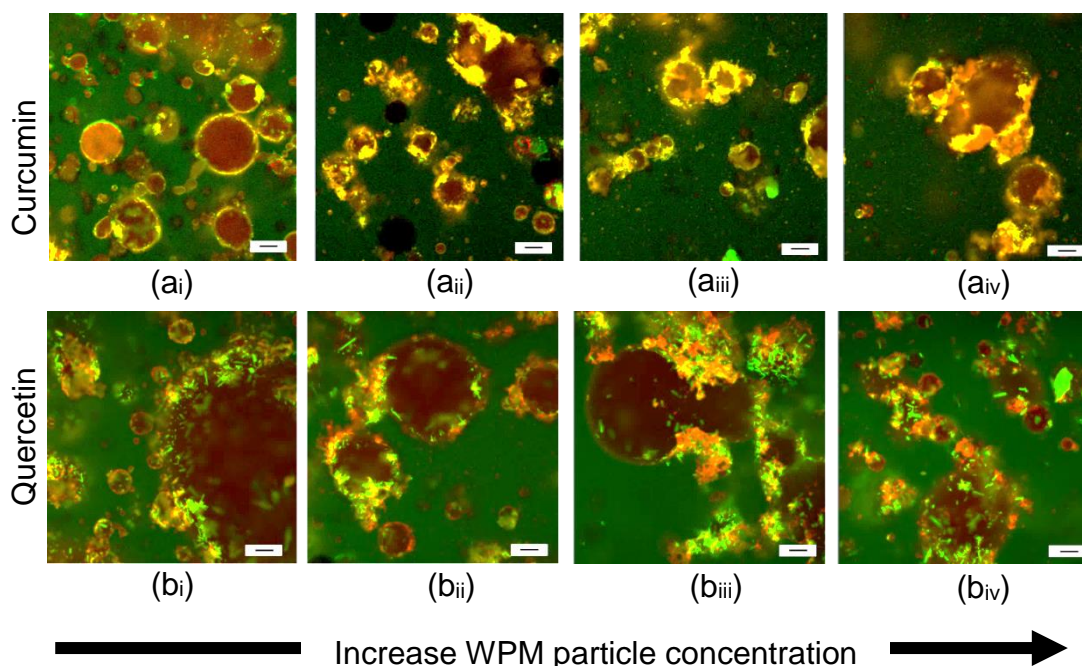


Figure 5.2. Confocal images of 10 wt% W/O Pickering emulsions stabilized by 0.14 wt% curcumin (a) and quercetin (b) crystals in the oil phase and different concentrations of WPM particles in the aqueous phase; 0.1 (i), 0.5 (ii), 1.0 (iii) and 2.0 wt% (iv) for freshly prepared samples. The green brightness in the images is caused by the auto-fluorescence of curcumin (488 nm excitation) or quercetin (405 nm excitation) crystals. The red brightness is due to the WPM particles stained by Rhodamine B (568 nm excitation). The scale bar represents 50 μm .

Confocal images of aged (for 21 days) emulsions stabilized by polyphenol crystals and 2.0 wt% WPM particles are shown in Figure 5.3. The appearances of both the curcumin and quercetin systems seemed to have remained stable over time and no coalescence was observed.

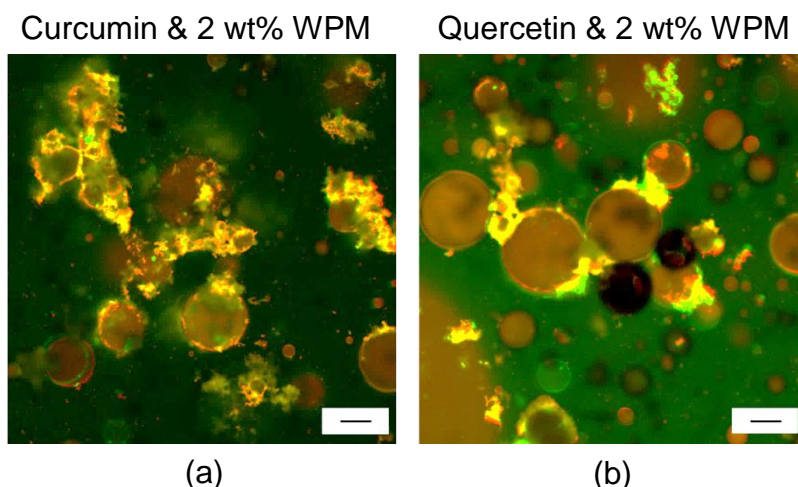


Figure 5.3. Confocal images of 10 wt% W/O Pickering emulsions stabilized by 0.14 wt% curcumin (a) and quercetin (b) crystals in the oil phase and 2.0 wt% WPM particles in the aqueous phase (pH 3.0) for 21 days old samples. The green brightness in the images is caused by the auto-fluorescence of curcumin (488 nm excitation) or quercetin (405 nm excitation) crystals. The red brightness is due to WPM particles stained by Rhodamine B (568 nm excitation). The scale bar represents 50 μm .

5.3.3.2. Effect of volume fraction of water droplets

Higher water:oil ratios (15, 20 and 30 wt% water) were tested for curcumin (0.14 wt%) or quercetin (0.14 wt%) crystals + 2.0 wt% WPM particles as Pickering stabilizers, since this WPM particle concentration provided enhanced stability to 10 wt% W/O emulsions. Figure 5.4 shows that the initial d_{32} of the emulsions with curcumin or quercetin crystals was not significantly different ($\sim 15 \mu\text{m}$, $p > 0.05$ see Appendix C, Table C3 and Table C4 for curcumin and quercetin, respectively) as the volume fraction increased from 15 to 20 wt%, whilst at 30 wt% water the size *decreased* significantly in both systems. Selected images of these emulsions, shown in Figure 5.4, illustrate the dense and uniform coverage of the droplets by polyphenol crystals (yellow). As the wt% water increases and therefore the absolute amount of WPM particles available increases (though the WPM particle concentration remains the same), the absolute amount of polyphenol available will decrease. However, the optimum ratio of WPM particles to polyphenol to achieve the most rapid interfacial complex formation *during* emulsification is difficult to calculate, given that the two types of particle approach the interface from the

two different phases. The WPM particles are generally smaller than those of the polyphenol crystals, so that possibly greater WPM particle coverage in the early stages of water droplet formation aids polyphenol co-adsorption (via the various attractive interactions proposed), explaining the initial reduction in the droplet size. More efficient adsorption of both components at the interface also apparently reduced the capacity for polyphenols to aggregate in the oil phase, as also shown in the confocal images.

The emulsions containing 15 wt% water were stable for more than 90 days (results are not shown) and had much the same microscopic appearance as those containing 10 wt% (Figure 5.2), as shown in Figure 5.4. The emulsions with 20 wt% stabilized by either curcumin or quercetin crystals were stable for 14 days whilst for all the emulsion systems containing 30 wt% water, a water layer at the bottom was observed after 1 day and the systems had completely phase separated after 3 days. Thus between 20 and 30 wt% water the systems became increasingly unstable, probably because there was not enough polyphenol crystals to fully cover the interface. The selected images shown in Figures 5.4 (a) and (b) of these higher wt% water systems also illustrate this increased instability in terms of larger apparent droplet sizes. (Note that the confocal images were obtained 3 to 5 h after emulsion preparation, during which significant coalescence may have occurred, which was not appeared in the light scattering results as the droplet size was measured only few minutes after emulsion preparation).

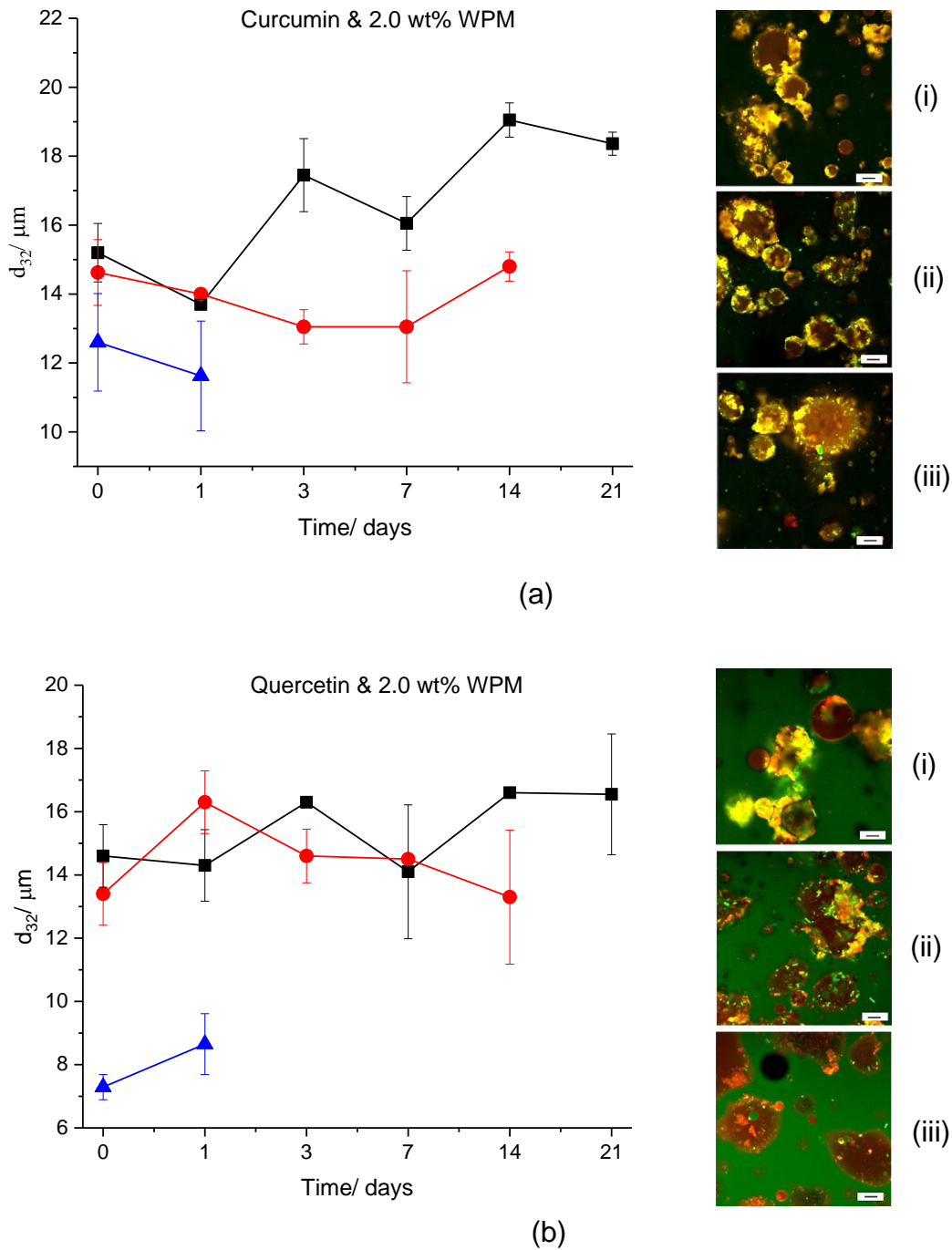


Figure 5.4. Mean size of water droplets (d_{32}) over time and confocal images (i-iii) of W/O emulsions stabilized by 0.14 wt% curcumin (a) and quercetin (b) crystals containing 15 wt% (■, i), 20 wt% (●, ii) and 30 wt% (▲, iii) water with 2.0 wt% WPM particles at pH 3.0. For statistical analysis according to Tukey's test, see Appendix C, Table C3 and Table C4 for curcumin and quercetin, respectively. The green brightness in the images is caused by the auto-fluorescence of curcumin (488 nm excitation) or quercetin (405 nm excitation) crystals. The red brightness is due to WPM particles stained by Rhodamine B (568 nm excitation). The scale bar represents 50 μm .

5.3.3.3. Microgel and polyphenol crystal interactions via monolayer experiments

The response of the film of adsorbed material to expansion and compression of the interface is a key factor determining the ease of formation and stability of a multitude of colloidal systems (Murray, 1997). Using Langmuir trough techniques at the air-water (A-W) interface we sought to obtain direct evidence for specific interactions between the protein microgels and the polyphenol crystals at an interface. Working at the A-W interface was a simplification of the system compared to the W/O emulsions, but allowed reproducible spreading of material at the interface resulting in more robust conclusions. However, manual spreading at the interface can never mimic exactly the processes of adsorption/desorption and the associated rates of conformational change during emulsification. Similarly, the solvency of air is not the same as oil and the affinity of both the microgels and polyphenol crystals for the W-O and A-W interfaces is probably not the same (Murray, 1997).

Upon adsorption, WPM particles undergo conformational changes which result from the balance between chain spreading - driven by surface activity - and microgel internal elasticity, promoted by cross-linking (Picard *et al.*, 2017). The extent of spreading therefore depends on various factors such as the microgel internal structure and cross-linking, their concentration, or process parameters (Picard *et al.*, 2017). Microgels tend to flatten at fluid interfaces, sometimes exhibiting a 'fried egg'-like structure (Destribats *et al.*, 2011). The extent of spreading has consequences for the capacity of adjacent microgels to entangle *via* their peripheral dangling chains, forming a two-dimensional elastic network of connected microgels (Destribats *et al.*, 2011). Microgels with low deformability barely form entanglements and fail to stabilize emulsions against mechanical disturbances. It has also been found that the conformation depends on the concentration of microgels from which they adsorb - at low concentration when the adsorption kinetics are slow the microgels flattened, whereas at high concentrations they were more compressed laterally (Picard *et al.*, 2017). Interfaces covered with flattened

microgels were adhesive, leading to bridging between adjacent interfaces, because the thin polymeric layer separating adjacent microgels could be more easily ruptured (Destribats *et al.*, 2013). Thus, more deformable microgels can lead to more bridging due to their flattened conformation (Destribats *et al.*, 2012). When the interfaces are covered with compressed microgels, the films are no longer adhesive because the higher polymer thickness prevents interfaces from bridging (Destribats *et al.*, 2012; Destribats *et al.*, 2013; Picard *et al.*, 2017) (Keal *et al.*, 2017). Other parameters such as energy input on stirring and homogenization and the size of microgels can also change the extent of spreading and thus the polymeric thickness at the interface, leading to similar consequences for bridging (Destribats *et al.*, 2014a; Destribats *et al.*, 2013; Keal *et al.*, 2017; Picard *et al.*, 2017).

Figure 5.5 (a) shows the isotherms obtained by spreading a solution of 0.34 wt% WPM particles at the A-W interface at pH 3.0. Surface pressure (π) is plotted against A_p , where A_p is the area per particle scaled against the cross-sectional area of the nominal particle size, *i.e.*, a sphere of radius 45 nm (see above). This size is therefore also used to calculate the number of particles in the 0.34 wt% solution, assuming the particles have the same density as the bulk gel from which they are formed. Films were repeatedly compressed then re-expanded and compressed again to increasingly higher maximum π values to test for reversibility. It is seen that π starts to rise significantly at $A_p > 1$ (somewhere between $A_p = 7$ and 8), which maybe taken as the region where the particles start to interact with each other in the interface, and thereafter π increases smoothly with increasing rapidity on further compression. By the time $\pi = 10 \text{ mN m}^{-1}$ the isotherm is quite steep but A_p is still > 4 . This suggests that on adsorption at low π , the particles are significantly more expanded than their initial unabsorbed size (the maximum packing fraction for monodisperse spheres on a plane, *i.e.*, circles, being 0.9069) and whilst they undergo significant compression (nearly a factor of two in area) up to $\pi = 10 \text{ mN m}^{-1}$, they are still significantly expanded at this π . However, this assumes that the particles are monodisperse, whilst clearly there is a range of sizes and also probably a range of shapes, so that the polydispersity of the microgels (Appendix C, Figure C1) and possibly differences in the compressibility of

different sized particles could account for some of this apparent increase in cross-sectional area. This interpretation of the isotherms also assumes that there is no irreversible desorption of particles on compression, but the reversibility and reproducibility of the isotherms, within experimental error (ca., 0.3 mN m^{-1}) suggested that this did not take place. Particles also tended to form networks at the interface because they are attracted via capillary interactions, causing this increase of π . This attraction between the particles helps rendering stability of the water droplets in the emulsion systems (explained above). Overall then, the isotherms suggest the WPM particles have a high tendency to adsorb and unfold at the A-W interface, substantiated by the emulsion results (and also the interfacial shear rheology results – see below).

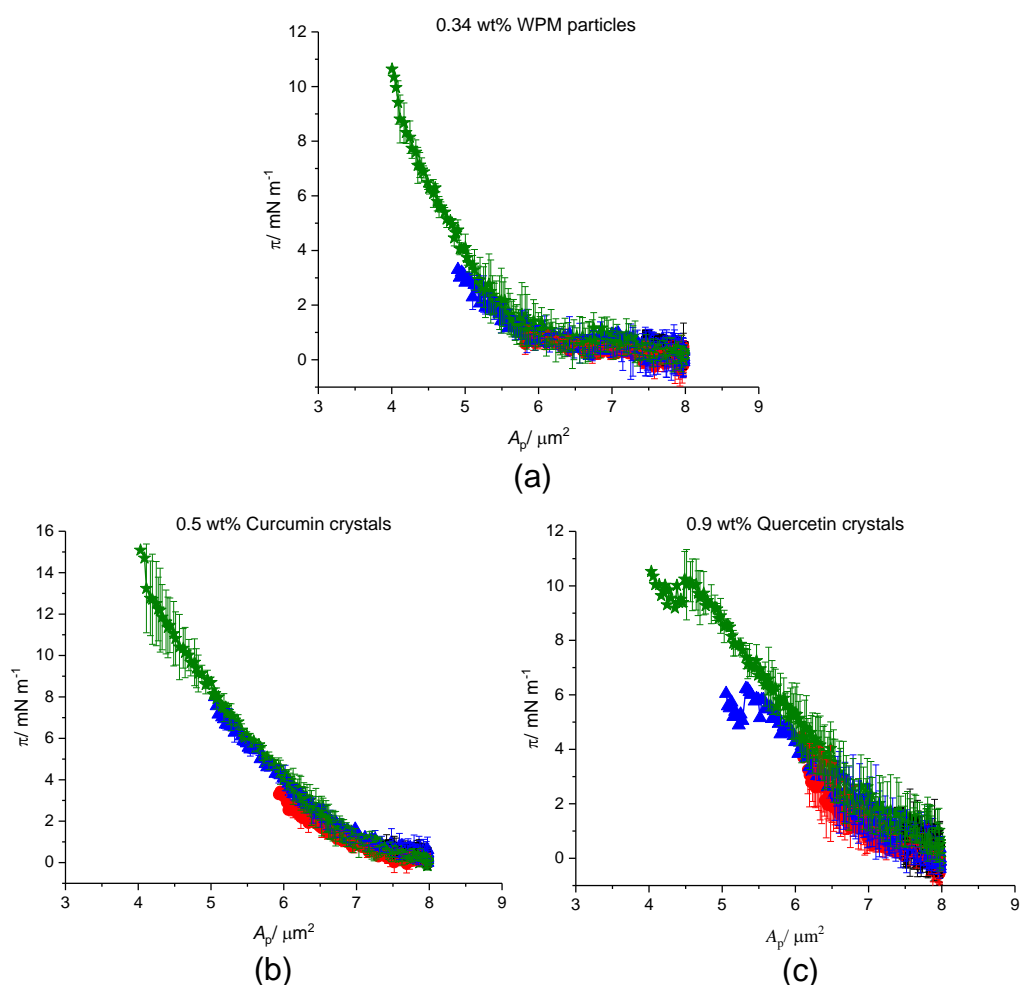


Figure 5.5. Surface pressure (π) versus (A_p) isotherms at A-W interface (aqueous phase at pH 3.0) spread solution of 0.34 wt% WPM particles (a), 0.5 wt% curcumin (b) and 0.9 wt% quercetin (c) particles under different compression and expansion times; 1st compression-expansion (■), 2nd compression-expansion (●), 3rd compression-expansion (▲) and 4th compression-expansion (★).

Figures 5.5 (b) and (c) shows isotherms for curcumin and quercetin crystals, respectively, after their precipitation at the A-W interface from solution (at 0.5 wt% and 0.9 wt% in hexane, respectively) and evaporation of the solvent. Expression of the isotherms in terms of A_p as in Figure 5.5 (a) immediately presents the problem of what particle size and cross-sectional area (and number of particles spread) to use for each polyphenol. The particle size and shape of the polyphenols crystals is even less precisely known. However, for illustrative purposes, since the main intention is to examine the behaviour of the mixed WPM + polyphenol films, here we assumed the quercetin crystals had a rectangular cross-section $7 \times 1 \mu\text{m}$, *i.e.*, each

occupied an area of $7 \mu\text{m}^2$ at the interface, whilst the curcumin crystals were spheres of radius $0.1 \mu\text{m}$ and so each occupied an area of $\pi(0.1)^2 = 0.031 \mu\text{m}^2$. The justification for this comes from our earlier characterization of the properties of the crystals dispersed in vegetable oil for the W/O emulsions (Zembyla *et al.*, 2019; Zembyla *et al.*, 2018), whereas here the materials are precipitated at the interface from hexane. Removal of the crystals floating at the interface and observations of their size and shape via microscopy did not suggest they were significantly different. Nevertheless, in view of these approximations, not too much significance should be attached to the fact that, the start of the increase in π begins at quite high $A_p \approx 6$, only slightly lower than for the WPM particles. The crystals clearly should not expand, so that this is probably explained by them having a wider range of sizes and aspect ratios than assumed. This suggests that they can interact and form a network at the interface at lower coverages than the assumed sizes predict. Irrespective of this, it is seen that the isotherms are reversible, suggesting irreversible attachment and orientation within the interface. The quercetin isotherm is slightly steeper than for curcumin. Note that the amounts of polyphenols spread were chosen to give an equivalent surface area of material as the WPM particles, based on the non-deformed particle dimensions assumed above. The absolute position on the A_p scale is not important for the reasons already discussed, but the isotherms for the individual components do allow us to compare the isotherms measured for the mixed systems with those predicted by ideal mixing. Thus, if one assumes there are no attractive or repulsive interactions between the WPM and polyphenol particles at the interface, then the surface pressures should be independent of one another and additive at the same overall trough area.

Figures 5.6 (a) and (b) show the measured and predicted isotherms for the combined systems of 0.34 wt% WPM + 0.5 wt% curcumin or 0.9 wt% quercetin, respectively. As indicated above, these concentrations would give equal interfacial areas of the non-deformed spread materials. Note that since both materials were initially spread at high area per particle, we have assumed that this will give them sufficient interfacial space to allow them to re-arrange into the same sort of mixed configuration as eventually forms on their

adsorption to the W-O interface in the emulsions, although it is very difficult to obtain direct evidence of this. The predicted isotherms are simply calculated from addition of the isotherms in Figure 5.5 and we have plotted π against the average area per particle for both particles. It is seen that for both WPM + curcumin and WPM + quercetin the measured isotherm for the mixed system is shifted to lower A_p at equivalent π in the predicted isotherm. In other words, the combined materials occupy lower areas at the same π , suggesting attractive interaction, or interpenetration of the crystals and microgels. In view of the above discussion of a possible attractive electrostatic interaction between the polyphenol crystals and WPM particles at the W-O interface, this perhaps not surprising, but this is nice additional support for this effect. It is also seen that the shift is most pronounced for curcumin, which is noted as having much smaller crystals and which might therefore more easily penetrate, or pack in between, the WPM particles. With quercetin, the measured and predicted isotherms are coincident, within experimental error, up until *ca.*, $\pi = 7 \text{ mN m}^{-1}$, beyond which the mixed area increasingly starts to diverge to lower areas compared to that predicted by ideal mixing. Note that qualitatively these trends will be independent of the actual choice of particle cross-sectional areas, as long as one is consistent for the single and mixed systems. Although at present we have no way of knowing what are the actual *adsorbed* (*i.e.*, rather than spread) surface concentrations of the two components at the W-O interface in the emulsions, the monolayer results provide interesting direct evidence for an attractive interaction between WPM particles and curcumin or quercetin crystals at interfaces.

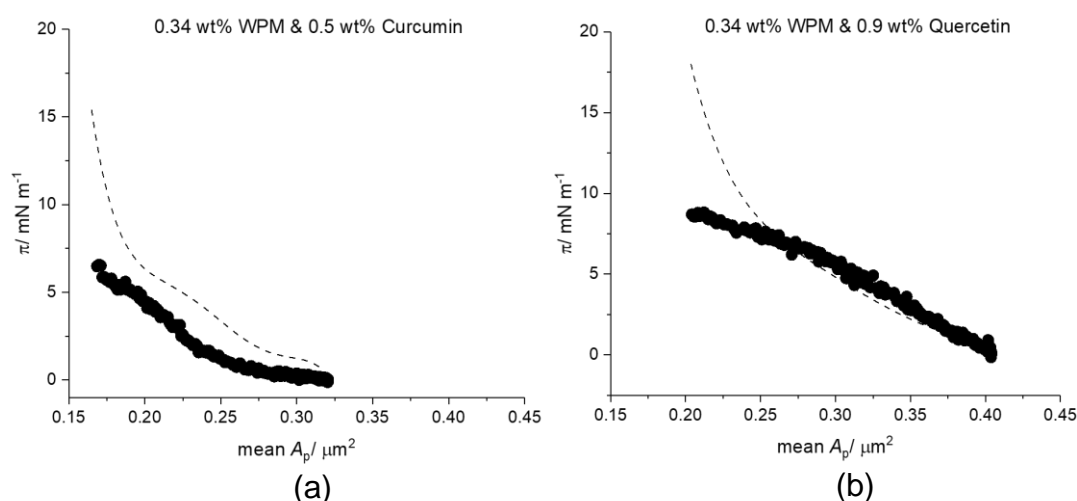


Figure 5.6. Surface pressure (π) versus mean area per particle (A_p) isotherms of mixtures of 0.34 wt% WPM particles plus 0.5 wt% curcumin (a), or 0.9 wt% quercetin (b) crystals. The symbols (●) are the experimentally measured points (average of 3 runs) whilst the dashed lines are the theoretical results based on ideal mixing (*i.e.*, no interactions) of WPM particles and curcumin or quercetin crystals.

5.3.4. Interfacial shear viscosity (η_i)

In order to further test for evidence of interfacial complex formation, measurements of interfacial shear viscosity (η_i) were undertaken as discussed on our previous work (Zembyla *et al.*, 2019; Zembyla *et al.*, 2018). Interfacial shear viscosity is a particularly sensitive method for monitoring any structural and compositional changes within adsorbed layers (Murray, 2002; Murray *et al.*, 1996a). Experiments were performed with purified soybean oil in order to remove any low molecular weight surface active components (mono and diglycerides), which tend to lower η_i because they are more surface active than proteins or particles (Murray, 2002). Figure 5.7 shows the values of interfacial shear viscosity after 24 h in the presence of 0.14 wt% curcumin or quercetin crystals dispersed in the oil with different concentrations of WPM particles in the aqueous phase, at pH 3.0. A control experiment with purified oil (*i.e.*, containing no polyphenol crystals) and Milli-Q water was performed but $\eta_i = 0 \text{ mN s m}^{-1}$ even after 24 h (results are not shown). Addition of 0.5 wt% WPM particles to the aqueous phase (but with only purified oil as the continuous phase) also showed a significant increase in η_i reaching a maximum of 711 mN s m^{-1} after 24 h (shown as the single blue point on the Figure 5.7).

As seen in Figure 5.7, for both curcumin and quercetin, the trend of η_i (24 h) versus WPM particle concentration at pH 3.0 was very similar. Below 0.1 wt% WPM particles, there was a significant increase of η_i , whereas above 0.1 wt% WPM particles, η_i decreased. Note that although the value for 0.5 wt% WPM particles after 24 h is high (similar to many pure globular proteins, including β -lactoglobulin and α -lactalbumin (Murray *et al.*, 1996a; Roth *et al.*, 2000)) the values for these mixed systems at low WPM particle concentration are considerably higher still. At low concentrations of WPM particles, the polyphenol crystals and WPM particles might easily co-adsorb at the interface and so form complexes, giving films that are much stronger than WPM particles on their own (at 0.5 wt% WPM particles, for example). A similar effect has been identified between polyphenol crystals and WPI (Zembyla *et al.*, 2019). However, at higher concentrations of WPM particles, WPM adsorption will tend to dominate over crystal adsorption, and so the η_i values decreased towards the values for WPM particles alone.

Curcumin gave the same η_i as quercetin at 0.05 and 0.1 wt% WPM particles (Figure 5.7), within experimental error, suggesting that both polyphenol crystals acted very similarly at lower WPM particle concentrations. However, as the concentration of WPM particles increased (> 0.1 wt%) η_i decreased more significantly ($p > 0.05$, see Appendix C, Table C5) for curcumin than quercetin. This could be due to stronger interactions between quercetin and WPM particles, similar to the stronger interaction between quercetin and WPI suggested previously by the same η_i measurement (Zembyla *et al.*, 2019). As the WPM particle concentration increased, more aggregated particles were present at the interface, indicating a microgel dominated system. During the interfacial shearing, these aggregated microgels may re-arrange at the interface or break down to single microgels, destroying the interfacial film, explaining the decrease of η_i (especially at WPM particle concentrations > 0.5 wt%).

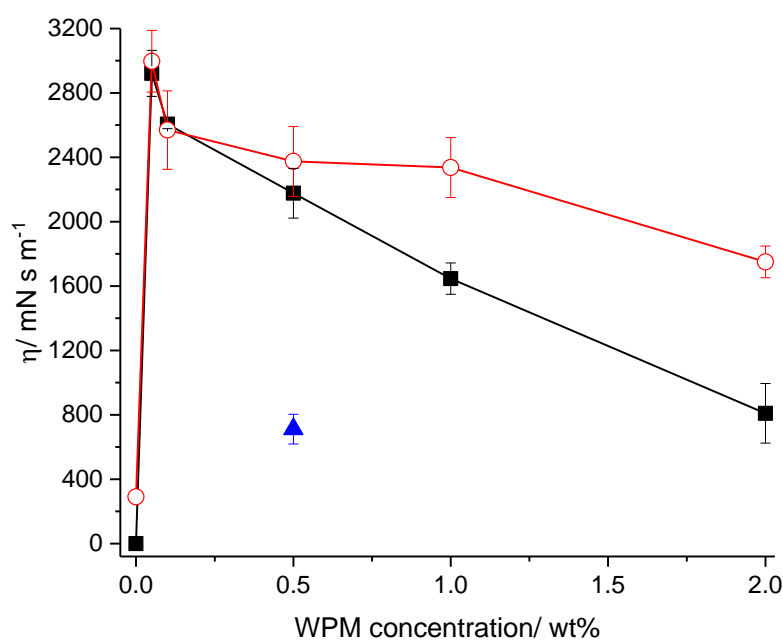


Figure 5.7. Interfacial shear viscosity at W-O interface without polyphenol crystals (only WPM particles) [▲], with 0.14 wt% curcumin [■] and quercetin [●] crystals dispersed in purified oil with different concentrations of WPM particles in the aqueous phase after 24 h of adsorption at pH 3.0. For statistical analysis according to Tukey's test, see Appendix C, Table C5 for both curcumin and quercetin.

5.4. Discussion

Drawing together the results of all these experiments, a possible mechanism of complex formation between the protein microgels and polyphenol crystals at the interface is schematically shown in Figure 5.8. At low concentration of WPM particles (< 1 wt%), both polyphenol crystals and WPM particles co-exist at the interface of the water droplets and synergistically improve the stability of the emulsions (Figure 5.8 (a)). For curcumin systems, where the curcumin crystals have nearly similar shape and size as the WPM particles, both curcumin and WPM particles efficiently form complexes together, improving the water droplet coverage and stability for more than 90 days. For quercetin systems, where the quercetin crystals are much bigger in size ($d_{32} \sim 5.9 \mu\text{m}$) (Zembyla *et al.*, 2018) than WPM particles (at low concentration, $\sim 90 \text{ nm}$), the complex was still formed but the water droplets were only stable for 21 days, probably due to the incomplete

coverage of the water droplets due to the larger size difference between the crystals and WPM particles. As the concentration of WPM particles increases, the size and shape of polyphenol crystals becomes less important with respect to stability. At WPM ≥ 1.0 wt% the WPM particles aggregate with each other, with polyphenol crystals in the bulk phase and at the interface and between the water droplets, acting as a sort of 'colloidal glue' for the whole system (Figure 5.8 (b)) that immobilizes the water droplets and inhibits their coalescence. Ultimately, this synergistic action of polyphenol crystals and WPM particles is due to electrostatic attraction between the oppositely-charged polyphenol crystals and WPM particles at the interface. This depends on the pH of the aqueous phase as explained before and in our previous work (Zembyla *et al.*, 2019), whilst hydrogen bonding probably also plays a role in enhancing the interaction.

Schmitt *et al.* (2013) explain how the particle packing in a microgel layer can cause bridging flocculation. If the particles' packing is looser and more heterogeneous due to non-uniformity of the microgel's internal structure or limited interconnectivity with adjacent particles, then there is a tendency for microgel layers to become shared between droplets (Destribats *et al.*, 2013; Schmitt *et al.*, 2013). This susceptibility to bridging flocculation is considered more likely to occur in emulsions containing large stiff microgel particles having a high degree of cross-linking (Destribats *et al.*, 2013; Schmitt *et al.*, 2013). Another factor affecting microgel packing at the interface is the intensity of hydrodynamic disturbance during emulsification. Highly intensive shearing induces pronounced microgel flattening at the droplet surface, leading to enhanced susceptibility towards bridging flocculation (Destribats *et al.*, 2013). On the other hand, a moderately low shear-rate applied during emulsification favours the formation of stable droplets with surfaces fully covered by dense uniform monolayers of laterally compressed microgel particles (Destribats *et al.*, 2013).

We have attempted to obtain evidence of the homogeneity of the typical arrangement (as distinct islands or mixed regions of each, for example) of the polyphenol crystals and the microgel particles at the W/O droplet interface via

a range of electron microscopy (cryo-SEM and TEM) techniques. However, although the above confocal images clearly show that both components are present together, so far electron microscopy has failed to resolve the individual WPM particles at the interface, no doubt due to their more delicate nature and thus the damaging effects of dehydration, freezing or the electron beam itself. Nor have we seen any clear evidence, with the range of crystal sizes and shapes, of capillary interactions influencing the deformation of the interface between droplets, which for large particles has been shown to be a significant contribution to the Pickering stabilization mechanism (Paunov *et al.*, 1993).

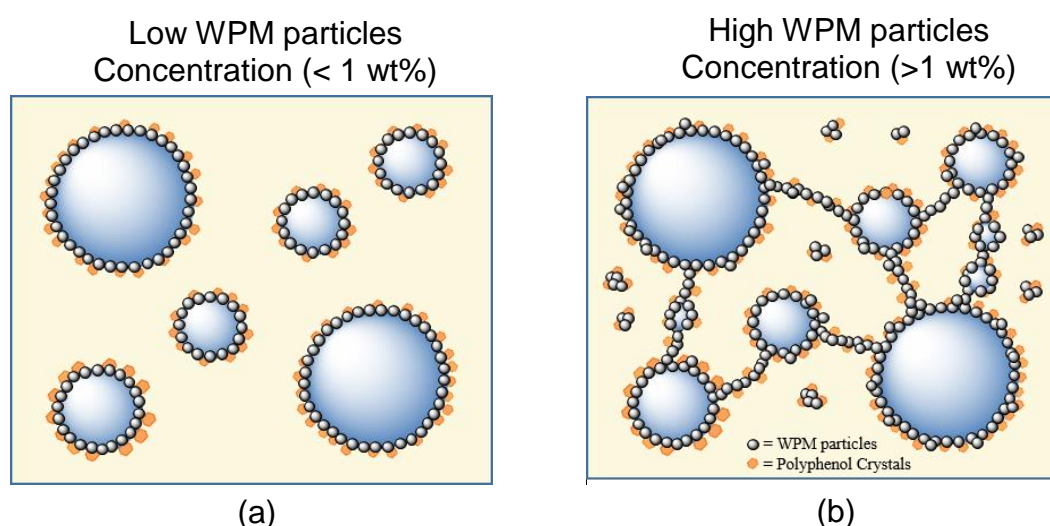


Figure 5.8. Schematic representation (not to scale) of curcumin or quercetin crystal + WPM particle-stabilized W/O emulsions, illustrating the effect of WPM particle concentration and the possible mechanism of water droplet stabilization.

5.5. Conclusion

In this work, we propose a novel way to stabilize W/O emulsions via a ‘double Pickering mechanism’, where polyphenol particles adsorb from the oil side and WPM particles co-adsorb from the aqueous side of the interface. This complex formation was strongly dependent on the concentration of WPM particles. At low WPM particle concentrations, both polyphenol crystals and WPM particles were present at the interface and through a synergistic action, they better stabilized the W/O emulsions. At higher WPM particle

concentrations, flocculation was observed where the WPM particles acted as a 'colloidal glue' between water droplets and polyphenol crystals enhancing the water droplet stability and preventing the coalescence. Via this mechanism, addition of WPM particles up to 1 wt% gave a significant improvement in the stability of the emulsions up to at least 20 wt% water. It is believed that this complex formation was mainly formed due to attractive electrostatic interactions between oppositely-charged polyphenol Pickering particles on the oil side of the interface and WPM 'Pickering' particles mainly on the aqueous side of the interface, which therefore was also dependent on the pH of the aqueous phase. Interfacial shear viscosity measurements and monolayer experiments at the A-W interface provided further evidence of strengthening of the film due to the complex formation at the interface. However, higher concentrations of WPM particles do not improve the stability further due to WPM particle adsorption dominating over polyphenol crystal adsorption. Combinations of such polyphenol crystals + microgels to form interfacial synergistic Pickering particle-particle complexes could be used more widely for designing water-in-oil emulsions for a variety of soft matter applications.

In the following chapter (**Chapter 6**) the process stability of the W/O emulsions stabilized by curcumin or quercetin crystals dispersed in the oil phase, with or without the presence of WPI (**Chapter 3 and 4**) or WPM particles (**Chapter 5**) in the aqueous phase will be characterized. This characterization will be undertaken using controlled rheological tests (shear rates and temperatures) combined with particle sizing and confocal laser scanning microscopy.

References

- Araiza-Calahorra, A., & Sarkar, A. (2019). Pickering emulsion stabilized by protein nanogel particles for delivery of curcumin: Effects of pH and ionic strength on curcumin retention. *Food Structure*, *21*, 100113.
- Arts, T., Laven, J., van Voorst Vader, F., & Kwaaitaal, T. (1994). Zeta potentials of tristearoylglycerol crystals in olive oil. *Colloids and Surfaces A: Physicochemical and Engineering Aspects*, *85*(2-3), 149-158.
- Atarés, L., Marshall, L. J., Akhtar, M., & Murray, B. S. (2012). Structure and oxidative stability of oil in water emulsions as affected by rutin and homogenization procedure. *Food chemistry*, *134*(3), 1418-1424.
- Binks, B. P., & Horozov, T. S. (2006). *Colloidal particles at liquid interfaces*: Cambridge University Press.
- Destribats, M., Eyharts, M., Lapeyre, V., Sellier, E., Varga, I., Ravaine, V., & Schmitt, V. (2014a). Impact of pNIPAM microgel size on its ability to stabilize Pickering emulsions. *Langmuir*, *30*(7), 1768-1777.
- Destribats, M., Lapeyre, V., Sellier, E., Leal-Calderon, F., Ravaine, V., & Schmitt, V. (2012). Origin and control of adhesion between emulsion drops stabilized by thermally sensitive soft colloidal particles. *Langmuir*, *28*(8), 3744-3755.
- Destribats, M., Lapeyre, V., Sellier, E., Leal-Calderon, F., Schmitt, V., & Ravaine, V. (2011). Water-in-oil emulsions stabilized by water-dispersible poly (N-isopropylacrylamide) microgels: Understanding anti-Finkle behavior. *Langmuir*, *27*(23), 14096-14107.
- Destribats, M., Rouvet, M., Gehin-Delval, C., Schmitt, C., & Binks, B. P. (2014b). Emulsions stabilised by whey protein microgel particles: towards food-grade Pickering emulsions. *Soft Matter*, *10*(36), 6941-6954.
- Destribats, M., Wolfs, M., Pinaud, F., Lapeyre, V., Sellier, E., Schmitt, V., & Ravaine, V. (2013). Pickering emulsions stabilized by soft microgels: influence of the emulsification process on particle interfacial organization and emulsion properties. *Langmuir*, *29*(40), 12367-12374.
- Dickinson, E. (2010). Food emulsions and foams: stabilization by particles. *Current opinion in colloid & interface science*, *15*(1-2), 40-49.
- Dickinson, E. (2015). Microgels—an alternative colloidal ingredient for stabilization of food emulsions. *Trends in Food Science & Technology*, *43*(2), 178-188.
- Dickinson, E. (2017). Biopolymer-based particles as stabilizing agents for emulsions and foams. *Food Hydrocolloids*, *68*, 219-231.
- Ghosh, S., & Rousseau, D. (2011). Fat crystals and water-in-oil emulsion stability. *Current Opinion in Colloid & Interface Science*, *16*(5), 421-431.

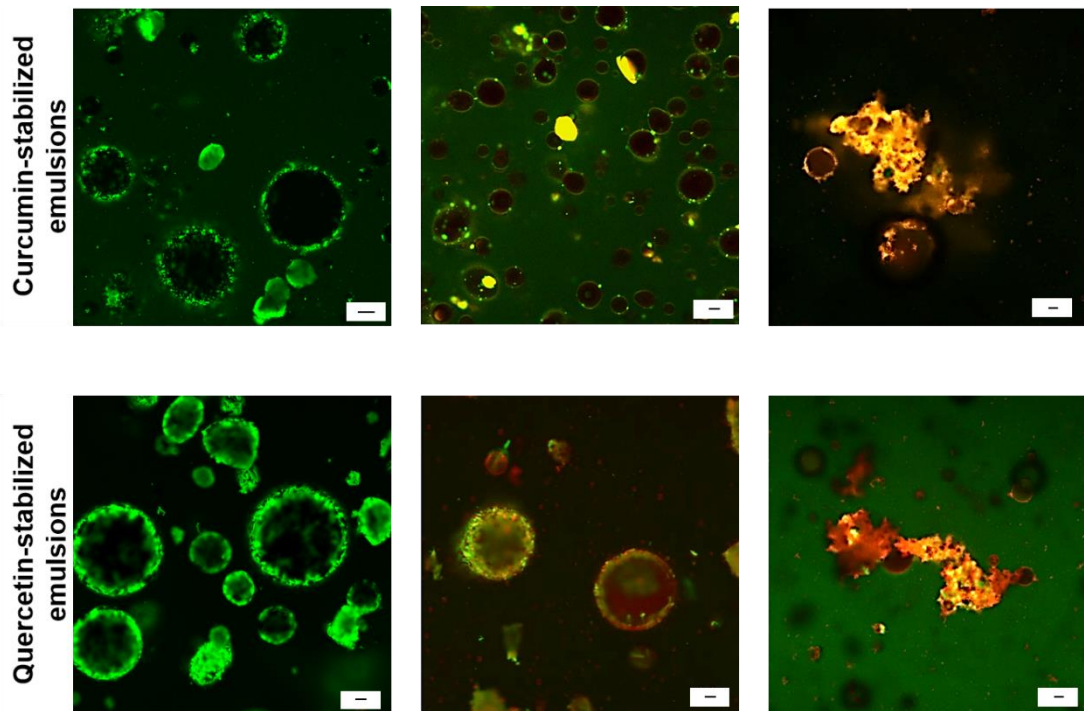
- Keal, L., Lapeyre, V., Ravaine, V., Schmitt, V., & Monteux, C. (2017). Drainage dynamics of thin liquid foam films containing soft PNIPAM microgels: influence of the cross-linking density and concentration. *Soft Matter*, 13(1), 170-180.
- Morrison, I. D. (1993). Electrical charges in nonaqueous media. *Colloids and Surfaces A: Physicochemical and Engineering Aspects*, 71(1), 1-37.
- Murray, B. S. (1997). Equilibrium and dynamic surface pressure-area measurements on protein films at air-water and oil-water interfaces. *Colloids Surfaces A: Physicochemical Engineering Aspects*, 125(1), 73-83.
- Murray, B. S. (2002). Interfacial rheology of food emulsifiers and proteins. *Current Opinion in Colloid & Interface Science*, 7(5-6), 426-431.
- Murray, B. S. (2019). Pickering Emulsions for Food and Drinks. *Current Opinion in Food Science*, 27, 57-63.
- Murray, B. S., Cattin, B., Schüler, E., & Sonmez, Z. O. (2002). Response of adsorbed protein films to rapid expansion. *Langmuir*, 18(24), 9476-9484.
- Murray, B. S., & Dickinson, E. (1996a). Interfacial rheology and the dynamic properties of adsorbed films of food proteins and surfactants. *Food Science and Technology International*, 2(3), 131-145.
- Murray, B. S., & Nelson, P. V. (1996b). A novel Langmuir trough for equilibrium and dynamic measurements on air-water and oil-water monolayers. *Langmuir*, 12(25), 5973-5976.
- Murray, B. S., & Phisarnchananan, N. (2016). Whey protein microgel particles as stabilizers of waxy corn starch plus locust bean gum water-in-water emulsions. *Food Hydrocolloids*, 56, 161-169. doi:10.1016/j.foodhyd.2015.11.032
- Nallamilli, T., Binks, B. P., Mani, E., & Basavaraj, M. G. (2015). Stabilization of Pickering emulsions with oppositely charged latex particles: influence of various parameters and particle arrangement around droplets. *Langmuir*, 31(41), 11200-11208.
- Nallamilli, T., Mani, E., & Basavaraj, M. G. (2014). A model for the prediction of droplet size in Pickering emulsions stabilized by oppositely charged particles. *Langmuir*, 30(31), 9336-9345.
- Nicolai, T., Britten, M., & Schmitt, C. (2011). β -Lactoglobulin and WPI aggregates: formation, structure and applications. *Food Hydrocolloids*, 25(8), 1945-1962.
- Patel, M. N., Smith Jr, P. G., Kim, J., Milner, T. E., & Johnston, K. P. (2010). Electrophoretic mobility of concentrated carbon black dispersions in a low-permittivity solvent by optical coherence tomography. *Journal of Colloid and Interface Science*, 345(2), 194-199.

- Paunov, V., Kralchevsky, P., Denkov, N., & Nagayama, K. (1993). Lateral capillary forces between floating submillimeter particles. *Journal of colloid interface science*, *157*(1), 100-112.
- Picard, C., Garrigue, P., Tatry, M.-C., Lapeyre, V. r., Ravaine, S., Schmitt, V. r., & Ravaine, V. r. (2017). Organization of microgels at the air–water interface under compression: Role of electrostatics and cross-linking density. *Langmuir*, *33*(32), 7968-7981.
- Pushpam, S. D. C., Basavaraj, M. G., & Mani, E. (2015). Pickering emulsions stabilized by oppositely charged colloids: Stability and pattern formation. *Physical Review E*, *92*(5), 6. doi:10.1103/PhysRevE.92.052314
- Rosenholm, J. B. (2018). Evaluation of particle charging in non-aqueous suspensions. *Advances in colloid and interface science*.
- Roth, S., Murray, B. S., & Dickinson, E. (2000). Interfacial shear rheology of aged and heat-treated β -lactoglobulin films: Displacement by nonionic surfactant. *Journal of agricultural and food chemistry*, *48*(5), 1491-1497.
- Sahasrabudhe, S. N., Rodriguez-Martinez, V., O'Meara, M., & Farkas, B. E. (2017). Density, viscosity, and surface tension of five vegetable oils at elevated temperatures: Measurement and modeling. *International journal of food properties*, *20*(sup2), 1965-1981.
- Sarkar, A., Ademuyiwa, V., Stublely, S., Esa, N. H., Goycoolea, F. M., Qin, X., . . . Olvera, C. (2018). Pickering emulsions co-stabilized by composite protein/polysaccharide particle-particle interfaces: Impact on in vitro gastric stability. *Food Hydrocolloids*, *84*, 282-291.
- Sarkar, A., Kanti, F., Gulotta, A., Murray, B. S., & Zhang, S. (2017a). Aqueous Lubrication, Structure and Rheological Properties of Whey Protein Microgel Particles. *Langmuir*, *33*(51), 14699-14708. doi:10.1021/acs.langmuir.7b03627
- Sarkar, A., Murray, B., Holmes, M., Ettelaie, R., Abdalla, A., & Yang, X. (2016). In vitro digestion of Pickering emulsions stabilized by soft whey protein microgel particles: influence of thermal treatment. *Soft Matter*, *12*(15), 3558-3569.
- Sarkar, A., Zhang, S., Murray, B., Russell, J. A., & Boxal, S. (2017b). Modulating in vitro gastric digestion of emulsions using composite whey protein-cellulose nanocrystal interfaces. *Colloids and Surfaces B: Biointerfaces*, *158*, 137-146.
- Schmidt, S., Liu, T., Rütten, S., Phan, K.-H., Möller, M., & Richtering, W. (2011). Influence of microgel architecture and oil polarity on stabilization of emulsions by stimuli-sensitive core–shell poly (N-isopropylacrylamide-co-methacrylic acid) microgels: Micking versus Pickering behavior? *Langmuir*, *27*(16), 9801-9806.

- Schmitt, C., Moitzi, C., Bovay, C., Rouvet, M., Bovetto, L., Donato, L., . . . Stradner, A. (2010). Internal structure and colloidal behaviour of covalent whey protein microgels obtained by heat treatment. *Soft Matter*, 6(19), 4876-4884.
- Schmitt, V., & Ravaine, V. (2013). Surface compaction versus stretching in Pickering emulsions stabilised by microgels. *Current Opinion in Colloid & Interface Science*, 18(6), 532-541.
- Xu, R., Dickinson, E., & Murray, B. S. (2007). Morphological changes in adsorbed protein films at the air- water interface subjected to large area variations, as observed by Brewster angle microscopy. *Langmuir*, 23(9), 5005-5013.
- Zembyla, M., Murray, B. S., Radford, S. J., & Sarkar, A. (2019). Water-in-oil Pickering emulsions stabilized by an interfacial complex of water-insoluble polyphenol crystals and protein. *Journal of Colloid and Interface Science*, 548, 88-99.
- Zembyla, M., Murray, B. S., & Sarkar, A. (2018). Water-In-Oil Pickering Emulsions Stabilized by Water-Insoluble Polyphenol Crystals. *Langmuir*, 34(34), 10001-10011. doi:10.1021/acs.langmuir.8b01438

Chapter 6

Shear and Temperature Stability of Water-in-Oil Emulsions Co-Stabilized by Polyphenol Crystals-Protein Complex ⁴



Abstract

The process stability of water-in-oil (W/O) Pickering emulsions (10 or 20 wt% water), co-stabilized by crystals of the polyphenols (curcumin or quercetin, 0.14 wt%) dispersed in the oil phase, plus whey protein isolate (WPI, 2.0 wt%) or whey protein microgel (WPM, 0.1 - 2.0 wt%) particles present in the inner aqueous phase, was assessed by measuring the apparent viscosity (η), water droplet size (light scattering) and microstructural changes (confocal laser

⁴ Zembyla, M., Lazidis, A., Murray, B.S., & Sarkar, A. (2019). Shear and Temperature Stability of Water-in-Oil Emulsions Co-Stabilized by Polyphenol Crystals- Protein Complex. *Submitted to Journal of Food Engineering*.

scanning microscopy, CLSM). Stability was measured as a function of temperatures (25, 35 and 50 °C), using a shear rate cycle between 10^{-1} to 10^2 s^{-1} to highlight shear- and time-dependent hysteresis (if any) of η . All the emulsions showed shear-thinning to some extent, but those without added WPI or WPM particles in the aqueous phase exhibited coalescence at increasing shear rate, that was more pronounced at higher temperatures. Emulsions containing WPI in the dispersed phase were stable, whilst those containing WPM particles showed a decrease in mean droplet size (d_{43}) on shearing due to the disruption of the aggregates of droplets, polyphenol crystals and/or WPM particles in the continuous oil phase, but with no droplet coalescence. The low shear rate ($0.1 s^{-1}$) viscosity showed an increase with increasing WPM particle concentration. This increase, plus CLSM of the emulsions, suggested that the WPM particles increased W/O emulsion stability not only via their adsorption to the inner surface of the water droplets, but also due to their promotion of a mixed network of WPM particles, water droplets and polyphenol crystals in the oil phase.

6.1. Introduction

Emulsions are metastable colloids where one liquid phase is dispersed into another immiscible liquid as droplets, which are created via external shear energy and the droplets can be stabilized by surface-active molecules or particles (Mason, 1999). Emulsions therefore tend to revert to their two-phase state, usually via a combination of creaming/sedimentation, aggregation, coalescence and Ostwald ripening, as well as due to various chemical and biological actions (Leal-Calderon *et al.*, 2007; Sarkar *et al.*, 2016b). Apart from creaming and sedimentation, all these other instability mechanisms can be accelerated by shearing and mixing occurring during emulsion transportation and processing.

Food emulsions are often complex systems containing many different surface active ingredients and stabilizers – lipids, proteins, polysaccharides, particles, etc. (McClements, 2015). Pickering emulsions, stabilized by solid particles that strongly adsorb at the interface between two fluid phases, were

largely ignored even after their re-discovery by Pickering in 1907 (Chevalier *et al.*, 2013). However, in the past decades there has been renewed interests in Pickering stabilization, partly because of the increasingly novel and wide ranging types of particles available. As far as applications in foods is concerned, a continuing challenge is to find effective Pickering particles that are acceptable for use in the food industry (Berton-Carabin *et al.*, 2015; Dickinson, 2012, 2013; Morris, 2011)·(Anvari *et al.*, 2017; Sarkar *et al.*, 2018). In particular, there are relatively limited number of biocompatible particles that have been used so far in literature to stabilize W/O emulsions (Ghosh *et al.*, 2011; Rousseau, 2013; Rutkevičius *et al.*, 2018; Toro-Vazquez *et al.*, 2013; Zembyla *et al.*, 2019b; Zembyla *et al.*, 2018). Although Pickering emulsions are extraordinarily stable to coalescence and Ostwald ripening, their process stability have attracted rare attention in literature to date, which is part of what this work aimed to investigate particularly in W/O emulsions.

In our previous work, we demonstrated the ability of water-insoluble polyphenol crystals, such as curcumin and quercetin, to stabilize water droplets via the Pickering mechanism (Zembyla *et al.*, 2018). Micro-structural evaluation at various length scales revealed that quercetin crystals had a more rod-like shape and curcumin crystals were smaller having a more polyhedral shape (Zembyla *et al.*, 2018). It was observed that both polyphenol crystals were able to adsorb at the W-O interface and provide stabilization of water droplets for several days. However, formation of a hybrid polyphenol-biopolymer complex at the W-O interface revealed a pronounced improvement in the kinetic stability of the emulsions (Zembyla *et al.*, 2019b). This complex formation occurred between the Pickering polyphenol particles adsorbing from the oil side and whey protein isolate (WPI) biopolymer co-adsorbing from the aqueous side of the interface, which strengthened the mechanical properties of the adsorbed composite film (Zembyla *et al.*, 2019b). Furthermore, by changing the physical nature of the protein – forming it into WPI-based microgel (WPM) particles that are formed by controlled shearing of heat set whey protein gels, the stability of W/O emulsions was further improved and higher stable water volume fraction was possible (up to 20 wt%) (Zembyla *et al.*, 2019a). In this case, the water droplets were stabilized by a

sort of 'double Pickering mechanism', where one type of particle (polyphenol crystals) adsorbed from the oil side and another (WPM particles) co-adsorbed from the aqueous side. Nevertheless, this double Pickering stabilization was strongly dependent on the concentration of WPM particles. At low WPM particle concentration, both polyphenol crystals and WPM particles were present at the interface and synergistically improved the W/O emulsion stability (Zembyla *et al.*, 2019a). At higher WPM particle concentration, droplet flocculation was observed where the WPM particle appeared to bridge between the water droplets and polyphenol crystals. The formation of this mixed particle network in the oil phase seemingly enhanced the resilience of the emulsions to coalescence even further. Evidence was also presented that the principal origin of the complex formation (for both WPI and WPM particles) was electrostatic attraction between the oppositely charged polyphenol particles and protein, although hydrogen bonding between the two components may have also contributed to the stability (Zembyla *et al.*, 2019a; Zembyla *et al.*, 2019b). However, in none of the afore-mentioned studies, emulsions were tested for their process stability to shear, which is best done using a combination of controlled rheological tests combined with particle sizing and confocal laser scanning microscopy (CLSM).

As well as rheological stability being used as a measure of colloidal stability (Gallegos *et al.*, 2004), rheological control is, of course, vital in the manufacture of foods, *e.g.*, design of material handling systems plus maintenance of quality control and the desired sensory aspects of products (Krop *et al.*, 2019; Rao, 2010). In general, emulsion viscoelasticity depends on droplet size distribution, rheology of the continuous phase and inter-particle interactions, all of which are strongly influenced by processing conditions, such as energy input during emulsification, residence time, application of thermal treatments, mixing efficiency, etc. (Gallegos *et al.*, 2004; McClements, 2015). In order to test the likely process stability of the Pickering emulsions created using polyphenol crystals alone and/or in combination with WPI and WPM particles as stabilizers, the apparent viscosity (η), water droplet size and microstructural changes were measured as a function of water volume fractions, plus cycles of shear rate and temperature. To our knowledge, this

is the first study that has systematically characterized the process stability of W/O Pickering emulsions stabilized by complex interfaces.

6.2. Materials and methods

6.2.1. Materials

Curcumin (orange-yellow powder) from turmeric rhizome (96 % total curcuminoid content) was obtained from Alfa Aesar (UK). Quercetin (≥ 95 %) in the form of a yellow crystalline solid was purchased from Cayman Chemicals (USA). Both polyphenol crystals were used without further purification. Soybean oil (KTC Edibles, UK) was purchased from a local store. Whey protein isolate (WPI) containing 96.5 % protein was obtained from Fonterra (New Zealand). Water, purified by treatment with a Milli-Q apparatus (Millipore, Bedford, UK), with a resistivity not less than $18 \text{ M}\Omega \text{ cm}^{-1}$, was used for the preparation of the emulsions. A few drops of hydrochloric acid (0.1 M HCl) or sodium hydroxide (0.1 M NaOH) were used to adjust the pH of the emulsions. Sodium azide was purchased from Sigma-Aldrich (USA).

6.2.2. Preparation of oil dispersion of curcumin or quercetin crystals

Curcumin or quercetin dispersions were prepared by dispersing these polyphenol crystals in the continuous phase (soybean oil) using an Ultra-Turrax T25 mixer (Janke & Kunkel, IKA-Labortechnik) with a 13 mm mixer head (S25N-10 G) operating at 9,400 rpm for 5 min.

6.2.3. Preparation of aqueous dispersion of whey protein isolate (WPI)

The WPI (4 wt%) was dissolved in aqueous phase for at least 2 h at room temperature to ensure complete hydration. The WPI solution was then diluted to the desired WPI concentration and 0.02 wt% sodium azide was added as a preservative. The pH of the aqueous phase was adjusted to 3.0, by adding few drops of 0.1 M HCl or NaOH.

6.2.4. Preparation of aqueous dispersion of whey protein microgel (WPM) particles

An aqueous dispersion of WPM particles was prepared based on a slight modification of the methods previously described (Araiza-Calahorra *et al.*, 2019); Murray *et al.* (2016); (Sarkar *et al.*, 2017). Whey protein solution (10 wt%) was prepared by dissolving WPI powder in 20 mM phosphate buffer solution at pH 7.0 for 2 h. The WPI solution was then heated at 90 °C for 30 min and cooled at room temperature for 30 min followed by storage at 4 °C overnight to form whey protein hydrogels. The gels were mixed with 20 mM phosphate buffer solution (1:1 w/w) at pH 7.0 and were pre-homogenized using a blender (HB711M, Kenwood, UK) for 3 min before homogenization using two passes through the Leeds Jet homogenizer (University of Leeds, UK) operating at a pressure of 300 ± 20 bar. Sodium azide (0.02 wt%) was added to the final 5 wt% WPM particles stock solution.

6.2.5. Preparation of W/O emulsions

W/O emulsions were prepared at room temperature (21 to 26 °C) based on the procedure described in our previous work (Zembyla *et al.*, 2019a; Zembyla *et al.*, 2019b; Zembyla *et al.*, 2018). Curcumin or quercetin dispersions were prepared by dispersing the polyphenol crystals (0.14 wt%) in the continuous phase (soybean oil) using an Ultra-Turrax T25 mixer (Janke & Kunkel, IKA-Labortechnik) with a 13 mm mixer head (S25N- 10G) operating at 9,400 rpm for 5 min. The aqueous phase was prepared with Milli-Q water, WPI (2.0 wt%) or WPM particles (0.1 - 2.0 wt%). Coarse W/O emulsions were prepared by homogenizing 10 or 20 wt% of this aqueous phase with soybean oil in an Ultra-Turrax mixer for 2 min at 13,400 rpm. Fine emulsions were prepared by passing the coarse emulsions through the Leeds Jet homogenizer, twice, operated at 300 bar. Immediately after preparation, emulsions were sealed in 25 mL cylindrical tubes (internal diameter = 17 mm) and stored at room temperature in a dark place.

6.2.6. Rheology

A modular compact rheometer, MCR-302 (Anton Paar, Austria) was used to measure the viscosity of soybean oil, curcumin and quercetin dispersions, WPI and WPM particles aqueous dispersions and emulsions at different temperatures (25, 35 and 50 °C). Cone-and-plate geometry (CP50-2, diameter: 50 mm cone angle: 2°) was used for all measurements. The rheometer was initialized with 0.2 mm gap between the cone and plate. The shear rate was set in the range of 10^{-1} to 10^2 s^{-1} . For each measurement, a small amount of sample was pipetted onto the top of the plate, excluding any air bubbles. Samples were left in the rheometer for approximately 2 min to achieve a steady state. The viscosity was measured at shear rates of 10^{-1} to 10^2 s^{-1} for 15 min, where subsequently the shear rate was kept constant at 10^2 s^{-1} for 30 min. Then, the shear rate returned back to 10^{-1} s^{-1} (within 15 min) to check for any hysteresis. Although the normal force was nominally set to zero, during measurements it typically fluctuated between 0.3 and 0.5 N. Viscosity at each concentration was measured three times on separate samples.

6.2.7. Particle size measurements

The particle size distributions (PSD) of emulsions were measured using static light scattering via a Mastersizer Hydro SM small volume wet sample dispersion unit (Malvern Instruments, UK). The size was measured before and after shearing in the rheometer at different temperatures. Average droplet size was monitored via the Sauter mean diameter, d_{32} , or volume mean diameter, d_{43} , defined by:

$$d_{ab} = \frac{\sum n_i d_i^a}{\sum n_i d_i^b} \quad (6.1)$$

where n_i is the number of the droplets of diameter d_i .

For water droplet size measurements, refractive indices of 1.33 and 1.47 were used, for water and soybean oil, respectively. Absorption coefficients of 0.01, 0.1 and 0.01 for curcumin, quercetin and water, were

used, respectively. All measurements were made at room temperature on at least three different samples.

6.2.8. Confocal laser scanning microscopy (CLSM)

The microstructure of the W/O emulsions was observed using a confocal microscope (Zeiss LSM700 inverted, Germany). The emulsions were prepared as discussed above. Approximately, 80 μL of sample were placed into a laboratory-made well slide and a cover slip (0.17 mm thickness) was placed on top, ensuring that there was no air gap (or bubbles) trapped between the sample and coverslip. The samples were scanned at room temperature (25 ± 1 °C) using a 20 \times /0.5 objective lens. Auto-fluorescence from the crystals was excited using 488 and 405 nm wavelength lasers for curcumin and quercetin crystals, respectively. Rhodamine B was used as a dye for whey protein and was excited using a 545 nm wavelength laser. The emitted fluorescent light was detected at wavelengths of 525, 460 and 580 nm for curcumin, quercetin and Rhodamine B, respectively.

6.2.9. Statistical analysis

Significant differences between samples were determined by one-way ANOVA and multiple comparison test with Tukey's adjustment performed using SPSS software (IBM, SPSS statistics) and the level of confidence was 95 %.

6.3. Results and discussion

6.3.1. Control experiments

Before measuring the viscosity of the emulsions, it was necessary to check the effect of the particles on the viscosity of the dispersed and continuous phases alone.

6.3.1.1. Viscosity of curcumin and quercetin dispersions in soybean oil

The viscosity (η) of curcumin and quercetin dispersions (0.14 wt%) in soybean oil was measured at a range of shear rates ($\dot{\gamma} = 10^{-1} - 10^2$ s $^{-1}$) at

different temperatures (25, 35 and 50 °C) as shown in Figure 6.1. The η of soybean oil alone (*i.e.*, without added polyphenol crystals) was also measured as a control. All the samples showed Newtonian behaviour at all temperatures, *i.e.*, the viscosity remained stable as the shear rate increased. The η results for soybean oil, curcumin and quercetin dispersions were indistinguishable at 25 °C indicating that the concentration of particles (0.14 wt%) added to the oil did not cause any significant change in the η of the oil. As the temperature increased from 25 to 50 °C, the viscosity of all the samples decreased slightly, but remained Newtonian as expected for most oils (Diamante *et al.*, 2014; Esteban *et al.*, 2012; Fasina *et al.*, 2008), showing again that the η values of curcumin and quercetin dispersion were very similar to the control (soybean oil alone).

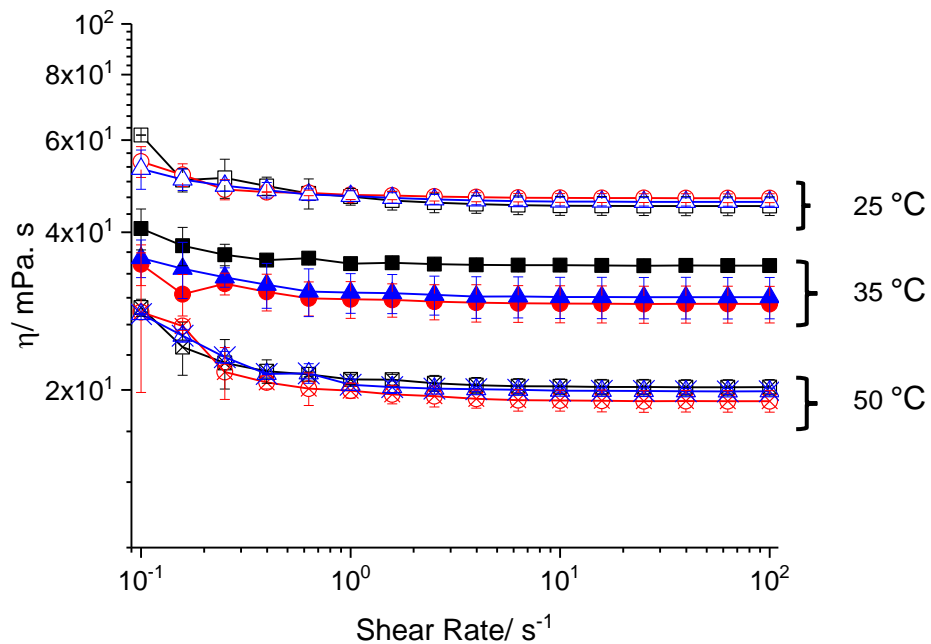


Figure 6.1. Viscosity (η) against shear rate ($\dot{\gamma}$) curves of soybean oil (control, ■), 0.14 wt% curcumin (●) and 0.14 wt% quercetin (▲) dispersions in soybean oil at different temperatures 25 (open symbols), 35 (closed symbols) and 50 °C (crossed symbols).

6.3.1.2. Viscosity of 2.0 wt% WPI or WPM particle dispersions in aqueous phase at pH 3.0

The η of 2.0 wt% WPI or WPM particles in aqueous phase (pH 3.0) at different shear rates and temperatures (25, 35 and 50 °C) are shown in Figure 6.2. The

solutions/dispersions were sheared from 10^{-1} to 10^2 s^{-1} and then kept at this high shear rate for 30 min to check their stability (as described in the Methods section). The solution of 2.0 wt% WPI did not show strong shear-thinning behaviour, indicating biopolymer entanglements were not formed, as expected for globular proteins at this concentration. In addition, the change in the temperature from 25 to 50 °C did not significantly affect the viscosity of the WPI solutions at low shear rates (< 1 s^{-1}) where the flow curves were indistinguishable. At higher shear rates (> 1 s^{-1}) η decreased slightly with the increase of the temperature. No hysteresis was observed in the WPI solutions at 25 °C but a hysteresis loop was identified at higher temperatures (35 and 50 °C), where the η values, as $\dot{\gamma}$ was decreasing (Figure 6.2 (a), open symbols), were slightly lower at low shear rates (< 1 s^{-1}) than those when $\dot{\gamma}$ was ramped up (Figure 6.2 (a), closed symbols). This was probably due to the start of unfolding of WPI molecules at higher temperatures (Murray *et al.*, 1996; Zembyla *et al.*, 2019b).

Protein microgels are soft colloidal particles that exhibit complex surface (Murray, 2019) and bulk rheological behaviour (Sarkar *et al.*, 2017; Zembyla *et al.*, 2019a) since they do not have a true surface in the usual sense, but consist of particles of a gel network. Thus, their surface is expected to be porous and “fuzzy”, while the particles may be deformable or even be able to interpenetrate to some extent (Sarkar *et al.*, 2017). The interaction between microgel particles in the bulk and at the interface – the electrostatic repulsion between them, their interpenetration and/or deformation – are factors that are still not fully understood (Murray, 2019; Plamper *et al.*, 2017). It has been suggested that at interfaces both bulk phases interpenetrate such particles (Gumerov *et al.*, 2016), illustrating that it is misleading to conceive of microgels as having a fixed and finite contact angle like true Pickering particles (Destribats *et al.*, 2011; Murray, 2019). Nevertheless, such particles can act as excellent stabilizers of emulsions and foams.

WPM particles (2 wt%) at all temperatures showed strong shear-thinning behaviour, typical of microgel dispersions. This is due to inter-particle entanglements and other interactions that occur at relatively low particle

volume fraction but that are disrupted by shear (Lazidis *et al.*, 2016; Sarkar *et al.*, 2017). For example, η of the WPM particle dispersions (at 25 °C) was three orders of magnitude higher than that of WPI (at 25 °C) even though the overall protein concentration in these samples was 10× lower (*i.e.*, 0.2 wt% whey protein isolate), taking into account the water content of the microgel particles themselves. In previous work Murray *et al.* (2016) identified a strong dependence of WPM particle dispersion rheology on pH, attributed to changes in the protein charge and thence WPM particle aggregation. WPM particles display polyampholyte character in line with their constituent proteins, with an isoelectric point (pI) at pH 4.7, where their overall charge is zero (Destribats *et al.*, 2014). Below and above this pH value, WPM particles are positively and negatively charged, respectively (Araiza-Calahorra *et al.*, 2019; Sarkar *et al.*, 2016a; Zembyla *et al.*, 2019b). Such particles are generally stable against aggregation when the ζ -potential exceeds the absolute value of 20 mV (Schmitt *et al.*, 2010). Electrostatic repulsion plays an important role in determining the rheology of concentrated dispersions in general (Lizarraga *et al.*, 2008). At low shear rates, particles are not able to approach closely because of the electrostatic repulsion and their effective volume fraction is greater. At high shear rates the stresses are large enough to overcome the electrostatic repulsion between the particles and force them closer together, exhibited as a shear-thinning effect (Lizarraga *et al.*, 2008). However, charge effects are magnified with ampholytic microgel particles, due to the expansion and contraction of their diffuse surface polymer layers as they become more charged or uncharged, respectively.

The effect of temperature on η of the WPM particle dispersions was also more pronounced than on that of the WPI solutions. The initial η of the WPM particle dispersions (at $\dot{\gamma} = 10^{-1} \text{ s}^{-1}$, 25 °C) was higher ($\eta \sim 10^4 - 10^5 \text{ mPa}\cdot\text{s}$) than that at 35 or 50 °C ($\eta \sim 10^4 \text{ mPa}\cdot\text{s}$) and remained higher at all the shear rates applied ($10^{-1} - 10^2 \text{ s}^{-1}$). The η values decreased with increasing temperature, suggesting either shrinkage of the microgel particles and/or a reduction in entanglements between them (Sarkar *et al.*, 2017). The viscosity curves of the WPM particle dispersions at 35 and 50 °C were very similar at all the shear rates. All the WPM particle dispersions at any

temperature showed hysteresis, where the η values on decreasing $\dot{\gamma}$ (Figure 6.2 (b), open symbols) were much lower than those when $\dot{\gamma}$ increased (Figure 6.2 (b), closed symbols).

Finally, it should be emphasized that the much higher η values of the 2 wt% WPM particle dispersions compared to the 2 wt% WPI solutions persisted after application of $\dot{\gamma} = 100 \text{ s}^{-1}$, even though the WPM particles were highly shear-thinning. Thus the WPM particles may have aggregated or interpenetrated as a function of shear rate to some extent, but they were certainly not completely destroyed by subjecting them to these conditions, so such interactions must be reversible, *i.e.*, the WPM particles are resilient under these conditions of shear.

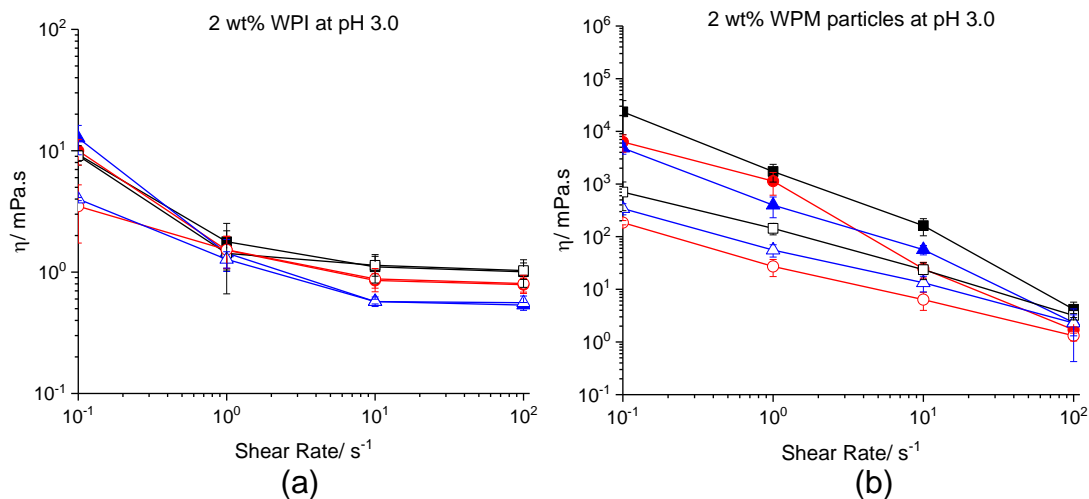


Figure 6.2. Viscosity (η) against shear rate ($\dot{\gamma}$) curves of 2.0 wt% WPI (a) and 2.0 wt% WPM particles (b) at different temperatures; 25 °C (■, □), 35 °C (●, ○) and 50 °C (▲, △). All the aqueous dispersions have been prepared at pH 3.0. Viscosity values are shown for ramping up (closed symbols) at shear rates from 0.1 - 100 s^{-1} and ramping down (open symbols) at shear rates from 10² – 10⁻¹ s^{-1} .

6.3.2. Stability of 10 wt% W/O emulsions stabilized by curcumin or quercetin crystals with or without 2 wt% WPI or WPM particles

Figure 6.3 shows η against $\dot{\gamma}$ for emulsions stabilized by 0.14 wt% curcumin or quercetin crystals dispersed in the oil phase + water (*i.e.*, 0 wt%

protein) or 2.0 wt% WPI or WPM particles at different temperatures; 25, 35 and 50 °C. The emulsions were prepared at pH 3.0 due to the formation of stronger interfacial complexes between the oppositely charged polyphenol crystals present in the oil phase and WPI or WPM particles in the aqueous phase, as shown earlier (Zembyla *et al.*, 2018). All the systems showed shear-thinning behaviour; they had a higher η at low shear rates which decreased dramatically as the shear rate increased. The trends for the emulsions stabilized by either curcumin or quercetin were very similar, with the latter having slightly higher η values, possibly due to the rod-like shape and larger mean size ($d_{32} \sim 5.9 \mu\text{m}$) (Zembyla *et al.*, 2018) of quercetin crystals than curcumin (polyhedral shape, $d_{32} \sim 0.2 \mu\text{m}$) (Zembyla *et al.*, 2018), at all temperatures. For both curcumin and quercetin systems at all temperatures, the initial η (at 10^{-1} s^{-1}) decreased in the order WPM particles > WPI > water. The η of the emulsions with or without WPI decreased slightly (from 10^4 to 10^3 mPa·s) as the shear rate increased from 10^{-1} to 10^2 s^{-1} at 25 °C (Figure 6.3 (a_i) and (b_i)) reaching a final η value of $\sim 10^2$ mPa·s at $\dot{\gamma} = 10^2 \text{ s}^{-1}$. This was 1 - 2 orders of magnitudes higher than the η of the polyphenol dispersions in oil ($\sim 5 \times 10^1$ mPa·s, Figure 6.1) or the 2.0 wt% WPI solutions (1 mPa·s, Figure 6.2 (a)) at this shear rate, respectively. As the temperature increased from 25 to 50 °C (Figure 6.3 (a_{ii} – a_{iii}) and (b_{ii} – b_{iii})) the initial η at $\dot{\gamma} = 10^{-1} \text{ s}^{-1}$ without WPI (or WPM particles) decreased significantly, especially for the quercetin-stabilized system (one order of magnitude lower at 50 °C compared to at 25 °C). This decrease was possibly due to the re-arrangement of the polyphenol crystals at the interface. In the presence of WPI a slight decrease in the initial η was observed, suggesting disruption of flocculated particles, again mainly for the quercetin-stabilized system. The final η value at $\dot{\gamma} = 10^2 \text{ s}^{-1}$ decreased slightly for all the systems as the temperature increased from 25 to 50 °C. However, the WPM particle systems showed a very high initial η ($\sim 10^5$ mPa·s at 10^2 s^{-1}) compared to the systems with or without WPI (10^3 - 10^4 mPa·s). These higher η values were presumably due to flocculation of WPM particles in the continuous oil phase as already first noted in our previous work (Zembyla *et al.*, 2019a). The WPM particles seemed to form aggregates with polyphenol crystals in the bulk oil phase, at the interface and also between the

water droplets, acting as a sort of 'colloidal glue' for the whole system, immobilizing the water droplets and helping to inhibit coalescence under quiescent conditions (Zembyla *et al.*, 2019a). Therefore, as expected for flocculated systems, shear-thinning behaviour was very pronounced, as explained above (Buján-Núñez *et al.*, 1994; McClements, 2015; Tadros, 2004). No significant effect of temperature increase from 25 to 50 °C was observed on the emulsions containing WPM particles.

Hysteresis was observed in all the above emulsions, but was more pronounced in those containing WPM particles, again probably due to more flocculated nature of the latter systems. Interestingly, η at $\dot{\gamma} = 10^{-1} \text{ s}^{-1}$ of the WPM particle systems at 25 °C ($10^3 - 10^4 \text{ mPa}\cdot\text{s}$) returned to values close to the initial values observed in the systems without (or with) WPI at the same initial shear rate. This suggests that flocculating effects of the WPM particles were broken by the application of the shear cycle. Hysteresis was less pronounced in the emulsions with or without WPI, presumably because these were less flocculated in the first place compared to the WPM particle systems. As the temperature increased (from 35 to 50 °C, Figure 6.3 (a_{ii} – a_{iii}) and (b_{ii} – b_{iii})), η decreased slightly, probably mainly due to the decrease of η of the continuous phase as observed in Figure 6.1. At 50 °C, both curcumin- and quercetin-stabilized systems with or without WPI reached η values close to $10^2 \text{ mPa}\cdot\text{s}$ at all shear rates (10^2 to 10^{-1} s^{-1}), indicating convergence to the same sort of state of droplet and/or protein aggregation.

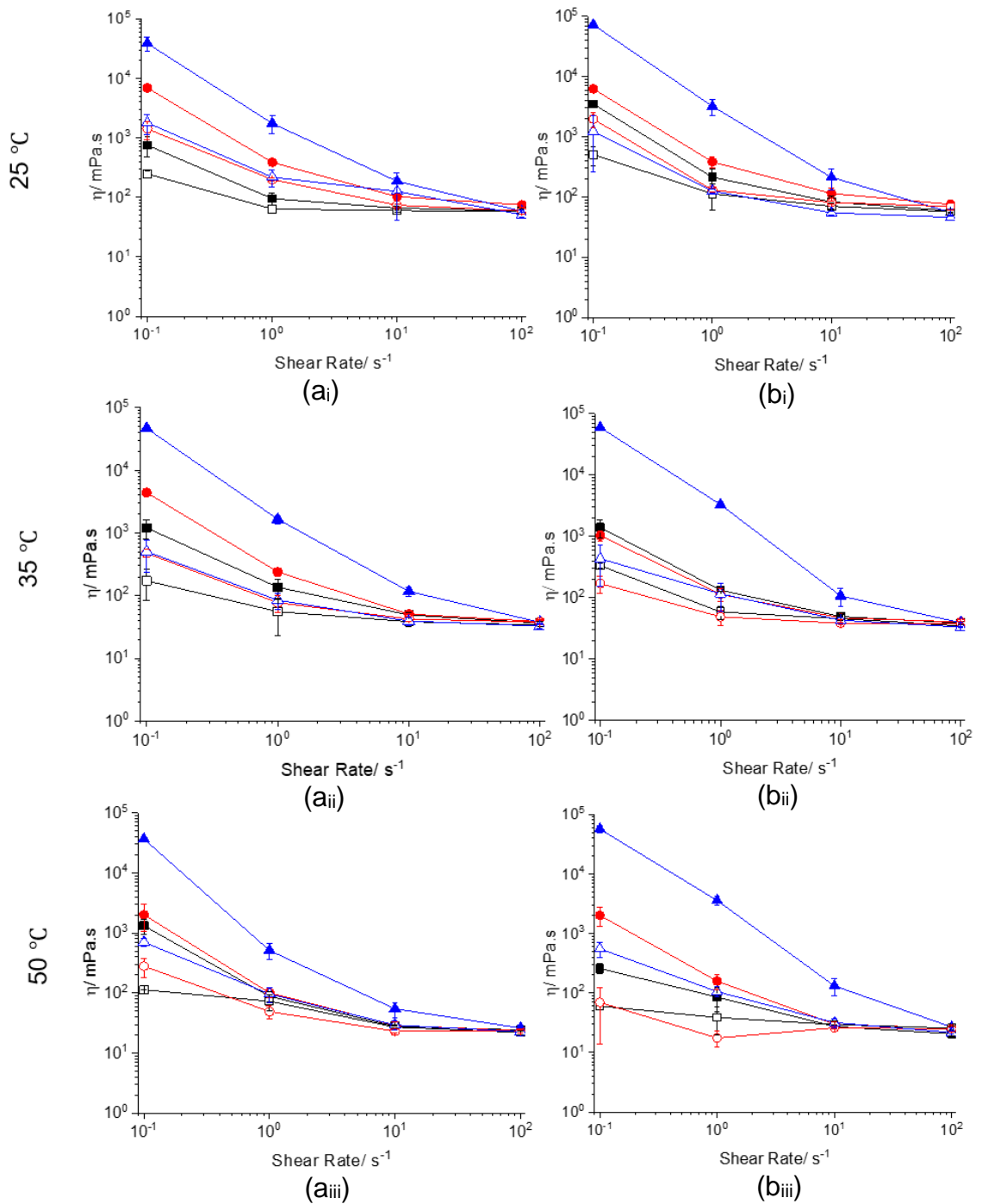


Figure 6.3. Viscosity (η) against shear rate ($\dot{\gamma}$) curves of 10 wt% W/O emulsions stabilized by 0.14 wt% curcumin (a) or quercetin (b) crystals dispersed in oil + water (\blacksquare , \square) or 2.0 wt% WPI (\bullet , \circ) or 2.0 wt% WPM particles (\blacktriangle , \triangle) as an aqueous phase (pH 3.0) at different temperatures 25 (i), 35 (ii) and 50 (iii) °C. Viscosity values are shown for ramping up (closed symbols) at shear rates from 0.1 - 100 s^{-1} and ramping down (open symbols) at shear rates from $10^2 - 10^{-1}$ s^{-1} .

Figure 6.4 shows the CLSM images of the same fresh 10 wt% W/O Pickering emulsions stabilized by curcumin or quercetin crystals (0.14 wt%) with or without 2.0 wt% WPI or WPM particles. Figures 6.4 (a_i) and (b_i) show that the water droplets were surrounded by a dense layer of curcumin or quercetin crystals, respectively, confirming the preferential location of the polyphenol crystals at the W-O interface. The green brightness in the images was due to the auto-fluorescence of the polyphenol particles. Furthermore, some droplets appeared to be not completely spherical, which is another good indication of Pickering stabilization (Dickinson, 2010). Images of the emulsions including 2.0 wt% WPI plus curcumin or quercetin crystals are shown in Figures 6.4 (a_{ii}) and (b_{ii}), respectively, demonstrating that again the water droplets were surrounded by a dense layer of polyphenol particles (green). Rhodamine B (red) was used to visualize the location of protein and so the intensity of the red colour indicates a higher concentration of WPI on the inside of the water droplets, as expected. Thus, both polyphenol crystals and WPI appeared to be in close proximity at the interface. Images of fresh emulsions including 2.0 wt% WPM particles plus curcumin or quercetin crystals are shown in Figure 6.4 (a_{iii}) and (b_{iii}), respectively. As already discussed above, it is seen that in both these systems there was an increased tendency for the whole system to aggregate in the oil phase. WPM particles seemed to be aggregated at the interface of the individual droplets and between interfaces of adjacent droplets, *i.e.*, causing flocculation of the water droplets. The polyphenol crystals seemed to be mixed in with these aggregates. In other words, there was increased tendency for microgels and polyphenol crystals to become shared between droplets (Zembyla *et al.*, 2019a).

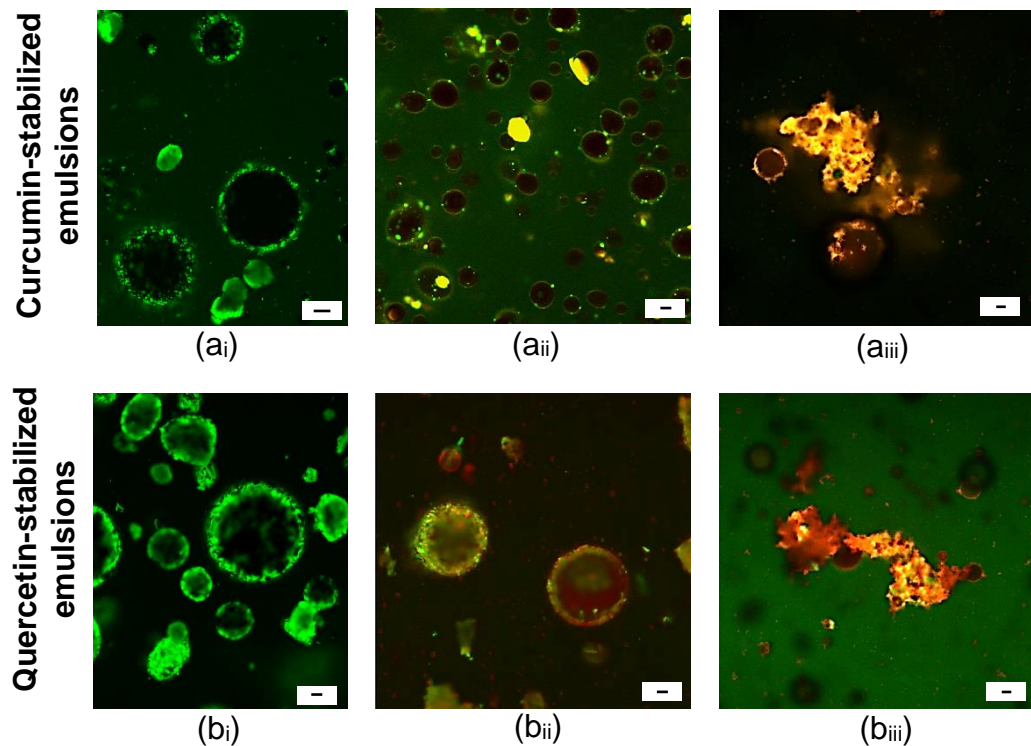


Figure 6.4. Confocal images of 10 wt% W/O Pickering emulsions stabilized by 0.14 wt% curcumin (a) and quercetin (b) crystals in the oil phase + water (i), 2.0 wt% WPI (ii) or 2.0 wt% WPM particles (iii) in the aqueous phase at pH 3.0 for fresh samples. The green brightness in the images is caused by the auto-fluorescence of curcumin (488 nm excitation) or quercetin (405 nm excitation) crystals. The red brightness is due to the WPM particles stained by Rhodamine B (568 nm excitation). The scale bar represents 20 μm .

The PSDs of the systems were measured before and after the shear cycle at the different temperatures. Tables 6.1 and 6.2, show the d_{32} and d_{43} results for the curcumin- and quercetin-stabilized systems, respectively. It was seen that the size of the water droplets before shearing at 25 °C increased in the order of water < WPI < WPM particles, possibly indicating the presence of a thicker adsorbed particle-protein or particle-particle layer at the interface in the case of WPI and WPM particles, respectively. However, it should be remembered that the light scattering technique used cannot distinguish between water droplets, polyphenol crystals, WPM particles or their aggregates as scattering centers (Atarés *et al.*, 2012). After shearing, the mean size (d_{32} and d_{43}) for both curcumin- and quercetin-stabilized emulsions without WPI or WPM particles increased significantly in size ($p < 0.05$, Table 6.1 and 6.2), at all the temperatures, showing that these systems were

unstable to shear and that coalescence occurred. In contrast, d_{32} and d_{43} for the samples containing WPI showed a small increase ($p < 0.05$, Table 6.1 and 6.2) due to shearing at 25 °C, *i.e.*, the systems were more stable. However, as the temperature increased, d_{32} and d_{43} did not change ($p > 0.05$, Table 6.1 and 6.2). Furthermore, the samples containing WPM particles showed an approximate halving of the d_{43} values after shearing ($p < 0.05$, Table 6.1 and 6.2) at all temperatures, again indicating a flocculated system disrupted by shear, whilst d_{32} remained the same ($p > 0.05$, Table 6.1 and 6.2) before and after the shearing, suggesting that no coalescence was occurred.

From the above results, it can be concluded that the curcumin- and quercetin-stabilized emulsions containing WPI or WPM particles were more stable to shear and elevated temperatures than without these two forms of protein. Thus, interfacial complex formation between the oppositely charged polyphenol crystals in the oil phase + biopolymer or biopolymer microgel particles in the aqueous phase, not only improves the storage stability under quiescent conditions (as discussed in our previous work (Zembyla *et al.*, 2019a; Zembyla *et al.*, 2019b)) but also enhances stability to shear and temperature.

Table 6.1. d_{32} and d_{43} values (μm) before and after shearing of 10 wt% W/O emulsions stabilized by 0.14 wt% curcumin crystals & water, 2.0 wt% WPI or 2.0 wt% WPM particles as an aqueous phase (pH 3.0) at different temperatures; 25, 35 and 50 °C. Samples with the same letter differ significantly ($p < 0.05$) according to Tukey's test for each component in the aqueous phase before and after shearing.

Aqueous phase	Before Shearing		After Shearing					
	25 °C		25 °C		35 °C		50 °C	
	d_{32}	d_{43}	d_{32}	d_{43}	d_{32}	d_{43}	d_{32}	d_{43}
Water	$7.4 \pm 1.6^{a,b,c}$	$23.8 \pm 1.2^{d,e,f}$	21.5 ± 2.8^a	59.5 ± 3.2^d	24.2 ± 0.8^b	59.6 ± 3.1^e	27.2 ± 2.3^c	60.3 ± 5.7^f
WPI	18.5 ± 1.1^g	$51.5 \pm 0.9^{h,i}$	16.2 ± 0.9^g	47.7 ± 4.6^h	19.0 ± 1.2	42.4 ± 1.7^i	19.2 ± 1.8	50.4 ± 9.0
WPM particles	20.8 ± 0.5	$110.0 \pm 8.5^{j,k,l}$	18.0 ± 5.7	49.6 ± 6.1^j	18.0 ± 4.8	44.6 ± 10.0^k	20.6 ± 3.6	49.3 ± 2.4^l

Table 6.2. d_{32} and d_{43} values (μm) before and after shearing of 10 wt% W/O emulsions stabilized by 0.14 wt% quercetin crystals & water, 2.0 wt% WPI or 2.0 wt% WPM particles as an aqueous phase (pH 3.0) at different temperatures; 25, 35 and 50 °C. Samples with the same letter differ significantly ($p < 0.05$) according to Tukey's test for each component in the aqueous phase before and after shearing.

Aqueous phase	Before Shearing		After Shearing					
	25 °C		25 °C		35 °C		50 °C	
	d_{32}	d_{43}	d_{32}	d_{43}	d_{32}	d_{43}	d_{32}	d_{43}
Water	$11.7 \pm 2.7^{a,b,c}$	$41.0 \pm 5.4^{d,e,f}$	18.9 ± 0.6^a	60.1 ± 1.4^d	23.6 ± 1.3^b	73.1 ± 5.4^e	32.7 ± 13.4^c	66.2 ± 6.9^f
WPI	$11.4 \pm 2.0^{g,h,i}$	$42.1 \pm 5.7^{k,l}$	14.1 ± 0.1^g	42.9 ± 0.4	18.2 ± 0.6^h	49.3 ± 1.4^k	18.6 ± 3.1^i	54.3 ± 13.4^l
WPM particles	18.5 ± 3.0^m	$92.7 \pm 21.6^{n,o,p}$	15.4 ± 0.8^m	49.8 ± 3.0^n	16.4 ± 1.3	51.0 ± 2.3^o	22.7 ± 5.2	42.9 ± 8.4^p

6.3.3. Stability of 10 wt% W/O emulsions stabilized by curcumin or quercetin crystals + wt% different concentrations of WPM particles

The curcumin and quercetin systems containing WPM particles were chosen for further testing since these had the highest viscosity values at high shear rates and different temperatures and no coalescence was observed. Emulsions stabilized by 0.14 wt% curcumin or quercetin crystals + different WPM particle concentrations (0.1, 0.5, 1.0 and 2.0 wt%) in the aqueous phase were tested. Figure 6.5 shows the results of η against WPM particle concentration at $\dot{\gamma} = 0.1 \text{ s}^{-1}$. It is seen that η of the emulsions stabilized by curcumin crystals were slightly lower than those stabilized by quercetin, possibly due to the smaller size of curcumin crystals compared to quercetin (Zembyla *et al.*, 2018). In addition, η increased as the concentration of WPM particles increased for both curcumin and quercetin emulsions confirming the tendency for the whole system to become more aggregated as more WPM particles were added.

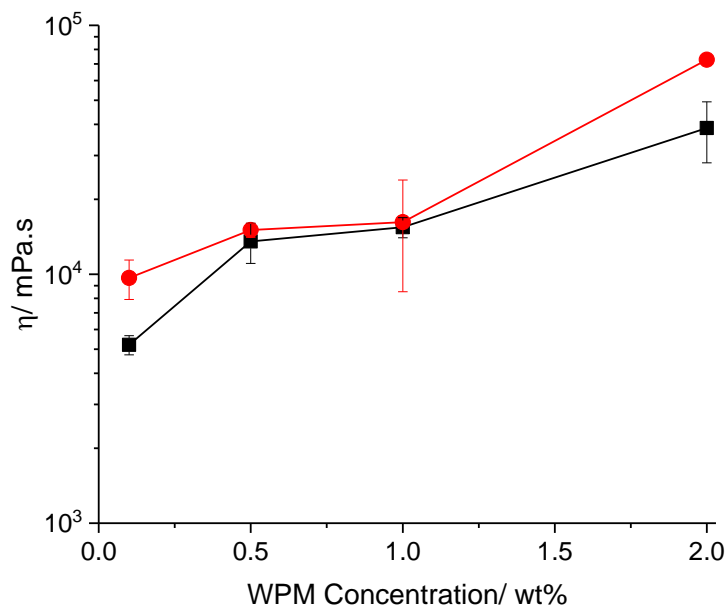


Figure 6.5. Viscosity (η) against WPM particle concentration at 0.1 s^{-1} shear rate of 10 wt% W/O emulsions stabilized by 0.14 wt% curcumin (■) or quercetin (●) crystals dispersed in oil & WPM particles as an aqueous phase (pH 3.0) at different concentrations; 0.1, 0.5, 1.0 and 2.0 wt%. The temperature was kept constant at $25 \text{ }^\circ\text{C}$.

Tables 6.3 and 6.4 show the d_{32} and d_{43} values of the W/O emulsions stabilized by curcumin or quercetin crystals, respectively with different concentrations of WPM particles added in the dispersed phase, before and after shearing at 25 °C. All the emulsions had very similar d_{32} values ($p > 0.05$, Table 6.3 and 6.4) before shearing but the d_{43} values increased ($p < 0.05$, Table 6.3 and 6.4) as the concentration of WPM particles increased, again suggesting increased flocculation of the system as WPM particles were added. After shearing, both curcumin- and quercetin-stabilized emulsions + 0.1 wt% WPM particles showed a significant increase in both d_{32} and d_{43} values ($p < 0.05$, statistical data are not shown). This possibly showed some coalescence, but at the higher WPM particle concentrations (0.5, 1.0 and 2.0 wt%) only d_{43} decreased significantly ($p < 0.05$, statistical data are not shown), indicating greater stability with increased wt% WPM particles.

Table 6.3. d_{32} and d_{43} values (μm) before and after shearing of 10 wt% W/O emulsions stabilized by 0.14 wt% curcumin crystals & WPM particles as an aqueous phase (pH 3.0) at different concentrations; 0.1, 0.5, 1.0 and 2.0 wt%. Samples with the same letter differ significantly ($p < 0.05$) according to Tukey's test for each WPM particle concentration.

WPM particle concentration/ wt%	Before Shearing		After Shearing	
	d_{32}	d_{43}	d_{32}	d_{43}
0.1	$22.0 \pm 1.7^{a,b}$	54.3 ± 0.8^c	$41.9 \pm 5.4^{d,e,f}$	61.1 ± 15.3^g
0.5	19.2 ± 1.4^a	83.5 ± 2.6^c	23.1 ± 3.0^d	70.9 ± 8.2^e
1.0	19.2 ± 3.2^b	92.7 ± 3.9^c	19.2 ± 0.3^e	$78.6 \pm 2.3^{g,f}$
2	20.8 ± 0.5	110.0 ± 8.5^c	18.0 ± 5.7^f	$49.6 \pm 6.1^{e,f}$

Table 6.4. d_{32} and d_{43} values (μm) before and after shearing of 10 wt% W/O emulsions stabilized by 0.14 wt% quercetin crystals & WPM particles as an aqueous phase (pH 3.0) at different concentrations; 0.1, 0.5, 1.0 and 2.0 wt%. Samples with the same letter differ significantly ($p < 0.05$) according to Tukey's test for each WPM particle concentration.

WPM particle concentration/ wt%	Before Shearing		After Shearing	
	d_{32}	d_{43}	d_{32}	d_{43}
0.1	20.3 \pm 1.1 ^{a,b,c}	65.8 \pm 6.9 ^d	38.1 \pm 13.6 ^{g,h,i}	77.3 \pm 1.3 ^j
0.5	18.5 \pm 1.4 ^a	70.4 \pm 7.3 ^e	25.3 \pm 7.5 ^g	65.9 \pm 23.8 ^k
1.0	17.5 \pm 1.0 ^b	73.5 \pm 6.2 ^f	17.3 \pm 0.0 ^h	68.1 \pm 5.0 ^l
2.0	18.5 \pm 3.0 ^c	92.7 \pm 21.6 ^{d,e,f}	15.4 \pm 0.8 ⁱ	49.8 \pm 3.0 ^{j,k,l}

6.3.4. Stability of 20 wt% W/O emulsions stabilized by curcumin or quercetin crystals + 2.0 wt% WPM particles

The shear stability of emulsions containing a higher water:oil ratio (20 wt% water) was tested for systems stabilized by 0.14 wt% curcumin or quercetin crystals + 2.0 wt% WPM particles acting as Pickering stabilizers, since this WPM particle concentration appeared to impart enhanced stability for 10 wt% W/O emulsions, (Figure 6.5 and Tables 6.3 and 6.4) (Zembyla *et al.*, 2019a). Figure 6.6 shows η against $\dot{\gamma}$ at different temperatures (25, 35 and 50 °C). The emulsions were taken through the same shear cycle as described earlier. As at 10 wt% water, all the systems showed shear-thinning behaviour at all temperatures. No significant differences were identified in the initial η (at $\dot{\gamma} = 10^{-1} \text{ s}^{-1}$) at any temperature. In addition, the initial η value (at all temperatures) was in the same range ($10^4 - 10^5 \text{ mPa}\cdot\text{s}$) as that of the emulsions containing 10 wt% water (Figure 6.3). At high shear rates (10^2 s^{-1}), a slight decrease of η was observed as the temperature increased for both the curcumin- and quercetin-stabilized systems. Hysteresis was observed for all the systems, with the final η in the same range ($\sim 10^3 \text{ mPa}\cdot\text{s}$) at all

temperatures and similar to the value for the emulsions containing 10 wt% water (Figure 6.3).

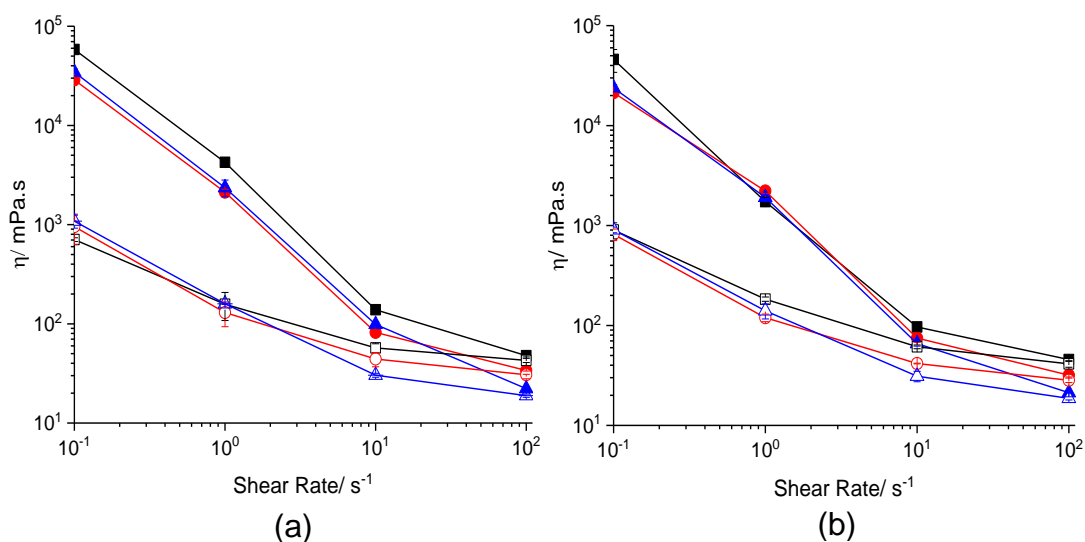


Figure 6.6. Viscosity (η) against shear rate ($\dot{\gamma}$) curves of 20 wt% W/O emulsions stabilized by curcumin (a) or quercetin (b) crystals dispersed in oil & 2.0 wt% WPM particles as an aqueous phase (pH 3.0) at different temperatures; 25 (■, □), 35 (●, ○) and 50 °C (▲, △). Viscosity values are shown for ramping up (closed symbols) at shear rates from 0.1 - 100 s⁻¹ and ramping down (open symbols) at shear rates from 10² - 10¹ s⁻¹.

Table 6.5 shows the size of the water droplets before and after shearing at different temperatures. The mean particle sizes in emulsions containing 20 wt% water were smaller in size (~ 15 μm , Table 6.5) compared to those with 10 wt% water (~ 20 μm , Tables 6.1 and 6.2). This is possibly due polyphenol crystal adsorption at the interface dominating over crystal aggregation in the bulk oil as the area of interface is increased. Also the d_{43} value was lower in the emulsions with 20 wt% (65 – 75 μm , Table 6.5) than those with 10 wt% water (108 – 110 μm , Table 6.1 and 6.2), suggesting less aggregation in the continuous oil phase due to limited amount of unabsorbed WPM particles. After shearing, both d_{32} and d_{43} decreased slightly for both crystal types at all temperatures, due to the disruption of the aggregates, reaching mean sizes similar to those containing 10 wt% water. In summary, the 20 wt% W/O systems including 2 wt% WPM particles were at least, if not more stable, than the 10 wt% water emulsions.

Table 6.5. d_{32} and d_{43} values (μm) before and after shearing of 20 wt% W/O emulsions stabilized by 0.14 wt% curcumin or quercetin crystals & 2.0 wt% WPM particles as an aqueous phase (pH 3.0) at different temperatures; 25, 35 and 50 °C. Samples with the same letter differ significantly ($p < 0.05$) according to Tukey's test for each polyphenol crystal before and after shearing.

Particle Type	Before Shearing		After Shearing					
	25 °C		25 °C		35 °C		50 °C	
	d_{32}	d_{43}	d_{32}	d_{43}	d_{32}	d_{43}	d_{32}	d_{43}
Curcumin	16.0 ± 1.0	$77.7 \pm 11.7^{\text{a,b,c}}$	12.9 ± 2.9	$50.5 \pm 7.9^{\text{a}}$	15.5 ± 1.6	$54.6 \pm 1.6^{\text{b}}$	13.6 ± 0.3	$54.9 \pm 0.4^{\text{c}}$
Quercetin	$14.2 \pm 0.3^{\text{d}}$	$65.9 \pm 6.9^{\text{e,f,g}}$	$12.3 \pm 1.4^{\text{d}}$	$52.4 \pm 6.8^{\text{e}}$	13.5 ± 2.4	$54.1 \pm 6.5^{\text{f}}$	14.0 ± 1.9	$50.6 \pm 4.1^{\text{g}}$

6.4. Conclusion

In this study, the viscosity (η) and mean particle size of W/O emulsions stabilized by curcumin or quercetin crystals dispersed in the oil phase, with or without WPI or WPM particles present in the aqueous phase at pH 3.0, were measured at different shear rates and temperatures. All the emulsions were shear-thinning. The emulsions stabilized by the polyphenol crystals alone without the addition of WPI or WPM particles in the aqueous phase exhibited coalescence after shearing, with the size of the water droplets increasing significantly. More pronounced destabilization was observed at higher temperatures. The emulsions containing WPI in the dispersed phase were stable over shear and temperature without a significant increase in mean particle size. The emulsions with WPM particles showed a decrease in the d_{43} values on shearing, indicating disruption of flocculated droplets, polyphenol crystals and WPM particles in the continuous oil phase. Aggregation appeared to be enhanced by increasing WPM particle concentration, but at ≥ 0.5 wt% WPM particles no droplet coalescence occurred and the systems were significantly stable even at 20 wt% water content. In summary, co-adsorbing biopolymers or biopolymer-based microgels to polyphenol crystal stabilized W/O emulsions appear as a promising new technique to improve the process stability of water droplets and can have applications in designing new formulations in food industries.

References

- Anvari, M., & Joyner, H. S. (2017). Effect of formulation on structure-function relationships of concentrated emulsions: Rheological, tribological, and microstructural characterization. *Food hydrocolloids*, *72*, 11-26.
- Araiza-Calahorra, A., & Sarkar, A. (2019). Pickering emulsion stabilized by protein nanogel particles for delivery of curcumin: Effects of pH and ionic strength on curcumin retention. *Food Structure*, *21*, 100113.
- Atarés, L., Marshall, L. J., Akhtar, M., & Murray, B. S. (2012). Structure and oxidative stability of oil in water emulsions as affected by rutin and homogenization procedure. *Food chemistry*, *134*(3), 1418-1424.

- Berton-Carabin, C. C., & Schroën, K. (2015). Pickering emulsions for food applications: background, trends, and challenges. *Annual review of food science technology*, 6, 263-297.
- Buján-Núñez, M. C., & Dickinson, E. (1994). Brownian dynamics simulation of a multi-subunit deformable particle in simple shear flow. *Journal of the Chemical Society, Faraday Transactions*, 90(18), 2737-2742.
- Chevalier, Y., & Bolzinger, M.-A. (2013). Emulsions stabilized with solid nanoparticles: Pickering emulsions. *Colloids Surfaces A: Physicochemical Engineering Aspects*, 439, 23-34.
- Destribats, M., Lapeyre, V., Wolfs, M., Sellier, E., Leal-Calderon, F., Ravaine, V., & Schmitt, V. (2011). Soft microgels as Pickering emulsion stabilisers: role of particle deformability. *Soft Matter*, 7(17), 7689-7698.
- Destribats, M., Rouvet, M., Gehin-Delval, C., Schmitt, C., & Binks, B. P. (2014). Emulsions stabilised by whey protein microgel particles: towards food-grade Pickering emulsions. *Soft Matter*, 10(36), 6941-6954.
- Diamante, L. M., & Lan, T. (2014). Absolute viscosities of vegetable oils at different temperatures and shear rate range of 64.5 to 4835 s⁻¹. *Journal of food processing*, 2014.
- Dickinson, E. (2010). Food emulsions and foams: stabilization by particles. *Current opinion in colloid interface science*, 15(1-2), 40-49.
- Dickinson, E. (2012). Use of nanoparticles and microparticles in the formation and stabilization of food emulsions. *Trends in Food Science Technology*, 24(1), 4-12.
- Dickinson, E. (2013). Stabilising emulsion-based colloidal structures with mixed food ingredients. *Journal of the Science of Food Agriculture*, 93(4), 710-721.
- Esteban, B., Riba, J.-R., Baquero, G., Rius, A., & Puig, R. (2012). Temperature dependence of density and viscosity of vegetable oils. *Biomass bioenergy*, 42, 164-171.
- Fasina, O., & Colley, Z. (2008). Viscosity and specific heat of vegetable oils as a function of temperature: 35 C to 180 C. *International Journal of Food Properties*, 11(4), 738-746.
- Gallegos, C., Franco, J. M., & Partal, P. (2004). Rheology of food dispersions. *Rheology reviews*, 1, 19-65.
- Ghosh, S., & Rousseau, D. (2011). Fat crystals and water-in-oil emulsion stability. *Current opinion in colloid interface science*, 16(5), 421-431.
- Gumerov, R. A., Rumyantsev, A. M., Rudov, A. A., Pich, A., Richter, W., Möller, M., & Potemkin, I. I. (2016). Mixing of two immiscible liquids within the polymer microgel adsorbed at their interface. *ACS Macro Letters*, 5(5), 612-616.

- Krop, E. M., Hetherington, M. M., Holmes, M., Miquel, S., & Sarkar, A. (2019). On relating rheology and oral tribology to sensory properties in hydrogels. *Food hydrocolloids*, 88, 101-113.
- Lazidis, A., Hancocks, R., Spyropoulos, F., Kreuz, M., Berrocal, R., & Norton, I. (2016). Whey protein fluid gels for the stabilisation of foams. *Food hydrocolloids*, 53, 209-217.
- Leal-Calderon, F., Schmitt, V., & Bibette, J. (2007). *Emulsion science: basic principles*: Springer Science & Business Media.
- Lizarraga, M., Pan, L., Anon, M., & Santiago, L. (2008). Stability of concentrated emulsions measured by optical and rheological methods. Effect of processing conditions—I. Whey protein concentrate. *Food hydrocolloids*, 22(5), 868-878.
- Mason, T. (1999). New fundamental concepts in emulsion rheology. *Current opinion in colloid interface science*, 4(3), 231-238.
- McClements, D. J. (2015). *Food emulsions: principles, practices, and techniques*: CRC press.
- Morris, V. (2011). Emerging roles of engineered nanomaterials in the food industry. *Trends in biotechnology*, 29(10), 509-516.
- Murray, B. S. (2019). Pickering Emulsions for Food and Drinks. *Current Opinion in Food Science*, 27, 57-63.
- Murray, B. S., & Discinson, E. (1996). Interfacial rheology and the dynamic properties of adsorbed films of food proteins and surfactants. *Food Science Technology International*, 2(3), 131-145.
- Murray, B. S., & Phisarnchananan, N. (2016). Whey protein microgel particles as stabilizers of waxy corn starch+ locust bean gum water-in-water emulsions. *Food hydrocolloids*, 56, 161-169.
- Plamper, F. A., & Richtering, W. (2017). Functional microgels and microgel systems. *Accounts of chemical research*, 50(2), 131-140.
- Rao, M. A. (2010). *Rheology of fluid and semisolid foods: principles and applications*: Springer Science & Business Media.
- Rousseau, D. (2013). Trends in structuring edible emulsions with Pickering fat crystals. *Current opinion in colloid interface science*, 18(4), 283-291.
- Rutkevičius, M., Allred, S., Velev, O. D., & Velikov, K. P. (2018). Stabilization of oil continuous emulsions with colloidal particles from water-insoluble plant proteins. *Food hydrocolloids*, 82, 89-95.
- Sarkar, A., Kanti, F., Gulotta, A., Murray, B. S., & Zhang, S. (2017). Aqueous lubrication, structure and rheological properties of whey protein microgel particles. *Langmuir*, 33(51), 14699-14708.
- Sarkar, A., Murray, B., Holmes, M., Ettelaie, R., Abdalla, A., & Yang, X. (2016a). In vitro digestion of Pickering emulsions stabilized by soft whey protein microgel particles: influence of thermal treatment. *Soft Matter*, 12(15), 3558-3569.

- Sarkar, A., & Singh, H. (2016b). Emulsions and foams stabilised by milk proteins. In *Advanced dairy chemistry* (pp. 133-153): Springer.
- Sarkar, A., Zhang, S., Holmes, M., & Ettelaie, R. (2018). Colloidal aspects of digestion of Pickering emulsions: Experiments and theoretical models of lipid digestion kinetics. *Advances in colloid interface science*.
- Schmitt, C., Moitzi, C., Bovay, C., Rouvet, M., Bovetto, L., Donato, L., . . . Stradner, A. (2010). Internal structure and colloidal behaviour of covalent whey protein microgels obtained by heat treatment. *Soft Matter*, 6(19), 4876-4884.
- Tadros, T. (2004). Application of rheology for assessment and prediction of the long-term physical stability of emulsions. *Advances in colloid and interface science*, 108, 227-258.
- Toro-Vazquez, J. F., Mauricio-Pérez, R., González-Chávez, M. M., Sánchez-Becerril, M., de Jesús Ornelas-Paz, J., & Pérez-Martínez, J. D. (2013). Physical properties of organogels and water in oil emulsions structured by mixtures of candelilla wax and monoglycerides. *Food research international*, 54(2), 1360-1368.
- Zembyla, M., Lazidis, A., Murray, B. S., & Sarkar, A. (2019a). Water-in-Oil Pickering Emulsions Stabilized by Synergistic Particle-Particle Interactions. *Langmuir*.
- Zembyla, M., Murray, B. S., Radford, S. J., & Sarkar, A. (2019b). Water-in-oil Pickering emulsions stabilized by an interfacial complex of water-insoluble polyphenol crystals and protein. *Journal of colloid interface science*, 548, 88-99.
- Zembyla, M., Murray, B. S., & Sarkar, A. (2018). Water-In-Oil Pickering Emulsions Stabilized by Water-Insoluble Polyphenol Crystals. *Langmuir*, 34(34), 10001-10011.

Chapter 7

General Discussion

7.1. Introduction

Considering the global uprise of obesity and food-linked cardiovascular diseases, the addition of non-calorific water into fat-based products, in the form of water-in-oil (W/O) emulsions, seems the most promising way to reduce the fat and calorific content of these products. Although this appears to be the most promising approach in theory, lack of stability of these emulsion systems presents one of the key challenges because they are thermodynamically unstable and prone to phase separation over time. Traditionally, chemically-synthesized surfactants (e.g., PGPR) and/or chemically modified particles (e.g., silica particles), have widely used as stabilizers for W/O emulsions, making them less appealing to consumers (**Chapter 2**). Consequently, there is a huge driving force from food industries to replace these chemically-synthesized materials with natural, biodegradable and affordable ingredients that will give a '*clean label*' on the final product.

In recent years, there has been a resurgence of interests in Pickering emulsions particularly for W/O emulsions due to the limited range of suitable biocompatible emulsifiers in existence for the stabilization of food- and pharmaceutical-based emulsions, designed for human ingestion (**Chapter 2**). Polyphenols are a group of phytochemicals from plant-based foods such as fruits, vegetables, tea, coffee etc., and recent studies have shown that polyphenols act as Pickering stabilizers at the O-W interface. However, to our knowledge no work has been done on the action of these particles on stabilizing W/O emulsions. The interactions between polyphenol crystals and proteins (when both are present in water) have been examined by a lot of authors showing their ability to interact with each other through hydrophobic interaction, electrostatic attraction and hydrogen bonding (Andersen *et al.*, 2005; Bordenave *et al.*, 2014; Le Bourvellec *et al.*, 2012; Riihimaki *et al.*, 2008). However, a research question remains on how protein and polyphenol

crystals interact at the interface when polyphenol crystals are dispersed in the oil phase and protein is present in the aqueous phase. Therefore, the main aim of this PhD was to use polyphenol crystals to stabilize W/O emulsions and to identify if complexes between proteins or protein-based particles and polyphenol crystals at the interface can be exploited to enhance the stability of those emulsions.

In view of the above, the microstructure, hydrophilicity, size and shape of polyphenol crystals (curcumin and quercetin) were first analysed (Figure 7.1, **Chapter 3**). W/O emulsions were then prepared stabilized by curcumin or quercetin crystals and they were evaluated based on different polyphenol concentrations, pH values and water volume fractions (Figure 7.1, **Chapter 3**). The stability of these emulsions was improved by the incorporation of WPI in the aqueous phase where complexes were formed at the interface between polyphenol crystals (from the oil side) and WPI (from the aqueous side) through hydrogen bonding and electrostatic attraction. The stability of the corresponding W/O emulsion droplets was evaluated as a function of different WPI concentrations, pH values, water volume fractions and different NaCl concentrations in the aqueous phase (Figure 7.1, **Chapter 4**). All these emulsions showed a good stability with only 5 wt% water. In order to further increase the water volume fraction, a physical modification of the WPI was undertaken where WPM particles formed, using the top-down technique, and were used in the aqueous phase (pH 3.0) of the emulsions. Therefore, W/O emulsions stabilized by 'double Pickering stabilization' were formed via an interfacial complexation between polyphenol crystals adsorbed from the oil side and WPM particles co-adsorbed from the aqueous side of the interface. This mechanism of stabilization used to improve the stability of W/O emulsions and increase the water volume fraction for up to 20 wt%. The stability of the corresponding W/O emulsion droplets was evaluated as a function of different WPM particle concentrations and water volume fractions (Figure 7.1, **Chapter 5**). The last part of this study was to characterize the process stability of the W/O emulsions stabilized by curcumin or quercetin crystals dispersed in the oil phase (**Chapter 3**), with or without the presence of WPI (**Chapter 3 and 4**) or WPM particles (**Chapter 5**) in the aqueous phase. This characterization

was undertaken using controlled rheological tests (shear rates and temperatures) combined with particle sizing and confocal laser scanning microscopy (Figure 7.1, **Chapter 6**).

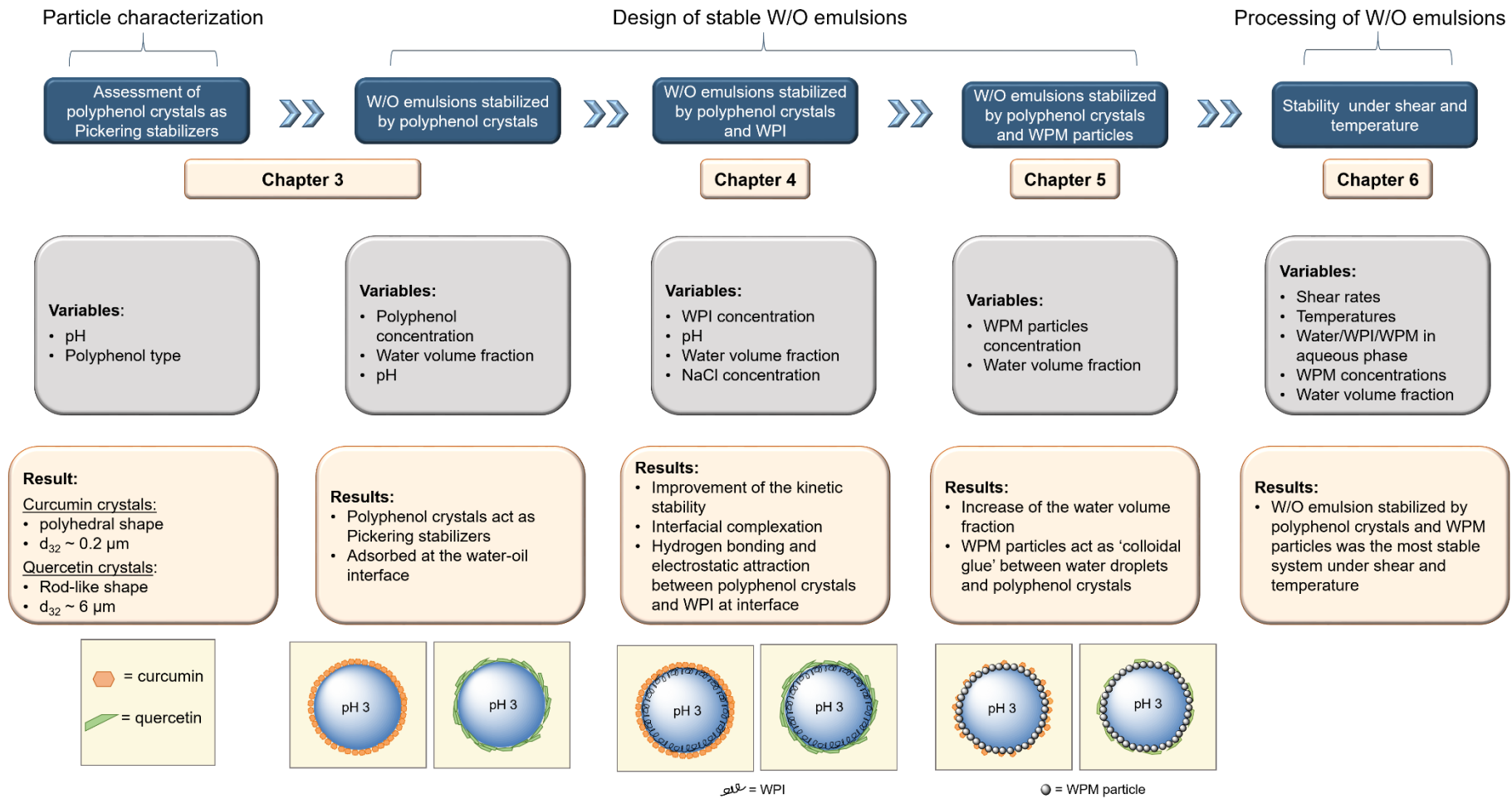


Figure 7.1. Schematic framework of this thesis.

7.2. Summary of the main results

7.2.1. Assessment of particles as Pickering stabilizers

Table 7.1 summarizes the different characteristics of curcumin and quercetin crystals based on their size in oil (d_{32}), contact angle of water droplet (θ_w), oil droplet (θ_o), interfacial tension (γ_T) at oil-water (O-W) interface, ζ -potential (in water) and electrophoretic mobility (in oil) (**Chapter 3**). Microstructural evaluation at various length scales revealed that quercetin crystals had a more rod-like shape and larger size ($d_{32} \sim 5.9 \mu\text{m}$, Table 7.1) than curcumin crystals, the latter being smaller ($d_{32} \sim 0.2 \mu\text{m}$, Table 7.1) and having a more polyhedral shape. The differences in the shape and size of the polyphenols were reflected in the Pickering stabilization efficiency of the two materials.

Curcumin and quercetin have been chosen for this study, since both of them are insoluble in water, partially soluble in oils but they are considered as hydrophobic due to their high $\log P$ value (3.29 and 2.16 for curcumin and quercetin, respectively; where P is the partition coefficient between n-octanol and water). The $\log P$ value can be used to identify the hydrophilicity/hydrophobicity of a polyphenol molecule. However, Pickering stabilization depends on the hydrophilic/hydrophobic balance of particles, not their molecules, and no simple relationship seemed to exist between $\log P$ and the ability to stabilize W/O emulsions. Therefore, the hydrophilicity/hydrophobicity of the polyphenol particles was measured via their wettability (sessile drop method). It was assumed that when the contact angle of water droplet (θ_w) significantly exceeds the contact angle of oil droplet (θ_o), the particles can be categorized as hydrophobic and thus will tend to stabilize W/O rather than O/W emulsions. As shown in Table 7.1, both curcumin and quercetin crystals had θ_w values exceeding their θ_o values (at both pH 3.0 and 7.0), indicating that both possess a hydrophobic character. In addition, neither of these particle dispersions suppressed the interfacial tension (at oil-water interface) significantly comparing the interfacial tension

values of pure water and oil ($\gamma_T \sim 33 \text{ mN m}^{-1}$), indicating a Pickering stabilization mechanism (**Chapter 3**).

In order to predict how the particles might behave when they adsorb at the W-O interface, the ζ -potential of those particles dispersed in the aqueous phase was measured because this might have some relevance to the behaviour of the particles when partially wetted by water at the W-O interface (Table 7.1 and **Chapter 3**). The curcumin particles had a positive charge at pH 3.0 but at pH 7.0, they became strongly anionic. Under alkaline conditions, curcumin can be dissolved sparsely in water as its acidic phenolic group donates its H^+ ion, forming the phenolate ion enabling dissolution (Araiza-Calahorra *et al.*, 2018). On the other hand, quercetin had negative charge at both pH values (Table 7.1). The $\text{C}_7\text{-OH}$ on the quercetin nucleus also behaves as a polyprotic acid undergoing dissociation at alkaline conditions ($> \text{pH } 7.0$) by imparting a negative charge (Luo *et al.*, 2012). As particles become more highly charged, they are likely to be less hydrophobic and less surface-active (Luo *et al.*, 2012). Thus, the ζ -potential results predict that both curcumin and quercetin would be more surface active at lower pH (~ 3.0). Most notably, curcumin at pH 3.0 is predicted as the most hydrophobic from the above contact angle measurements, which agrees with the lowest absolute magnitude of ζ -potential in contact with water. The electrophoretic mobility results for curcumin and quercetin crystals dispersed in the oil phase are shown in Table 7.1 (**Chapter 5**). Due to the very high viscosity ($57.1 \pm 1.1 \text{ mPa}\cdot\text{s}$ (Sahasrabudhe *et al.*, 2017)) of the soybean oil, the mobility of the particles is expected to be low. Both polyphenol crystals showed a small negative mobility value indicating the presence of some negative charge at the particle surface when they are dispersed in the soybean oil.

Table 7.1. Comparison of the characteristics of 0.14 wt% curcumin and quercetin crystals based on their size in oil (d_{32}), contact angle of water droplet (θ_w), oil droplet (θ_o) at pH 3.0 and 7.0, interfacial tension (γ_T) at oil-water (O-W) interface, ζ -potential (in water, pH 3.0 and 7.0) and electrophoretic mobility (in oil). Samples with the same letter do not differ significantly ($p > 0.05$) according to Tukey's test.

Characteristics	Curcumin crystals	Quercetin crystals
$d_{32}/ \mu\text{m}$	0.2 ± 0.0	5.9 ± 0.1
$\theta_w/ ^\circ$ (pH 3.0)	85.6 ± 0.4	60.2 ± 0.7^a
$\theta_w/ ^\circ$ (pH 7.0)	73.4 ± 1.2	59.4 ± 0.4^a
$\theta_o/ ^\circ$	11.9 ± 2.0	19.8 ± 0.5
$\gamma_T/ \text{mN m}^{-1}$ (O-W)	32.5 ± 0.3^c	33.4 ± 0.4^c
ζ -potential/ mV (in water, pH 3.0)	12.0 ± 2.2	-26.2 ± 1.2
ζ -potential/ mV (in water, pH 7.0)	-47.6 ± 2.4^d	-48.1 ± 1.2^d
Electrophoretic mobility/ $\mu\text{m cm V}^{-1} \text{s}^{-1}$ (in oil)	-0.0031 ± 0.0009	-0.0035 ± 0.0002

The size of particles dispersed in the continuous phase is an important parameter on the Pickering functionality. It is used for the estimation of the amount of surface active particles require for surface coverage in order to form stable emulsions (Luo *et al.*, 2011). Additionally, the overall stability of an emulsion is inversely proportional to particle size, with smaller particles giving a higher packing efficiency and therefore providing a more homogeneous layer at the interface preventing coalescence (Duffus *et al.*, 2016; Hunter *et al.*, 2008). Therefore, attempts have been made to minimize the size of the polyphenol crystals dispersed in oil in order to improve their packing efficiency at the interface. The size of curcumin and quercetin crystals dispersed in the oil phase was measured after treatment with ultra-Turrax (9,400 rpm for 5 min) only or ultra-Turrax (9,400 rpm for 5 min) followed by ultrasound bath (2, 5

and 10 min), heat (60 - 65 °C for 1h) or Jet homogenizer (twice, operating at 300 bar). According to the results shown in Figure 7.2 and Table 7.2, only heat treatment reduced the size of curcumin particles, from 0.2 to 0.1 µm, compared to the other methods. The particle size distribution plots showed that curcumin particles were polydispersed under ultra-Turrax, ultrasound bath and Jet homogenizer treatment whilst under heat they were bimodal. These results indicated that most of the curcumin crystals were dissolved in oil phase at 60 - 65 °C, which this has also proved from the turbidity of the dispersions which was decreased upon heating from 25 to 60 °C. Interestingly, upon cooling back to 25 °C, the turbidity of the dispersions was still low indicating that curcumin remained dissolved in the oil phase. This might be attributed to either curcumin being below its saturation temperature (even at 25 °C), or the curcumin concentration did not exceed the super-saturation level to form curcumin crystals (McClements, 2012). However, heat treatment was considered as unappropriated method for curcumin size reduction because prolonged heat exposure of curcumin in the oil phase can cause decomposition of curcumin (Wang *et al.*, 2016). In addition, the idea of this PhD was to use polyphenol crystals as particles, thus, any dissolution of the crystals in the oil phase will affect the stabilization efficiency and adsorption at the interface. On the other hand, for quercetin crystals (Figure 7.2 (b) and Table 7.2) neither ultrasound bath nor heat reduced the size of particles significantly ($p > 0.05$). However, Jet homogenizer significantly ($p < 0.05$) reduced the size of quercetin crystals from 5.9 to 4.0 µm. The Jet homogenizer produced a slight milling effect, but this appeared to predominantly affect the larger crystals or their aggregates (> 10 µm). Thus, the overall particle distributions, which were quite broad remained largely in the micrometer range. Therefore, both curcumin and quercetin crystals were used into the oil phase without further treatment (only Ultra-Turrax at 9,400 rpm for 5min) with an average size (d_{32}) of 0.2 and 5.9 µm for curcumin and quercetin in oil, respectively.

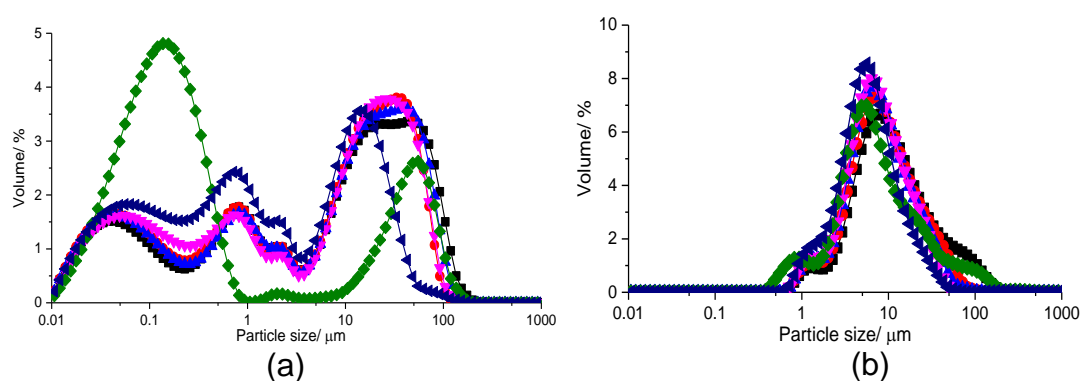


Figure 7.2. Particle size distribution plots for 0.14 wt% curcumin (a) and quercetin (b) crystals dispersed in oil under different treatments; ultra-Turrax only (9,400 rpm for 5 min) (■), ultra-Turrax (9,400 rpm for 5 min) followed by: ultrasound bath for 2 (●), 5 (▲) or 10 min (▼), heat (60 °C for 1h) (◆) or Jet homogenizer (twice at 300 bar) (►).

Table 7.2. d_{32} values for 0.14 wt% curcumin and quercetin crystals dispersed in oil under different treatments; ultra-Turrax only (9,400 rpm for 5 min), ultra-Turrax (9,400 rpm for 5 min) followed by: ultrasound bath for 2, 5 or 10 min, heat (60 °C for 1 h) or Jet homogenizer (twice at 300 bar). Samples with the same letter do not differ significantly ($p > 0.05$) according to Tukey's test.

Treatment	$d_{32}/ \mu\text{m}$	
	Curcumin crystals	Quercetin crystals
Ultra-Turrax	0.2 ± 0.0^a	5.9 ± 0.1
Ultrasound bath, 2 min	0.2 ± 0.0^a	5.5 ± 0.3
Ultrasound bath, 5 min	0.2 ± 0.0^a	5.2 ± 0.2^b
Ultrasound bath, 10 min	0.2 ± 0.0^a	$5.0 \pm 0.2^{b,c}$
Heat 60 °C for 1 h	0.1 ± 0.0	4.7 ± 0.5^c
Jet homogenizer, twice, at 300 bar	0.1 ± 0.0	4.0 ± 0.2

7.2.2. W/O emulsions

Regarding the results obtained from the assessment of particles, it was identified that both curcumin and quercetin act as Pickering stabilizers and are considered as hydrophobic based on their contact angle measurements, thus,

they can stabilize W/O emulsions. Therefore, W/O emulsions (5 wt% water) were prepared using curcumin or quercetin crystals dispersed in the oil phase at different concentrations. A low concentration of curcumin or quercetin particles (0.06 wt%) was not able to cover the water droplets fully, whereas at a much higher concentration (0.5 and 1.5 wt%), a significant proportion of particles still remained unabsorbed, leading to aggregation of water droplets and particle sedimentation. An optimum concentration of particles with the smallest water droplets and fewer free particles in the continuous phase was identified at ~ 0.14 wt% for both quercetin and curcumin. In addition, the pH value played a significant effect on the stability of the emulsions. Increasing the pH of the aqueous phase from 3.0 to 7.0 gave more coarse emulsions, possibly related to an increase in the magnitude of the ζ -potential (more negative) of the particle surface when in contact with water. Interfacial shear viscosity results also show stronger film formation in the presence of particles. Confocal microscopy (see Figures 3.11 and 3.12, **Chapter 3**) and SEM images (Figure 7.3) showed the adsorbed particles at the W-O interface proving once again the ability of polyphenol crystals to act as Pickering stabilizers.

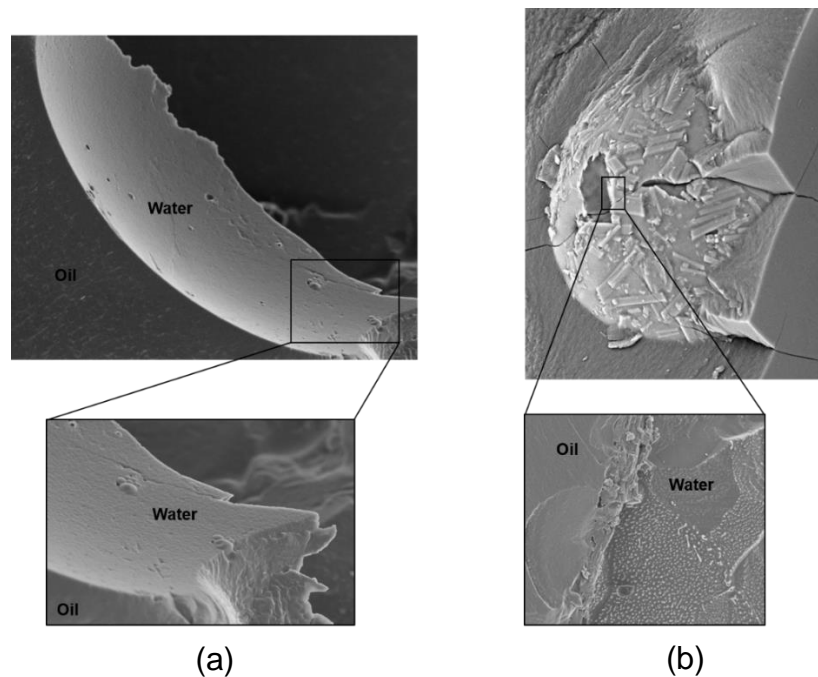


Figure 7.3. SEM images of 5 wt% W/O emulsions stabilized by (a) curcumin and (b) quercetin crystals at an aqueous phase of pH 3.0.

Curcumin and quercetin particles at 0.14 wt% imparted stability to coalescence of W/O emulsions for several days of storage, but the size (up to 6 μm) of the droplets resulted in significant sedimentation of both droplets and particles over this time period. This happened due to the large size range of the stabilizing particles, making the efficient coverage of small water droplets difficult (**Chapter 3**). Thus, although polyphenol crystals show potential as W/O emulsion stabilizers, improvements were required to extend the kinetic stability of such emulsions. To improve the stability of these systems a biopolymer, WPI, was added into the aqueous phase to identify if protein-polyphenol interactions exist at the W-O interface (**Chapter 4**). Therefore, W/O emulsions (5 wt% water) were prepared with polyphenol crystals adsorbing from the oil-continuous phase and WPI co-adsorbing from the aqueous phase (at either pH 3.0 or 7.0) of the interface. Addition of WPI up to 0.5 wt% gave a significant increase in the stability of the emulsions over time and strengthened the mechanical properties of the adsorbed film. Based on the interfacial shear viscosity measurements, the main factors affecting complex formation and strengthening of the film was the electrostatic attraction between oppositely charged polyphenol particles and protein at the interface, which therefore also depends on the pH of the aqueous phase. This agrees with correspondingly more stable emulsions at pH 3.0 compared to pH 7.0. At pH 3.0, WPI was positively charged whilst polyphenol crystals were slightly negatively charged which this promoted the electrostatic attraction between the two components at the interface and thus, formations of stronger films. On the other hand, at pH 7.0, both WPI and polyphenol crystals had a strong negative charge which this caused chemical instability on the emulsions and maybe degradation of the polyphenol crystals at this more alkaline pH. Higher concentrations of WPI do not improve the stability further due to protein adsorption dominating over polyphenol particle adsorption. Higher water:oil ratios (10 and 20 wt% water) were tested at pH 3.0 for 0.14 wt% curcumin or quercetin crystals + 0.5 wt% WPI as Pickering stabilizers. However, both curcumin- and quercetin-stabilized emulsions containing 10 or 20 wt% water showed an obvious water layer at the bottom of the samples after 1 day and the systems had completely phase separated after 3 days,

suggesting that at these higher water volume fractions there were not enough polyphenol crystals or WPI to fully cover the interface.

To further increase the water volume fraction (from 5 to 20 wt%), protein microgels were formed by using a top-down technique of forming a physically cross-linked heat-set hydrogel in the first stage. Then microgel particles were produced by breaking the gel down under high shear forces using a homogenizer. W/O emulsions were then formed where polyphenol particles were adsorbed from the oil side and WPM particles co-adsorbed from the aqueous side of the interface. In this work, we proposed a novel way to stabilize W/O emulsions via a 'double Pickering mechanism' (**Chapter 5**). This complex formation was strongly dependent on the concentration of WPM particles. At low WPM particle concentrations, both polyphenol crystals and WPM particles were present at the interface and through a synergistic action, they better stabilized the W/O emulsions. At higher WPM particle concentrations, flocculation was observed where the WPM particles acted as a 'colloidal glue' between water droplets and polyphenol crystals enhancing the water droplet stability and preventing the coalescence. Via this mechanism, addition of WPM particles up to 1 wt% gave a significant improvement in the stability of the emulsions up to at least 20 wt% water. It is again believed that this complex formation was mainly formed due to attractive electrostatic interactions between oppositely-charged polyphenol Pickering particles on the oil side of the interface and WPM 'Pickering' particles mainly on the aqueous side of the interface, which therefore was also dependent on the pH of the aqueous phase. Interfacial shear viscosity measurements and monolayer experiments at the A-W interface provided further evidence of strengthening of the film due to the complex formation at the interface. However, higher concentrations of WPM particles do not improve the stability further due to WPM particles adsorption dominating over polyphenol particle adsorption.

Chapter 6 demonstrated the effects of the application of different shear rates (cycle between 10^{-1} to 10^2 s^{-1}) and temperatures (25, 35 and 50 °C) on the viscosity (η) and mean particle size of W/O emulsions stabilized by

curcumin or quercetin crystals dispersed in the oil phase, with or without WPI or WPM particles present in the aqueous phase at pH 3.0. All the emulsions were shear-thinning. The emulsions stabilized by polyphenol crystals alone, without the addition of WPI or WPM particles in the aqueous phase, exhibited coalescence after shearing, with the size of the water droplets increasing significantly. More pronounced destabilization was observed at higher temperatures. The emulsions containing WPI in the dispersed phase were stable over shear and temperatures without a significant increase in mean particle size. The emulsions with WPM particles showed a decrease in the d_{43} values on shearing, indicating disruption of the flocculated droplets, polyphenol crystals and WPM particles in the continuous oil phase. At low shear rate (0.1 s^{-1}) viscosity showed an increase with increasing WPM particle concentration. This suggests that at higher WPM particle concentrations, the W/O emulsion stability increased, not only via their adsorption to the inner surface of the water droplets, but also due to their promotion of a mixed network of WPM particles, water droplets and polyphenol crystals in the oil phase.

To summarize, W/O emulsions stabilized by WPM particles were the most stable systems over time and under shear and temperatures. At WPM particle concentration $\geq 0.5 \text{ wt}\%$, no droplet coalescence or phase separation were observed and the systems were significantly stable even at 20 wt% water content. The action of WPM particles as “colloidal glue” between water droplets and polyphenol crystals have showed to be the key mechanism of the improvement of the stability of this system. The presence of polyphenol crystals in the oil phase and WPM particles in the aqueous phase have shown to improve the interfacial film formation. This was achieved due to the complex formation mainly due to attractive electrostatic interactions between oppositely charged polyphenol crystals and WPM ‘Pickering’ particles, which therefore was also dependent on the pH of the aqueous phase. Under shear, this “colloidal glue” network was disrupted but no any coalescence or phase separation was observed.

7.3. Concluding remarks and recommendations for future studies

7.3.1. Concluding remarks

A schematic overview of the approach of this thesis was presented at the beginning of this chapter (Figure 7.1), highlighting the main outcome of this thesis: assessment of polyphenol crystals as Pickering stabilizers (**Chapter 3**); stabilization of W/O emulsions using polyphenols crystals + with or without WPI or WPM particles in the aqueous phase (**Chapters 4 and 5**); and characterization of the stability of these emulsions under shear rates and temperatures (**Chapter 6**).

This thesis highlights the importance of replacing the chemically-synthesized emulsifiers with some natural, biodegradable and from renewable resource ingredients. A novel way for stabilization of W/O emulsion through a complex formation between polyphenol crystals (curcumin or quercetin) adsorbing from the oil side and WPI or WPM particles co-adsorbing from the aqueous side of the interface, is proposed. This complex formation depends on the concentration of WPI or WPM particles present in the aqueous phase, as well as, to the pH of the aqueous phase. Under an acidic pH (~ 3.0), the emulsions showed an improvement of the stability due to hydrogen bonding and electrostatic attraction between the oppositely charged WPI or WPM particles (positive) and polyphenol crystals (negative). On the other hand, at pH 7.0, WPI or WPM particles and polyphenol crystals had a strong negative charge which this caused chemical instability on the emulsions and thus, weak complex formation. Also, at this more alkaline pH, there was a higher probability for chemical degradation of both curcumin and quercetin crystals at the interface when they are in contact with water. Emphasis was placed on the effect of different processing conditions such as shear rates (cycle between 10^{-1} to 10^2 s⁻¹) and temperatures (25, 35 and 50 °C) on the stability of these emulsions. Emulsions stabilized by interfacial complexes were stable to shear rates and temperatures and no any coalescence and phase separation was observed.

In summary, co-adsorbing biopolymers or biopolymer-based particles to polyphenol crystal, coming from different phases, to stabilize W/O emulsions appeared as a promising new technique to improve the process stability of water droplets. This method can have applications in designing new formulations for a variety of soft matter applications (*i.e.*, food, pharmaceuticals, personal care, agriculture etc.) but also more widely, where there is a lack of biocompatible Pickering particles for stabilization of aqueous droplets in an oily phase.

7.3.2. Future studies

This thesis has demonstrated the potential of polyphenol crystals to act as Pickering stabilizers and form interfacial complexation with WPI or WPM particles and polyphenol crystals. Based on these findings, further research could be undertaken in order to fully unleash the application potential of these complexed W/O emulsions:

a) Characterization

- In this thesis, we have used a range of structural and rheological techniques to characterize the complexed emulsions. However, a lot of problems have been noticed on the quality of the images from cryo-SEM. Fat continuous phase crystallized during the freezing stage of the emulsions using liquid nitrogen, making the process of identification of the water droplets and W-O interface very complicated. Therefore, it is recommended to optimize the conditions of the sample preparation prior to the cryo-SEM analysis. It is suggested to use liquid ethane or propane instead of liquid nitrogen for faster solidification. In addition, another parameter that must be tested is the use of a pure organic phase instead of a commercial oil, which it will not contain any fatty acids and triglycerides.
- The oxidative stability of the emulsions, *i.e.*, antioxidant capacity, total phenolic compounds and chemical composition must be determined.

This will be a useful indication of the usefulness of emulsions in technological processes, as well as, shelf life.

b) Materials

- Extraction and isolation of polyphenol compounds from vegetables and fruits. In this thesis, purified polyphenol crystals were used in order to identify the mechanism of stabilization through the interfacial complexation. However, future work must be done on how to extract and isolate these polyphenol crystals from vegetables and fruits using 'green' methods and identify if they have the same efficiency on stabilizing W/O emulsions as the purified ones.
- There could be potential in testing different types of polyphenol crystals (*i.e.*, tiliroside, crocetin, naringin etc.) and biopolymers (*i.e.*, casein, gelatine, chitosan, carrageenan, cellulose, starch etc.) to determine if the interfacial complexation is still formed by using different components in each phase.

c) Application tests

- Water-soluble compounds (*i.e.*, vitamins) can be encapsulated into the aqueous phase of the emulsions and control their release during digestion. It is important as well, to investigate their behaviour under *in vitro* oral and gastrointestinal digestion using biological assays and biophysical membranes.
- It would be of great interest to incorporate these complexed W/O emulsion into real composite food systems, such as chocolates. Particularly, further research is needed to replace the soybean oil phase with a more viscous oil such as, cocoa butter or palm oil to understand whether these emulsions retain their mechanical integrity during processing, such as exposure to shear, temperature or interactions with other food components (*i.e.*, sugars, fatty acids, thickeners etc.).

References

- Andersen, O. M., & Markham, K. R. (2005). *Flavonoids: chemistry, biochemistry and applications*: CRC press.
- Araiza-Calahorra, A., Akhtar, M., & Sarkar, A. (2018). Recent advances in emulsion-based delivery approaches for curcumin: From encapsulation to bioaccessibility. *Trends in food science technology*, *71*, 155-169.
- Bordenave, N., Hamaker, B. R., & Ferruzzi, M. G. (2014). Nature and consequences of non-covalent interactions between flavonoids and macronutrients in foods. *Food function*, *5*(1), 18-34.
- Duffus, L. J., Norton, J. E., Smith, P., Norton, I. T., & Spyropoulos, F. (2016). A comparative study on the capacity of a range of food-grade particles to form stable O/W and W/O Pickering emulsions. *Journal of colloid interface science*, *473*, 9-21.
- Hunter, T. N., Pugh, R. J., Franks, G. V., & Jameson, G. J. (2008). The role of particles in stabilising foams and emulsions. *Advances in colloid interface science*, *137*(2), 57-81.
- Le Bourvellec, C., & Renard, C. (2012). Interactions between polyphenols and macromolecules: quantification methods and mechanisms. *Critical reviews in food science nutrition*, *52*(3), 213-248.
- Luo, Z., Murray, B. S., Ross, A.-L., Povey, M. J., Morgan, M. R., & Day, A. J. (2012). Effects of pH on the ability of flavonoids to act as Pickering emulsion stabilizers. *Colloids Surfaces B: Biointerfaces*, *92*, 84-90.
- Luo, Z., Murray, B. S., Yusoff, A., Morgan, M. R., Povey, M. J., & Day, A. J. (2011). Particle-stabilizing effects of flavonoids at the oil- water interface. *Journal of agricultural food chemistry*, *59*(6), 2636-2645.
- McClements, D. J. (2012). Crystals and crystallization in oil-in-water emulsions: Implications for emulsion-based delivery systems. *Advances in colloid interface science*, *174*, 1-30.
- Riihimaki, L. H., Vainio, M. J., Heikura, J. M., Valkonen, K. H., Virtanen, V. T., & Vuorela, P. M. (2008). Binding of phenolic compounds and their derivatives to bovine and reindeer β -lactoglobulin. *Journal of agricultural food chemistry*, *56*(17), 7721-7729.
- Sahasrabudhe, S. N., Rodriguez-Martinez, V., O'Meara, M., & Farkas, B. E. (2017). Density, viscosity, and surface tension of five vegetable oils at elevated temperatures: Measurement and modeling. *International journal of food properties*, *20*(sup2), 1965-1981.
- Wang, C., Liu, Z., Xu, G., Yin, B., & Yao, P. (2016). BSA-dextran emulsion for protection and oral delivery of curcumin. *Food hydrocolloids*, *61*, 11-19.

Appendix A

Supporting information for Chapter 3

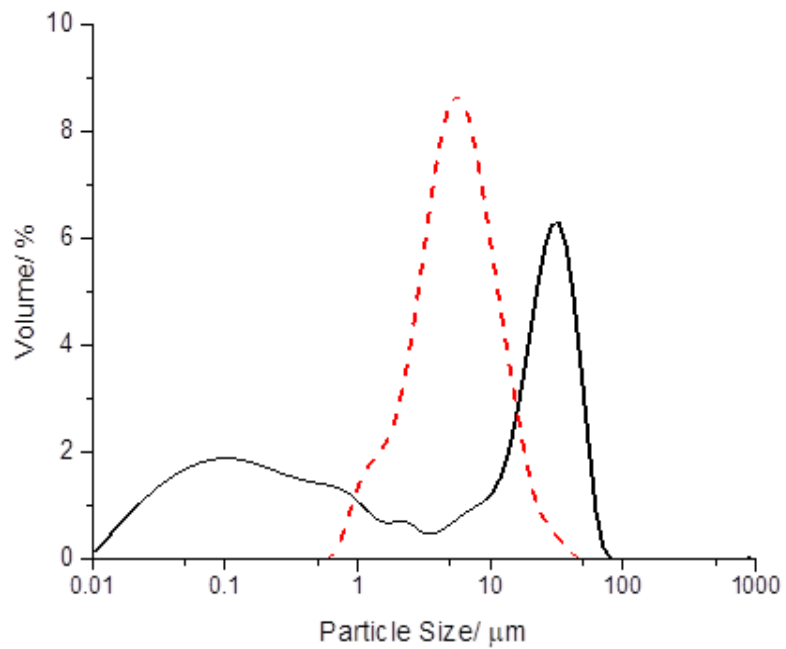
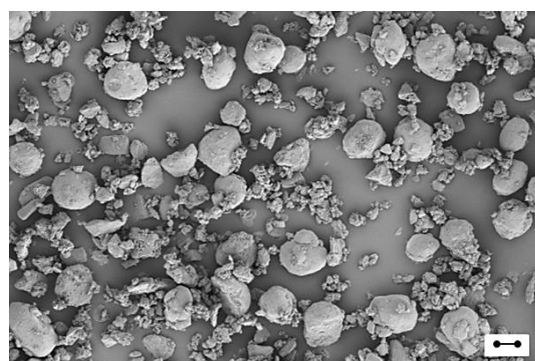


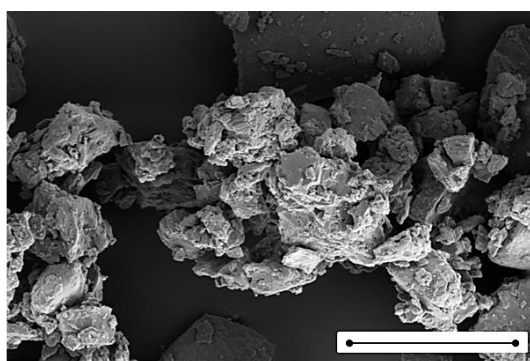
Figure A1. Particle size distribution of 0.14 wt% curcumin (black solid line) and 0.14 wt% quercetin (red dashed line) particles dispersed in soybean oil after passing through all stages of emulsification process (Ultra-Turrax at 9,400 rpm/ 5 min, 13,400 rpm/ 2 min and Jet homogenization for two passes, at 300 bar), respectively.

Table A1. Average size of curcumin and quercetin crystals (0.14 wt%) dispersed in oil under different mixing conditions; Ultra-Turrax at 9,400 rpm/ 5 min or after passing through all stages of emulsification process (Ultra-Turrax at 9,400 rpm/ 5 min, 13,400 rpm/ 2 min and Jet homogenization for two passes, at 300 bar). Samples with the same letter do not differ significantly ($p > 0.05$) according to Tukey's test.

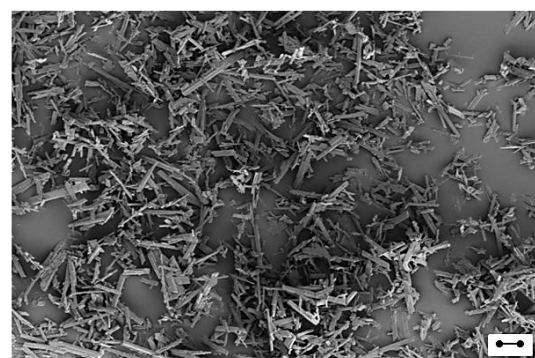
Polyphenol crystal dispersion	$d_{32}/ \mu\text{m}$		$d_{43}/ \mu\text{m}$	
	Ultra-Turrax only	All stages of emulsification process	Ultra-Turrax only	All stages of emulsification process
Curcumin	0.2 ± 0.0^a	0.2 ± 0.0^a	20.5 ± 1.6	15.2 ± 1.8
Quercetin	5.9 ± 0.1	4.0 ± 0.2	14.9 ± 1.7	6.8 ± 0.9



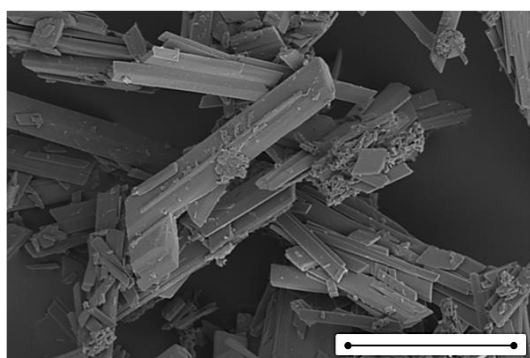
(a)



(b)



(c)



(d)

Figure A2. SEM images of curcumin (a and b) and quercetin (c and d) dry powders at different magnifications: (a) and (c) at lower magnifications (250 \times) and (b) and (d) at higher magnification (2,000 \times). Scale bar is 20 μm .

The oil was purified with aluminium oxide to eliminate free fatty acids and surface active impurities that may affect the measurements. A mixture of oil and aluminium oxide in proportion 2:1 w/w was stirred for 3 h and centrifuged at 4,000 rpm for 30 min.

Table A2. Surface tension (γ) between aqueous phase and air (A-W) and non-purified soybean oil phase and air (O-A) in the presence or not of 0.14 wt% curcumin and quercetin crystals. Samples with the same letter do not differ significantly ($p > 0.05$) according to Tukey's test.

Particle type	$\gamma / \text{mN m}^{-1}$	
	A-W	O-A
No Polyphenol Crystal	71.6 ± 0.5^a	33.1 ± 0.4^b
Curcumin	70.8 ± 1.3^a	32.5 ± 0.3^b
Quercetin	71.5 ± 0.3^a	33.4 ± 0.4^b

Table A3. Interfacial tension (γ_T) between aqueous phase at pH 3.0 and curcumin or quercetin crystals (0.14 wt%) dispersed in purified or non-purified soybean oil phase. Samples with the same letter do not differ significantly ($p > 0.05$) according to Tukey's test.

Particle type	$\gamma_T / \text{mN m}^{-1}$		
	Aqueous phase (pH 3.0)	Purified oil phase	Non-purified oil phase
Soybean oil	Milli-Q water	32.2 ± 0.7^a	25.8 ± 1.0^b
Curcumin in oil	Milli-Q water	32.0 ± 1.4^a	24.6 ± 1.8^b
Quercetin in oil	Milli-Q water	32.1 ± 0.7^a	25.3 ± 0.8^b

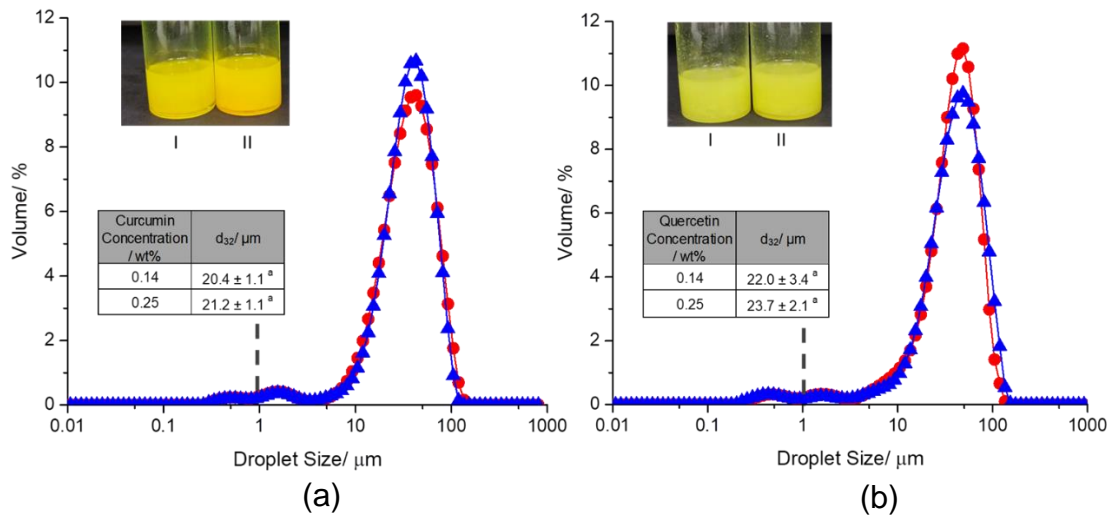


Figure A3. Mean water droplet size distribution and corresponding visual images of W/O Pickering emulsions (10:90 wt% w:o ratio) stabilized by curcumin (a) and quercetin (b) crystals at different particle concentrations; 0.14 wt% [●] and [I] and 0.25 wt% [▲] and [II] at pH 3.0. Dashed line separates the unabsorbed particles remained into the continuous phase ($\leq 1 \mu\text{m}$) and water droplets. Samples with the same letter do not differ significantly ($p > 0.05$) according to Tukey's test.

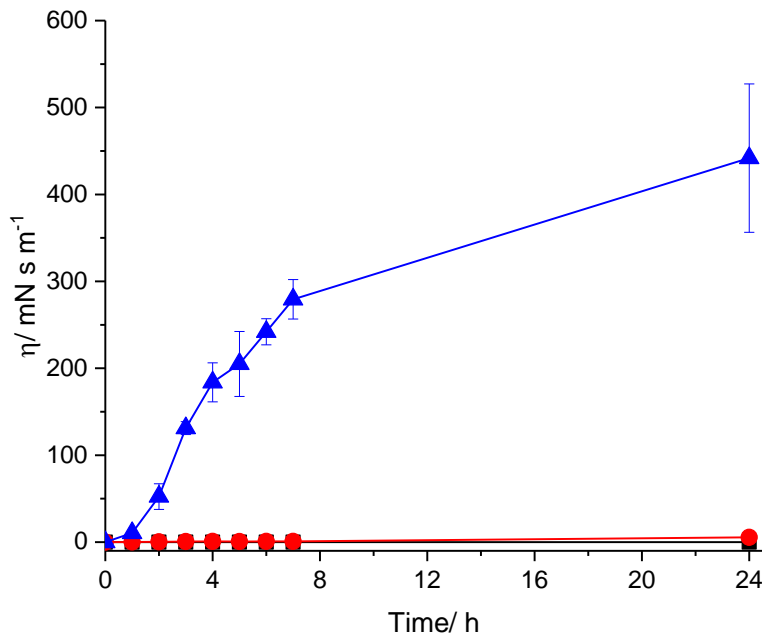


Figure A4. Interfacial shear viscosity at interface of Milli-Q water with purified oil [■], purified oil with 0.14 wt% curcumin particles [●] and purified oil with 0.14 wt% quercetin particles [▲]. The pH of the aqueous phase was adjusted to pH 3.0. Error bars represent standard deviation of at least two independent experiments.

Appendix B
Supporting information for Chapter 4

Table B1. Size of water droplets (d_{32}) over time of 5 wt% W/O emulsions stabilized by 0.14 wt% curcumin particles containing 0, 0.05, 0.5, 1, 2 and 4 wt% WPI in the aqueous phase at pH 3.0. Samples with the same letter differ significantly ($p < 0.05$) according to Tukey's test for each concentration of WPI.

WPI/ wt%	$d_{32}/ \mu\text{m}$					
	0 day	1 day	3 days	7 days	14 days	21 days
0	12.9 ± 2.1^a	28.9 ± 3.4^a				
0.05	13.3 ± 5.1^b	30.6 ± 2.0^b				
0.5	20.0 ± 4.0^c	24.8 ± 0.9	22.2 ± 6.9	26.4 ± 7.0^c	21.1 ± 6.2	21.6 ± 5.9
1	26.1 ± 6.5^d	25.6 ± 1.9	20.2 ± 9.1	22.3 ± 1.4	21.9 ± 1.8	20.0 ± 1.6^d
2	26.4 ± 2.4^e	26.4 ± 2.2^f	$20.9 \pm 4.4^{e,f}$	22.8 ± 3.2	$20.3 \pm 5.4^{e,f}$	22.2 ± 4.9
4	21.3 ± 3.2	19.5 ± 1.0	19.7 ± 4.3	20.3 ± 3.0	18.6 ± 2.8	19.5 ± 3.3

Table B2. Size of water droplets (d_{32}) over time of 5 wt% W/O emulsions stabilized by 0.14 wt% quercetin particles containing 0, 0.05, 0.5, 1, 2 and 4 wt% WPI in the aqueous phase at pH 3.0. Samples with the same letter differ significantly ($p < 0.05$) according to Tukey's test for each concentration of WPI.

WPI/ wt%	$d_{32}/ \mu\text{m}$					
	0 day	1 day	3 days	7 days	14 days	21 days
0	20.7 ± 2.0^a	22.9 ± 1.9^a				
0.05	18.7 ± 2.8^b	24.9 ± 0.9^b				
0.5	30.8 ± 1.6^c	32.9 ± 2.4^d	32.0 ± 4.3^e	$35.6 \pm 4.2^{c,f}$	30.0 ± 4.0^f	$27.4 \pm 3.5^{d,e,f}$
1	25.4 ± 2.0	26.5 ± 7.9^g	22.1 ± 2.1^g	22.7 ± 3.0^g	24.6 ± 2.5	22.4 ± 2.7^g
2	30.2 ± 2.4^h	28.3 ± 2.0^i	28.8 ± 1.1^j	$28.6 \pm 4.1^{i,k}$	$23.0 \pm 3.2^{h,i,j,k}$	$26.0 \pm 1.3^{h,k}$
4	25.4 ± 2.7^l	24.8 ± 2.2	24.2 ± 1.5	26.0 ± 2.7^m	$21.5 \pm 3.9^{l,m}$	$21.3 \pm 3.4^{l,m}$

Table B3. Size of water droplets (d_{32}) over time of 5 wt% W/O emulsions stabilized by 0.14 wt% curcumin particles containing 0, 0.05, 0.5, 1, 2 and 4 wt% WPI in the aqueous phase at pH 7.0. Samples with the same letter differ significantly ($p < 0.05$) according to Tukey's test for each concentration of WPI.

WPI/ wt%	$d_{32}/ \mu\text{m}$				
	0 day	1 day	3 days	7 days	14 days
0	10.3 ± 1.8 ^a	31.3 ± 5.0 ^a			
0.05	10.3 ± 0.7 ^b	23.1 ± 2.7 ^b			
0.5	20.2 ± 3.5 ^c	25.4 ± 1.3 ^c	25.3 ± 1.8 ^c	22.6 ± 2.6 ^d	27.0 ± 5.7 ^{c,d}
1	28.8 ± 1.4 ^e	28.4 ± 2.3 ^f	25.5 ± 2.1 ^e	23.9 ± 2.4 ^{e,f}	22.8 ± 2.9 ^{e,f}
2	21.8 ± 2.4 ^g	24.1 ± 2.0	24.8 ± 1.7 ^{g,h}	22.6 ± 1.4 ^h	23.3 ± 1.8
4	14.5 ± 3.3 ^{i,j,k,l}	23.7 ± 0.8 ⁱ	23.9 ± 1.4 ^j	21.2 ± 1.5 ^k	22.8 ± 1.9 ^l

Table B4. Size of water droplets (d_{32}) over time of 5 wt% W/O emulsions stabilized by 0.14 wt% quercetin particles containing 0, 0.05, 0.5, 1, 2 and 4 wt% WPI in the aqueous phase at pH 7.0. Samples with the same letter differ significantly ($p < 0.05$) according to Tukey's test for each concentration of WPI.

WPI/ wt%	$d_{32}/ \mu\text{m}$			
	0 day	1 day	3 days	7 days
0	14.5 ± 1.4 ^a	28.3 ± 2.8 ^a		
0.05	18.4 ± 1.3 ^b	32.0 ± 2.2 ^b		
0.5	17.0 ± 2.1 ^{c,d,e}	29.3 ± 1.3 ^c	26.4 ± 1.8 ^d	23.6 ± 3.1 ^e
1	16.1 ± 3.8 ^{f,g,h}	24.3 ± 2.8 ^f	22.5 ± 1.9 ^g	21.7 ± 2.3 ^{f,g,h}
2	16.5 ± 3.9 ^{i,j}	28.9 ± 2.0 ^{i,k}	28.7 ± 1.7 ^j	24.5 ± 1.8 ^{i,j,k}
4	14.3 ± 2.9 ^{l,m}	26.0 ± 1.8 ^{l,n}	27.4 ± 1.6 ^m	23.3 ± 2.6 ^{l,m,n}

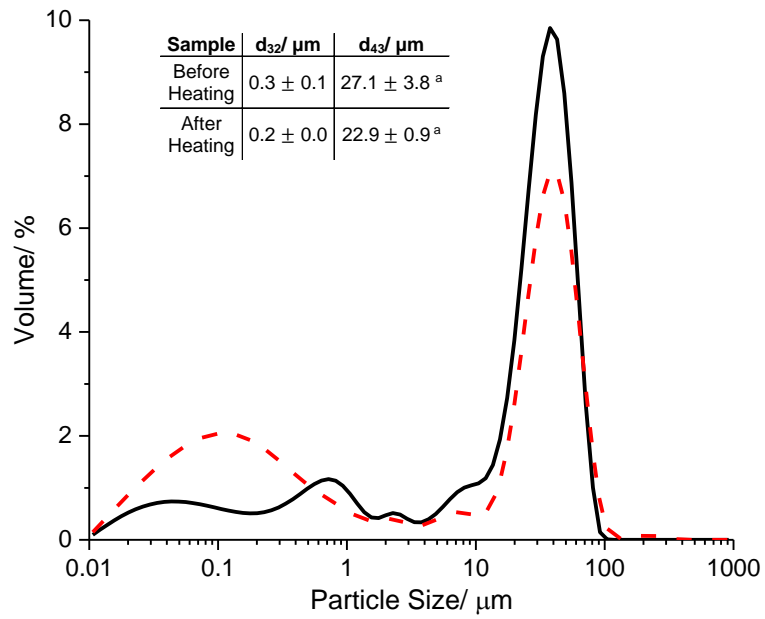


Figure B1. Particle size distribution of 0.14 wt% curcumin in soybean oil before heating (black solid line) and after heating at 45 °C (red dashed line) particles dispersed in soybean oil, respectively. Samples with the same letter differ significantly ($p < 0.05$) according to Tukey's test.

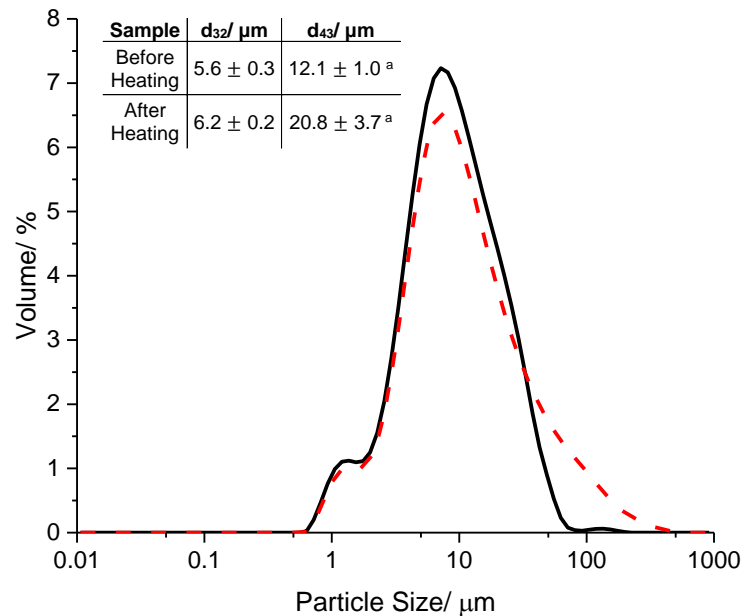


Figure B2. Particle size distribution of 0.14 wt% quercetin in soybean oil before heating (black solid line) and after heating at 45 °C (red dashed line) particles dispersed in soybean oil, respectively. Samples with the same letter differ significantly ($p < 0.05$) according to Tukey's test.

Appendix C

Supporting Information of Chapter 5

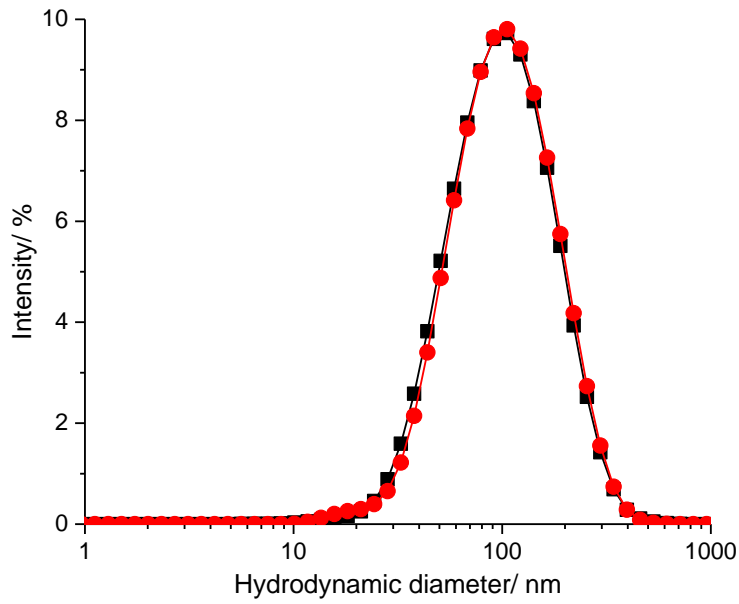


Figure C1. Intensity distribution of 0.5 wt% WPM particles at pH 3.0 (■) and pH 7.0 (●).

Table C1. Size of water droplets (d_{32}) over time of 10 wt% W/O emulsions stabilized by 0.14 wt% curcumin crystals containing 0.05, 0.1, 0.5, 1 and 2 wt% WPM particles in the aqueous phase at pH 3.0. Samples with the same letter differ significantly ($p < 0.05$) according to Tukey's test for each concentration of WPM particles.

WPM particles/ wt%	$d_{32}/ \mu\text{m}$								
	0 day	1 day	3 days	7 days	14 days	21 days	60 days	80 days	90 days
0.05	23.1 ± 0.3 a,b,c	25.5 ± 0.4 a,b,c	28.9 ± 1.8 a,c	32.0 ± 0.1 a,b,c	27.1 ± 1.0 a,b	27.7 ± 0.4 ^a			
0.1	22.9 ± 1.3 ^a	23.8 ± 0.3 b	26.1 ± 0.4	28.7 ± 1.4	26.0 ± 1.1	26.8 ± 0.1 a,b,c	25.5 ± 1.2	23.5 ± 2.9 ^c	24.4 ± 1.3
0.5	19.9 ± 1.0 ^a	20.8 ± 1.9 b	24.4 ± 0.6 a,b,c	24.4 ± 0.6 a,b,d	23.0 ± 0.8 a,b	24.6 ± 1.9 a,b,e	22.2 ± 1.8 a,b,f	21.3 ± 1.7 c,d,e	21.2 ± 0.1 c,d,e,f
1	20.8 ± 2.5 ^a	21.3 ± 0.8 b	24.4 ± 1.6 a,b,c	24.0 ± 1.6 a,d	24.0 ± 1.3 a,b,e	25.8 ± 1.3 a,b,f	19.9 ± 0.8 c,d,e,f	21.9 ± 1.9 c,e,f	20.5 ± 0.3 c,d,e,f
2	20.4 ± 4.0 ^a	19.9 ± 0.1 b	22.4 ± 0.5 ^c	25.2 ± 3.3 a,b,d	23.0 ± 0.1 b,e	20.0 ± 3.1 d,e	16.5 ± 2.1 a,c,d,e	18.7 ± 1.8 c,d,e	17.8 ± 0.4 c,d,e

Table C2. Size of water droplets (d_{32}) over time of 10 wt% W/O emulsions stabilized by 0.14 wt% quercetin crystals containing 0.05, 0.1, 0.5, 1 and 2 wt% WPM particles in the aqueous phase at pH 3.0. Samples with the same letter differ significantly ($p < 0.05$) according to Tukey's test for each concentration of WPM particles.

WPM particles/ wt%	$d_{32}/ \mu\text{m}$								
	0 day	1 day	3 days	7 days	14 days	21 days	60 days	80 days	90 days
0.05	25.4 ± 10.2 a,b,c,d,e	42.8 ± 12.4 a,b	48.7 ± 5.3 a,c	55.7 ± 3.0 a,d	53.1 ± 9.4 a,e				
0.1	20.2 ± 1.0 ^a	20.9 ± 2.8	22.7 ± 2.8 ^a	20.3 ± 1.5 ^b	23.1 ± 2.9 a,b	20.7 ± 1.3			
0.5	18.5 ± 1.5 ^a	19.7 ± 2.3	21.0 ± 1.8	20.3 ± 0.4	22.8 ± 1.3	23.6 ± 3.0 ^a			
1	17.3 ± 1.0 ^a	18.7 ± 1.6 a,b	17.9 ± 1.2 ^c	19.3 ± 1.0 a,d	20.6 ± 1.2 a,b,c,e	21.5 ± 0.6 a,b,c,d,f	16.3 ± 0.4 b,c,d,e,f	17.0 ± 0.3 b,d,e,f,g	14.7 ± 0.7 a,b,c,d,e,f,g
2	16.8 ± 0.6 ^a	19.4 ± 1.1 ^b	17.9 ± 0.6 ^c	19.4 ± 2.0 a,d	20.5 ± 0.9 a,b,c,e	20.5 ± 1.7 a,b,c,f	16.8 ± 1.0 d,e,f	17.7 ± 1.0 e,f	16.6 ± 0.8 d,e,f

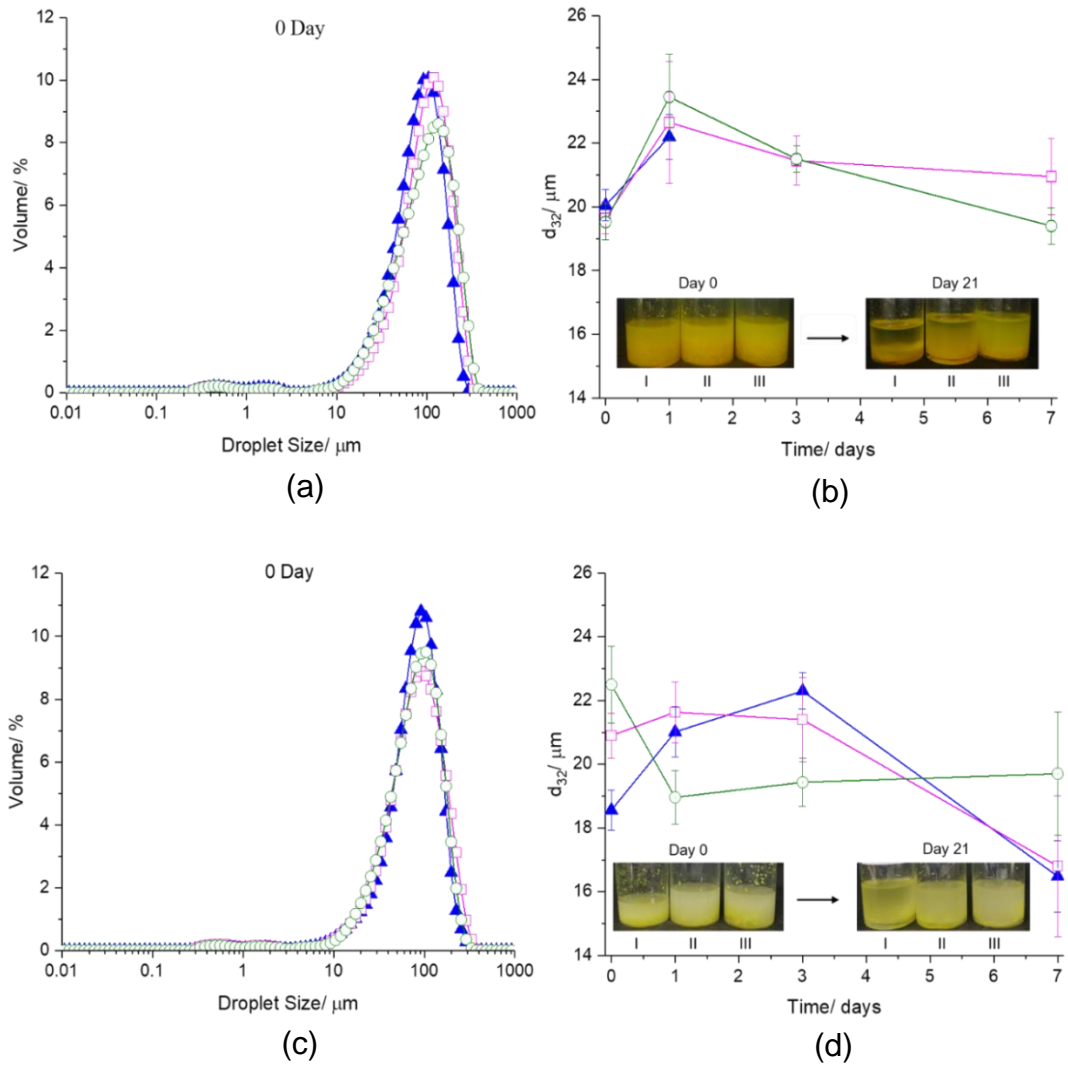


Figure C2. Droplet size distribution [(a) and (c)] and mean droplet size (d_{32}) of water droplets over time with visual images [(b) and (d)] of 10 wt% W/O emulsions stabilized by 0.14 wt% curcumin [(a) and (b)] and quercetin [(c) and (d)] crystals in the oil phase and 0.5 wt% [\blacktriangle] [I], 1 wt% [\square] [II] and 2 wt% [\circ] [III] WPM particles in the aqueous phase at pH 7.0, respectively.

Table C3. Size of water droplets (d_{32}) over time of 15, 20 and 30 wt% W/O emulsions stabilized by 0.14 wt% curcumin crystals & 2 wt% WPM particles in the aqueous phase at pH 3.0. Samples with the same letter differ significantly ($p < 0.05$) according to Tukey's test for each concentration of WPM particles.

Water volume fraction/ wt%	$d_{32}/ \mu\text{m}$					
	0 day	1 day	3 days	7 days	14 days	21 days
15	$15.2 \pm 0.8^{a,b,c}$	$13.7 \pm 0.1^{a,b,c}$	$17.5 \pm 1.1^{a,b,c}$	$16.1 \pm 0.8^{b,c,d}$	$19.1 \pm 0.5^{a,b,c,d}$	$18.4 \pm 0.3^{a,b,d}$
20	14.6 ± 1.0	14.0 ± 0.1	13.1 ± 0.5	13.1 ± 1.6	14.8 ± 0.4	
30	12.6 ± 1.4^a	11.6 ± 1.6^a				

Table C4. Size of water droplets (d_{32}) over time of 15, 20 and 30 wt% W/O emulsions stabilized by 0.14 wt% quercetin crystals & 2 wt% WPM particles in the aqueous phase at pH 3.0. Samples with the same letter differ significantly ($p < 0.05$) according to Tukey's test for each concentration of WPM particles.

Water volume fraction/ wt%	$d_{32}/ \mu\text{m}$					
	0 day	1 day	3 days	7 days	14 days	21 days
15	14.6 ± 1.0	14.3 ± 1.1^a	16.3 ± 0.0^b	$14.1 \pm 2.1^{b,c}$	$16.6 \pm 0.0^{a,c}$	$16.6 \pm 1.9^{a,c}$
20	13.4 ± 1.0^a	$16.3 \pm 1.0^{a,b}$	14.6 ± 0.8^b	14.5 ± 0.1^b	13.3 ± 2.1^b	
30	7.3 ± 0.4	8.7 ± 1.0				

Table C5. Interfacial shear viscosity at W-O interface with 0.14 wt% curcumin and quercetin crystals dispersed in purified oil with different concentrations of WPM particles in the aqueous phase after 24 h of adsorption at pH 3.0. Samples with the same letter differ significantly ($p < 0.05$) according to Tukey's test for each polyphenol crystal.

System	$\eta / \text{mN s m}^{-1}$					
	0 wt% WPM	0.05 wt% WPM	0.1 wt% WPM	0.5 wt% WPM	1 wt% WPM	2 wt% WPM
Curcumin	0.0 ± 0.0 ^{a,b,c,d}	2921.4 ± 142.8 ^{a,b,d}	2605.6 ± 27.2 ^{a,c}	2176.9 ± 154.2 ^{a,b,d}	1646.3 ± 97.5 ^{a,b,c,e}	809.6 ± 185.1 ^{a,b,c,d,e}
Quercetin	289.9 ± 0.0 ^{a,b,c,d}	2997.2 ± 191.9 ^{a,b}	2569.4 ± 243.4 ^{a,c}	2374.4 ± 216.9 ^a	2336.7 ± 186.2 ^{a,d}	1750.2 ± 98.4 ^{a,b,c,d}

As you set out for Ithaka
hope your road is a long one,
full of adventure, full of discovery.
Laistrygonians, Cyclops,
angry Poseidon—don't be afraid of them:
you'll never find things like that on your way
as long as you keep your thoughts raised high,
as long as a rare excitement
stirs your spirit and your body.
Laistrygonians, Cyclops,
wild Poseidon—you won't encounter them
unless you bring them along inside your soul,
unless your soul sets them up in front of you.

Hope your road is a long one.
May there be many summer mornings when,
with what pleasure, what joy,
you enter harbours you're seeing for the first time;
may you stop at Phoenician trading stations
to buy fine things,
mother of pearl and coral, amber and ebony,
sensual perfume of every kind—
as many sensual perfumes as you can;
and may you visit many Egyptian cities
to learn and go on learning from their scholars.

Keep Ithaka always in your mind.
Arriving there is what you're destined for.
But don't hurry the journey at all.
Better if it lasts for years,
so you're old by the time you reach the island,
wealthy with all you've gained on the way,
not expecting Ithaka to make you rich.

Ithaka gave you the marvellous journey.
Without her you wouldn't have set out.
She has nothing left to give you now.

And if you find her poor, Ithaka won't have fooled you.
Wise as you will have become, so full of experience,
you'll have understood by then what these Ithakas mean.

C. P. Cavafy,
"The City" from *C.P. Cavafy: Collected Poems*.
